ACOUSTIC EMISSION ANALYSIS OF PRESTRESSED CONCRETE STRUCTURES

HISHAM A. ELFERGANI

Ph.D. May 2013

DECLARATION

This work has not been submitted in substance for any other degree or award at this or any other university or place of learning, nor is being submitted concurrently in candidature for any degree or other award.

Signed…………………………. (candidate)   Date……………………

STATEMENT 1

This thesis is being submitted in partial fulfilment of the requirements for the degree of PhD.

Signed…………………………. (candidate)   Date……………………

STATEMENT 2

This thesis is the result of my own independent work/investigation, except where otherwise stated. Other sources are acknowledged by explicit references. The views expressed are my own.

Signed…………………………. (candidate)   Date……………………

STATEMENT 3

I hereby give consent for my thesis, if accepted, to be available for photocopying and for inter-library loan, and for the title and summary to be made available to outside organisations.

Signed…………………………. (candidate)   Date……………………

ACOUSTIC EMISSION ANALYSIS OF PRESTRESSED CONCRETE STRUCTURES

PhD Thesis

HISHAM A. ELFERGANI (BEng (Hons), MSc)

School of Engineering
Cardiff University, Cardiff
UK
May 2013

Prifysgol Caerdydd   SUMMARY OF THESIS   Cardiff University

Candidate's Surname: Elfergani
Candidate's Forenames: Hisham
Candidate for the Degree of: PhD
Institution at which study pursued: Cardiff University, Wales, UK
Full Title of Thesis: AE Analysis of Prestressed Concrete Structures

Summary:

This thesis examines the role of Acoustic Emission (AE) as a non-destructive testing (NDT) technique for prestressed and reinforced concrete structures. The work focuses on the development of experimental techniques and data analysis methods for the detection, location and assessment of AE from prestressed and reinforced concrete specimens.

This thesis reveals that AE can be used to detect the onset of corrosion activity in wire in the interface between prestressed concrete and mortar as found in prestressed concrete pipes. Furthermore, this technique can be used to locate the corrosion activity on different size prestressed concrete samples.

By correlation between three parameters of classical AE analysis techniques (traditional parameters), damage can be detected and located whilst the corrosion area, macro crack and crack propagation can be identified. However, it cannot classify the crack type.

Different damage modes, including corrosion activity, micro/macro cracking formation, crack propagation and wire failure generate different types of AE signals with varying amplitudes and absolute energy emitted.

A novel analysis approach has been used on composite materials (concrete, mortar and steel) to evaluate differing crack types by a combination of the classical acoustic emission analysis technique and advanced analysis Rise time / Amplitude (RA) and Average Frequency (AF), results proved the effectiveness of the developed techniques for damage detection and classification crack types.

The relationship between RA value and AF value can be used to determine the crack area and classify it as either tensile crack type, other type (shear movement) or no crack.

The results of the research have demonstrated that the AE technique is valid in larger scale monitoring and hence the potential for monitoring real structures such as prestressed concrete pipes.

Use of Kernel Density Estimation Function (KDEF) provides improved visualisation of the data to represent clearly the RA/AF values.

Key Words: Acoustic Emission, Corrosion, Reinforced Concrete, Prestressed Concrete, Micro and Macro Concrete Cracks, Crack classification, Source Location, Damage Assessment, Monitoring.

ACKNOWLEDGEMENTS

INDEX OF CONTENTS

SUMMARY

ACKNOWLEDGEMENTS

Contents

APPENDIX A: SUMMARY OF TEST DETAILS

APPENDIX B: SENSOR CALIBRATION CERTIFICATES)

APPENDIX C: PUBLISHED PAPERS

LIST OF FIGURES

LIST OF Tables

CHAPTER 1: INTRODUCTION

Structures such as bridges, buildings, concrete pipes, strong tanks, dams, nuclear reactor protective shells, railway sleepers, piles and pressure vessels are made of prestressed concrete in which prestressing steel wires are put into a permanent state of tension to compensate for the inadequate tensile strength of the concrete. Tensile cracking in the concrete is minimised by ensuring that the concrete is in compression under normal working loads by prestressing the steel reinforcement. Generally prestressed steel is between four to five times stronger than mild steel. The main advantages of prestressed concrete structural materials are that they are stronger, lighter and "crack free" (Singh 2000) and hence these materials offer cost benefits over other materials. prestressed Concrete Cylinder Pipe (PCCP) has proven to be one of the most durable pipe materials for large diameter pipes because it has high resistance to large inner pressure and external loading. PCCP is widely utilised in several parts of the world to convey water and wastewater such as the USA (Elliott et al 2006, Travers 1997), Europe, the Middle East, Australia, South America, North Africa, and China. The Great Man Made River (GMMR) in Libya and the South-to-North Water Diversion (SNWD) in China are significant projects which required extremely large diameter embedded PCCP for water transmission (Xiong et al 2010).

Corrosion is a big problem in numerous structures. The cost due to corrosion is estimated in billions of dollars every year. The Department of Transport in the UK evaluated that the cost of repairing of concrete structures damaged by corrosion problems is £755 million a year (Ann et al., 2009). Moreover, Tucson Water (in Arizona, United States) has a total of 21 miles of PCCP in its network (48-96 inches diameter). In 1999, a 96-inch pipe ruptured, causing over $4 million in damage and repair costs (Elliott et al., 2006). The problem of corrosion is more general in reinforced and prestressed concrete and it can

be very dangerous. Therefore in this type of structure it must be given special consideration because failure may result in huge loss of life and money. Most of the studies indicate the main reason of deterioration of bridges and prestressed concrete pipes is corrosion during a relatively short period after construction. The concrete provides the ideal environment to protect the steel wires which are embedded in it possibly for over 50 years (Bertolini et al. 2004). However, the life of a concrete structure becomes shorter due to steel corrosion which occurs by aggressive ion attack such as chloride or carbonation (Ann et. al 2009).

The concrete pipes which transport water are one such structure that has suffered from corrosion. For example, the pipes of The Great Man-Made river project of Libya have suffered from the effect of corrosion. Five pipe failures due to corrosion have occurred since their installation. Another example, in 1990, widespread corrosion and failure of the reinforcing wire on over 6 miles of the prestressed concrete pipe used for the Central Arizona project in USA was found. This pipe had been in service for less than 15 years which is significantly shorter than the expected design life. (Travers 1997). However, the big problem which faces the engineers is to find the best way to detect the corrosion and prevent the pipes from deteriorating (Singh 2000).

This project aims to use the Acoustic Emission (AE) technique to detect the early stages of corrosion prior to deterioration of reinforced concrete structures.

1.1 Construction of PCCP at Great Man-Made River Project

The Great Man-Made River Project (GMRP) is the one of the major civil engineering projects of the 20th century located in Libya. The project is concerned with water transportation from the aquifers deep in the Sahara desert to the coastal region where over 90% of the population lives and the main regions of agriculture and industry are located. The high quality ground water is conveyed throughout almost 4000 km of prestressed concrete cylinder

pipe (PCCP) networks. The PCCP networks consist mainly of four metre diameter pipes and 6.6 million cubic metres of water is transported every day. Access to the pipe network is crucial for many reasons, therefore within the pipe network there are many manholes, located approximately at 600 m intervals. These provide access to the inside of the pipe for collection of water samples or measurement of flow rate. These also allow access to the outside of the pipe structure at these locations.

The purpose of the project is to transform thousands of hectares of semi-desert into rich fertile agricultural land (Singh 2000, Kuwairi 2006, Essamin and Holley 2004).
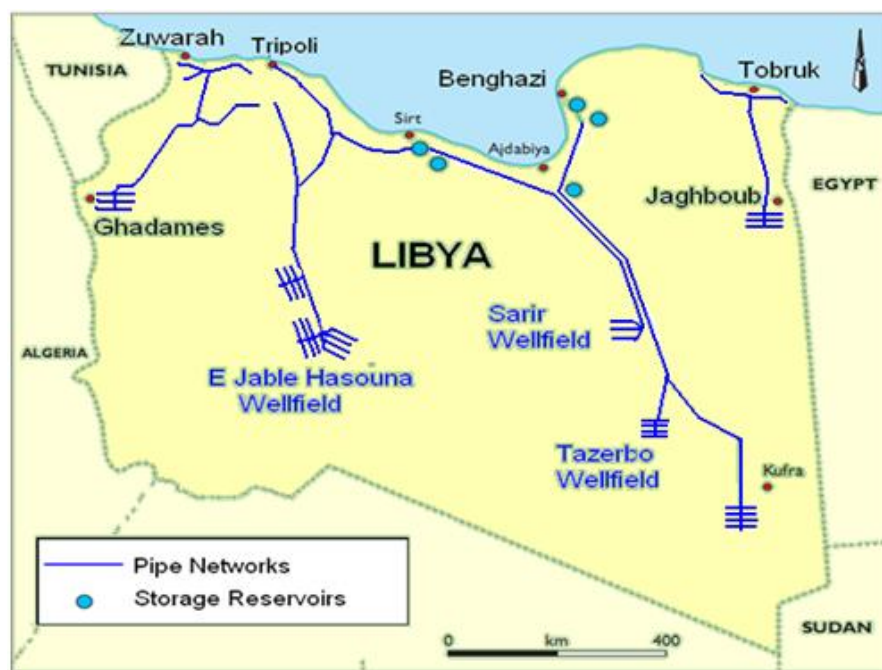
Figure 1. 1 Layout of the various phases of Great Man-Made River Project
(Kuwairi 2006)

1.1.1 Project main components

The total length of the fifth phase pipeline is 4071 km; Sarir/Sirt - Tazerbo/Benghazi is 1600 km, 1277 km of Hasouna/Jeffara, 190 km of

Assdada /Ajdabiya, 38 km is the length of Tazerbo/kufra link and 621 km the length of the Ghdames/Zwara pipeline.

The six open circular concrete reservoirs were constructed with different diameters larger than 1 km. Each reservoir has a different storage capacity ranging from 4 to 24 million cubic metres as shown in Table 1.

Table 1. 1 Reservoir storage capacity

Reservoirs	Storage Capacity
Omar EL-Mokhtar Grand reservoir	24,000,000 cubic metres
Ghordabiya Grand reservoir	15,400.000 cubic metres
Ghordabiya reservoir	6,800.000 cubic metres
Omar EL-Mokhtar reservoir	4,700.000 cubic metres
Ajdabiya holding reservoir	4,000.000 cubic metres
Total storage capacity	**54,900.00 cubic meters**

- **Great Man-Made River Project Statistics**

1. The total number of pipes is 585,296

2. The length of pre-stressing wire used in the project is six million km which is equivalent to 280 times the circumference of the earth.

3. The amount of aggregate used in the project is 30 million ton sufficient to build 20 pyramids the size of the Great Pyramid.

4. The total amount of cement used in the project is seven million tones, sufficient to construct a concrete road from Tripoli to Mumbai.

5. The volume of trench excavation was 250 million m^3.

6. The total number of wells is 1,350 which produce approximately 6.5 million m^3 of water daily.

1.2 Manufacturing of Pre-stressed Concrete Cylinder Pipe (PCCP)

Pre-stressed concrete cylinder pipes are designed to take best advantage of the compressive strength and corrosion-inhibiting property of Portland cement concrete and mortar and the tensile strength of prestressing wire. Each transportation line pre-stressed concrete cylinder pipe is mainly 4.0 m in inner diameter; with a length of 7.5 m, and over 70 tonnes in weight. The concrete

4

pipe consists of a 225 mm thick concrete core within an embedded thin steel cylinder and externally wrapping prestressed wires. The cured concrete core is prestressed by applying over-wrapping with high tensile steel wire at a close pitch under uniform tension. The prestressed wires are coved by a 19 mm thick layer of cement mortar to protect the wires against corrosion and mechanical harm. This type of pipe is called a 'white' pipe and is used in non corrosive soil whilst a 'black' pipe is used in more aggressive conditions. In black pipes the cement mortar is coated by a black coal tar epoxy. A typical cross-section of the PCCP is shown in Figure 1.2.

PIPE MAKE-UP

MORTAR COATING   STEEL PRE-STRESSING WIRE

OUTER CONCRETE CORE

STEEL LINER

INNER CONCRETE CORE

Length of Pipe = 7.52 meters
Pipe Diameters   1.6-4.0 meters
Weight of Pipe = 75-83 tonnes
Pressure Rates   6-26 bar
17-18 km of prestressed Wire
12-16 tonnes of Cement
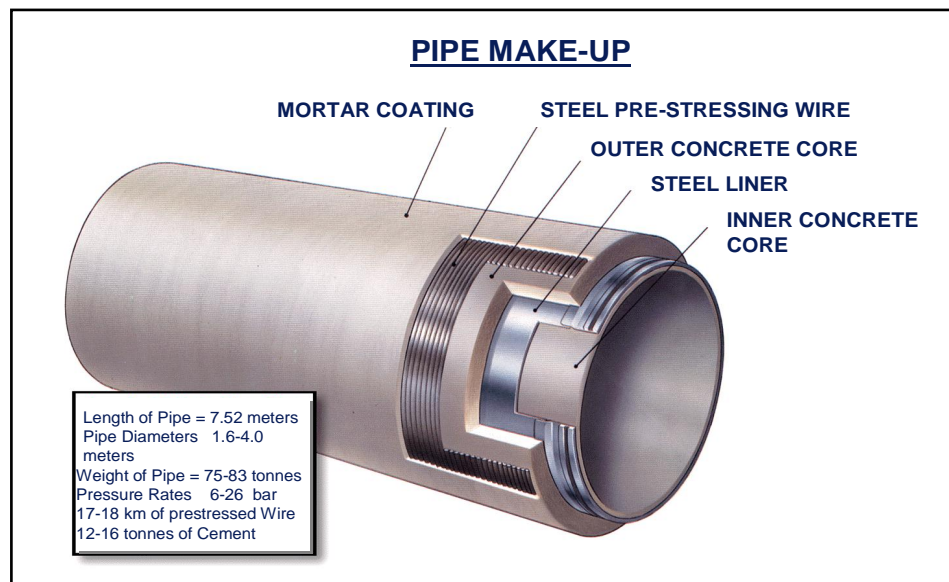
Figure 1. 2 Typical Cross-Section of the PCCP

Pre-stressed concrete cylinder pipes are resistant to external soil, surface loadings and internal pressure by being dependent on their inherent strength.

The pipe is designed in accordance to AWWA standard C301 (Al NAHR CO. LTD. July 1999). The pressure evaluation is based on the maximum steady state operating pressure plus a safety factor of about 5m head of water, and accommodates transients up to 140% of rated pressure. Classifications of the primary transportation system range from 6 bar to 28 bar in 2 bar increases, the different classifications are controlled by changes in prestressing wire

diameter, pitch and number of layers during pipe manufacture as shown in Figure 1.3. In order to protect the pipelines from the risks including temperature variations and other environmental conditions they are laid in seven metre deep trenches.

Figure 1. 3 Pipe Construction

1.3 Damage and damage assessment

Due to prestressed wire corrosion in the concrete pipes induced by chloride ions absorbed from the aggressive soil, five catastrophic failures in four metre diameter white pipes have occurred after ten years of operation. The first failure was in August 1999 in the Sarir-Sirt (ss) line. The following month another pipe failed on the parallel Tazerbo-Benghazi line of the SS/TB conveyance. Three more failures, one on the Sarir-Sirt line and two on Tazerbo-Benghazi line occurred between January 2000 and April 2001. The

main reason for the damage is corrosion of prestressed wires in the pipes due to attack from the chloride ions from soil. Detection of the corrosion in initial stages has been very important to avoid other failures and the interruption of water flow. Figure 1.4 shows photographs of corrosion of the prestessing wires and examples of pipe failures.

Figure 1. 4 Pipe failures

Initially traditional techniques such as potential mapping, tapping and close-interval potential surveys were used to make a vast survey of the current pipelines. Then, experts used electromagnetic inspection and Acoustic monitoring was used to inspect and monitor the rate of deterioration of pipes which had not been removed. The time and location of wire break events can be determined by this method. Even though most of the non-destructive methods, which are used in the project, are able to detect wire break, they cannot detect the presence of corrosion. Hence in areas where no excavation has been completed, areas of serious damage can go undetected.

1.4 Aims and Objectives

The substantial challenges which faces engineers, apart from future corrosion protection, is to find the best way to detect the corrosion and macro cracking at an early stage and prevent the pipes from deteriorating further.

The aims of this research are:

I.   To investigate the role of acoustic emission in detecting each stage of corrosion in reinforced concrete structures.

II.   To further the understanding of the AE technique for use in structural monitoring of prestressed concrete pipes and reinforced concrete structures.

III. To developed procedures to accurately locate, identify and characterise damage types.

CHAPTER 2: LITERATURE REVIEW

2.1 Corrosion

Corrosion is defined as an electrochemical process that occurs in metals due to environmental conditions. Metal oxide is more stable than metal, therefore metal has a tendency to convert to metal oxide or other compounds. Although naturally occurring it is possible to induce corrosion artificially using a corrosion cell. Every corrosion cell consists of four essential elements which are an anode, a cathode, an electrolyte and an electrical connection. The anode is located in the position where corrosion is required whilst the cathode is another cell site which is not consumed in the corrosion process. The electrolyte aqueous environment provides a path for ionic conduction between the anode and the cathode. The electrical connection allows the electrons to be transmitted through it. The corrosion cell can be illustrated as in Figure 2.1 below (Bradford 1993, Scully1990, Fontana 1978).
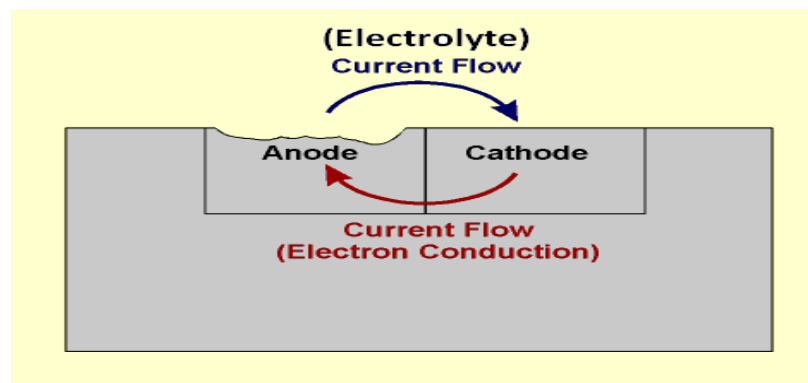
Figure 2. 1 The corrosion cell

- **Basic chemical attack in concrete**

One of the principal components of concrete is Portland cement which reacts with water to create hydrated products. These products help to bind together other elements such as aggregate and sand, to produce a strong material with a porous matrix. Alkalinity in concrete, which is in the form of calcium

hydroxide and small amounts of potassium and sodium hydroxide, is produced during the hydration process. In typical concrete, the alkalinity is high, often with a pH value between 12.5 and 13.5.

The steel used in reinforced concrete is situated within this highly alkaline environment meaning it will be passivated due to the water-insoluble layers formed on the surface therefore, protecting it from the corrosion process. Loss of passivity and the onset of corrosion can occur due to either a reduction in the alkalinity or the conversion of the oxide film to a soluble form by external influences. The loss of alkalinity occurs due to carbonation, while the protective oxide film destruction is attributed to the influence of aggressive ions, such as chlorides (Berkeley and Pathmanaban 1990, Schiessl 1988).

- **Carbonation**

Carbonation can be defined as attack of concrete by carbon dioxide, which comes from the atmosphere. Carbon dioxide can penetrate into concrete through contact with water or soil, providing carbon dioxide is dissolved within the contact material. Carbon dioxide causes destruction of the alkaline environment which as previously discussed maintains the protective oxide film on the steel surface.

The rate of penetration of atmospheric carbon dioxide depends on concrete permeability and moisture concrete. Carbonic acid is formed by dissolving carbon dioxide in pore water, moist soils or groundwater as follows in the reaction below:

$$CO_2 + H_2O \rightarrow H_2CO_3 \qquad\qquad (2.1)$$

Hydrogen and bicarbonate ions can be dissociated from carbonic acid. Then carbonate and hydrogen ions may be dissociated from the bicarbonate ions.

The carbonic acid reacts with $Ca(OH)_2$ in the hardened cement paste to form neutral insoluble $CaCO_3$. The general reaction is as follows:

$$Ca(OH)_2 + H_2CO_3 \rightarrow CaCO_3 + 2H_2O$$

(2.2)
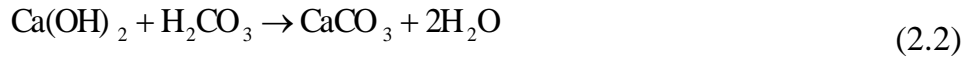
These results in an increasing strength and reduction in permeability due to the insoluble calcium carbonate formation in the concrete so the ability of the concrete to withstand the environment is further improved.

Soluble calcium bicarbonate will be formed from reacting further with carbon dioxide and with the $CaCO_3$ that has already been formed:

$$CaCO_3 + H_2CO_3 \rightarrow Ca(HCO_3)_2$$

(2.3)
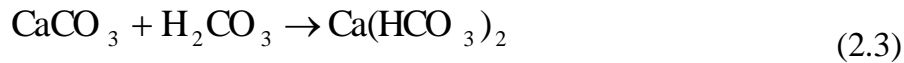
Calcium bicarbonate is easily soluble and can be leached from the concrete; consequently the concrete alkalinity and strength of the concrete are decreased. As a result of loss of concrete alkalinity, which is responsible for stability of the protective passive film on the steel surface, the protective film will be destroyed and so steel corrosion is initiated (Berkeley and Pathmanaban 1990).

- **Chloride attack**

The principle of steel protection in concrete from corrosion is a passivating gamma ferric oxide film which initiates on the steel surface due to cement hydration by producing the highly alkaline environment. Steel corrosion in concrete can be initiated when the chloride ions reach the steel-concrete interface with a concentration sufficient to break down the protective passive film on the steel surface and the presence of sufficient oxygen and moisture to sustain the reaction.

There are two types of source of chloride in concrete:

7. Internal source; when the mix materials (water, cement and aggregate) are contaminated with chlorides.

8. External source; such as de-icing salts, seawater, salt-spray particles.

To destroy the protective film on the surface of steel, the chloride must be in its free ionic form, if it remains bound in the matrix, the start of corrosion is postponed (Melchers 2009, Berkeley and Pathmanaban 1990, Schiessl 1988).

The main two factors, which lead to an increase in free chlorides, are carbonation and the presence of sulphates. Consequently they have a synergistic effect on chloride-induced corrosion.

- **Mechanics of corrosion of steel in concrete**

In the presence of chloride ions, water, and oxygen in concrete, the anodic and cathodic reactions are represented as follows:

Anodic reaction:

The metallic Fe is oxidized to form positively charged ferrous ions:

$$Fe + 2Cl^- \rightarrow FeCl_2 + 2e^- \rightarrow Fe^{2+} + 2Cl^- + 2e^- \tag{2.4}$$
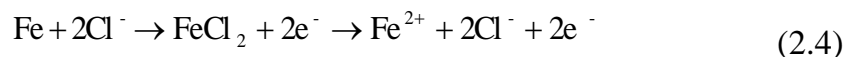
The net reaction of equation (2.4) is expressed:

$$Fe \rightarrow Fe^{2+} + 2e^- \tag{2.5}$$

Cathodic reaction:

The free electrons which are released from Anodic reaction react with O_2 and H_2O to form hydroxyl ions as:

$$2H^+ + 2e^- \rightarrow H_2 \tag{2.6}$$

$$O_2 + 2H_2O + 4e^- \rightarrow 4OH^- \tag{2.7}$$

Hydroxyl ions migrate towards the anode and react with the ferrous ions to form ferrous hydroxide Fe (OH)$_2$ as shown in Figure 2.2 and Equation 2.8:

$$2Fe^{2+} + 4(OH)^- \rightarrow 2Fe(OH)_2 \qquad (2.8)$$
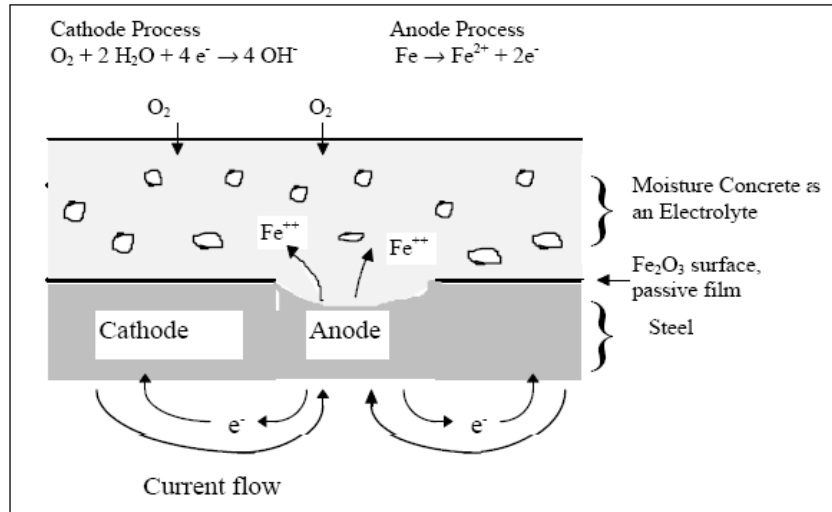
Figure 2. 2 Mechanism of corrosion of steel in concrete (Schiessl 1988)

Further oxidation reactions of the ferrous hydroxide can occur by reacting with O$_2$ and H$_2$O which are present in the concrete matrix to form hydrous ferric oxide (Fe$_2$O$_3$.3H$_2$O) (haematite) which is commonly known as ordinary red-brown rust, and black magnetite (Fe$_3$O$_4$) preceded by the formation of green hydrated magnetite (Fe$_3$O$_4$. H$_2$O):

$$4Fe(OH)_2 + O_2 \longrightarrow Fe(OH)_3 \rightarrow Fe_2O_3.H_2O + 2H_2O \qquad (2.9)$$

$$6Fe(OH)_2 + O_2 \longrightarrow 2Fe_3O_4.H_2O + 4H_2O \qquad (2.10)$$

$$Fe_3O_4.H_2O \rightarrow Fe_3O_4 + H_2O \qquad (2.11)$$
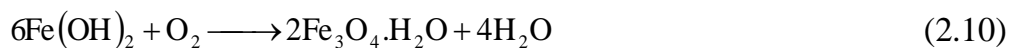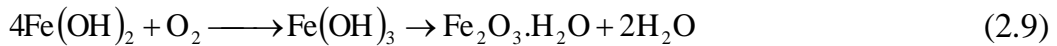
Since the volume of rust products is much bigger (about 4 to 6 times) than the metallic Fe in the primary situation it will lead to cracking of the cover

concrete when high stress exceeds the tensile strength of the concrete, and reduction of steel reinforcing cross section may eventually cause the failure of the structure (Schiessl 1988).

2.2 Non-destructive Testing

Flaws and cracks can cause a dramatic reduction in the performance of structures. It is therefore essential that as part of quality control of engineering structures for their safety and efficiency in service life, the detection and monitoring of defects in solids and the structures is of paramount importance.

Non-destructive testing (NDT) is defined as the method which is used to test a material or system without damaging it. To date non-destructive testing has been widely used for the monitoring of the condition of metallic structures but as far as concrete structures are concerned, its use is still in its early stages because of the heterogeneous nature of the material (Giannoulakis 2008).

In general, there are several NDT methods that are used; visual inspection, liquid penetrant testing, magnetic particle testing, eddy current testing, radiographic testing, ultrasonic testing, leak testing, infrared and thermal testing, acoustic emission and other methods. However, the application of a method is dependent on the test object or component (Miller et. al 2005, Hellier 2001).

Applications of non-destructive testing in reinforced and prestressed concrete structures at an early stage are important to avoid serious implications related to loss of asset use, financial loss and in some instances loss of life. Common methods used to monitor reinforced concrete and prestressing steel are; visual inspection, half-cell potential measurements, linear polarization resistance (LPR), concrete resistance, resistivity measurements, ultrasonic testing, eddy current and acoustic emission methods.

2.2.1 Visual Inspection

Visual inspection is a traditional and simple method. It is used by reflecting or transmitting light from the test object which is viewed with the naked eye or a light-sensing device. It should be applied as the first non-destructive technique of a test object.

However, applications of the method are limited because it is used only to detect surface discontinuities. Furthermore, it cannot supply enough information for an extensive survey.

2.2.2 Half-cell Potential Measurements

One of the most common techniques currently used in monitoring reinforced concrete is a half cell potential measurement. It is used to measure the electrical potential between the reinforced steel in the concrete and a reference electrode placed on the concrete surface (Ha et. al. 2007) such as saturated calomel electrode (SCE), copper/copper sulphate electrode (CSE), silver/ silver chloride electrode etc. The value of potential is an indicator of the degree of degradation which has occurred due to steel corrosion.

The potential of reinforcement is measured by using a voltmeter connected by an electrical wire between the reinforcing steel in the concrete and a reference electrode in contact with the surface of the concrete, as shown in Figure 2.3. The standard of testing is described in BS1881: Part 201 (1986).
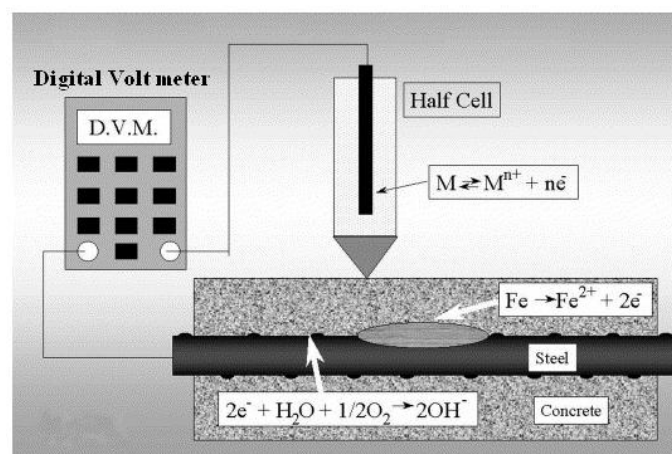
Figure 2. 3 Half cell potential measurement (Broomfield 2002)

This method provides an indication of the possibility of corrosion at the time of measurement nevertheless; it cannot give any information about the corrosion rate of reinforcing steel (Broomfield et al. 2002). The probability of corrosion is higher when the reading is more negative. The relationship between the half cell reading and corrosion potential has been well documented. As per ASTM C 876 standards, the probability of reinforcement corrosion is as follows in Table 2.1.

Table 2. 1Corrosion condition related with half-cell potential (HCP) measurements (ASTM C 876)

Open circuit potential (OCP) values		Corrosion condition
(mV vs. SCE)	(mV vs. CSE)	
< -426	< -500	Severe corrosion
< -276	< -350	High (<90% risk of corrosion)
-126 to -275	-350 to -200	Intermediate corrosion risk
> -125	> -200	Low(10% risk of corrosion)

This method is widely utilized to evaluate the stage of corrosion of reinforcing steel and prestressed concrete structures. The two most common reference electrodes, which are used in concrete, are the silver/silver chloride and copper/copper sulphate reference electrode.

Although half-cell potential measurement is the simplest of all methods used for monitoring steel wire corrosion, it is not able to provide any quantitative information (Ahmad 2003).

2.2.3 Linear Polarization Resistance (LPR)

In this method the reinforced steel in concrete is polarized for a certain amount of current by an external source. The polarization is required to be within the linear area of the current density potential curve (-20 and +20 mV with regard to corrosion potential). It is noted that the applied current is a

linear function of electrode potential within -10 to +10 mV, as shown in Figure 2.4. In this figure, E_{corr} is used as an over-voltage reference point and a plot of over voltage vs. applied anodic and cathodic currents is shown on a linear scale (Perez 2004). The slope of this line refers to the kinetic parameter of the system as follows:

$$\frac{\Delta E}{\Delta i_{app}} = \frac{\beta a \beta c}{2.3 i_{corr}(\beta a + \beta c)}$$

(2.12)

Where

$\beta_a, \beta c$ = anodic and cathodic Tafel slopes, respectively, and

$\frac{\Delta E}{\Delta i_{app}} = r_p$, the polarisation resistance (Ω)

Hence i_{corr} can be estimated by measuring the value of r_p
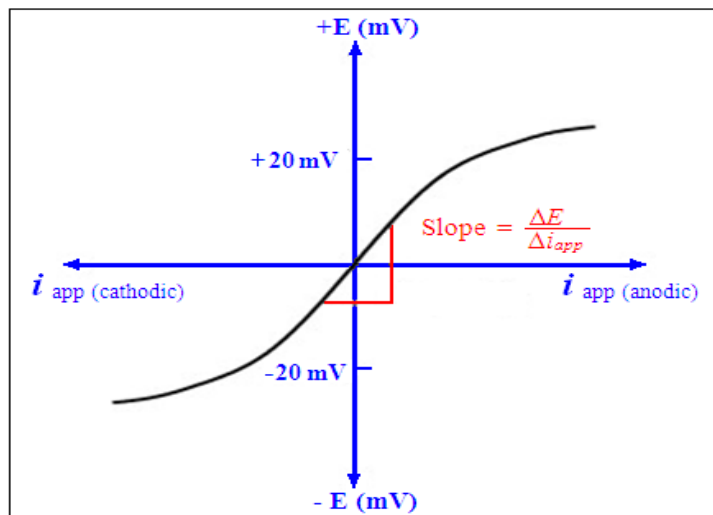
Figure 2. 4 Applied-current Liner Polarisation Curve (Poursaee 2010)

The corrosion rate can be determined by including other data such as sample area and material equivalent weight. (Bunnori 2008, Broomfield et al. 2002, Singh 2000).

The linear polarization method is commonly used in both the laboratory and in the field to measure the corrosion current density, but its use in practice is more difficult. The principal difficulty in this method is the definition of area over which the applied potential is going to act (Song and Saraswathy , 2007).

2.2.4   Concrete resistance and resistivity measurements

This method is dependent on measuring the electrical resistivity of concrete which is related to moisture movement and permanent changes associated with chloride ingress. A lower concrete resistivity indicates a greater chance of corrosion of the steel in concrete and also a greater corrosion rate. However, the corrosion probability is very small at high resistance. The resistivity of concrete can vary extensively depending on the local conditions and environmental influences. Therefore the combination of resistivity and potential measurement improves the information about the corrosion condition of the steel.

A number of authors (Song and Saraswathy, 2007) have related corrosion and resistivity as follows in Table 2.2.

Table 2. 2 Corrosion risk from resistivity

Resistivity (Ohm.cm.)	Corrosion risk
Greater than 20,000	Negligible
10,000 to 20,000	Low
5,000 to 10,000	High
Less than 5,000	Very high

2.2.5 Ultrasonic methods

The ultrasonic method is a technique which is based upon acoustic waves at high frequency. Waves are generated by an electro-acoustical transducer which is attached to the concrete surface. The generated waves are transferred from the concrete surface into the concrete. Parts of the wave are reflected at defects surface like cracks or voids in the concrete. The reflected waves are received by another transducer, which converts these waves into electrical signals. The location of defects can be determined based on the velocity of the waves and their transit time (Acciani et al, 2008). This technique is used to locate surface and subsurface flaws in several materials such as metals, concrete, wood and plastics.

Ultrasonic techniques are also used to measure the thickness of materials and otherwise characterize material properties based on sound velocity and attenuation measurements. Figure 2.5 illustrates this method.
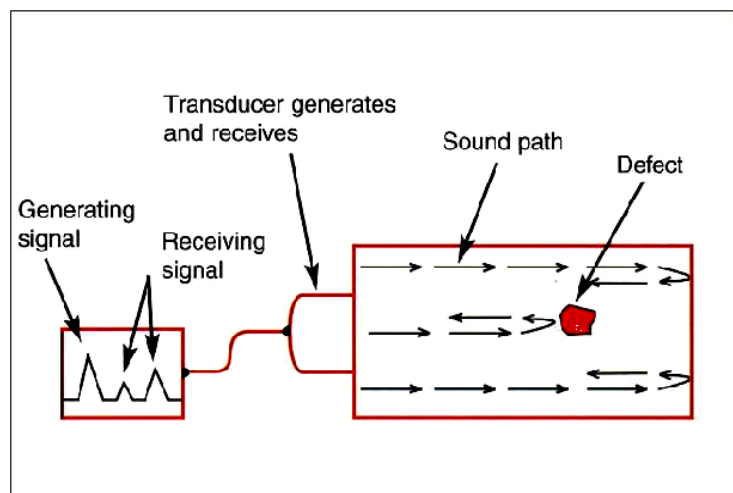
Figure 2. 5 Ultrasonic testing (Giannoulakis 2008)

2.2.6 Magnetic Particle Testing

During magnetic particle testing, a magnetic field is applied to a structure which has to be made from ferromagnetic material. The magnetic flux lines travel through the material and exit and re-enter the materials at the poles.

Flaws such as crack or voids can not support as much flux, and force some of the flux outside of the part. Magnetic particles distributed over the test object will be attracted to areas of flux leakage and generate a visible indication of damage (Hellier 2001, Giannoulakis 2008). Figure 2.6 shows the diagram of this method.
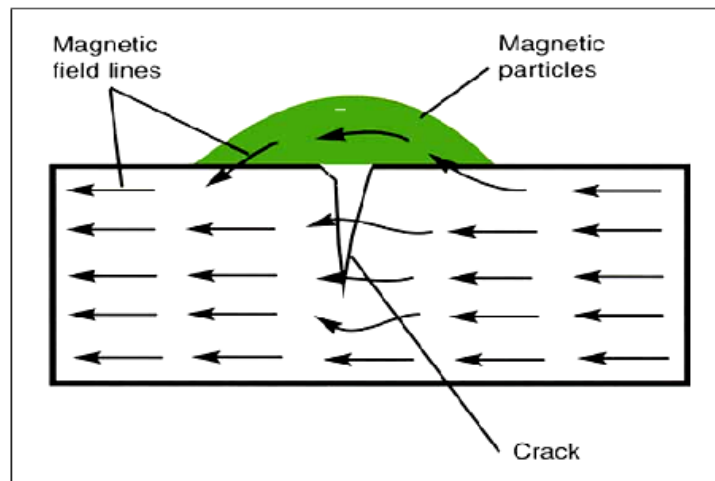
Figure 2. 6 Magnetic Particle Inspection (Giannoulakis 2008)

2.2.7 Eddy current

This technique is based on high frequency alternating electrical current being passed through a coil producing a magnetic field. This primary magnetic field induces eddy currents in the test object when the coil is placed near it. Eddy currents generate a secondary magnetic field that opposes the primary field and can be measured and used to find defects and characterize conductivity, permeability, and dimensional features.

Among the uses for this NDT method are crack detection, corrosion and material thickness measurements, sorting material, identification of heat-affected areas, coating thickness measurement, electrical conductivity measurement and metal detection. Figure 2.7 shows a graphic illustration of this method (Boving 1989, Hellier 2001, Miller and Hill 2005).
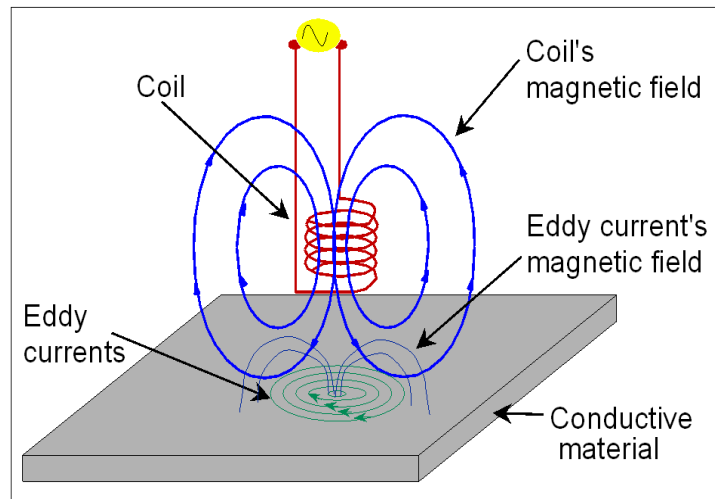
Figure 2. 7 Eddy current (Giannoulakis 2008)

2.2.8 Summary

NDT methods have been described for the assessment of reinforced concrete structures. The majority of these methods are still under research and have potential in relation to the assessment of corrosion and the condition of reinforced and prestressed concrete structures.

Choice of the most appropriate procedure is usually based on a combination of factors such as cost, speed, reliability, and accuracy of the given method. Each of the methods has certain advantages and disadvantages and adopting several testing methods and combining the results can often provide the best outcome (Idrissi and Liman, 2003).

 Although, most of these methods, such as electromagnetic inspections, have been used to monitor prestressed concrete pipes in Libya and although they can provide a probability of corrosion present they cannot detect the presence of corrosion. Hence, it is very important to find an innovative non destructive evaluation and monitoring technology with a much more accurate assessment of early stages of the presence and extent of deterioration. The major advantage of acoustic monitoring over other methods is the availability of real-time information on the deterioration rate of the pipe.

2.3   Acoustic Emission

2.3.1 Introduction

Acoustic emission (AE) is defined as the elastic energy liberated from materials which are undergoing deformation (Miller and Hill 2005). Also it can be defined as "the transient elastic waves which are generated by the rapid release of energy from localized sources within a material" (Moore et. al, 2005).

The rapid release of elastic energy, the AE event, propagates through the structure to arrive at the structure surface where a piezoelectric transducer is mounted. These transducers detect the displacement of the surface at different locations and convert it into a usable electric signal.

By analysis of the resultant waveform in terms of feature data such as amplitude, energy and time of arrival, the severity and location of the AE source can be assessed. Figure 2.8 and Figure 2.9 show a summary of the AE detection process.
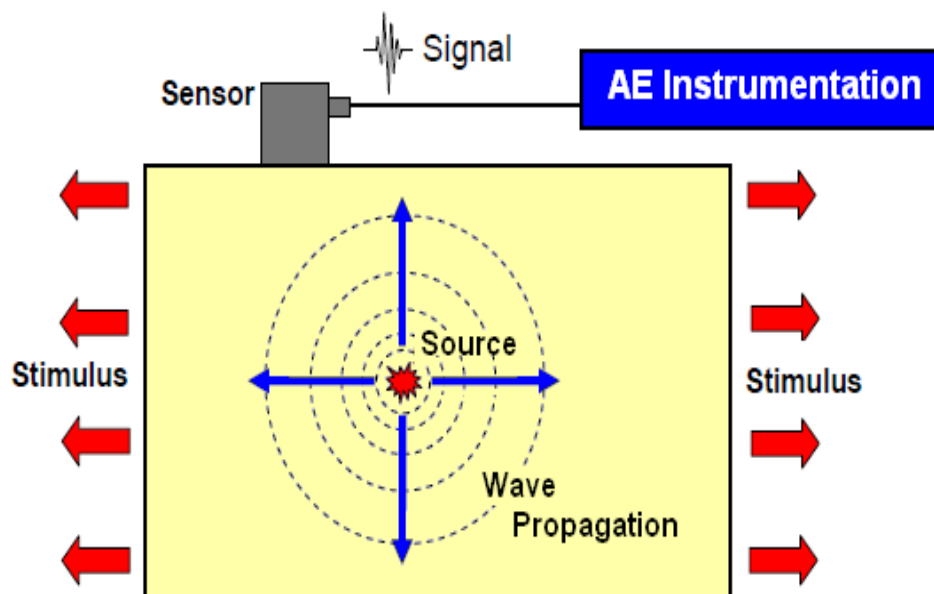
Figure 2. 8 Acoustic emission method (ASTM 1982)

Test object and application of load produce mechanical tensions
Source mechanisms release elastic energy
Wave propagation from source to sensor
Sensors converting a mechanical wave into electrical AE signal
Acquisition of measurement Data converting an AE signal into an electronic data set
Display of measurement data Plotting the recorded data into diagrams
Evaluation of the display from diagrams to safety-relevant interpretation

Figure 2. 9 The AE chain (Baxter 2007)

The phenomenon is also sometimes called stress wave emission, stress waves, microseismic activity, microseism and rock noise. AE testing is often considered the most sensitive method of non-destructive testing because it is the only technique which can detect the defect process as it is occurring. AE techniques can be used to monitor a wide range of structures and materials such as metals, non-metals and combinations of these when load is applied. There are two main differences between AE testing and other non-destructive techniques which are;

1. The energy which is detected is generated from the test object itself in AE testing.

2. The dynamic processes associated with the degradation of structures can be detected by only AE testing. (Miller and Hill 2005, Bunnori 2008).

The advantages of AE testing compared with other non-destructive methods include (Moore et. al, 2005, Hellier 2001):

1. AE testing is a dynamic test technique.
2. The significance of discontinuities in the entire structure during a single test can be detected and evaluated by AE testing (real-time evaluation).
3. AE testing can be applied to vessels and other pressure systems during service which requires no downtime.
4. Catastrophic failure of systems with unknown discontinuities can be prevented by AE monitoring.
5. AE testing requires only limited access to detect discontinuities.
6. AE testing can be used in all stages of testing such as pre-service testing, in-service testing, leak detection and location, in-process weld monitoring and mechanical property testing.

The limitations of AE testing include (Moore et. al, 2005, Hellier 2001):
1. Repeatability: AE is stress unique and each loading is different.
2. Attenuation: The AE wave in the component will be attenuated during testing.
3. History: Testing is highly effective when the loading history of a component is known.
4. Noise: Extraneous noise may affect AE testing.

There are several mechanisms which give rise to acoustic emission in materials. In metals source mechanisms include moving dislocations, slip, crack growth, grain boundary sliding, twinning and fracture and decohesion of inclusions. In composite materials matrix cracking and the debonding and fracture of fibres are AE sources.

According to Miller and Hill 2005 it is believed that artisans used the first AE monitoring application thousands of ago for assessing the quality of their manufactured pottery. However, it has been established that the first observation of acoustic emission was when copper smelting began in Asia Minor as early as 3700 B.C. In the eighth century, Arabian alchemist Geber made the first documented observations of AE. His book was published in 1545 in Berne in Latin. In 1933, in Japan, the first experiment to detect and record AE events of test objects was carried out by Fuyuhiko Kishinouye and in 1936, in Germany, some AE experiments were achieved by Friedrich Forster and Erich Schhil. They were able to measure immensely small voltage variations in steel wire by using an electrodynamic transmitter and receiver system. In 1948 in the United states experiments were performed by Warren P. Mason, Herbert J. McSimin and William Shockley to measure and monitor moving dislocations of 0.1 nm displacements.

In 1950, in the United Kingdom, Millard was able to detect twinning in single crystal wires of cadmium by using a Rochelle salt transducer. However the recent principle of AE technology is dependent on Josef Kaiser's work, undertaken in Germany.

The first comprehensive investigation of the AE phenomenon was reported by him in 1950. The irreversibility phenomenon was the most considerable finding that he discovered which is now called the Kaiser effect. In addition, he was able to differentiate between burst and continuous emission.

In 1954, in the United States, Bradford H. Schofild achieved the first extensive research about AE's phenomena following Kaiser's work. He concluded that AE is mostly a volume effect and not a surface effect. In the early 1960s, AE testing was finally classified as a new non-destructive testing technology.

2.3.2 Fundamentals of AE

The principal idea of acoustic emission is that elastic waves or acoustic emission is released from solid materials or components due to deformation or fracture which occurs during applied mechanical or thermal stress.

The purpose of the AE test is to detect and locate sources of the emission and to gain sufficient information about them. The detected waveform contains qualitative and quantitative information for characterization of a source. The main factors which influence the AE signals are the source's characteristics, a path between the source and transducer, transducer's characteristics and the measuring system.

The main parameters of waveform are AE hit, AE count, AE hit energy, signal amplitude, signal duration and signal rise time. Figure 2.10 shows the definitions for a simple waveform (Moore et al. 2005).
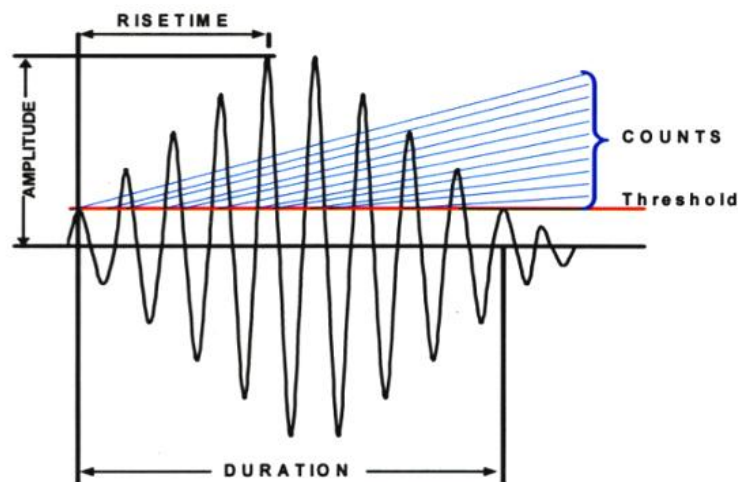
Figure 2. 10 Characteristics of a burst type of AE signal (Eaton 2007)

- **Emission Hits and Count**

Separate signal bursts, which are generated by local material changes, are called AE hits. However, the number of times a signal crosses a preset threshold is called hit count which depends on the transducer frequency, the

transducer damping characteristics, the damping characteristics of structure and the threshold level (Miller and Hill 2005).

- **Acoustic Emission Event Energy**

The acoustic emission event energy is the rapid release of energy in the material which can be expressed by the true energy which is proportional to the area under the AE waveform (Moore et al. 2005). The electrical energy, U, present in a transient hit can be defined as:

$$U = \frac{1}{R}\int_0^\infty V^2(t)dt$$

(2.13)

Where R is the electrical resistance (ohm) of measuring circuit, V is the output potential (volt) and t is time (second). Direct energy analysis can be achieved by digitizing and integrating the waveform signal or by special devices performing the integration electronically (Miller and Hill 2005).

- **Acoustic emission signal amplitude**

AE signal amplitude is the peak voltage of the signal waveform which depends on the intensity of the AE source in the material. Peak amplitude measurements are generally achieved using a log amplifier (logarithmic scale) to cope with a wide range of signal amplitudes (large and small signals) (Miller and Hill 2005).

A usual unit for measuring the amplitude of an acoustic signal is the decibel (dB). The decibel is not a fixed measurement unit but rather expresses a logarithmic ratio between two conditions of the same dimension. In acoustic emission, the reference level 0 dB_{AE} is defined as a signal of 1 µV at the transducer before any amplification.

The fundamental decibel is:

$$N_{dB} = 10 \log_{10} \frac{P}{P_0}$$

Where P is the measured power and P_0 is the reference power in watts.

In a sense, the power is a square function of voltage:

$$N_{dB} = 10 \log_{10} \left(\frac{V}{V_0} \right)^2$$

$$= 20 \log_{10} \frac{V}{V_0}$$

where V is the measured potential and V_o is the reference potential in volts.

Wave propagation in a solid material is complex. In an infinite medium, waves propagate as bulk waves in two fundamental modes; longitudinal waves (P-wave) and transverse waves (S-wave). Each has a special characteristic velocity depending on material properties such as the density and elastic constant. The characteristic of transverse waves is particle movement perpendicular to the wave propagation direction, whereas the motion of the particle in longitudinal waves is parallel to the wave's propagation direction. By introducing the surface boundary, the longitudinal and transverse waves combine in the region close to the surface, so that the overall particle motion is neither purely longitudinal nor transverse, this is called a Rayleigh wave or surface wave. Another kind of surface wave is known as a Lamb or plate wave. The Lamb wave is formed in a medium bounded by two surfaces (plates) (Holford 2000, Beck 2004, Giannoulakis 2008, Pullin 2001). Wave attenuation is another important AE characteristic. It can be described as the way in which the wave amplitude/energy decreases with distance. There are four main cases of attenuation which are geometric spreading, internal friction, dissipation of the wave into adjacent media and velocity dispersion (Pollock 1986).

- **Acoustic Emission Source Location**

AE source location is very important to assess the areas of active damage. The most commonly used source location technique is the time of arrival (TOA) approaches, which is an integral part of all commercially available AE software. There are other source location methods such as Single Sensor Modal Analysis Location (SSMAL), the recently developed DeltaT mapping method and energy based spatial location.

Time of arrival (TOA) technique is based on the source being located by several sensors in an array and measuring the time delay between pairs of sensors within the array. Several source location applications are appropriate for linear source location, i.e., where a single position along a measurement axis is adequate to define the location of a source. Most applications of AE source location are interested with locating a source in a fundamentally two-dimensional shell type component. Three-dimensional source location is required if the thickness of the object under test is significant relative to the other two dimensions or if the area of interest is internal to the specimen. For linear location, the minimum number of transducers is two; however three are required for two-dimensional location and four are required for three-dimensional location (Baron and Ying 1987). Pullin (2001) describes a technique that determines the location of an event in one dimension between two sensors where the propagating velocities of different wave modes of a signal and the time of arrival at a signal sensor is known.

- **Linear (1D) Location**

Figure 2.11 (a, b, c and d) shows a situation where three sensors are placed on a linear structure such as a beam. An AE event occurring at any point in this beam will emit stress waves propagating in both directions.

The simplest technique of locating this source is zonal location which examines the order in which the event reaches the sensors in the array, i.e. the "hit" sequence. With reference to Figure 2.11a, if the first sensor hit is sensor

2 then the region for possible location is the mid point between sensor 1 and 2 then the region for possible location is the mid point between sensor 1 and 2 to the mid point between sensor 2 and 3. Further location accuracy can be gained by examining the second sensor that is 'hit' in the array. In Figure 2.11b, sensor 1 is the second sensor to receive the hit and therefore the source can be located between the midpoint between sensors 1 and 2 and sensor 2.
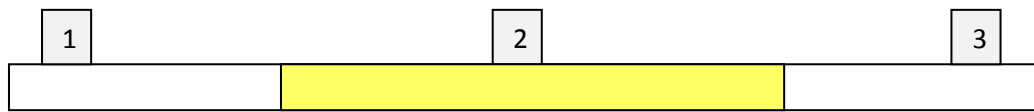
(a) Zone for first hits at sensor 2
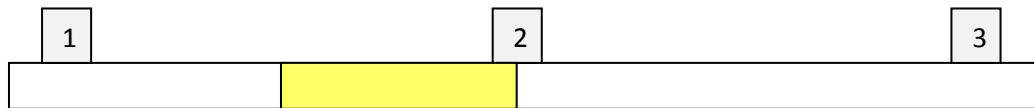
(b) Zone for first sensor at sensor 2 and second hits at sensor 1
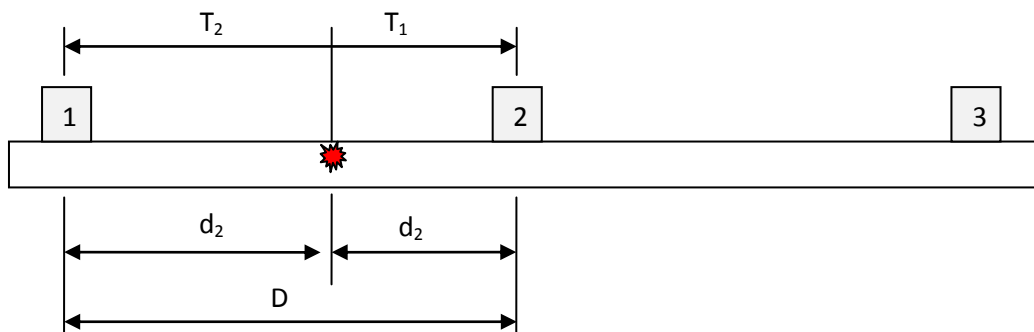
(c) Hits sequence, time difference measurement $\Delta t = T_2 - T_1$
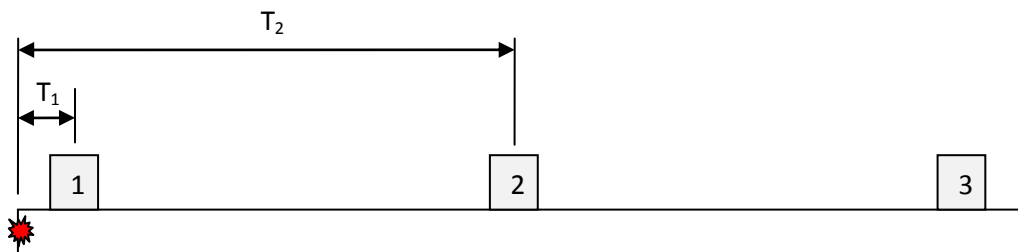
(d) Source outside of array $\Delta t = T_2 - T_1 =$ Constant

Figure 2. 11 Linear location using time of arrival (TOA) theory

(Miller and Mclntire 1987)

This method can be made more accurate by examining not only the hit order, but the difference in time arrival of the hit at the sensors. For instance, Figure 2.11c, represents a hit arriving at sensor 2 first followed by sensor 1. The time difference between these hits can be calculated as:

$$\Delta t = \frac{d_2 - d_1}{C_{AE}}$$

(2.14)

where C_{AE} = calculated wave velocity

Δt = time difference between sensor

d_1 = distance from source to first hit sensor

d_2 = distance from source to second hit sensor

This is however, commonly expressed in terms of d_1

$$d_1 = \frac{D - C_{AE}.\Delta t}{2}$$

(2.15)

where D is the total distance between sensors. If the source originates from outside the array, Figure 2.11d, then the time difference measurement always corresponds to the time of flight between the outer sensor pair. The source will be located at the sensor at the edge of the array; in the case of the example, at sensor 1.

- **Two dimensions (2D) Location**

The same method can be used for 2D location. Figure 2.12 considers two sensors placed a distance of D apart on an infinite plane. If the stress wave from a source is assumed to propagate at a constant velocity in all directions, then it can be shown that:
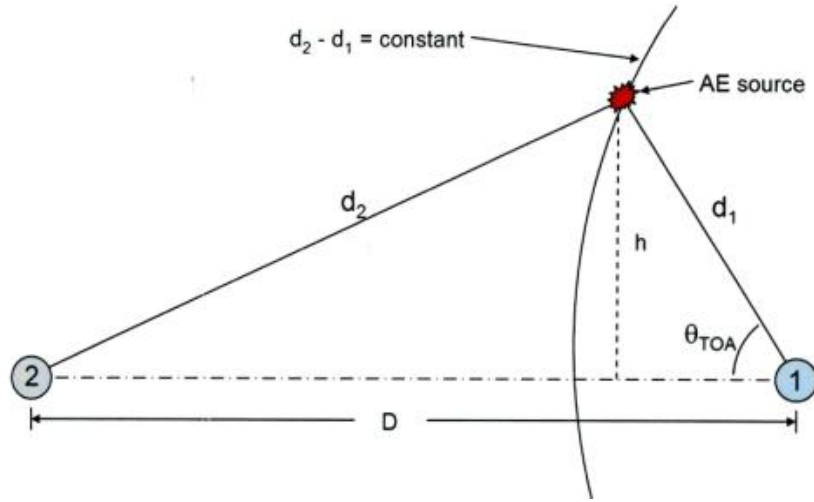
Figure 2. 12 D location on an infinite plate (Miller et al. 2005)

$$\Delta t.C_{AB} = d_2 - d_1 \tag{2.16}$$

and

$$h = d_1 \sin \theta_{TOA} \tag{2.17}$$

$$h^2 = d_2^2 - (D - d_1 \cos \theta_{TOA})^2 \tag{2.18}$$

then

$$d_1^2 \sin^2 \theta_{TOA} = d_2^2 - (D - d_1 \cos \theta_{TOA})^2 \tag{2.19}$$

$$d_1^2 = d_2^2 - D^2 + 2Dd_1 \cos \theta_{TOA} \tag{2.20}$$

Substituting $d_2 = d_1 + \Delta t.C_{AB}$ from equation 2.16 gives

$$d_1 = \left(\frac{1}{2}\right) \frac{(D^2 - \Delta t^2 C_{AE}^2)}{(\Delta t C_{AE} + D \cos \theta_{TOA})} \tag{2.21}$$
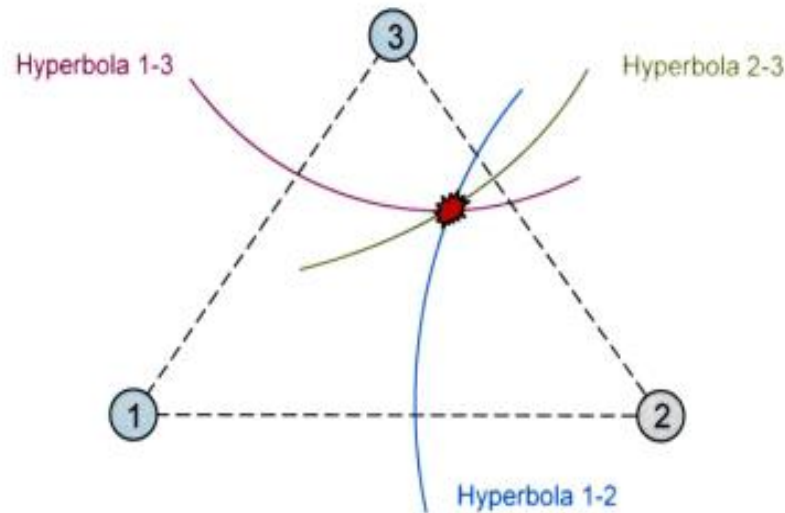
Figure 2. 13 2D location with three sensors (Miller et al. 2005)

This provides insufficient information to locate the source. However by adding a third sensor to the array as shown by Figure 2.13, it is possible to repeat this process for the three pairs of sensors 1-2, 2-3 and 1-3. The intersection point of three resulting hyperbola provides a more accurate 2D location. The adding of further sensors increases the number of hyperbola and consequently the accuracy and confidence of location.

2.4 The application of AE to concrete monitoring

According to Miller et al. (2005) the most significant application of acoustic emission to concrete started in the late 1970s when the primary technology, developed for metals, then it was modified to adapt heterogeneous materials.

Numerous researchers have shown that the AE monitoring technique can be applied to reinforced concrete applications such as bridges, viaducts, dams and buildings. By analysis of the resultant waveform in terms of feature data such as amplitude, energy and time of arrival, the severity and location of the AE source can be assessed (Hellier 2001 and Miller et al 2005). In concrete

research two primary areas of activity exist, application to structures and damage characterisation.

Successful applications of AE in dam structures have been demonstrated by Minemura et al. (1998), Bond et al. (2000) and Shiotani (2006). Furthermore the use of AE on concrete bridges has been reported by Nair (2010), Yuyama et al. (2007) and Yu et al. (2011). In addition, using AE to characterize the damage process of steel fibre reinforced concrete under bending was studied by Aggelis (2011), whilst classification of cracking modes in concrete were studied by Aggelis, (2011b) and Ohtsu (2010). Directly related to this work, the AE process was utilised to identify micro-macro fracture relationships in concrete by Landis (1999). Further investigations which identified the corrosion process in reinforced concrete have been demonstrated by Uddin et al. (2004), Ohtsu and Tomoda (2007) and Kawasaki (2010).

At Cardiff University, extensive research into damage assessment in concrete structures using acoustic emission has been carried out. This has been primarily reported by Beck (2004). These studies included identifying the most suitable sensor and method of attachment for optimum sensitivity for concrete structures, analysing laboratory-based concrete specimens using a Moment Tensor Analysis, source location of AE from fatigue cracks and the detection of damage within an in-service concrete hinge joint. Furthermore, the role of acoustic emission in the monitoring of laboratory-based and in-service reinforced concrete specimens and structures has been examined by Bunnori (2008). This research aimed to further the understanding of AE techniques for use in global and local structural monitoring of damaged reinforced concrete. It addressed an important aspect by determining the emissions associated with the onset of cracking and determined that this criterion can be used in a field test. Furthermore, some work into damage assessment in prestressed and reinforced composite concrete/mortar specimens using acoustic emission was performed. Recent work addressed the use of the AE technique to detect the early stages of corrosion prior to

deterioration of concrete structures. The results show that the onset of corrosion activity in wire in the interface between prestressed concrete and mortar as found in prestressed concrete pipes can be detected and located (Elfergani et al 2011). A novel analysis approach to this application has been used to evaluate differing crack types and the Kernel Density Estimation Function was used for better visualisation of the data (Elfergani et al 2012). The results show that the crack area and crack type can be identified and distinguished. In addition, further work performed by Elfergani et al (2013) shown that corrosion, macro cracks and crack propagation can be detected and distinguished.

An estimation of the fracture process zone size in concrete has been studied by Muralidhara (2010). Despite this research activity in concrete structures, only a few works for using AE techniques in prestressed concrete structures and composite concrete (mortar and concrete) currently exist. One study of the applicability of the acoustic emission technique for detecting corrosion of reinforced bar in concrete was performed by Zongjin et al. (1998). Their results demonstrated that there is a clear relationship between the AE events and reinforced bar corrosion in concrete.

A work has been interested in utilizing the AE technique to detect corrosion activities earlier than classical techniques such as Half-cell Potential Measurements and Linear Polarization Resistance (Leelalerkiet et al. 2005). Their experimental programmes show that the onset of rebar corrosion can be detected earlier using AE than other methods.

Idrissi and Liman (2003) performed a study utilizing AE combined with electrochemical methods. The electrochemical methods managed to evaluate the corrosive character of the medium used whilst the AE showed an activity characteristic of the corrosion initiation phase and the corrosion propagation phase.

Ing et al. (2005) applied AE methods to detect corrosion in a diverse range of reinforced concrete beams exposed to an accelerated corrosion current in the laboratory. It demonstrated the capability of the AE method for detecting reinforcement corrosion. In addition, it was shown that the AE method can easily identify the onset of corrosion prior to any visual damage being evident. Another study, performed by Ing (2003), showed that an acoustic emission technique is able to identify corrosion activity in concrete before conventional NDT techniques.

Beck (2004) reported extensive research into the damage assessment in concrete structures using the AE technique. The research included identifying the most appropriate sensor and technique of attachment for best sensitivity for concrete structures, analysing laboratory-based concrete specimens utilizing a Moment Tensor Analysis, source location of acoustic emission from fatigue cracking and the detection of damage within an in-service concrete hinge joint.

Bunnori et al. (2006a) carried out AE experiments on a reinforced concrete beam and slab, utilizing an artificial source to investigate the wave propagation in concrete structures over a diversity of source to sensor distances. In addition, an experimental programme to investigate the reinforced concrete structures behaviour when exposed to deterioration due to reinforcement corrosion by using AE monitoring was reported (Bunnori et al. 2006b). In this study, it was shown that AE has the ability to monitor the development of cracking in a concrete section. In addition, flexural cracking can be identified and located earlier than it can be visibly observed and its development under an increasing load can be traced.

Yuyama et al. (2007) carried out intensive studies in a laboratory for three kinds of beams post-tensioned by steel bar, strand and parallel wire cable to detect and locate the corrosion-induced failure by using AE monitoring. It was

found that important AE signals with very high amplitudes were detected when failures of bars and steel wires occurred. In addition, two highway bridges were monitored by the AE technique. It was found that AE is a very helpful method to detect and appraise failures of high-strength steel tendons in prestressed concrete bridges.

Another application of AE in prestressed concrete structure was performed by Ramadan et al. (2008). An experimental study was performed to monitor the stress corrosion cracking (SCC) of high-strength steel in pre-stressed concrete structures by AE. It demonstrated the presence of various stages related to crack initiation, crack propagation and steel failure respectively. Additionally, promising results for a potential in situ use of AE for real-time health monitoring of eutectoid steel cables utilized in prestressed concrete structures were demonstrated.

Studies on diverse laboratory loading tests of full scale models of real structural components have tried to relate observed AE characteristics to mechanisms of failure in pre-stressed or reinforced concrete (Othsu et al. 2002, Carpinteri 2007). However, only a few applications to real civil engineering structures like concrete buildings and prestressed concrete pipes have been reported.

Applying the AE method to estimate compressive failure in concrete samples using recycled aggregate has been performed by Watanabe et al (2007). They used RA values (rise time/ amplitude) and AF value (average frequencies counts/duration) to demonstrate the difference in failure mode behaviour and concrete mode with recycled concrete and that of normal concrete. It was further demonstrated that by AE monitoring in reinforced concrete and AE parameter analysis, the onset of reinforcement corrosion and the nucleation of corrosion cracking in concrete can be identified (Ohtsu and Tomoda 2007a, 2007b, Leelalerkiet et al. 2005).

Another study has been performed by Kawasaki et al. (2010) for applying the AE method to cyclic wet–dry tests of RC beams. It was confirmed that two periods of high AE activity coincided with the corrosion onset and the concrete cracking nucleation. Also, companion the of AE analysis with the Scanning Electron Micrographs of cross sections of the reinforcing bars showed that use of the AE method for monitoring the corrosion process in reinforced concrete structures has great promise.

To monitor the evolution of damage of concrete structure by using the AE method, Carpinteri et al. (2007) carried out a series of laboratory experiments on concrete specimens. He demonstrated that, based on an estimate of the amount of energy generated during fracture propagation, the criticality of the continual process can be observed via AE and therefore, the damage evaluation and the time of structure failure could be predicted.

AE behaviour of concrete under four-point bending was reported by Soulioti et al. (2009). It was demonstrated that AE parameters vary with the damage progress and can be utilized for the characterization of the failure process.

The applicability of AE methods for monitoring damage evolution in reinforced concrete beams strengthened in flexure with carbon fibre reinforced polymer (CFRP) sheets has been investigated by Yun et al. (2010). This study demonstrated that the acoustic emission method is an excellent non-destructive method to monitor the behaviour of reinforced concrete beams which are externally reinforced in flexure with CFRP sheets.

A study was performed by Wheat (2007) to determine whether the AE technique can offer more direct information about the extent of concrete damage. In this study, reinforced concrete specimens were exposed to salt water conditions as a function of time for one year and monitored by using

half-cell potentials, linear polarization resistance and AE technique. It was shown that the AE method is sensitive to cracks and crack propagation. It was further shown that by using AE it is possible to give indications of damage at earlier stages than traditional techniques.

Benin (2006) carried out experimental work to investigate deformation, crack generation, and fracture of reinforced concrete structures by using the AE technique. The study confirmed the potential of utilizing the AE method to investigate the kinetics of the accumulation of defects in reinforced concrete structures and theoretically predicting fracture when it is still unlikely to be detected on the basis of macroscopic observations.

2.4.1 AE Parameter analysis

AE parameter analysis is the fundamental method for identifying types of damage in a structure. It utilises features that describe the detected waveform. Typical parameters investigated include amplitude, energy, counts (number of threshold crossings), frequency, duration and rise time. According to many researchers (Aggelis 2011, Ohno and Ohtsu 2010, Ohtsu and Tomoda 2007, Soulioti et al 2009, JCMS-III 2003), the relationship between RA values (rise time/ amplitude) and AF value (average frequencies = counts/duration) can be used for classification of crack type in concrete structures. They reported that when an AE signal has low AF value and high RA value it is classified as shear type crack/movement. However when it has a high AF and low RA value is classified as tensile type crack as shown Figures 2.14 and 2.15. It should be noted that some researchers describe the shear movement as a shear "crack" but that this is not strictly correct; concrete will only crack under tensile forces and then move due to shear forces.
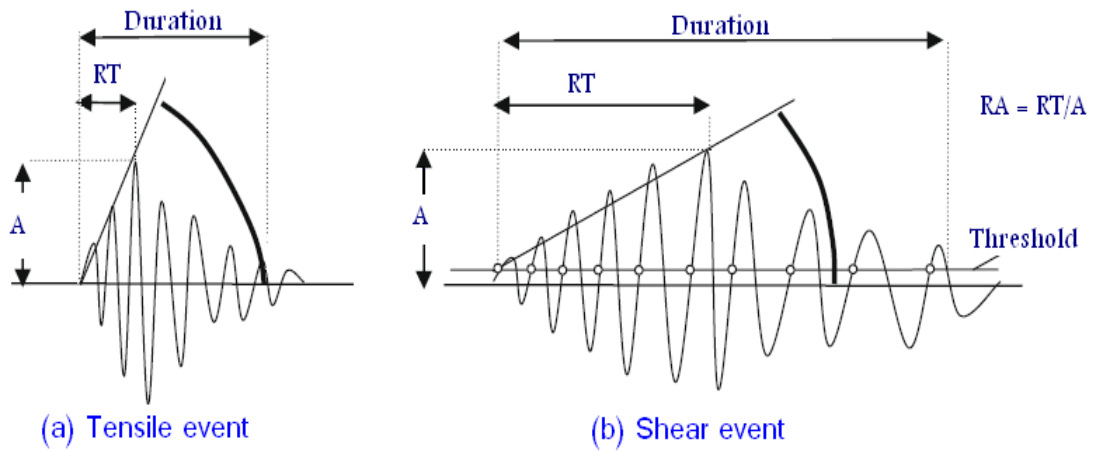
Figure 2. 14 Typical waveforms (Soulioti et al 2009)
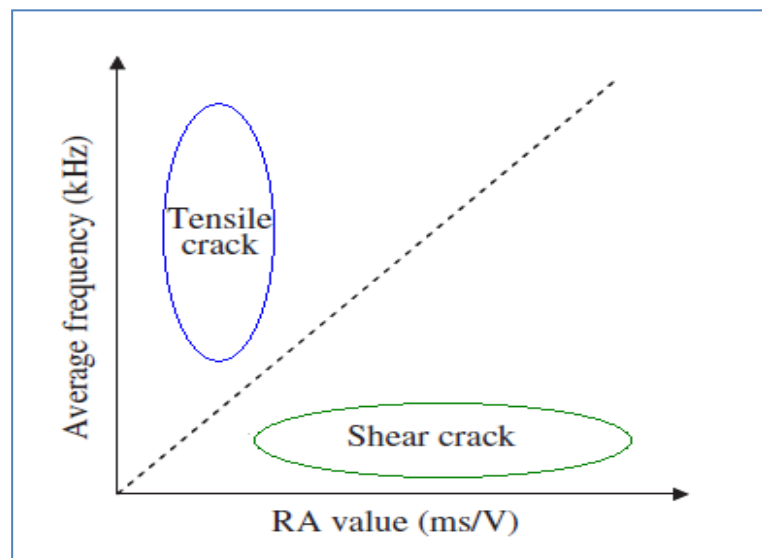
Figure 2. 15 Crack classifications (Ohno and Ohtsu 2010)

Furthermore, several works and studies on concrete fracture have shown that a single synthetic parameter, namely the b-value can be used to characterize fracture and damage growth (Carpinteri et al. 2009). The b-value is defined as the relationship between the number of AE events, N, and amplitudes, A, as

$$\text{Log}_{10}\,N = a - b\,\text{Log}_{10\,A} \hspace{4cm} (2.22)$$

Where a and b are empirical constants (Ohtsu and Tomoda 2007).

In the case that large scales of fracture are dominant then the b-value becomes small. Conversely, b-value is large when small scales of fracture are dominant (Aggelis 2011, Kawasaki et al 2010, Watanabe et al 2007). A size distribution of AE sources can be estimated by using the b-value. (Ohtsu and Tomoda 2007).

Moreover, crack kinematics on locations, types and orientations can be quantitatively determined by using moment tensor analysis (Uddin et al 2004, Ohtsu 1989).

2.5 Summary

In summary the literature review has shown that there is numerous research using AE techniques for monitoring laboratory-based reinforced concrete structure. However, there is limited research on prestressed concrete structures. Furthermore the prestressed and reinforced composite concrete/mortar structures are not covered well. Thus more work is required in this area. Furthermore, there is great potential in using the RA/AF approach for source characterisation.

The aim of this research was to further the understanding of the AE technique for use in global and local structural monitoring of concrete/mortar damage for the evaluation of prestressed concrete pipes and reinforced concrete structures and to provide improved techniques for source characterisation.

CHAPTER 3: PRELIMINARY EXPERIMENTAL STUDIES

3.1 Introduction

This chapter contains four main sections. The first section (3.3) details experiments to study the attenuation of AE waves from artificial sources through mortar in different directions; parallel, perpendicular and inclined (45° angle) to the wire direction over a variety of source to sensor distances.

Experiments were performed on reinforced concrete and mortar specimens using an artificial Hsu-Nelsen (H-N) source (ASTM, 1999). The second section (3.4) details an attenuation study through a composite wall (concrete, steel plate, and mortar) in order to determine the effect of the noise due to water flow inside a pipe on the externally mounted sensors. The third section (3.5) details a study of the acoustic emission from a concrete specimen loaded under tensile tests in order to promote only one type of crack signal. The fourth section (3.6) details a study of location accuracy using the Time of Arrival (TOA) method.

In all experimental tests, the method which was used to locate signals was the Time of Arrival (TOA) method (Miller and Mclntire 1987 and Rindorf 1981). This method is the simplest method for source location and is based on the arrival time of the source event at two or more sensors. When using this method, the wave velocity of the signals that propagate through the material needs to be determined.

3.2 Aims and objectives

The preliminary testing was undertaken to achieve the following:

- To investigate wave propagation and attenuation in composite material (concrete, reinforcing steel wire and mortar) over a variety of source-to-sensor distances.

- To investigate the attenuation of AE waves when propagating through the pipe structure.

- To identify the characteristics of AE signals gained from pure tensile cracks.

- To evaluate the location accuracy of the time of arrival method.

3.3 Study of propagation and attenuation along the structure

The heterogeneous nature of the composition of prestressed concrete cylinder pipe (e.g. concrete, mortar, aggregates, cracks, prestressing wire, the interface between concrete and mortar, steel plate, sand, and air voids) impacts the wave propagation by reflection and scattering causing a very complex wave field.

In order to study the impact of geometry on wave attenuation, experiments were performed on a composite of reinforced concrete by studying signal loss from artificial sources through the mortar in different directions; parallel, perpendicular and inclined (45° angle to the wire direction).

3.3.1 Experimental Procedure

• Concrete and mortar preparation

The concrete specimen (600×600×50mm), representative of the inner pipe, was prepared according to the technical specification for PCCP manufacturing used in GMRP, which is in accordance with AWWA C301-92 (Standard for Pre-stressed Concrete Pressure Pipe, Steel Cylinder Type, for Water and Other Liquids). Wires were placed on the upper surface of this specimen then the mortar 600×600mm and 20 mm thickness was coated on the upper surface of the concrete (The mortar consists of one part cement to not more than three parts fine aggregate by weight). The type of the cement which used is Portland cement CEM II/BV32.5R. The specimen was water cured for 28 days. The final construction is shown in Figure 3.1.

• **Acoustic emission set-up**

AE instrumentation typically consists of transducers, filters, amplifiers and analysis software. An AE sensor (R3I – resonant frequency 30 kHz) was mounted at the centre of the mortar surface (Figure 3.1). The AE sensor was mounted using silicon sealant and held in position until curing had occurred by a 0.5 kg weight mass. The AE system hardware was set-up with a threshold level of 40 dB. The sensitivity of the installed sensors was checked by using the Hsu-Neilson source (Hsu 1979).

Three lines were drawn; the first line was drawn parallel to the length of the wires from the sensor (centre) to the mortar edge then divided into six mark points 50 mm apart, a second line was drawn perpendicular to the wires from the sensor to edge, again with six positions at 50 mm centres. Finally a third line was drawn at a 45° angle to the wires from centre to edge. This was divided into eight points. The distance between these points was again 50 mm as shown in Figure 3.2.

In addition, a position located on the edge of the specimen was used to investigate the effect of out of plane waves in relation to the sensor position. Experiments were performed by using an artificial H-N source at the located marks on the three lines which were denoted as L, C and A respectively. The source was repeated five times at every mark and the signals were recorded.

Figure 3. 1 Concrete and mortar specimen
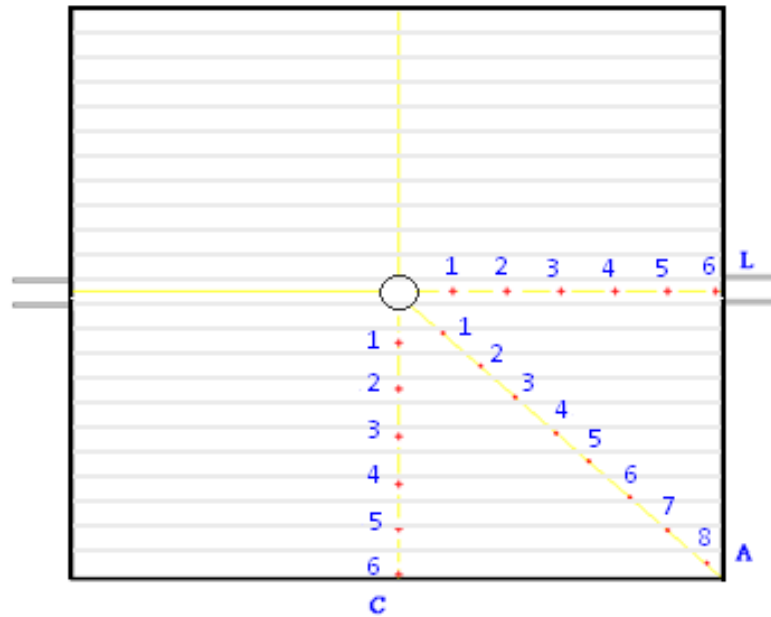
Figure 3. 2 Schematic Diagram of specimen

3.3.2 Results and Discussion

The average amplitudes detected from the H-N sources performed five times at every mark are shown in Table 3.1

Table 3. 1 Average amplitude of detected signal at varying positions

	dis.(mm)	L	C	A
		Amp.(dB)	Amp.(dB)	Amp.(dB)
1	50	100	94	96
2	100	97	92	93
3	150	93	91	92
4	200	90	89	89
5	250	90	89	86
6	300	95	96	93
7	350	-	-	89
8	400	-	-	87

Figure 3.3 shows the attenuation presenting the average amplitude in dB detected from H-N source versus distance from the sensor for waves propagating in three directions (L,C and A).
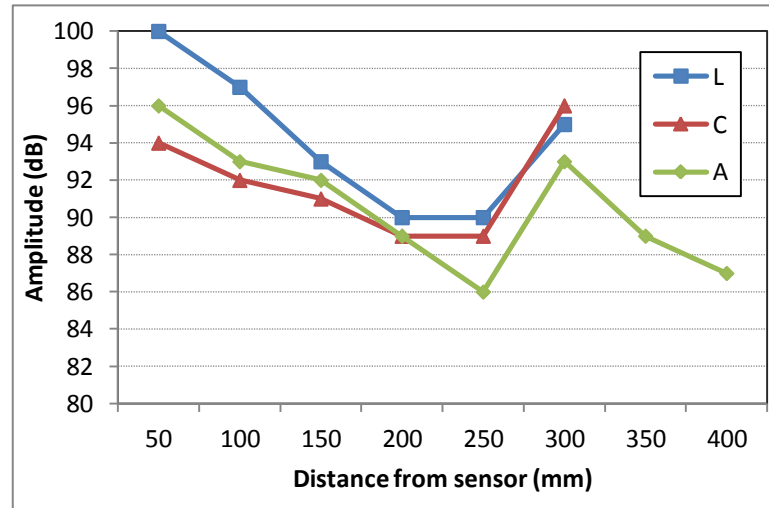
Figure 3. 3 Attenuation of signal with distance in three directions

It can be noted that the amplitudes decrease with distance from the sensor until 250 mm. However, the amplitudes increase significantly close to mortar edge (300mm from the sensor) due to the superposition phenomena which happens due to the combination of the main wave with edge reflections, as explained later in Figure 3.4.

It can be also seen from the plotted curves in Figure 3.3 that the amplitude of signals which have travelled parallel to the direction of the wire (L direction) are slightly higher than in other directions. This suggests the waves travel along the steel wire (with the wire acting as a wave guide) rather than mortar because the waves lose less energy when travelling through mortar.

Figure 3.4 (a, b, c and d) shows examples of waveforms recorded during the test within points L1, L3, L5 and L6. Figure 3.4 a, b and c displays example signals with the highest amplitude (100 dB), (93 dB) and (90 dB) gained from artificial sources on the mortar surface at 50 mm, 150 mm and 250 mm from the sensor parallel to the wire direction respectively. However Figure 3.4 d

displays the example for a superposition waveform with amplitude (95 dB) gained from artificial source on the mortar surface at a distance of 298mm from the sensor and 2mm from mortar edge.

(a) L1 (100dB)　　　　　　　　(b) L3 (93 dB)

(c) L5 (90 dB)　　　　　　　(d) L6 (95 dB) Superposition
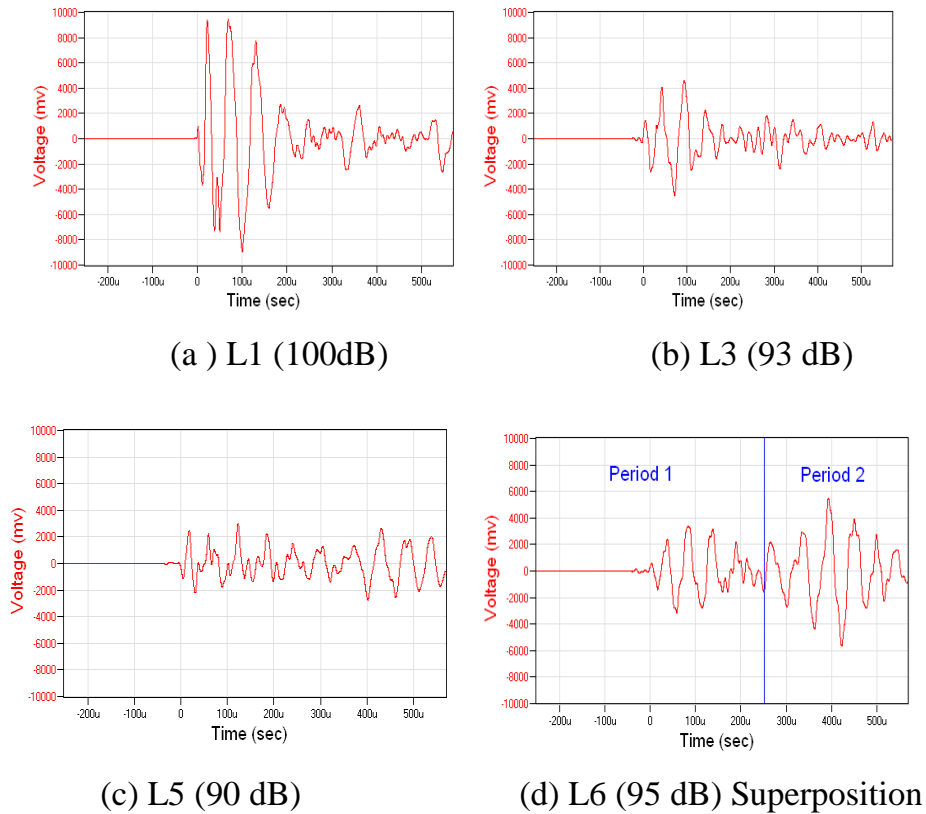
Figure 3. 4 Example waveforms

The difference between a wave with and without superposition is clearly evident as shown in Figure 3. 4 (d). The larger amplitude which is due to reflections from the edge of the specimen combining is seen in period 2 preformed based on the distance and wave velocity.

3.4　Study of attenuation through structure (pipe) wall.

In order to determine whether noise inside the pipe due to water flow would be detected by sensors on the outer face, experiments were performed by investigating wave propagation and attenuation through a thick composite specimen (concrete, steel plate, and mortar).

3.4.1 Experimental procedure

The specimen was manufactured as previously, however the dimensions were altered to represent the real dimensions of a pipe. These are shown in Figure 3.5.
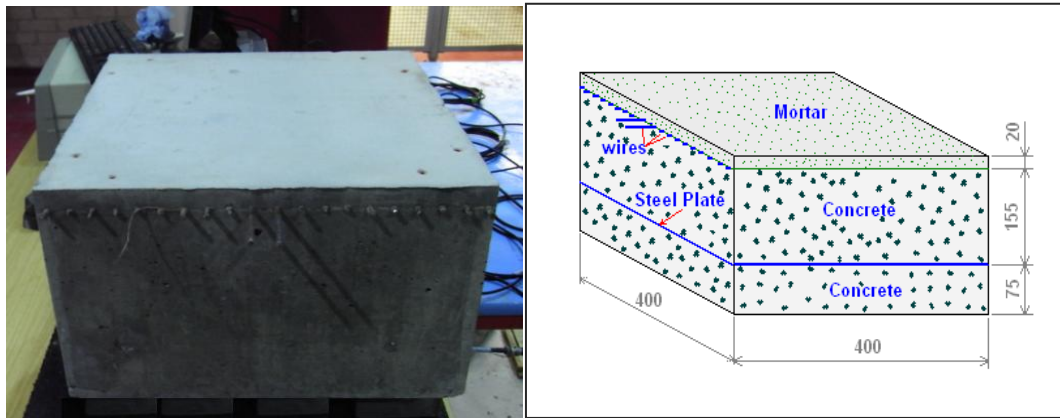
Figure 3. 5 Schematic Diagram and photo of specimen

Five AE sensors (R3I – resonant frequency 30 kHz) were mounted on the mortar surface. The AE sensors were again mounted using silicon sealant. The AE systems hardware was set-up with threshold level of 40 dB and the mounted sensitivity of the sensors was checked using the Hsu-Neilson source. The configuration of the specimen and sensors set up is given in Figure 3.6 Experiments were performed using an H-N source (ASTM, 1999) on the centre of the bottom surface of the concrete and repeated ten times for every test.
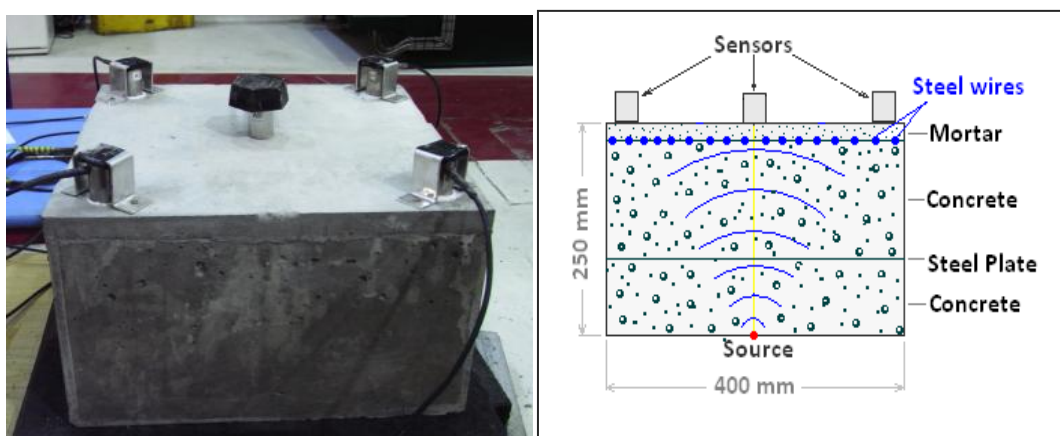
Figure 3. 6 Schematic diagram and photograph of specimen

3.4.2 Results and Discussion

Table 3.2 shows the average amplitude values obtained by sensors located on the centre of the upper surface of the mortar due to H-N sources on the bottom concrete surface; a distance of 250 mm from source. It is assumed that the amplitude of the source is 100 dB, as verified in previous sensor coupling verification tests.

Table 3. 2 Average amplitude received through wall

Test No.	Amplitude on the top surface of the mortar (distance 250 mm) (dB)	Attenuation (dB/250mm)
Test 1	76	24
Test 2	78	22
Test 3	77	23
Test 4	78	22
Test 5	77	23
Test 6	76	24
Test 7	77	23
Test 8	77	23
Test 9	78	22
Test 10	76	24
average	77	23

It can be clearly observed that the amplitude of the event declined dramatically (23 dB) from 100 dB to 77 dB through the distance of 250 mm compared with 10 dB decrease along the mortar at the same distance. as shown previously in Figure 3.3 and Table 3.1. The attenuation of the waves as they propagate through the composite wall of the pipe (concrete, steel plate, and mortar) is greater because the medium is more dispersive and highly damped due to both

the non-homogenous properties of concrete and signal reflection at the steel plate and at the interface between the concrete and the mortar. It is therefore suggested that the effect of the noise from the water flow would be insignificant given the degree of attenuation which the signals due to noise would be subjected to.

3.5 Study of AE arising from pure tensile cracks

In order to assess the proposed method for identifying the type of crack, it was necessary to undertake a further experimental investigation. In this section the details of two experimental tensile tests is presented. In order to achieve a pure tensile test on concrete, a bespoke specimen was designed.

3.5.1 Experimental Procedure

- **Specimen preparation**

The common problem when using the usual shape of sample (cylinder or prism) for uniaxial tension testing is that there is a stress concentration due to a mismatch between the Young's modulus and Poisson's ratio of concrete and steel when the steel loading plates are bonded onto the specimen. In order to avoid this problem, the specimen shape is designed as a dog-bone. Hence, the failure should occur in the narrow part of the specimen.

It was necessary to use a specimen geometry with a uniform tensile stress field over a large area which is unaffected by the loading arrangement, in order to observe the micro crack evolution (Benson 2003).

The dog-bone type shape as shown in Figure 3.7 ensures a central area in which the tensile stress is uniform and well defined.

Figure 3. 7 Concrete specimen

The dog-bone type shape has 740 mm length (500 mm of which is the spline), 100 mm width at the specimen's centre which increases gradually to 200 mm at the end of the spline and 35 mm thickness. Two specimens were prepared for testing. A combination of bonded plates and pinned plates was used to grip the specimen. This type of grip was adopted because it had proved effective previously (Benson 2003). A pair of plates was bonded, at both ends, using a commercial bonding agent (Sika bonding -Sikadur 31). In order to ensure that the adhesive had achieved its full strength, the specimens were left in the jig for 24 hours. These plates were pinned to a top plate which was attached to a coupling with a pin.

- **Test set-up**

A coupling was fixed on to a thick steel plate mounted on two I-beams. The top coupling was connected with the load cell attached to the actuator in the testing machine.

Two AE sensors (R3I – resonant frequency 30 kHz) were mounted to the centre of the mortar surface. The AE sensor was mounted using silicon sealant and fixed by adhesive tape. The AE systems hardware was set-up with threshold level of 40 dB and the sensitivity of the mounted sensors was checked by using the Hsu-Neilson source (Hsu 1979). The specimen was loaded gradually in tension and the AE system recorded the hits up to final failure. Figure 3.8 shows photographs of the specimen and the loading arrangement.

Figure 3. 8 Photographs of concrete specimen in the test machine

3.5.2 Results and Discussion

- **Test 1**

The variation of applied load against time is shown in Figure 3.9. The load was applied in two stages; in the first stage a rate of 0.002 mm/s was applied from the beginning until 310 sec and in the second stage the rate was decreased to 0.001mm/s until the failure in order to control the rate of crack growth prior to failure.

All the detected and located signals above a minimum amplitude of 45 dB detected by the two sensors for the whole duration of the tensile test are shown in Figure 3.10 as signal amplitude against time, while Figure 3.11 displays the same data set but this time as energy against time. The detected energy is attributed to a number of sources; micro and macro tensile cracking and load machine noise and specimen failure. It can be seen that the first hits occur before 100 seconds which the applied load reaches 2kN and the final failure occurred at 12.74 kN (543 sec).
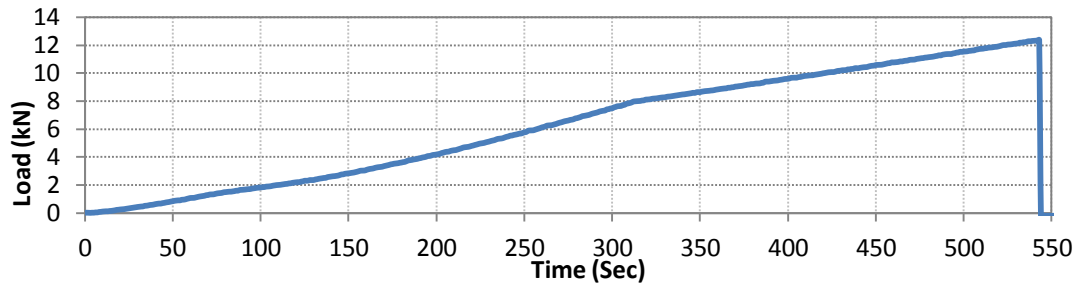
Figure 3. 9 Applied loads vs. Time
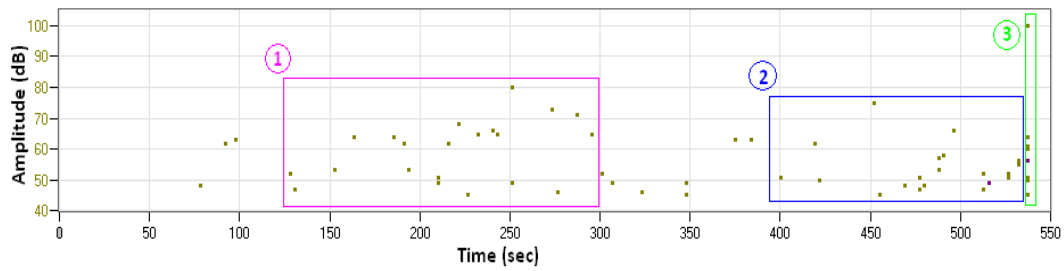
Figure 3. 10 Amplitude vs. Time
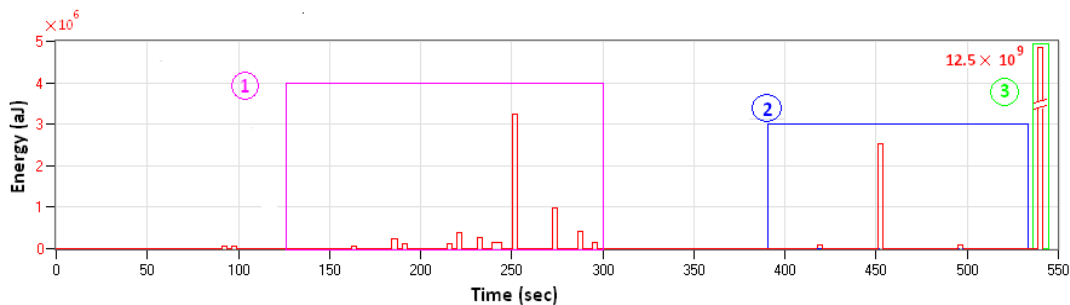
Figure 3. 11 Absolute energy vs. Time

It can be seen that in Figures 3.10 and 3.11 there are three significant periods of AE. Period 1 may be attributed to the energy release from the loading machine because no evidence of micro cracks was visually observed at this time. The emission in period 2 is attributed to micro crack and dislocation in the specimen from visual observation. It should be noted that period 1 has slightly more AE activity but this is attributed to higher load rate during that period. The highest energy and highest amplitude in a short time in period 3 corresponds to the formation of a tensile macro cracks and specimen failure.

Figures 3.12 (a, b and c) show the relationship between the RA value and average frequency of the three periods. Figure 3.12 (a) shows the relationship between RA value and AF for period 1 which is associated with the early period of the test before any crack occurred. It can be seen that most of the data points have wide RA value (RA values 0-25 ms/v) and with low AF values (less than 20 kHz). Figure 3.12 (b) shows the relationship between RA value and AF for period 2 associated with the period directly before failure. It can be seen that there is a tendency for the data points have a narrower range of RA values with higher AF values. However Figure 3.12 (c) represents the relationship between RA value and AF for period 3 the failure period. It can be noted that in this period the most of the data points have various AF and low RA value (less than 5 ms/v).

(a)

(b)

(c)
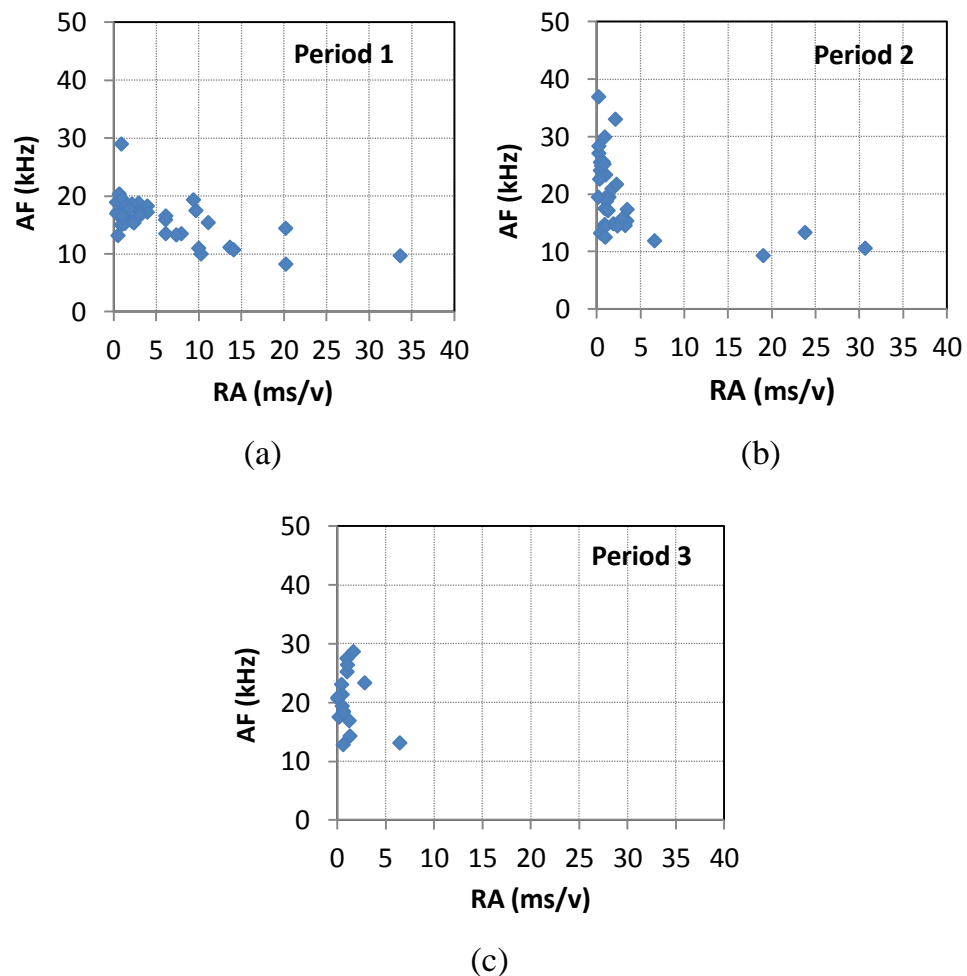
Figure 3.12 Relation between the RA value and average frequency of
(a)Period 1, (b) Period 2 and (c) Period 3

The location of signals with minimum amplitude of 45 dB for the whole period of the test is shown in Figure 3.13 as signal amplitude vs. position and Figure 3.14 displays the same data set but this time as energy vs. position. Figure 3.15 is a photograph of the mortar specimen after the end of the test, showing the crack location and crack shape.
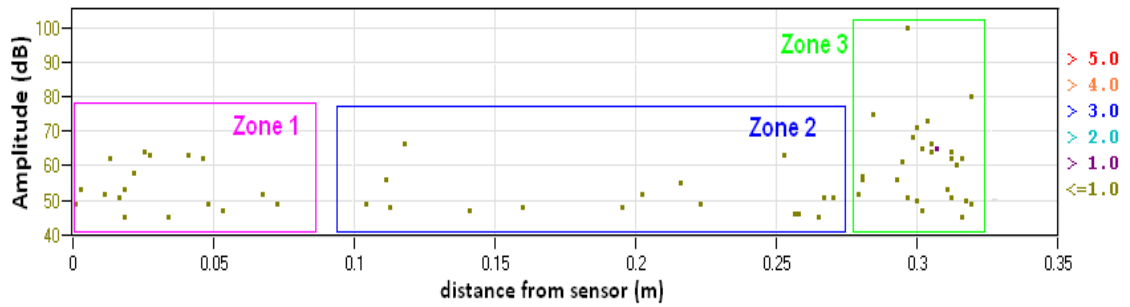
Figure 3. 13 Amplitude vs. liner location vs. Hits
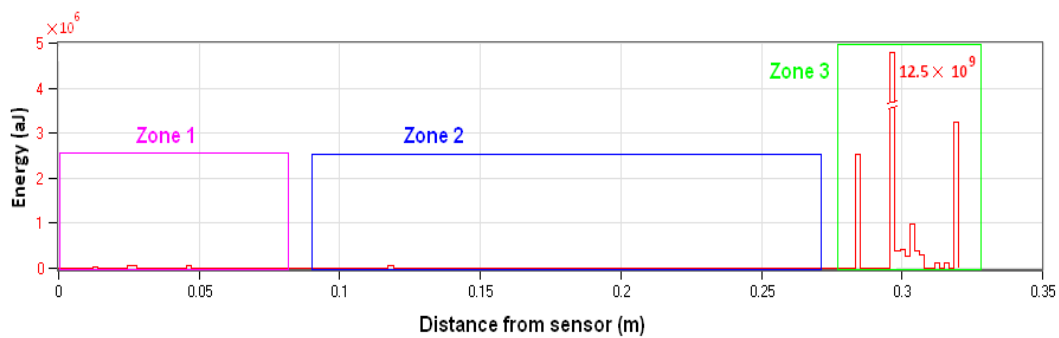
Figure 3. 14 Absolute energy vs. liner location
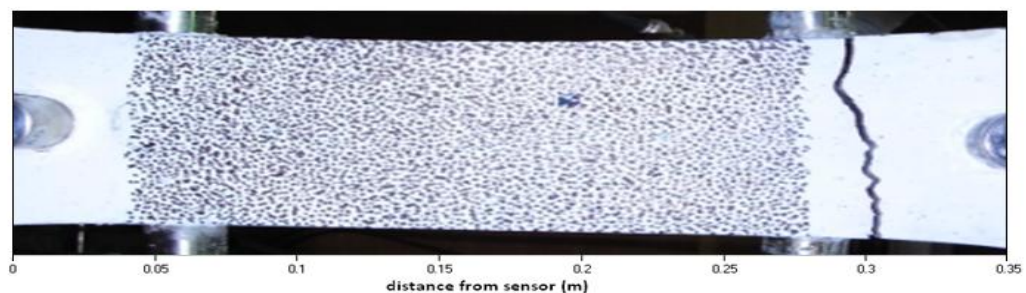
Figure 3. 15 Photos of specimen after failure

It can be noted that there are three zones in Figure 3.13 and 3.14. In zone 1 and 2 there are a small number of hits, low amplitude and with very low energy. By comparing with Figure 3.15 these zones are corresponding to areas with no crack. Zone 3 has higher hits concentration, high amplitude and

highest energy and coincides with the location of the crack which was visibly observed post test as shown in Figure 3.15.

Figure 3.16 (a, b and c) show the AF vs. RA values for the different three regions. Figure 3.16 (a and b) show the AF vs. RA for zones 1 and 2 which are associated with the no crack regions. It can be noted that in these areas the RA value have a wide distribution (RA values 0-35 ms/v). Figure 3.16 c shows the relationship between RA value and AF of zone 3 associated with the tensile crack type region. It can be seen that the most of data points have various AF and low RA value (less than 3 ms/v).

(a)

(b)

(c)
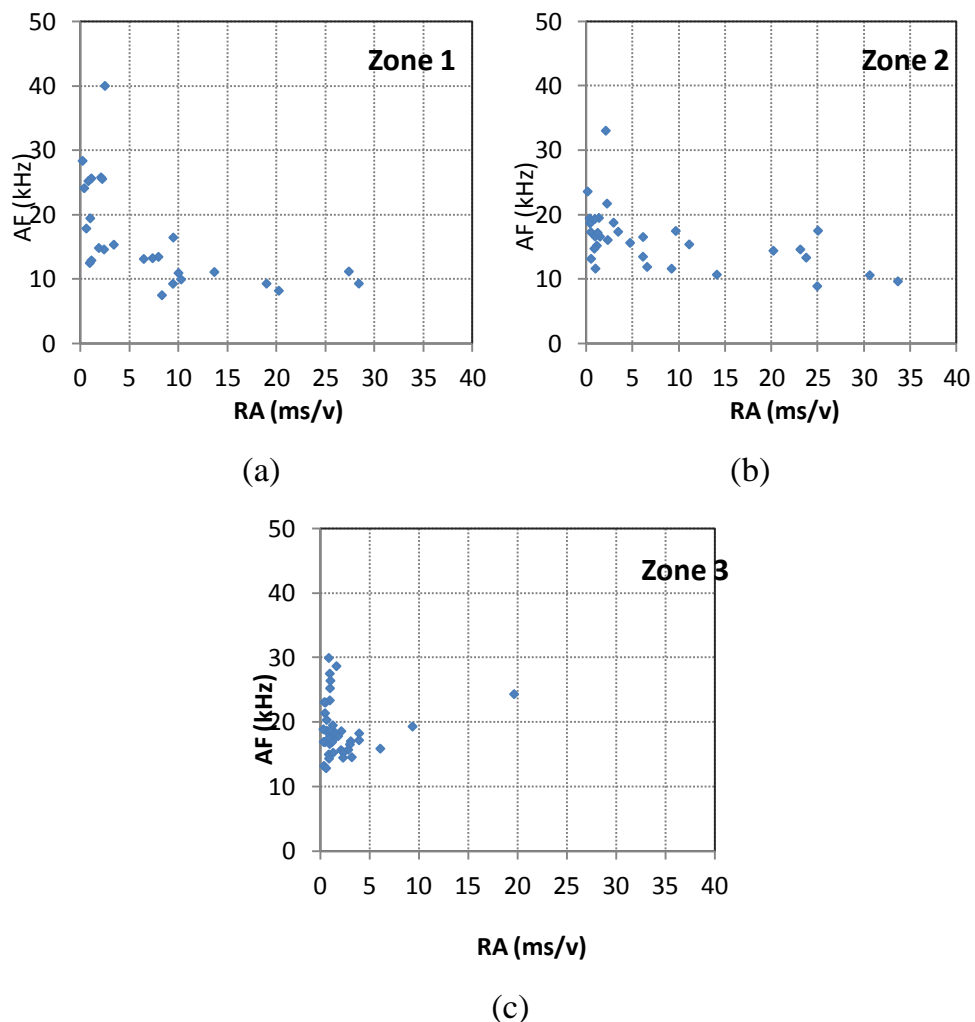
Figure 3. 16 Relation between the RA value and average frequency of (a)zone1, (b) zone2 and (c) zone3

- **Test 2**

Similar behaviour was observed in test 2. The variation of load applied against time is shown in Figure 3.17. The applied load was started with small rate (0.001 mm/s) until 250 sec then increased (0.002 mm/s).
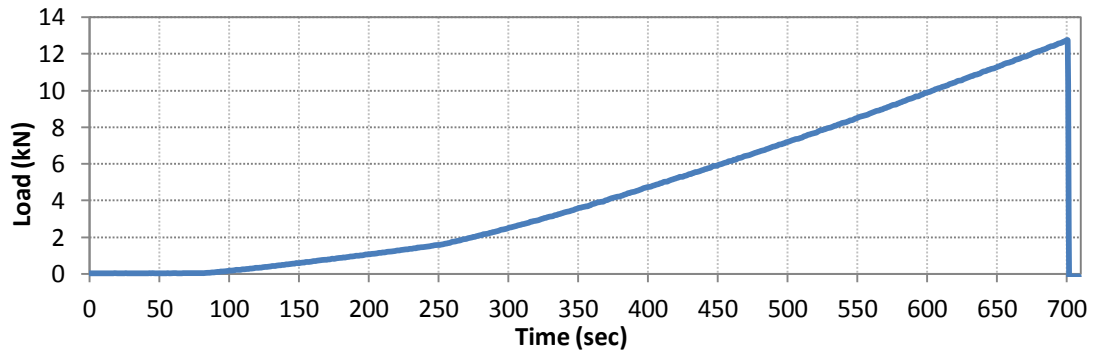
Figure 3. 17 Applied loads vs. Time

All the detected and located signals above a minimum amplitude 45 dB detected by two sensors for the whole duration of tensile test and continuous monitoring are shown in Figure 3.18 as signal amplitude against time, while Figure 3.19 displays the same data set but this time as energy against time. The detected energy is attributed to a number of sources; macro cracking, load machine noise and specimen failure.

It can be seen that the first hits occur before 300 seconds when the applied load reaches 2kN and the final failure occurred at 12.74 kN (695 sec).
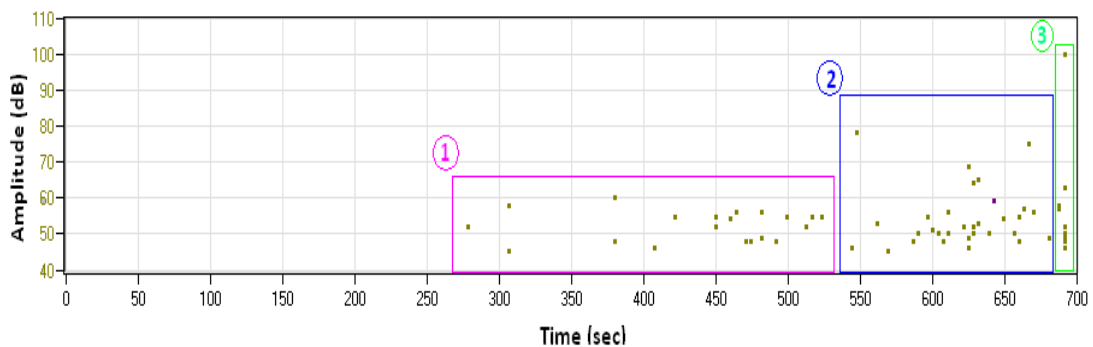
Figure 3. 18 Amplitude vs. Time
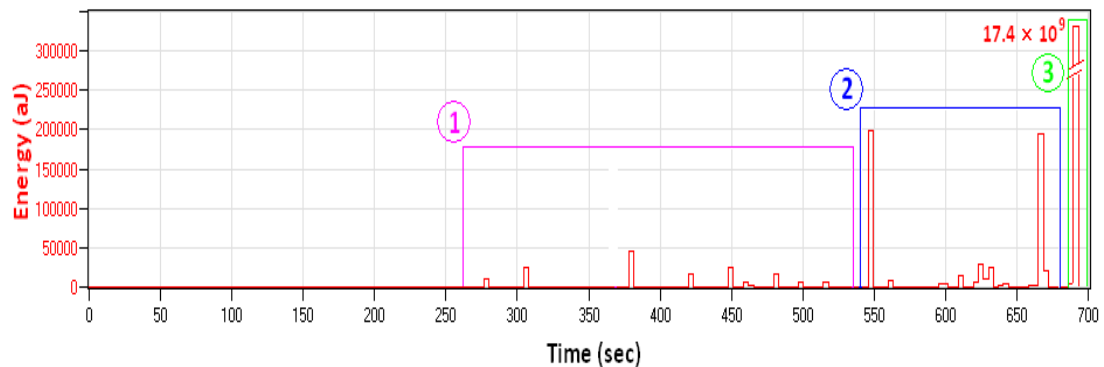
Figure 3.19 Absolute energy vs. Time

Figures 3.20 (a, b and d) show the relation between the RA value and average frequency of three periods.

Figure 3.20 (a) shows the relation of RA value and AF value in period 1 associated with the early period of the test before any crack occurred. It can be seen that the most of data points have broad RA value (RA values 0-25 ms/v) and with low AF values (less than 20 kHz) and Figure 3.20 (b) shows the relationship between RA value and AF in period 2 associated with the period directly before failure.

It can also be seen that there is a tendency for the data points to have narrower RA values and with higher AF values. Figure 3.20 (c) represents period 3 which is the failure period. It can be noted that in this period that most of the data points have various AF and very low RA values (less than 5 ms/v) which is termed a "vertical trend". Therefore, based on Figure 2.5 (in section 2.4.1) this indicates that the type of the crack is pure tensile.

It can be seen that the results in Figures 3.20 (a, b and c) exhibit very similar behaviour as those in Figures 3.12 (a, b and c) in test 1.

(a)

(b)

(c)
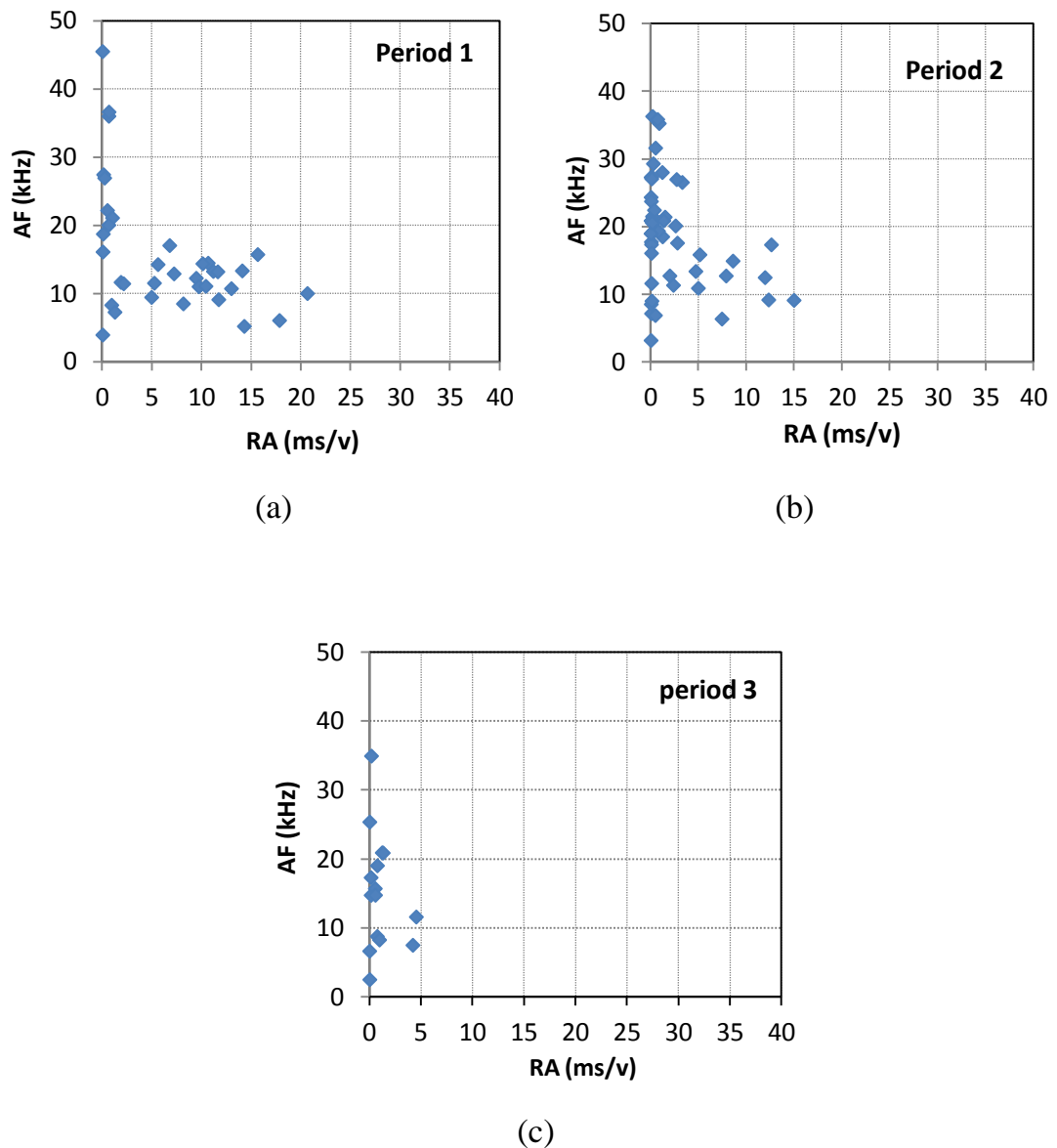
Figure 3. 20 Relation between the RA value and average frequency of
(a) period 1, (b) period 2 and (c) period 3

3.6 Preliminary location studies

It is important to know the effectiveness and accuracy of using the Time of Arrival (TOA) method in a concrete-mortar structure. This section presents details of a series of experimental tests performed to study location accuracy using this method on a series of concrete-mortar medium (400×400mm) and large (600×600) specimens.

3.6.1 Experimental Procedure

A concrete specimen (400×400×230mm – termed a medium size specimen) with a steel plate (400×400×1mm) was cast. Wires were placed on the upper surface of this specimen then the mortar 400×400mm and 20 mm thickness was coated on the upper surface of the concrete (The mortar consists of one part cement to not more than three parts fine aggregate by weight). The specimen was water cured for 28 days. The final construction is shown in Figure 3.21.

Figure 3. 21 Schematic diagram and photograph of specimen

Four AE sensors (R3I – resonant frequency 30 kHz) were mounted to the mortar surface as shown in Figure 3.22.

The AE sensors were mounted and systems hardware was set-up as detailed in previous section (3.4.1).
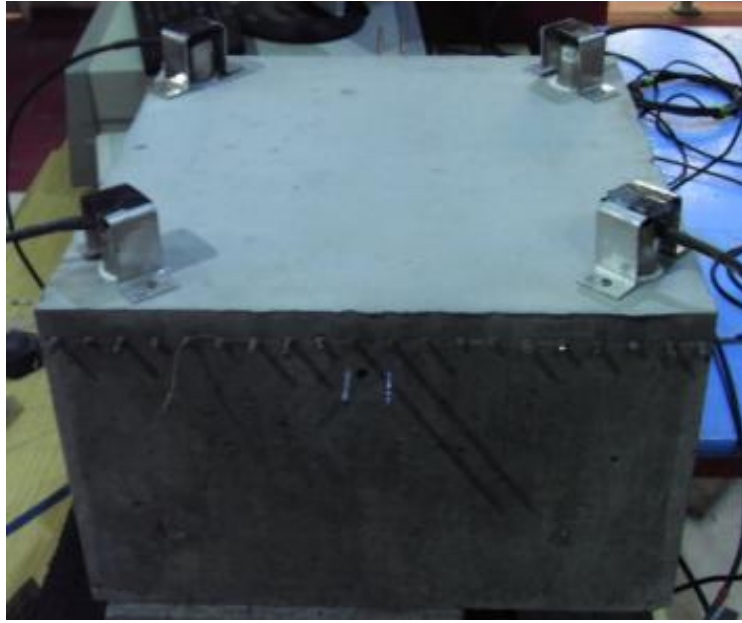
Figure 3. 22 Photograph of specimen with sensors setup.

Several experiments were performed using the H-N source (ASTM, 1999) on marked points at different locations on the upper surface of the mortar. Six sources were performed at every point. The locations of the H-N sources and sensors on upper mortar surface are shown in Figure 3.23.
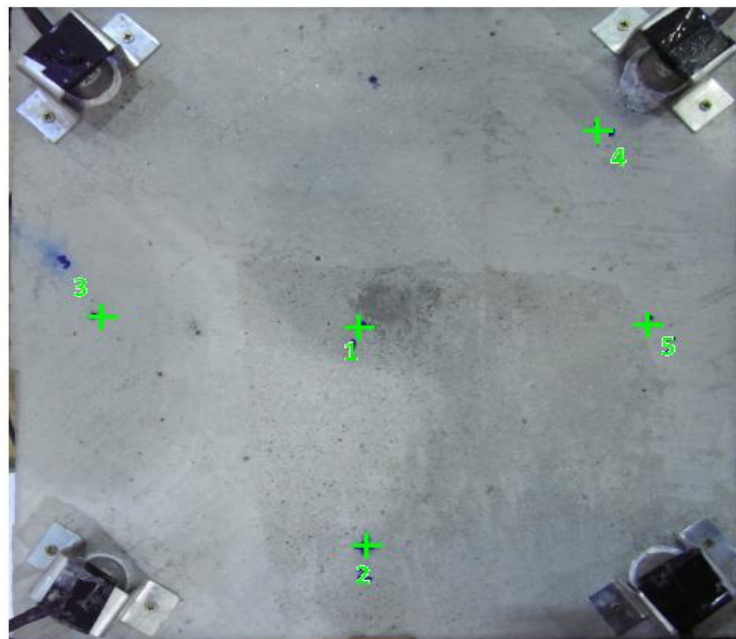
Figure 3. 23 Schematic Photo of specimen with five artificial source locations.

3.6.2 Results and Discussion

The location of signals above the minimum amplitude 40dB for six artificial source events at five different points is shown in Figure 3.24 (a and b). Figure 3.24 a displays planar location of the events including their absolute energy and Figure 3.25 b displays planar location of the events including their amplitudes.
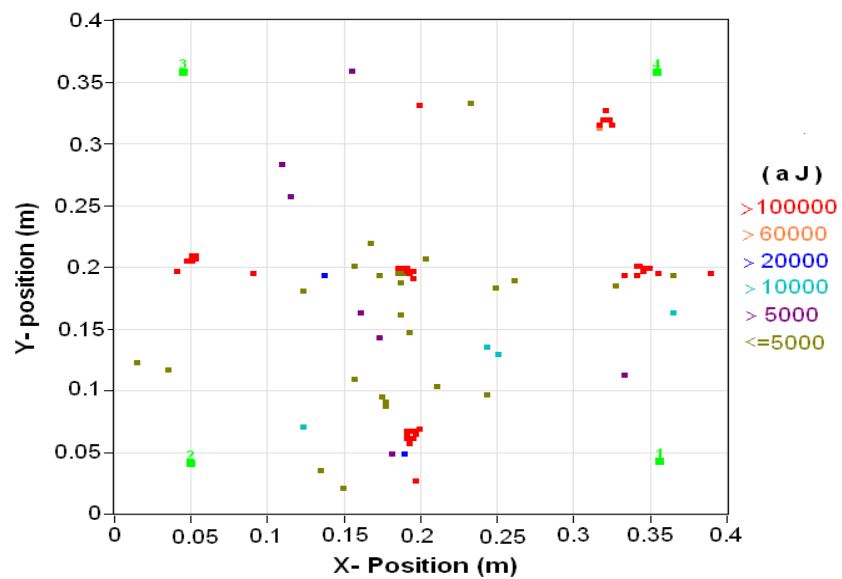
(a)
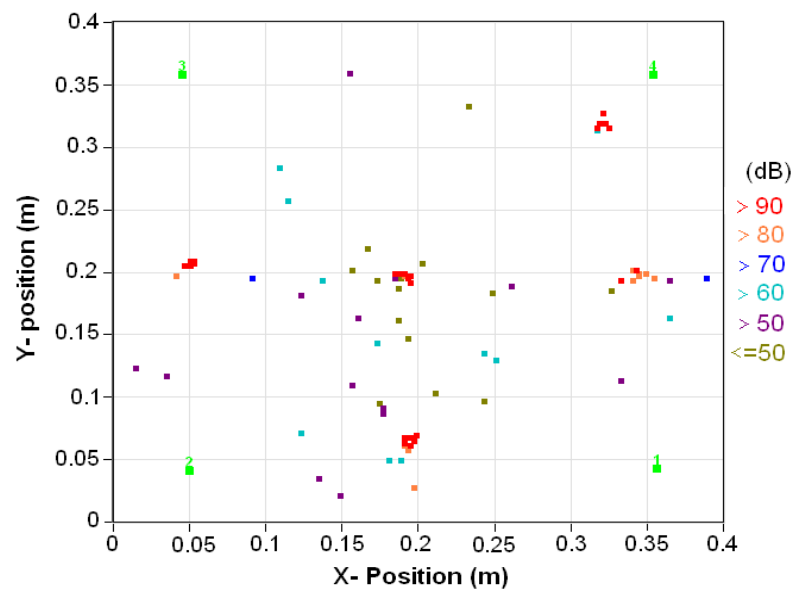
(b)

Figure 3. 24 Planar location of events with (a) Absolute energy (atto joules) (b) Amplitude (dB)

The location of events in Figure 3.24 a can be compared with Figure 3.23 which displays the planar location of sources on surface mortar in one Figure as shown in Figure 3.25.
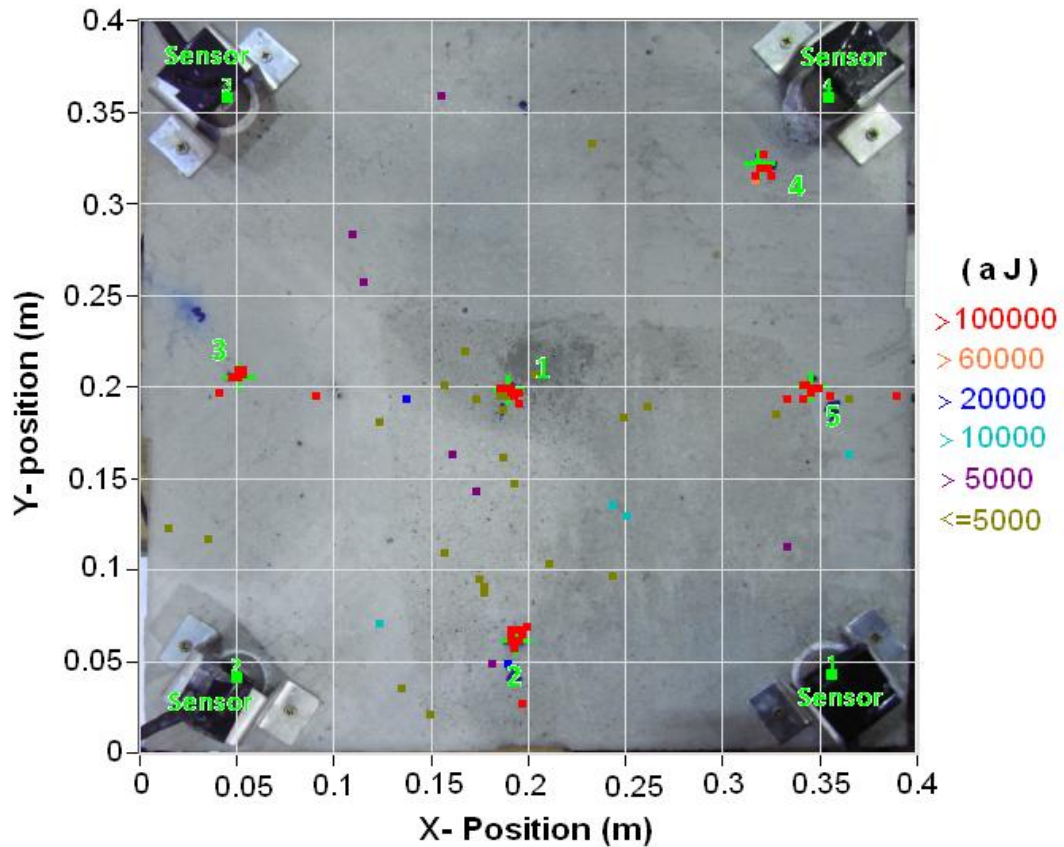
Figure 3. 25 Comparison of the H-N source location points with energy of events location

Figure 3.25 shows a comparison of the location of H-N source points on the mortar surface with the energy of events located determined using TOA. It can be seen that highest hits concentration and highest energy in the region coincides with the artificial source location marked as a green cross. However, there are some hits with low amplitude and low absolute energy distributed across the surface. These hits could be attributed to noise such as separation of the mortar from the concrete and shrinkage in concrete or mortar as observed in other investigations.

3.7 Conclusion and Summary

In this chapter, laboratory –based tests were conducted, it can be concluded that:

3.7.1 Study of propagation and attenuation along the structure

- Propagation of the elastic waves in the concrete-mortar structure is affected by the wire direction in the sample. This needs to be taken into consideration when mounting the sensors and locating the crack in the pipe.

- The wave propagation through the concrete-mortar specimen is faster along the wire length when compared with other directions, suggesting that the wave travels along the steel wire, possibly acting as a wave guide.

- The attenuation through the mortar is less than that through the concrete.

3.7.2 Study of attenuation through structure (pipe) wall.

- Attenuation of the elastic waves in crossing the concrete-mortar wall of the pipe is very high and is affected by the complex nature of the concrete, steel plate, and concrete-mortar interaction.

- The reason for high attenuation is complex, due to several factors such as waves passing through different medias, scattering on aggregate and, reflections on the steel plate and/or concrete-mortar interface.

- Since the attenuation of waves through the thick composite wall is high, the noise effect inside the pipe due to water flow in the real application is considered to be very small.

3.7.3 Study of AE a rising pure tensile cracks

- Tensile cracks can be identified and distinguished from other sources using the RA/AF value.
- Tensile type crack have small RA value (less than 5 ms/v).

3.7.4 Preliminary location studies

- The TOA method can be used effectively to locate signals on concrete/mortar specimen and has acceptable accuracy, the average error is approximately 6 mm for this sample.

CHAPTER 4: LABORATORY TESTING SMALLPRESTRESSED AND REINFORCED CONCRETE SPECIMENS

4.1 Introduction

This chapter demonstrates the use of acoustic emission (AE) to monitor and assess stages of damage of prestressed and reinforced mortar/concrete specimens induced by steel wire corrosion. A detailed description of the experimental work performed and the procedures followed are given. The materials, the initial casting and preparation of the specimens and test setup are described.

Laboratory tests were performed on a number of prestressed and reinforced concrete specimens. However, in this chapter, two tests for prestressed specimens and one of reinforced specimen are explained in detail, because they are indicative of all the other tests. However an overview of the main test results for all specimens is provided in Appendix A.

The data analysis involved the use of AE parameters such as hits, energy and location, corroborated by visual inspection as well as a study of the relationship between AF and RA values. Kernel Density Estimation (KDE) was used to visualise these results.

4.2 Aims and objectives

The aims and objective of these experiments using parameter analysis were:

- To assess the ability of AE to detect and locate damage areas at a very early stage in representative specimens due to corrosion.

- To investigate these areas in order to determine the presence of initial cracks which cannot be seen by visual inspection.

- To investigate, distinguish and classify the detected crack types.

- To investigate and distinguish active corrosion.

- To investigate and distinguish micro cracks, macro cracks, crack propagation and wire failure.

4.3 Prestressed concrete specimens Tests

4.3.1 Experimental procedure

The experimental program contains five key stages; development of a tension holding frame, wire preparation, concrete and mortar preparation, accelerated corrosion and AE monitoring for two prestressed specimens.

- **Tension holding frame**

Since it was intended in this work to simulate as close as possible the real physical conditions surrounding the high strength steel wires in concrete pipes, it was prudent to place and maintain all relevant wire samples under tension equal to 60% of their ultimate tensile strength in prestressed concrete cylinder pipe (PCCP). To achieve this objective a tension frame was especially designed and fabricated.

The frame consisted of two blocks (190mm x 45mm x 45mm) and two threaded steel bars (studding) having a diameter of 20 mm and a length of 500 mm. Two holes (20 mm diameter) and two (6mm) were drilled in each block. Figure 4.1 shows a schematic drawing for the tension holding frame. The two blocks were assembled via two threaded bars tightened by means of eight nuts.
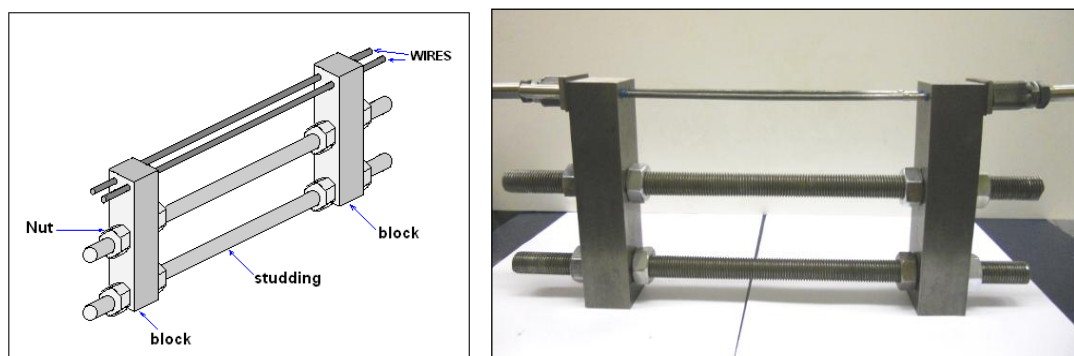
Figure 4. 1 Tension holding frame

- **Wire preparation**

The two working high strength steel wires samples were supplied from GMRP PCCP manufacturing plant in Libya. The metallurgical composition and mechanical properties as certified by the wire manufacturer can be summarised as follows:

Carbon steel (carbon 0.8-0.84%, 0.85-1.00%Mn, 0.030 %Max S, 0.035% Max P, 0.20-0.35% Si) (ASTM A663/A663M-88a). Typical mechanical properties are presented in Table 4.1.

Table 4. 1 Typical Mechanical Properties of Prestressing Wires

Tensile Strength	U.T.S (MPa)		Reduction in Area
Min(MPa)	Min	Max	Min (%)
1738	1736	1940	35

Three tensile tests were performed to confirm these mechanical properties. In addition, three tensile tests were carried out on the wires and using two strain gauges for every wire to plot the relationship between load and strain to determine the strain equivalent for the required load. Figure 4.2 shows the load-strain curve of one of these tests.
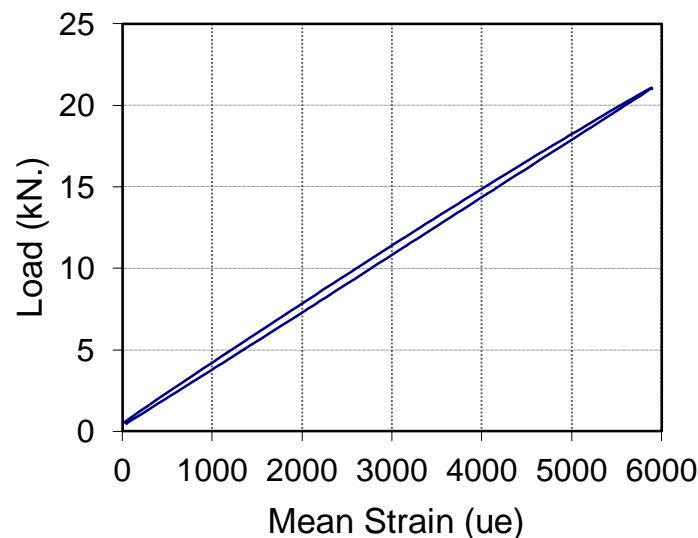
Figure 4. 2 Load-strain curves

The two working wire samples were passed through the 6 mm diameter holes which are in every two steel blocks and then two modified bolts and nuts, which are designed to control the tension load of every wire. Next, both ends of every wire were grasped via compressing a thick steel cylinder (12.5 mm outer diameter and 5 mm inner diameter). Figure 4.3 shows a schematic diagram and a photograph of the device. Three tests were carried out to ensure the effectiveness of this device.

Each monitored wire was subjected to a tensile force of 20 kN by adjusting the bolts and nuts and via the strain gauges mounted on the wires to monitor the strain.
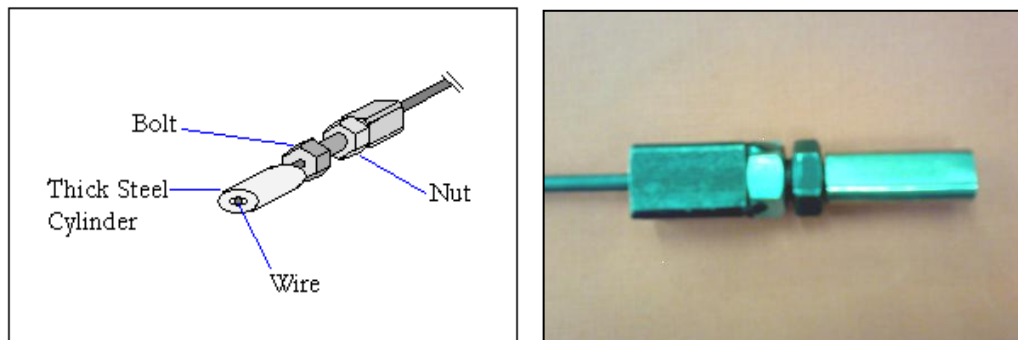
Figure 4. 3 Modified holed bolt and nut

- **Concrete and mortar preparation**

The concrete specimen (200×200×50mm) was prepared according to the Technical Specification for prestressed concrete cylinder pipe manufacturing used in the (GMRP), which is in accordance with AWWA C301-92 (Standard for Pre-stressed Concrete Pressure Pipe, Steel Cylinder Type, for Water and Other Liquids). The type of the cement which used is Portland cement CEM II/BV32.5R. The water to cement ratio used was 0.4 and the material proportions were 1:2:2.5:0.4 by weight of cement, sand, aggregate and water respectively and the concrete design strength was a 57.6MPa strength at 28 days. Three days later, when the concrete specimen had completely cured, the wires combined with their holding frame were placed on the upper surface of

this specimen. The mortar 200×200mm and 20 mm thickness was coated on the upper surface of the concrete encasing the wires. The water to cement ratio used was 0.4 and the material proportions were 1:2:0.4 by weight of cement, sand and water respectively and the concrete design strength was 56MPa strength at 28 days. The mortar should consist of one part cement to not more than three parts fine aggregate by weight. The construction is shown in Figure 4.4.
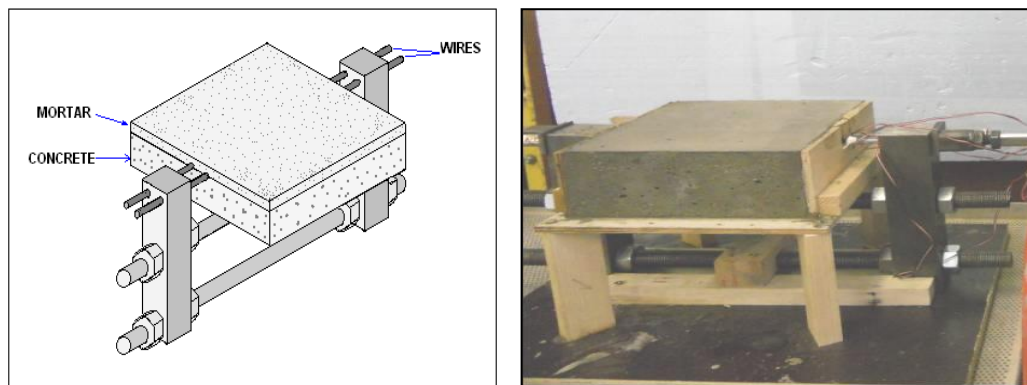
Figure 4. 4 Concrete and mortar specimen

- **Accelerated corrosion Technique**

To study the effects of corrosion within a realistic time-scale, it is sometimes necessary to accelerate the initiation period and occasionally control the rate of corrosion during the propagation stage. To simulate the corrosion of prestressing steel wires, the corrosion cell was induced by an impressed current (100µA/cm²). This is reported as corresponding to the maximum corrosion rate for concrete in laboratory conditions and has been used by several researchers in the laboratory as discussed by Li and Zhang (2008).

In this experimental work, wire corrosion was induced by impressed current (500µA/cm²). The prestressed wires were contacted in an electrical circuit with the positive pole of the power supply and the negative pole connected with a stainless steel plate (30×150 mm) resting on the upper mortar surface. A 4% NaCl solution was poured on the surface of the mortar. Silicon sealant was used to pool the solution on the upper surface (Elfergani et al. 2011).

- **Acoustic Emission Set-up**

AE instrumentation typically consists of transducers, filters, amplifiers and analysis software. Four AE sensors (R3I – 30 kHz resonant frequency) were mounted on the surface of the mortar. The experimental test set up is shown in Figures 4.5 and 4.6.
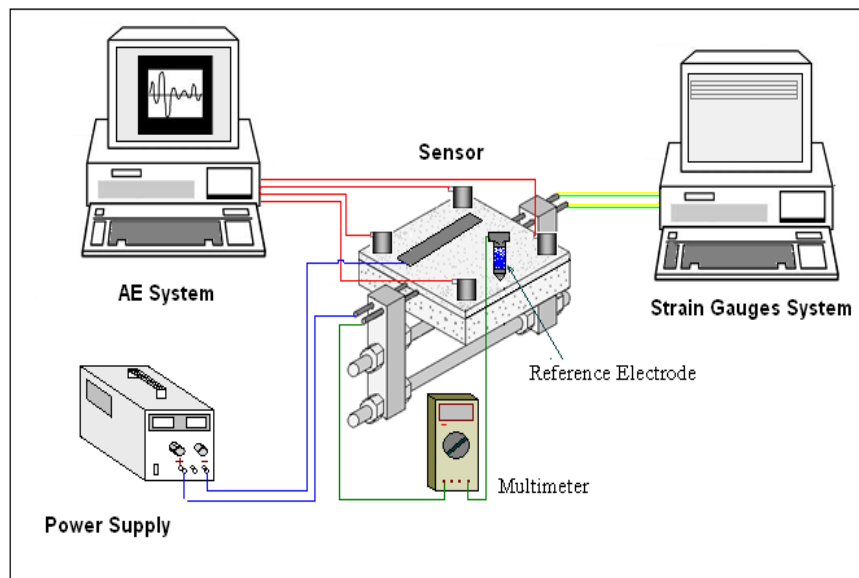
Figure 4. 5 Experimental set up
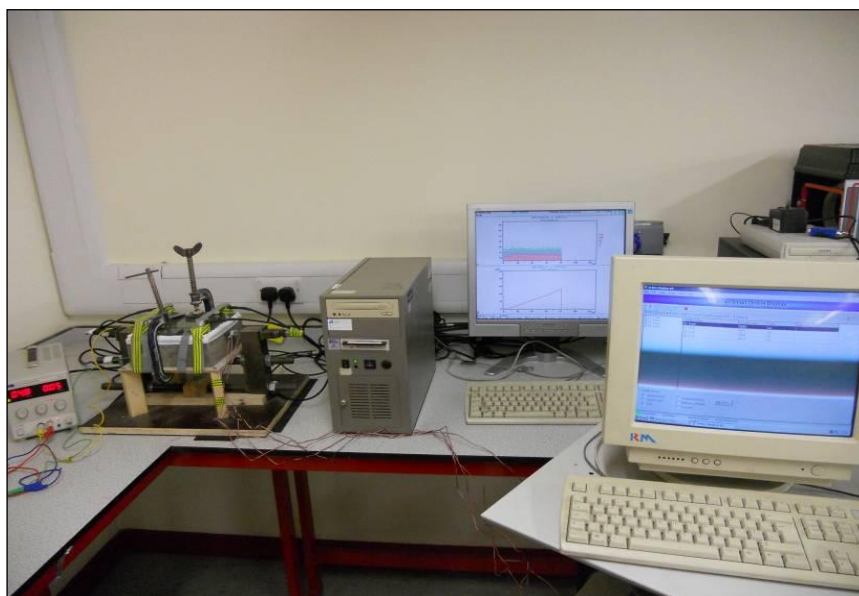
Figure 4. 6 Photograph of Experimental Set up

The four AE sensors were mounted using silicon sealant as an acoustic couplant and were fixed on the upper surface of mortar with a U shaped plate attached with screws holding the sensors and to ensure a good coupling as shown in Figure 4.7. The threshold level for AE data acquisition was set up at 40 dB. The sensitivity of the sensors was checked by using the Hsu-Neilson source (Neilson 1980).
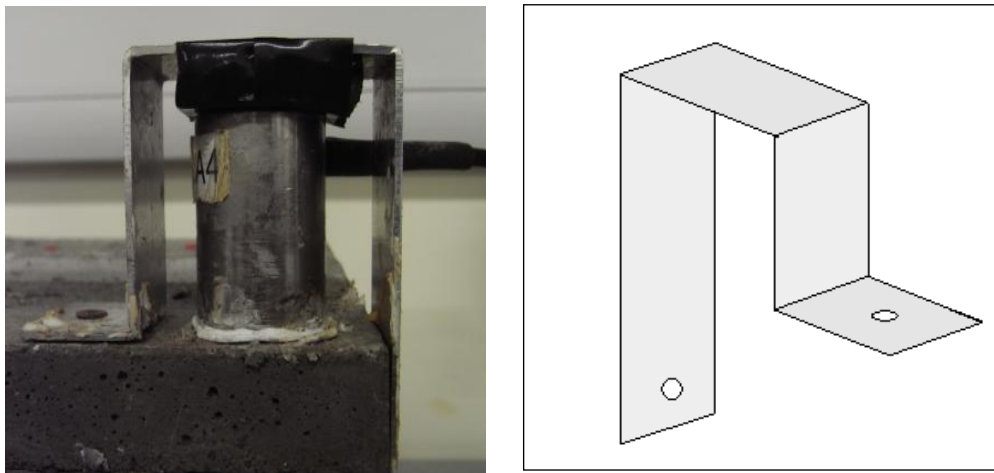
Figure 4.7 Steel clamp used to hold the sensor

4.3.2 Results and discussion of prestressed concrete specimens 1

Due to the extent of corrosion products, the specimen exhibited longitudinal cracks along the prestressed wire.

 Crack shape, wires, stainless plate, and sensors mounted on the mortar surface are shown in Figure 4.8 a and b. Figure 4.8a is a schematic diagram of the specimen after testing. Figure 4.8b is a photograph of the top mortar surface after the finish of the test.
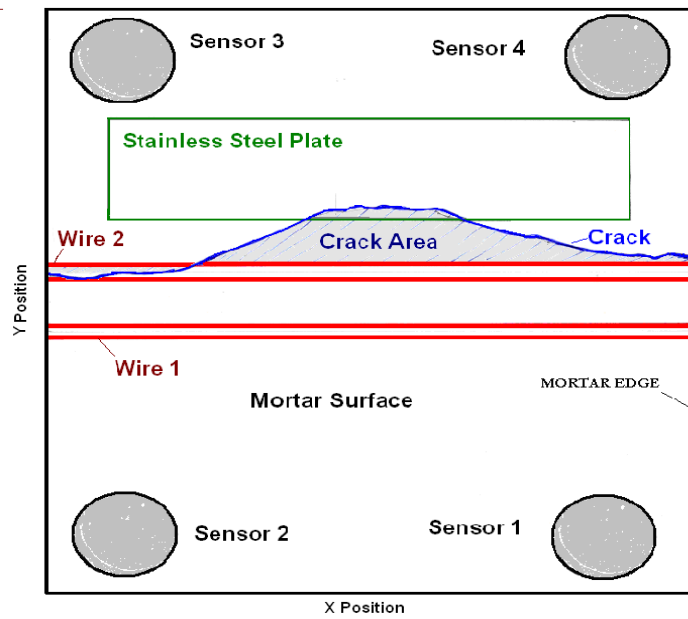
(a)
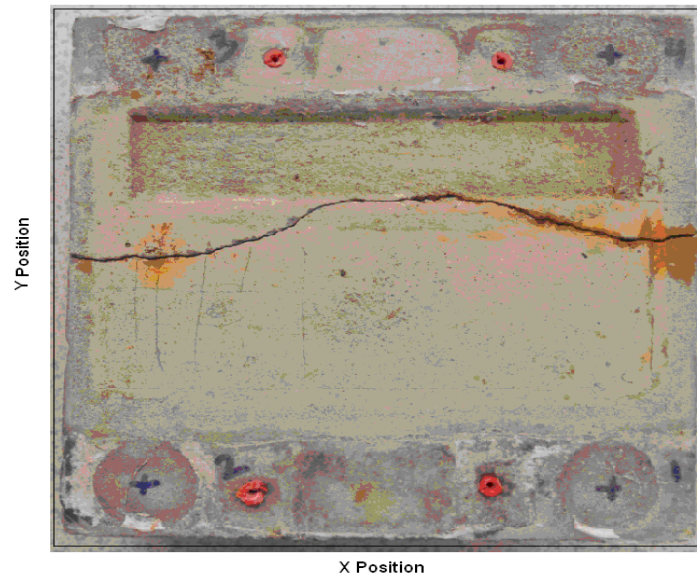
(b)

Figure 4. 8 Schematic Diagram and photo of top mortar surface

The location of hits with minimum amplitude 45dB for the whole period of the test is shown in Figure 4.9. It can be noted that the highest hits concentration and highest energy in the region coincides with the maximum wire corrosion products and the crack area which was visibly observed post test. Four zones have been chosen as examples to differentiate between cracks and non cracked areas (Figure 4.9).
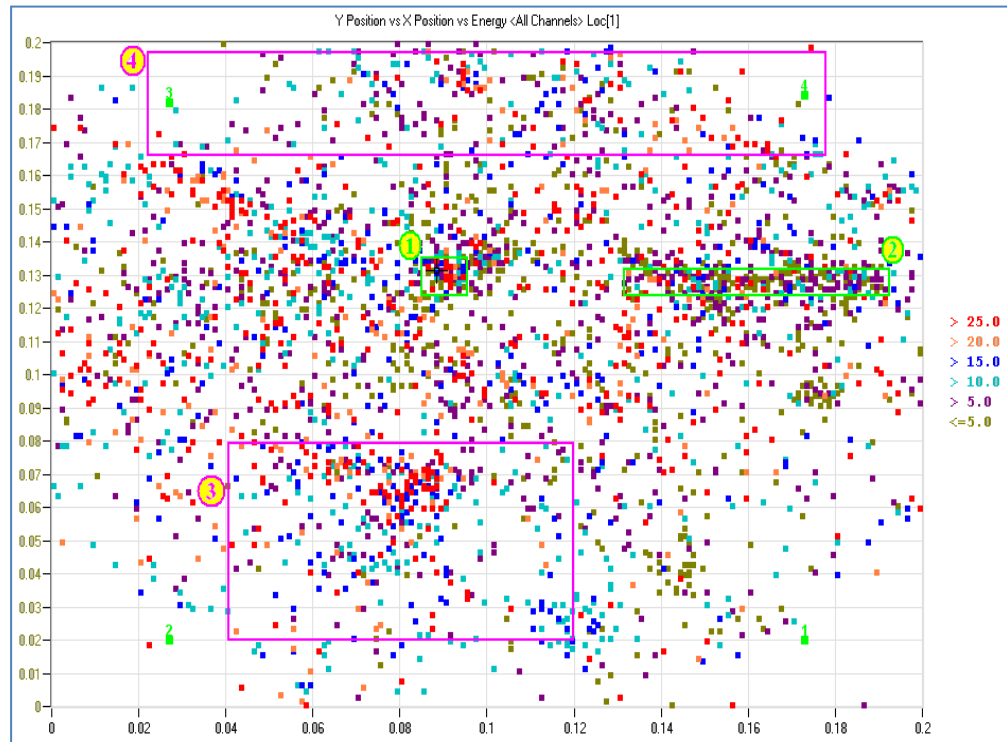
Figure 4. 9 Source locations for whole test with amplitudes greater than 45dB

Figure 4.10 (a, b, c, and d) shows the AF vs. RA values for the different regions of concentration of events on surface of mortar. Figure 4.10 (a and b) show the AF vs. RA for zones associated with the crack regions.

It can be seen that the majority of data points have various AF and low RA value (less than 5 ms/v). Therefore, based on Figure 2.5 (in Section 2.4.1) and Figure 3.12 (in Section 3.5.2), this indicates that this pattern represents a tensile crack. Furthermore, Figure 4.10 (c and d) shows the relationship between RA value and AF, for areas on the location with a low concentration of hits, where there was no tensile crack. It can be noted that the RA value has a wide distribution (0-50 ms/v).
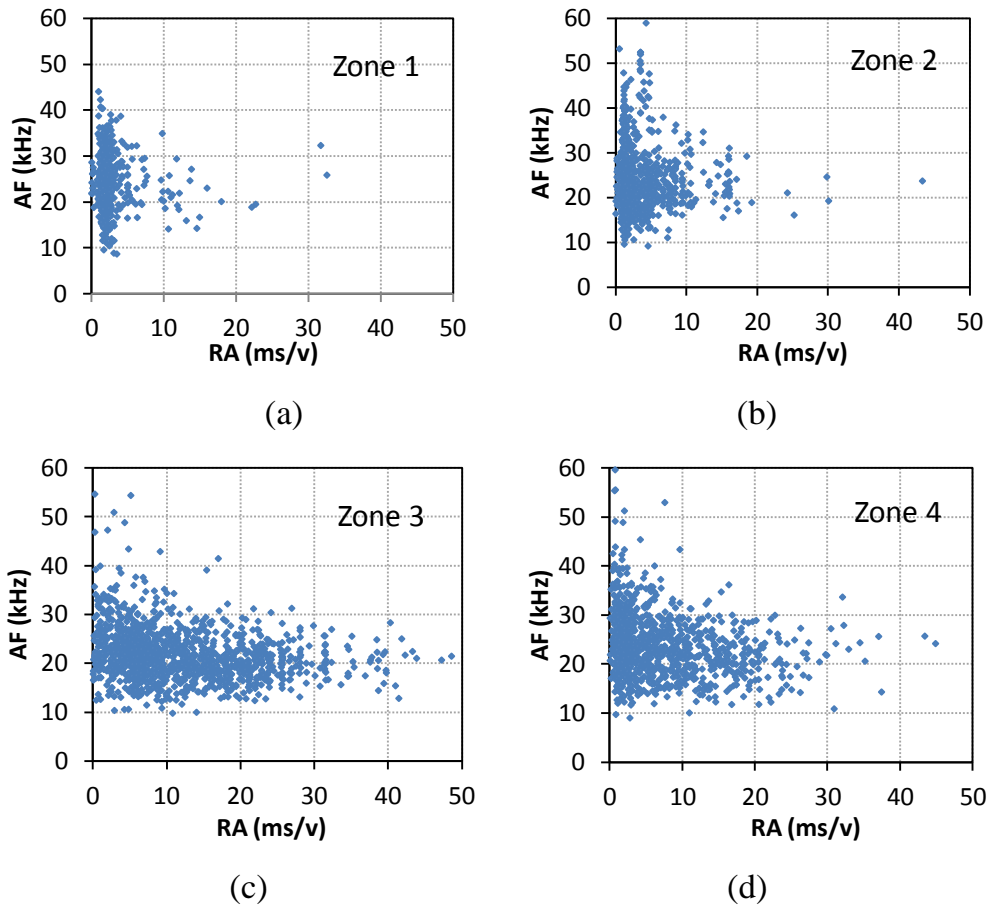
Figure 4. 10 Relation between the RA value and average frequency of (a)zone1, (b) zone2, (c) zone3 and (d) zone 4

Figure 4.11 shows the relationship between the RA value and average frequency of zone1 compared with zone 3. The blue data points represent the crack region, while the red represent the no crack region.
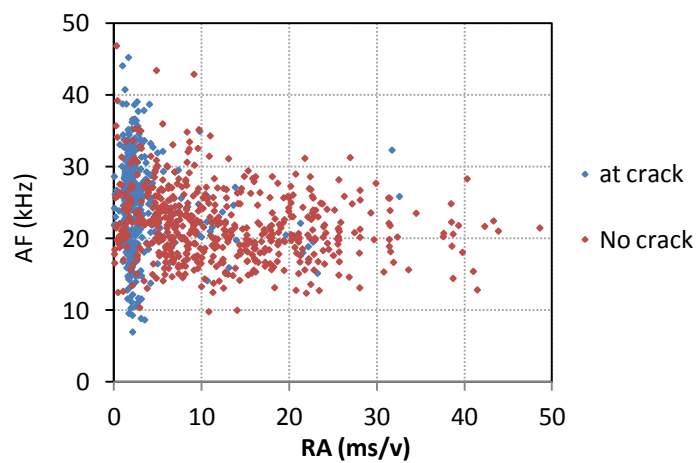
Figure 4. 11 Relation between the RA value and average frequency of zone1 and zone 3

This clearly demonstrates the difference between two zones. Thus a relationship is observed between crack and no crack areas; crack areas correspond with the blue data points and hereafter this type of relationship will be referred to as "a vertical trend" while those similar to the red data points will be referred to as "a horizontal trend" which represents signals in a region containing no tensile cracks.

Furthermore, these areas can be visualised using Kernel Density Estimation Function (KDEF) as shown in Figure 4.12 (a, b, c and d). Regions of high concentration are more easily identified. The concentration value of the data is represented by different colours, brown for the highest number of data points and blue for lowest.

(a)   (b)

(c)   (d)
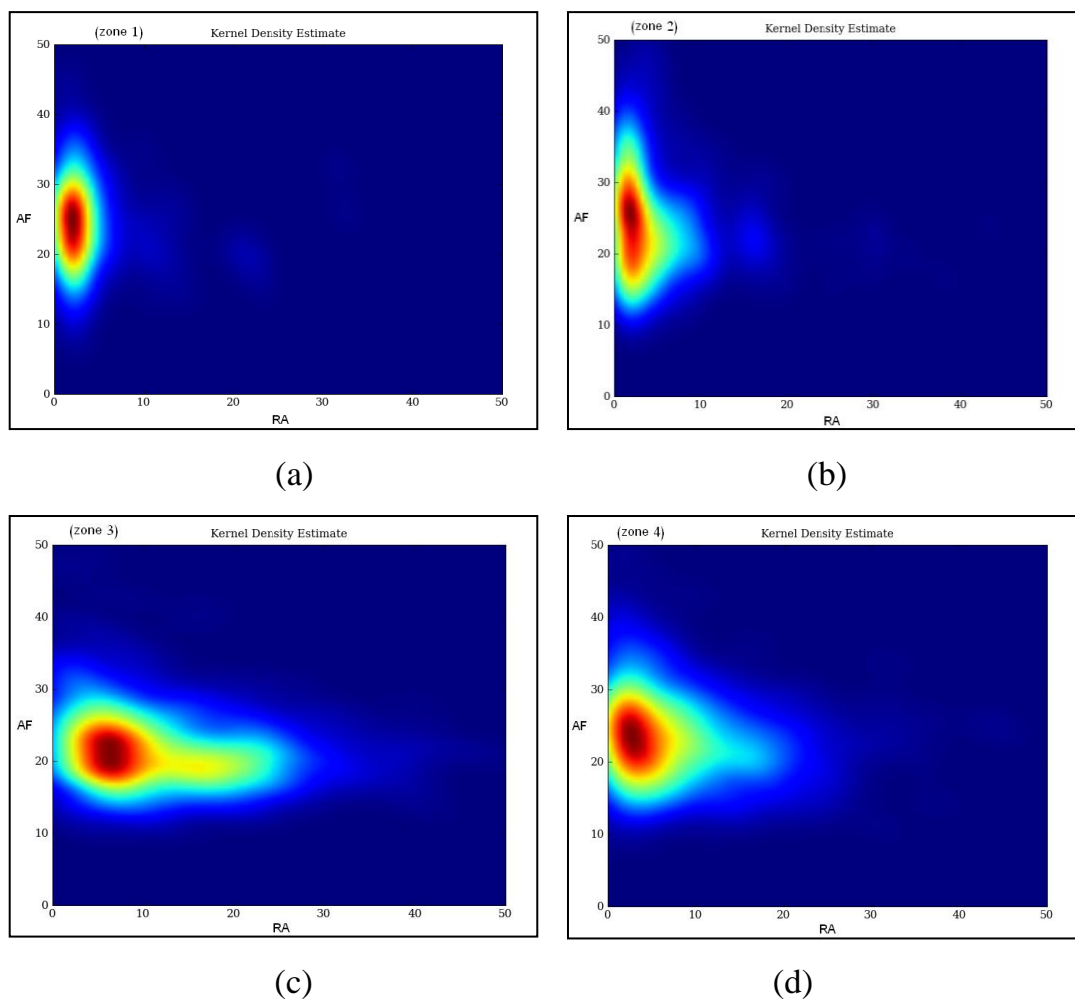
Figure 4.12 Kernel Density Estimation Function of (a) zone 1. (b) zone 2, (c) zone 3 and (d) zone 4

All the detected and located signals with a minimum amplitude 45 dB detected by all sensors for almost nine days of continuous monitoring are shown in Figure 4.13 as signal amplitude against time and Figure 4.14 displays the same data set but this time as the cumulative energy against time. The detected signals are attributed to background noise, active corrosion and mortar cracking through visual observation made during the tests. The graph demonstrates the behaviour of the energy emission in three regions of time. Each period of time marked represents approximately three days of monitoring.
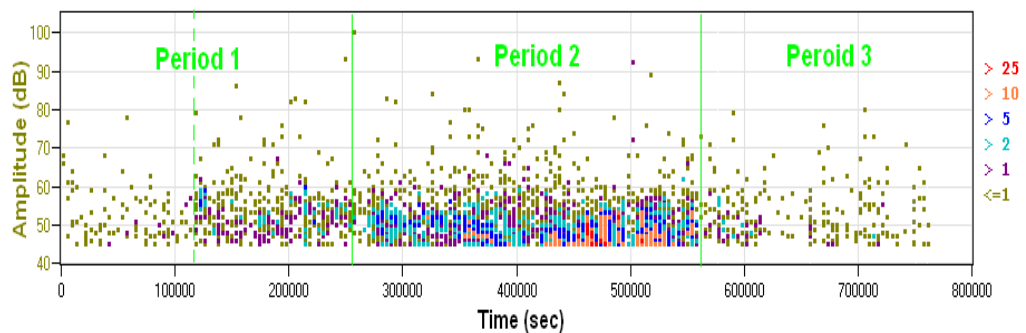
Figure 4. 13 Amplitude of detected signals for duration of investigation
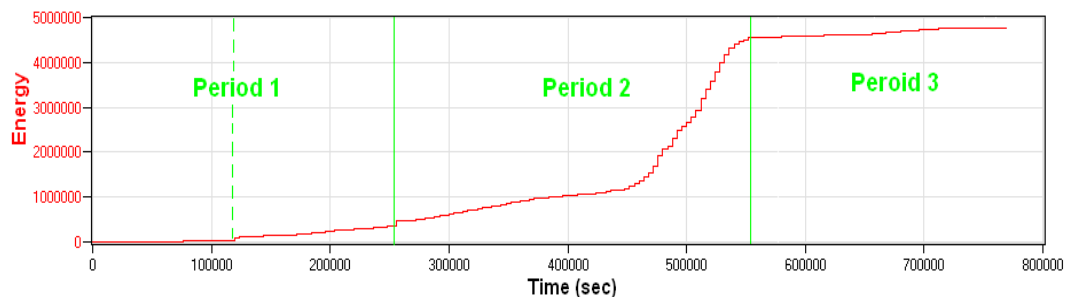
Figure 4. 14 Energy of detected signals for duration of investigation

The test is divided into three different stages as shown in Figure 4.13 and 4.14. The first stage, which is the first three days, is named period 1. It has a small number of hits and a small increase in energy. The energy emitted is attributed to constant corrosion activity (corrosion products accumulation at the interface prestressed wire / mortar and concrete and the friction of corrosion products at

the inner sides of the pores) and the separation of mortar from the concrete, as seen in the visual inspection.

Furthermore, Figure 4.15 shows the source location of signals within period 1. It can be seen that the number of hits and energy is small. All collected signals were analysed using the RA/AF comparison which is presented in Figure 4.16. It can be noted that the distribution of data points is a mixture between vertical and horizontal which is representative of tensile cracking together with other non-crack signals, i.e. a mixed area.
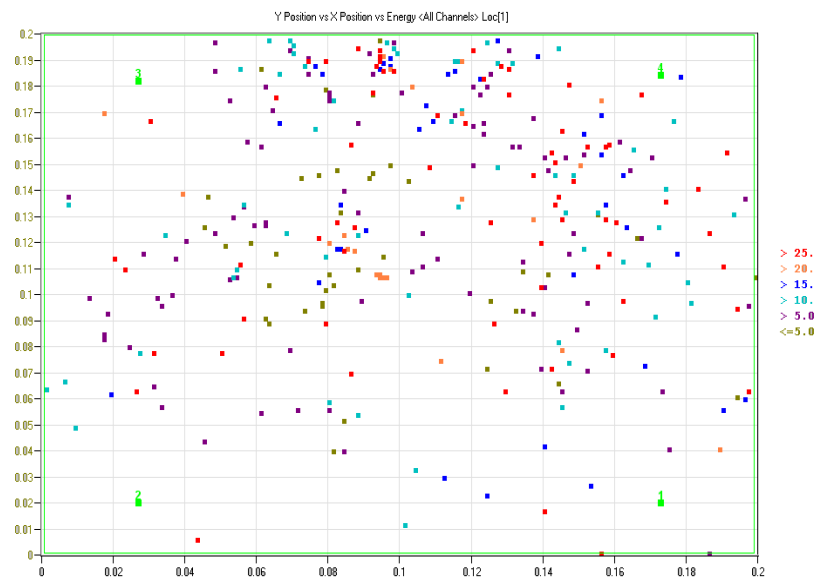
Figure 4. 15 Source locations for first three days (Period 1)

(a)   (b)
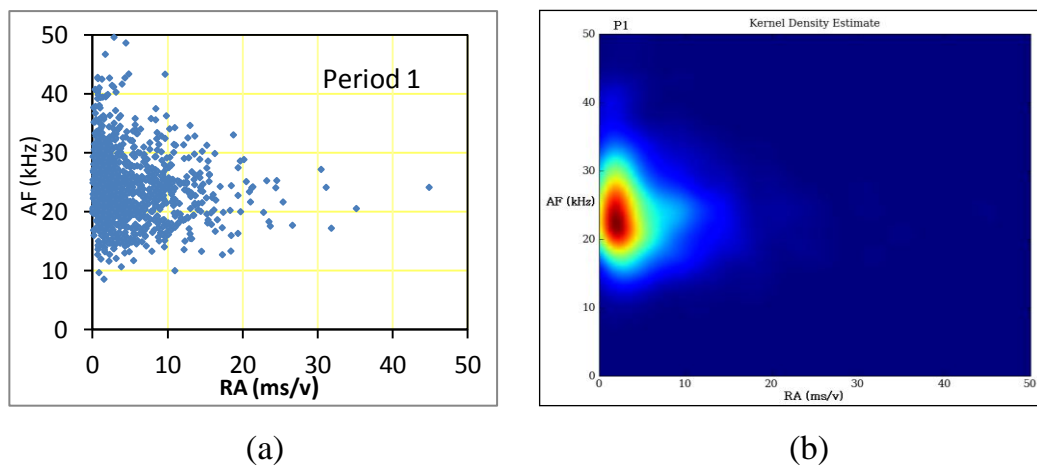
Figure 4. 16 Relation between the RA value and AF, (a) graph and (b) Kernel Density Estimation Function

The data was further analysed by dividing period 1 into two further periods; namely before and after the small increase in energy and the number of hits occurred as shown in Figure 4.13 and 4.14 by a dashed line.

By presenting these periods via a graph and KDEF as shown in Figure 4.17, it can be noted that the RA vs AF relationship is different for the two periods. In the second period the shape is more vertical which is indicative of tensile cracking.

(a)

(b)
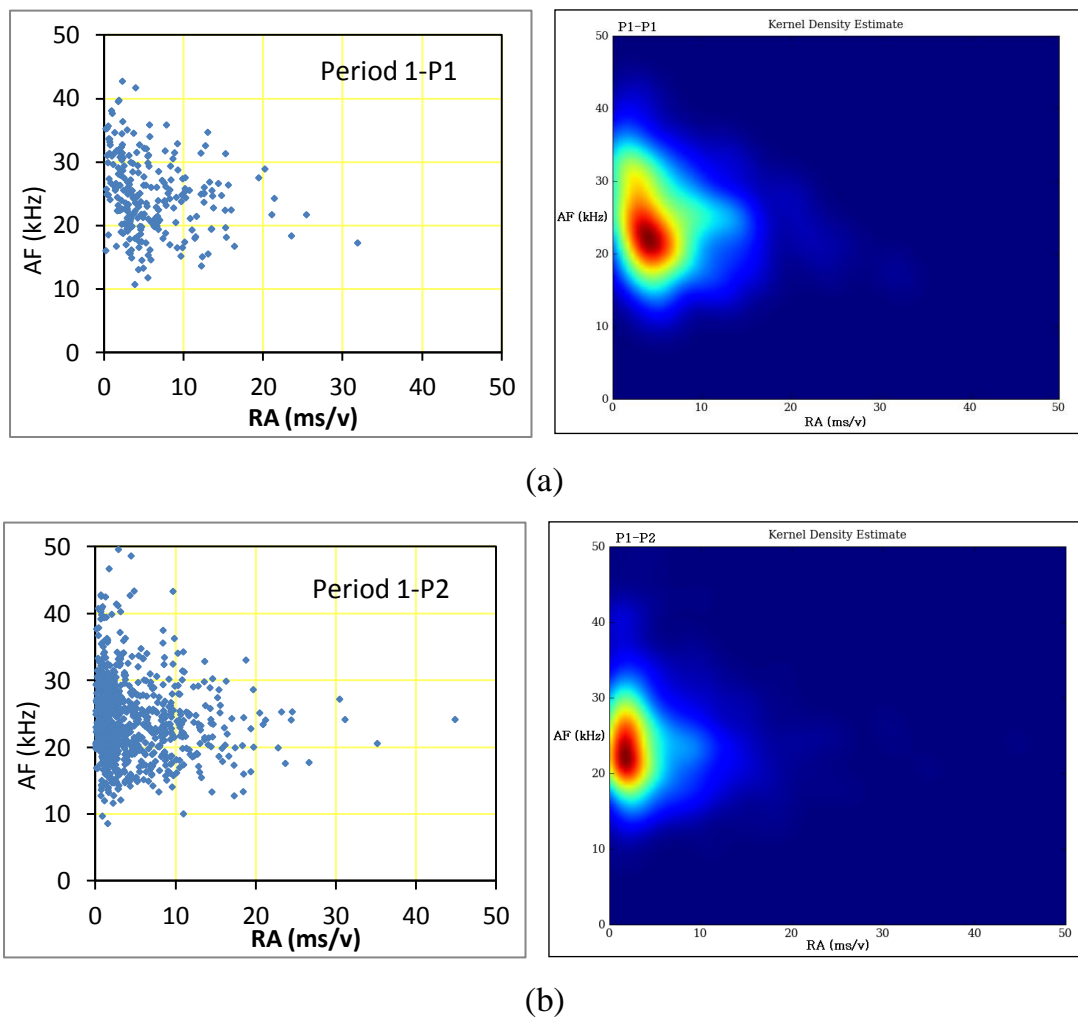
Figure 4.17 Relation between the RA value and AF of a and b period of period 1 (a)before and (b) after small increase of hits and energy.

The second stage is between the fourth day and the sixth day which is named period 2. In this stage, it can be seen that the number of hits and the emission energy increases significantly as shown in Figure 4.13 and 4.14. Furthermore,

it can be seen that in Figure 4.18 the number of located events increases considerably due to an increase in the number of macro cracks, crack propagation and the split of mortar from concrete, as observed visually. Also, a high concentration of hits in the observed area of cracking should be noted.
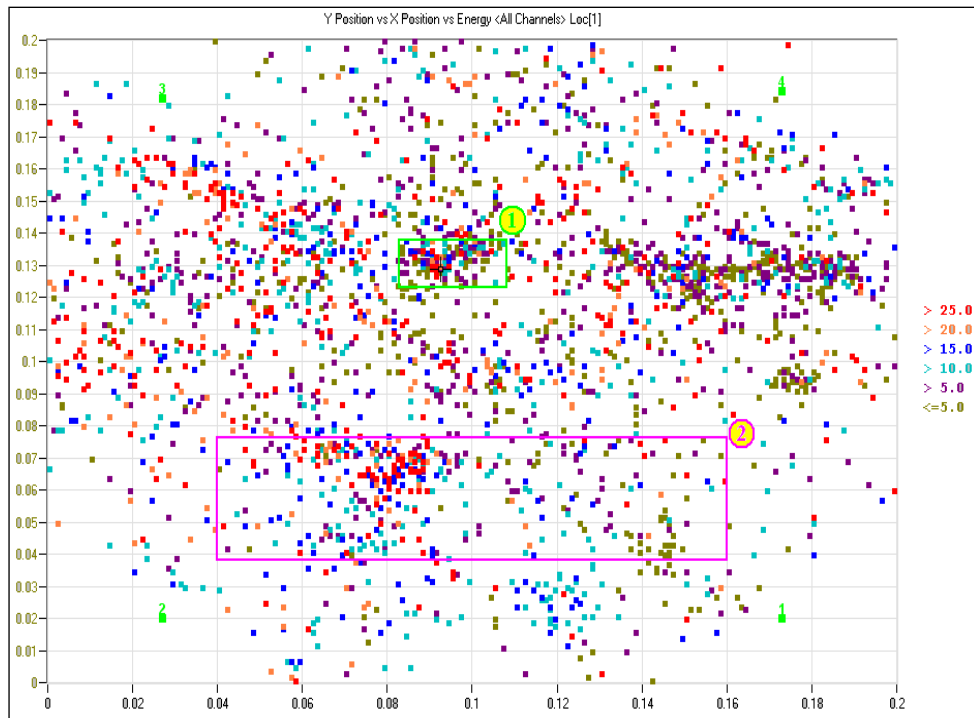
Figure 4. 18 Source locations for middle three days (Period 2)

To compare between the cracking region and no cracking area, two zones 1 and 2 are chosen as shown Figure 4.18. Zone 1 has a high concentration of hits and energy and is referred to the cracking area and zone 2 is the no cracking area.

As shown by comparing Figure 4.19a with Figure 4.19b representing zone1 and zone2 respectively via graph and KDEF, there are significant differences in behaviour. It can be noted that the distribution of data points in zone 1 (Fig 4.19a) has a vertical trend with low RA-value (less than 5 ms/v) and wide ranges of AF-value. This indicates that the trend is tensile crack type.

Conversely, in the Fig 4.19b (zone 2), there is a horizontal trend (low RA-value and wide variation of AF-value).

(a)

(b)
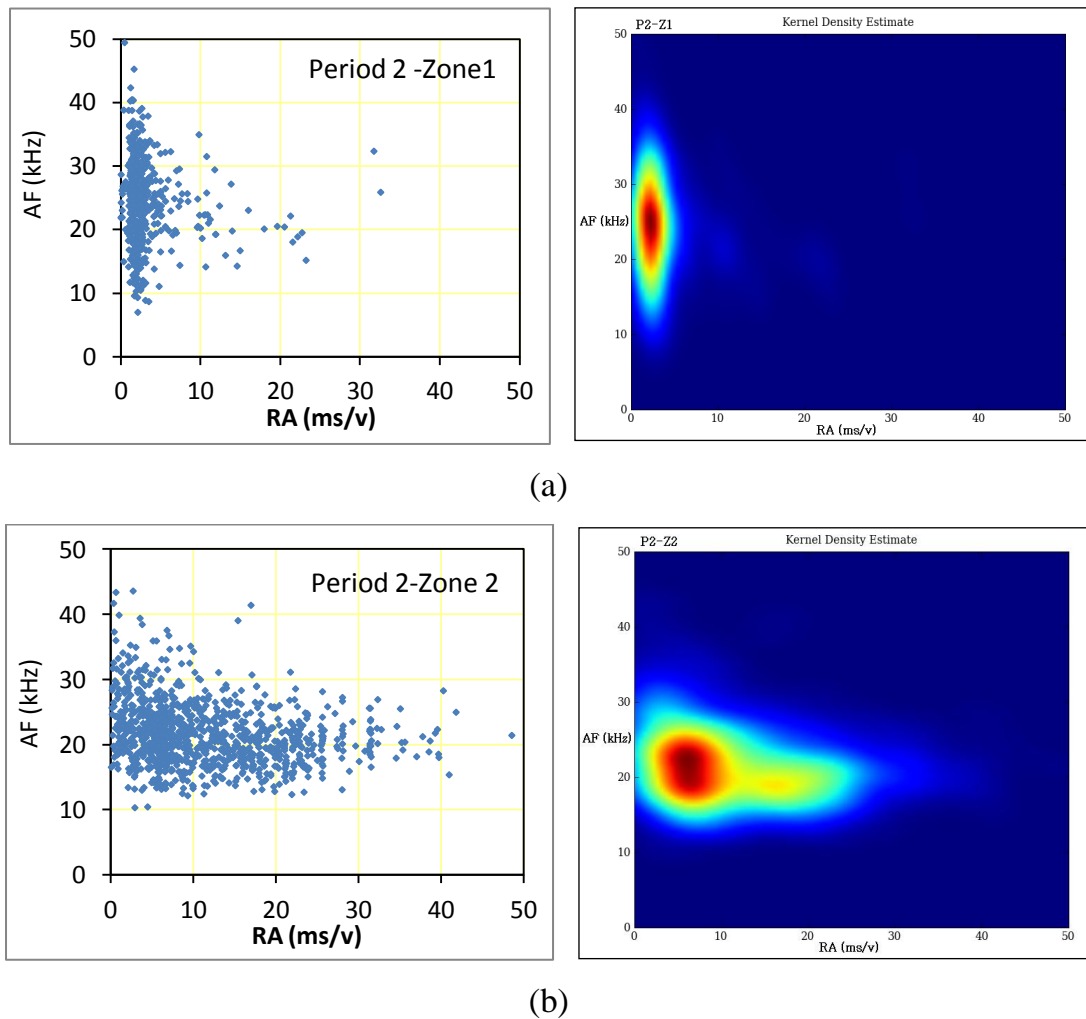
Figure 4. 19 Relation between the RA value and AF of (a) Zone1 and (b) zone2

During the final three days (period 3 in Figures 4.13 and 4.14) it can be noted that the energy decreases for two reasons; firstly all the cracks had opened at this point as observed visually and secondly due to the decrease of current (corrosion rate) and hence a decrease in the effects of corrosion on the concrete. In addition, Figure 4.20 shows source location on the mortar surface. It can be seen that the number of hits is decreased compared with period two.
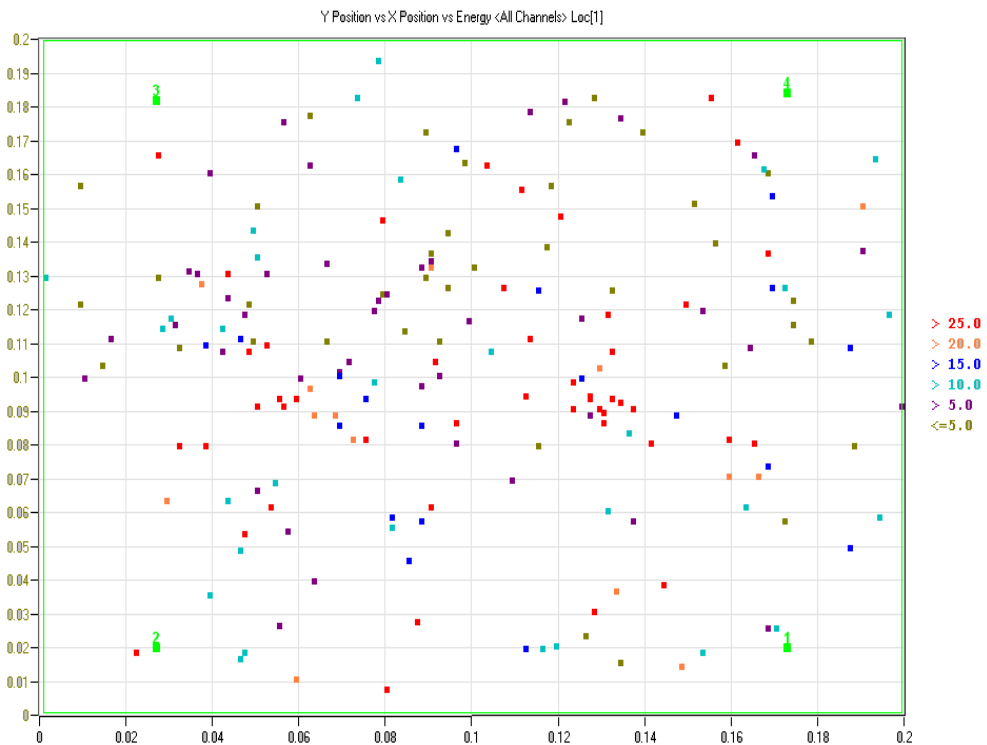
Figure 4. 20 Source location for last three days (Period 3)

Figure 4.21 illustrates the trends of relation between the RA-value and AF-value of all hits of period 3.

It can noted that the distribution of data points is mixed between the vertical and horizontal trend. (It develops over time from vertical to horizontal). This means that the dominant type of crack is another type rather than tensile type. This is because the hits detected include hits from noises (separation of mortar from the concrete) and a very small number of crack propagation hits.

The decrease in the number of crack propagation hits is due to the decrease in the corrosion activity (current applied) and the crack extending in the concrete above and along the wire becomes very slow (or completely opened).
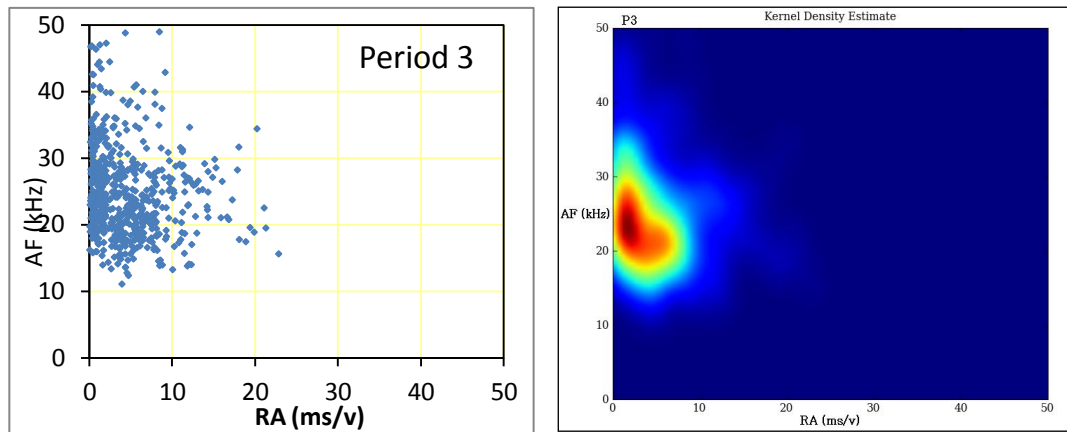
Figure 4. 21 Relation between the RA value and AF of period 3

It has been demonstrated that by using the relationship between RA and AF value, the crack area can be identified. Hence, it could be possible to provide a corrosion alarm and location to pipe engineers prior to any wire breaks. Furthermore, by knowing the crack types it could be possible to identify the damaged area before the mortar completely fails.

4.3.3 Results and discussion of prestressed concrete specimen 2

Due to a shorter curing time, specimen 2 exhibited a high level of background noise therefore a threshold of 50db was used, this was found to provide a better location of regions. All the detected and located signals with a minimum amplitude of 50 dB detected by all sensors for almost fourteen days of continuous monitoring are shown in Figure 4.22 as signal amplitude against time and Figure 4.23 displays the cumulative hits against time.

Figure 4.24 displays the same data set but this time as energy against time. The detected energy is attributed to a number of sources; active corrosion, micro cracking, macro cracking, propagation of mortar cracking, separation of the mortar from the concrete, noise and wire breaks, as observed by visual inspection.
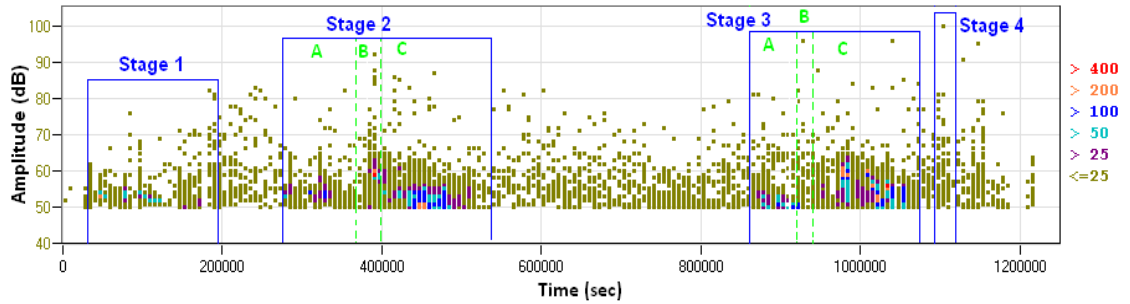
Figure 4. 22 Amplitude of detected signals for duration of investigation
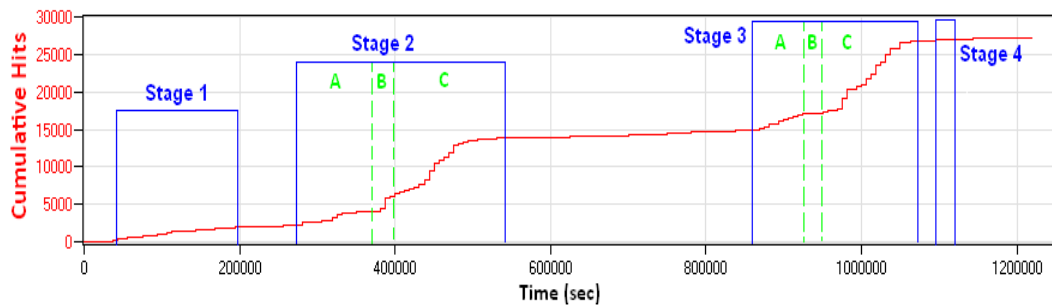
Figure 4. 23 Cumulative Hits Vs Time
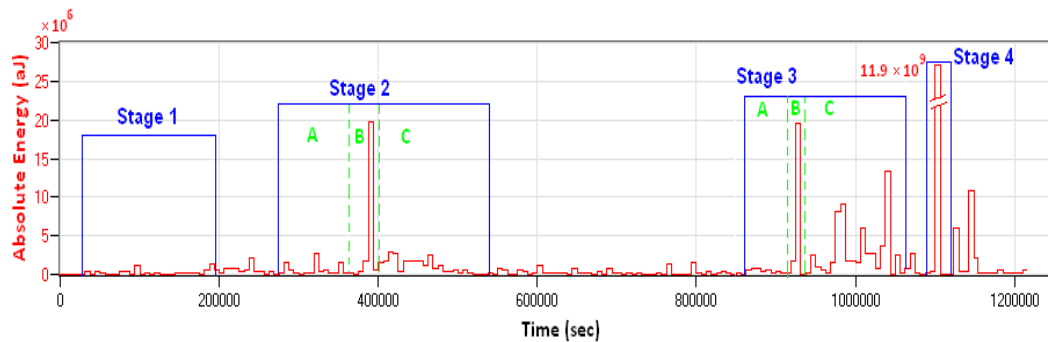
Figure 4. 24 Absolute energy of detected signals for duration of investigation

It can be seen that in Figure 4.22, 4.23 and 4.24 there are four significant stages which contain signals with a combination of large energy and an increased rate of hits. The increased hit rate, low amplitude and low energy in stage 1 is attributed to the energy release from the corrosion activity (corrosion products accumulation at the interface of the prestressed wire / mortar and concrete and the friction of corrosion products at the inner sides of the pores). Stage 2 is divided into three further stages; A, B, and C. The first stage (2A) is

84

the increase of the number of hits with a slightly higher energy and amplitude is attributed to micro crack formation. The following high energy and high amplitude over a short interval of time in stage 2B is attributed to the energy release from the formation of the macro longitudinal crack due to the products of corrosion from wire 1 as observed in visual inspection. In addition, the energy release from macro cracks formation is higher than micro cracks formation. This result shows good agreement with the results demonstrated by Aggelis (2011). The following increase in the number of hits with smaller energy and smaller amplitude than stage 2B and longer interval of time than stage 2A and 2B is attributed to macro crack propagation. (Stage 2C)

Stage 3 is divided to three stages A, B, and C. The first stage (3A) which has increased number of hits with a slightly higher energy and amplitude is attributed to micro crack formation. The high energy and high amplitude in stage 3B corresponds to the formation of a macro longitudinal crack due to the products of corrosion from wire 2 as observed in visual inspection. The following increase in the number of hits with variable energy (stage 3C) corresponds to mix of macro crack propagation and the formation of a macro inclined crack between two longitudinal cracks, as observed in visual inspection.

The highest energy and highest amplitude (100 dB) located in stage 4 is due to the wire 1 breaking as observed both in visual inspection and at this time the strain gauge reading suddenly decreased from approximately 6000 to around 500 μ strain .
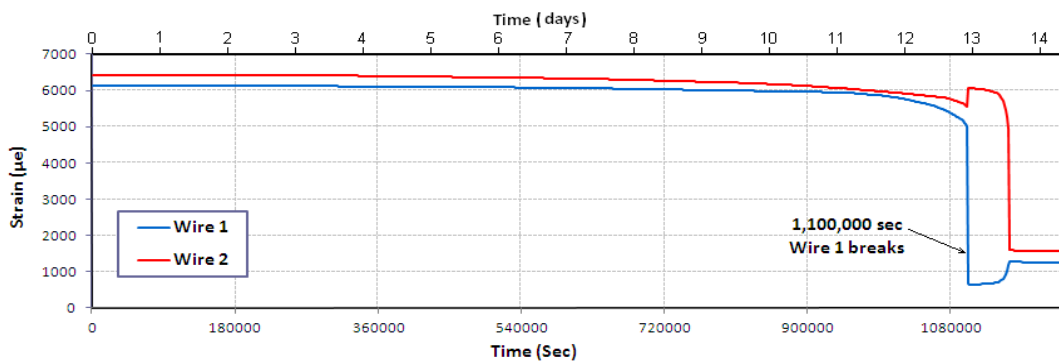
Figure 4. 25 Recorded strain for duration of investigation

85

It can be noted that different damage modes, including corrosion activity, micro/macro cracking formation, crack propagation and wire failure generate different types of AE signals with varying amplitudes and absolute energy emitted.

The increase in the number of hits, low amplitude and low energy is attributed to the energy release from the corrosion activity (corrosion products accumulation at the interface prestressed wire / mortar and concrete and the friction of corrosion products at the inner sides of the pores). This result shows a good agreement with results demonstrated by Assouli et al (2005) and Ohtsu et al (2010). Furthermore, this result is proved by a further test (short time test before micro crack occurs) which is explained in a subsequent section (Section 4.4).

The micro cracks emit a large number of waves with smaller amplitudes whereas macro cracks emit less waves but with larger amplitude. This result shows a good agreement with the results demonstrated by Colombo et al (2003).

In addition, the absolute energy released from macro crack formation is higher than micro crack formation. This result shows good agreement with the results demonstrated by Aggelis (2011). The results have shown that a gradual increase of the number of hits emitted with higher energy than those due to micro crack formation and lower than those due to macro crack formation corresponds to macro crack propagation. This result shows good agreement with the result demonstrated by Aggelis (2011) and Muralidhara (2010).

The variation of measured strain of the embedded wires against time is shown in Figure 4.25. It can be seen the load on the wires is constant for the entire period until wire 1 failure at about 1,100,000 seconds and the load is then transferred to wire 2 which subsequently failed

As previously, to eliminate background noise a threshold of 49dB was used, because this was found to provide a better distinction of location regions. The location of signals with minimum amplitude 49dB for the whole period of the test is shown in Figure 4.26. It can be noted that the highest hits concentration and highest energy region coincides with the position of maximum wire corrosion and the crack which was visibly observed post test as shown in Figure 4.27.
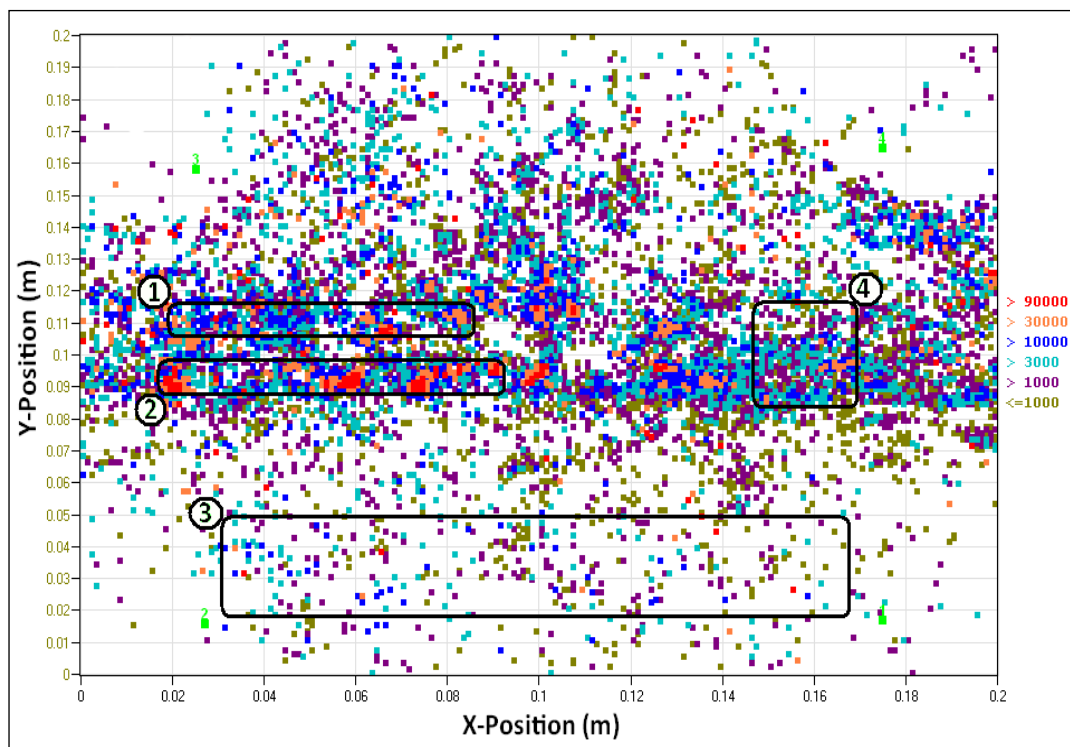
Figure 4. 26 Source locations for whole test with amplitudes greater than 49dB

Figure 4.27 is a photograph of the top mortar surface after the end of the test, showing the crack shape. Comparing this figure with the previous location plot reinforces the conclusion that the AE was detecting the concrete cracking as a result of wire corrosion within the specimen.
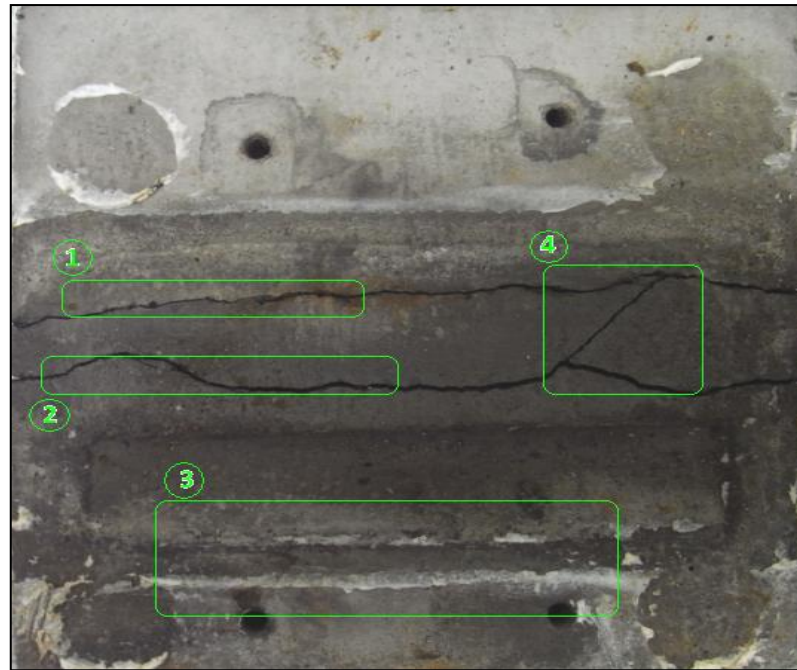
Figure 4. 27 Photo of top mortar surface

The corroded wires and corrosion product once the mortar had been removed is shown in Figure 4.28. It is evident that significant corrosion occurred in the upper wire and it was in this location that a large majority of AE signals were detected and located.

Figure 4. 28 Photo of upper concrete surface and wires

Four zones have been chosen as examples to distinguish between the crack area and noise and also to classify mode types. Areas were chosen based on visual observation (Figure 4.26 and Figure 4.27). Zones 1 and 2 represent crack areas where crack shapes are parallel to the corroded wires (longitudinal crack), zone 4 contains a crack that is inclined and which develops between the two longitudinal cracks, whereas in zone 3 no cracks were present. Figure 4.29 (a, b, c, and d) show the AF vs. RA values for different regions of concentration of events on surface of mortar.

(a)   (b)

(c)   (d)
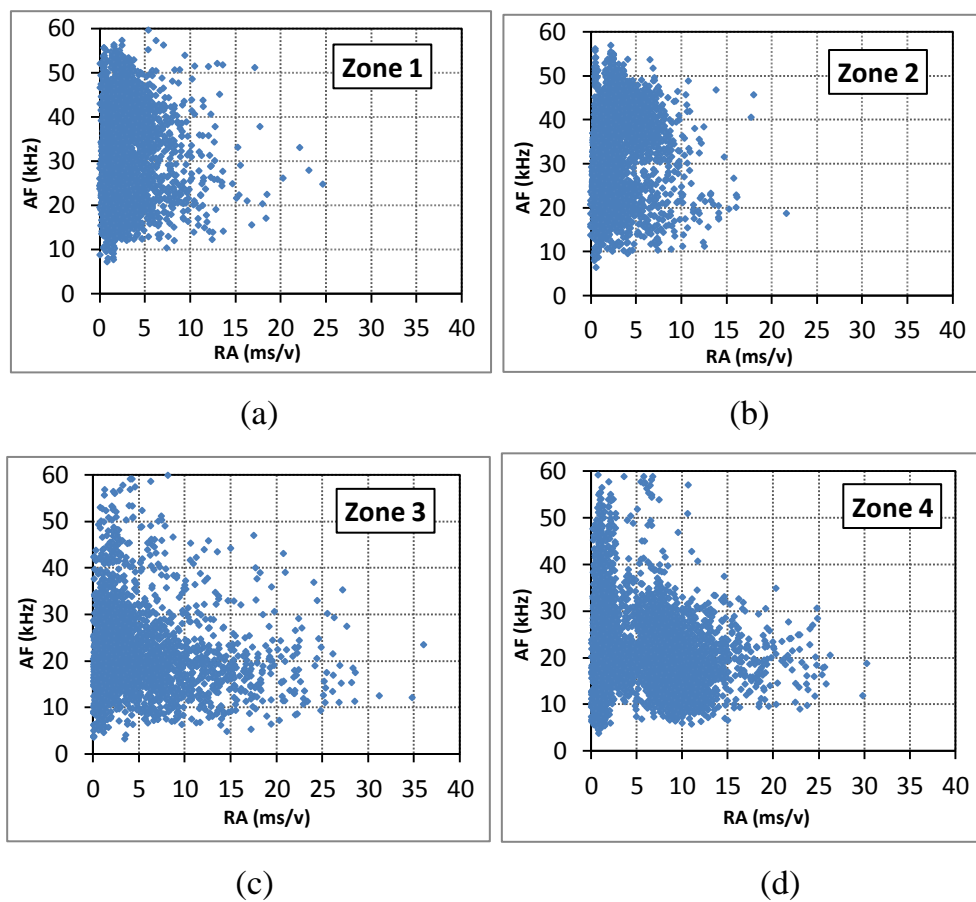
Figure 4. 29 Relation between the RA value and average frequency of (a) zone1, (b) zone2, (c) zone3 and (d) zone 4

Figure 4.29 (a and b) show the AF vs. RA for zones associated with the crack regions which is longitudinal crack due to the products of corrosion from wire 1 and wire 2 respectively (zones 1 and 2). It can be seen that the most of data points have various AF values and low RA values (less than 10 ms/v) which is

termed a "vertical trend". Therefore, based on Figure 2.5 (in section 2.4.1) and Figure 3.12 (in section 3.5.2), this indicates that the type of the crack is pure tensile. Figure 4.29 (c) shows the AF vs RA values for zone 3, an area where there is a low concentration of AE locations and no crack observed. It can be noted that in this area the RA value has a wide distribution (RA values 0-30 ms/v and AF values 10-40). This indicates that the trend no tensile crack type. The Figure 4.29 d shows the relationship between RA and AF values associated with zone 4, which is the inclined crack between the two longitudinal cracks. As previously explained, this indicates that the crack type is mixed between two modes; tensile crack and shear mode movement.

Furthermore, these figures can be better visualised using a KDEF as shown in Figure 4.30 (a, b, c and d).

(a)

(b)

(C)

(d)
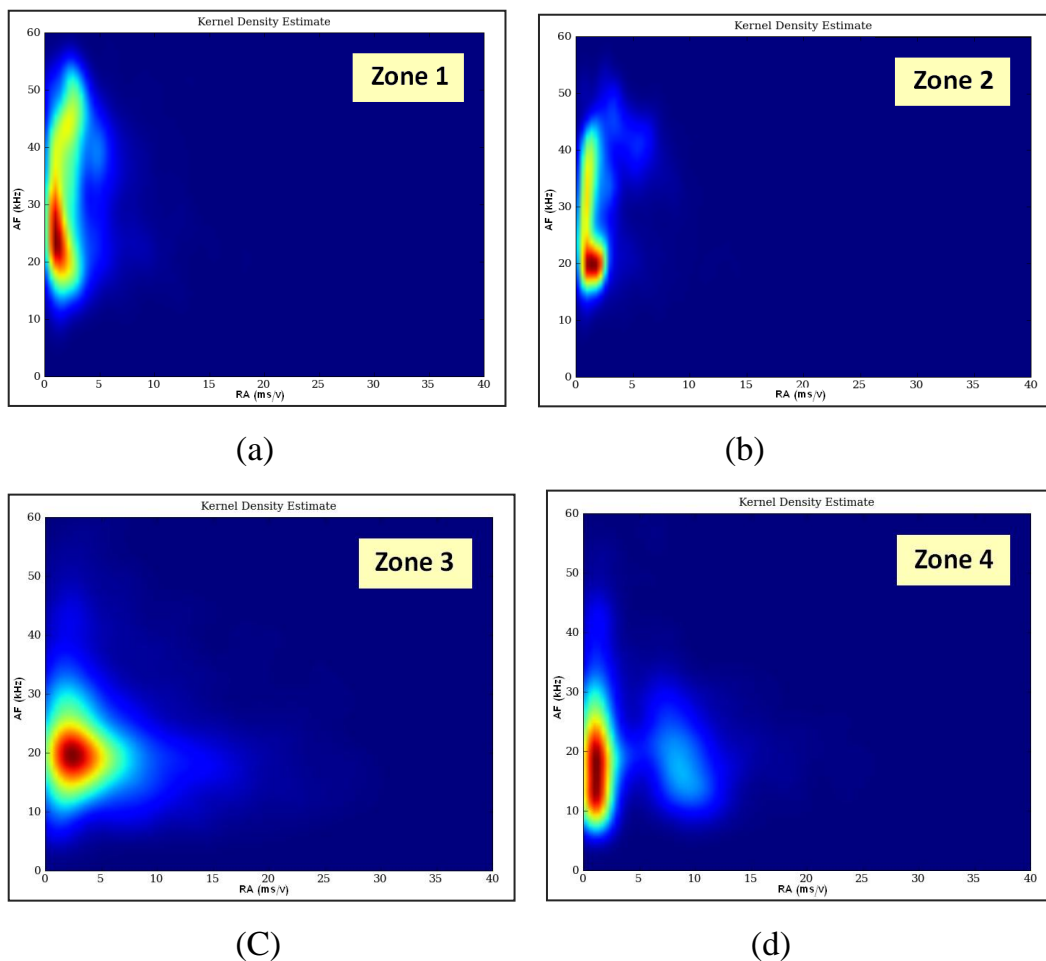
Figure 4. 30 Kernel Density Estimation of (a) zone 1. (b) zone 2, (c) zone 3 and (d) zone 4

It clearly can be seen that zones 1 and 2 have similar behaviour to Figure 4.10 (a and b) (vertical trend) however, zone 4 has two parts; one vertical trend and another horizontal trend.

During the corrosion process a number of key stages occur. Initially there is delamination and cracking of the steel wire, this leads to product expansion and a material volume increase. This increase then leads to the mortar cover moving upwards in this example or radially outwards on the real pipe causing a micro surface crack to form above the steel wires and this will develop to a visible crack (macro crack). The micro crack occurs when tensile stress due to internal corrosion product expansion pressure exceeds the mortar tensile strength.

It can be seen that in this area (Stage 1), before the micro crack occurred, an increasing number of signals with low amplitudes and low absolute energy as shown in Figure 4.22, 4.23 and 4.24. This increase in signals is associated with the initial stages of corrosion prior to the second increase in signals with larger amplitude signals and larger energy which it is associated with the micro cracking prior to mortar cover cracking. This demonstrates that the AE method can not only detect the cover cracking but evidence of the corrosion process can be observed.

In this example the longitudinal cracks grew along the lengths of both wires prior to a third crack forming at an incline/angle to the two already present (Figure 4.27- zone 4). This inclined crack would have initially been created by tensile forces, however as product expansion increases and the two faces of the mortar move upwards relative to each other a shear movement occurs. This is consistent with the findings in Figure 4.29 and 4.30 that show zone 4 is a mixed mode area of both tensile and shear movement whilst zones 1 and 2 are purely tensile. It has been shown that by using AE and the relationship between RA and AF value, the crack area can be located and identified (Figure

4.26, 4.29 and 4.30). Hence, it could be possible to provide a corrosion alarm and location to pipe engineers prior to any wire breaks. Furthermore, by knowing the crack type it is possible to identify the damaged area before the mortar completely fails.

4.3.4 The effect of distance between sensor and source on RA and AF value

In order to investigate the effect of distance between sensors and a source, two zones (A and B) containing different crack types were selected as examples as shown in Figure 4.31, which shows the location of hits with minimum amplitude 49dB (better distinction of location regions) for the whole period of the test and sensor locations.
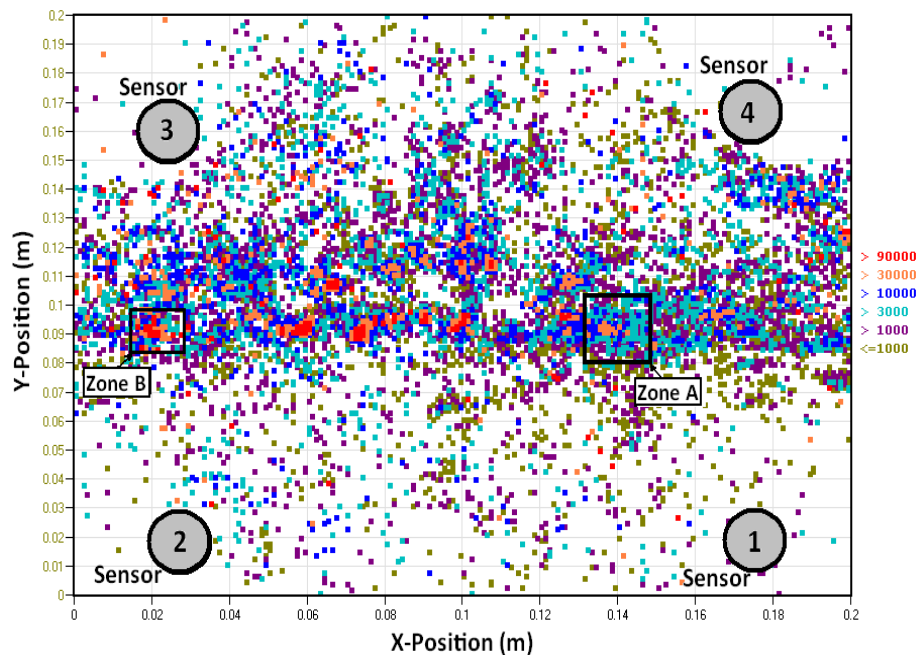
Figure 4. 31 Source locations for whole test with amplitudes greater than 49dB

The analysis of data of AF vs. RA values for all the signals detected by the four sensors of zone A is shown in Figure 4.32. This zone A corresponds to two types of crack mode; tensile and shear movement.
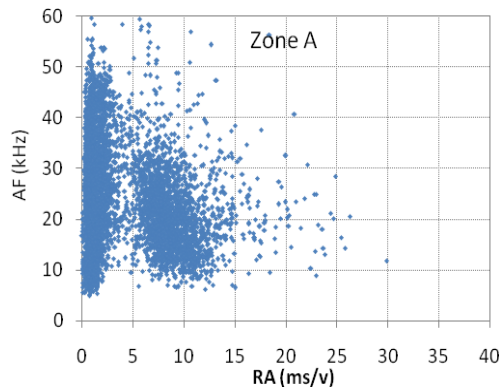
Figure 4. 32 Relation between the RA value and average frequency of data of all sensors of signals from zone A

It can be seen from Figure 4.31 that every sensor has a different distance from zone A. Figure 4.33 (a, b, c, and b) shows the AF vs. RA for each individual sensor for zone A. By comparing the data of RA and AF value in Figure 4.33, it can be seen that the data is similar for every channel, suggesting that the results will not be affected by distance to source.

(a)

(b)

(c)

(d)
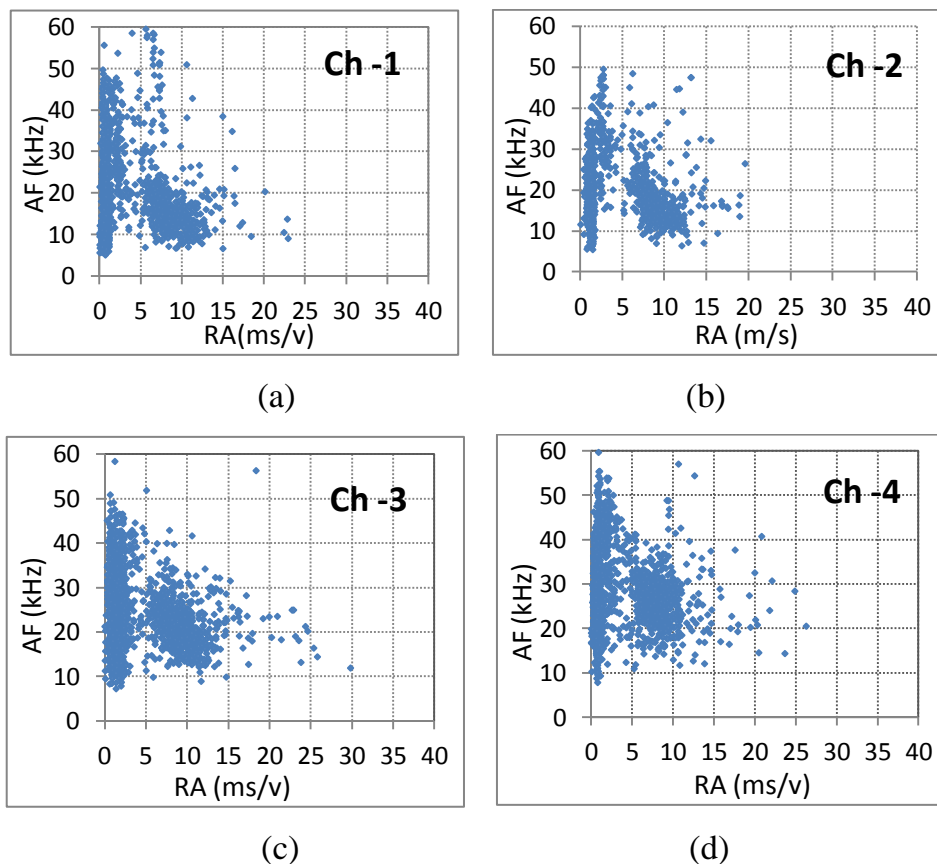
Figure 4. 33 Relation between the RA value and average frequency of data of (a) sensor 1, (b) sensor 2, (c) sensor 3 and (d) sensor 4

Furthermore, these figures can be visualised as before by using a KDEF as shown in Figure 4.34 and Figure 4.35 (a, b, c and d).
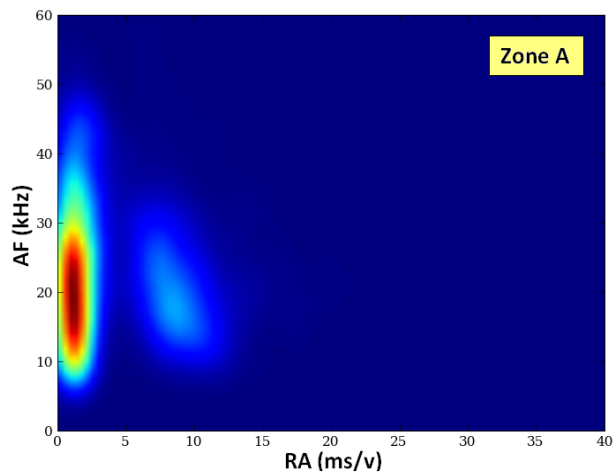
Figure 4. 34 Kernel Density Estimation of zone A

(a)

(b)

(c)

(d)
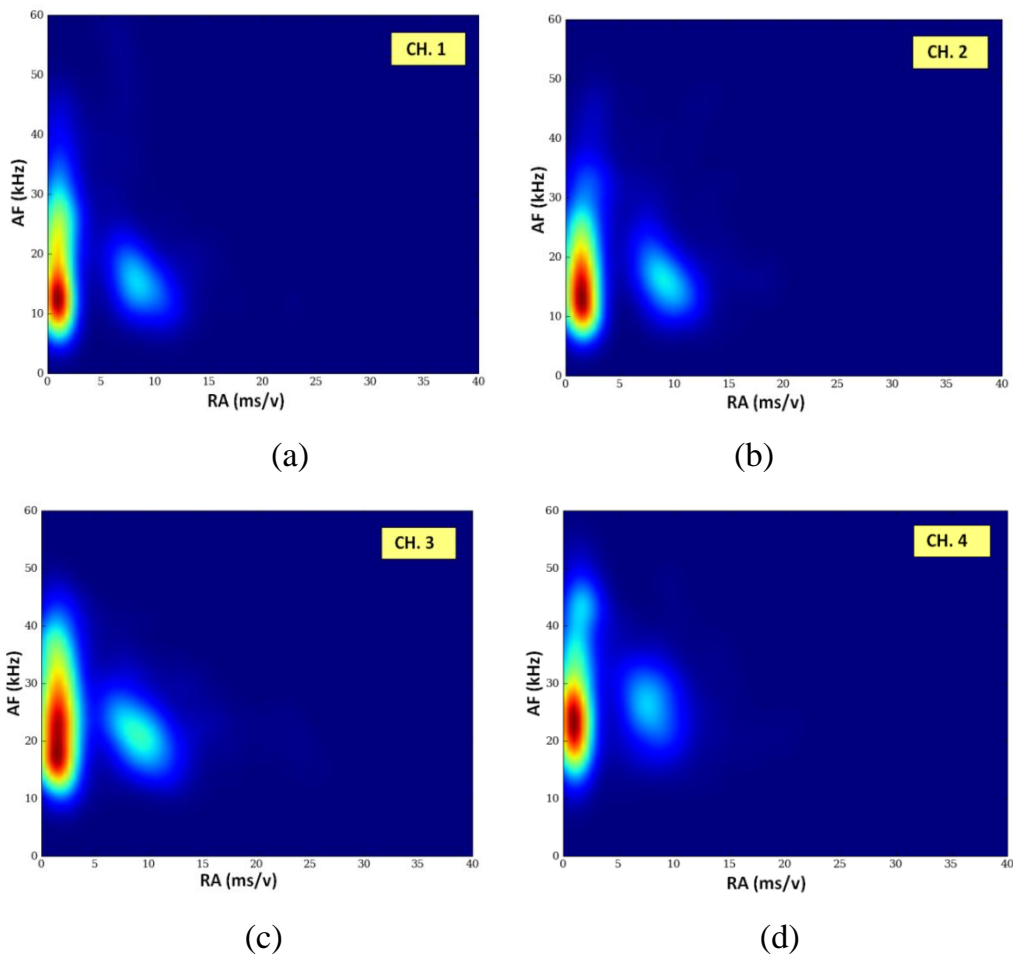
Figure 4. 35 Kernel Density Estimation of zone A (a) sensor 1. (b) sensor 2, (c) sensor 3 and (d) sensor 4

The analysis of data of AF vs. RA values for all the signals detected by the four sensors of zone B is shown in Figure 4.36. This zone B corresponds to tensile crack mode.
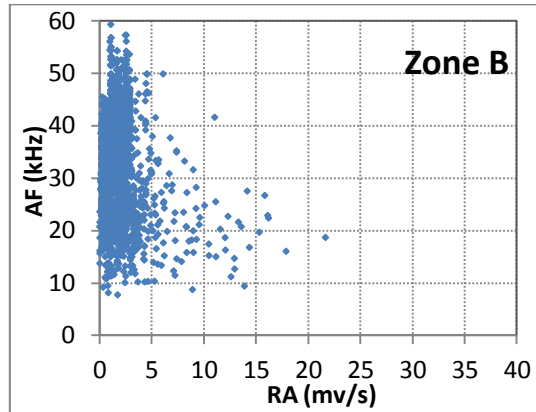
Figure 4. 36 Relation between the RA value and average frequency of data of all sensors of signals from zone B

(a)

(b)

(c)

(d)
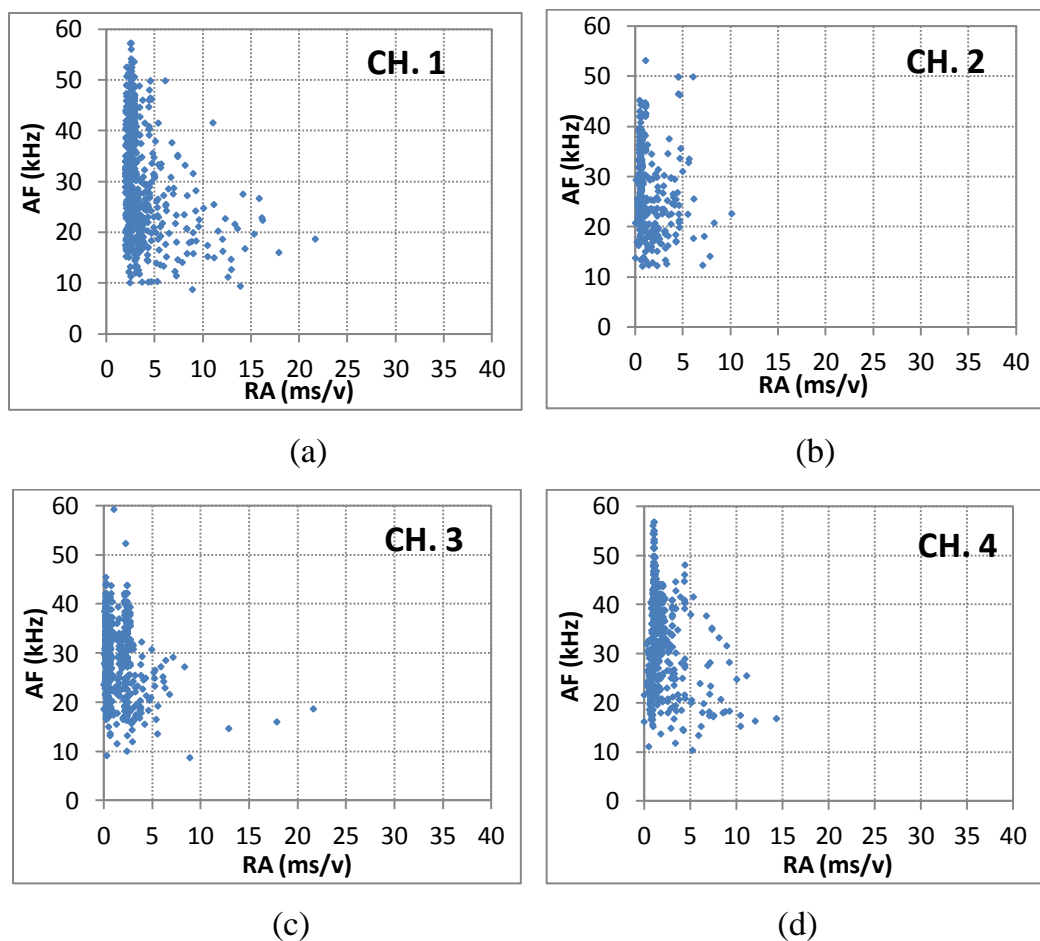
Figure 4. 37 Relation between the RA value and average frequency of data of Zone B (a) sensor 1, (b) sensor 2, (c) sensor 3 and (d) sensor 4

95

Every sensor has different distance from zone B as shown in Figure 4.31. Figure 4.33 (a, b, c, and b) shows the AF vs. RA for every sensor for zone A. By comparing the data of RA and AF value in Figure 4.37, it can be seen that the data is same tend for every channel, suggesting that the results will not be affected by distance to source.

These figures can be visualised using a Kernel Density Estimation Function (KDEF) as shown in Figure 4.38 and Figure 4.39 (a, b, c and d).

This result has demonstrated that the measured values are not affected by distance from damage source or sensor position making this an ideal approach.
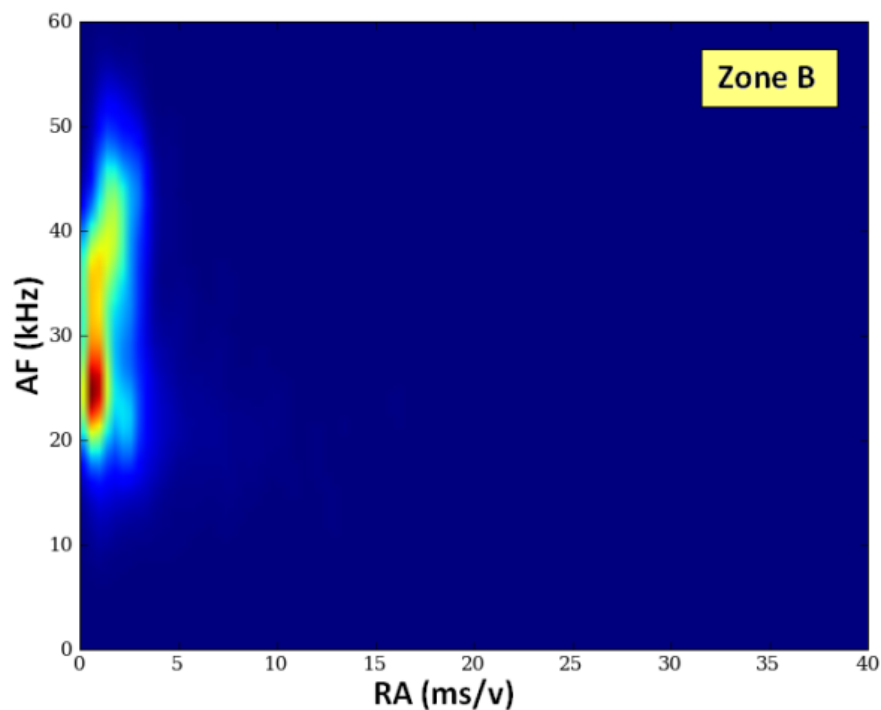
Figure 4. 38 Kernel Density Estimation of zone B

(a)

(b)

(c)

(d)
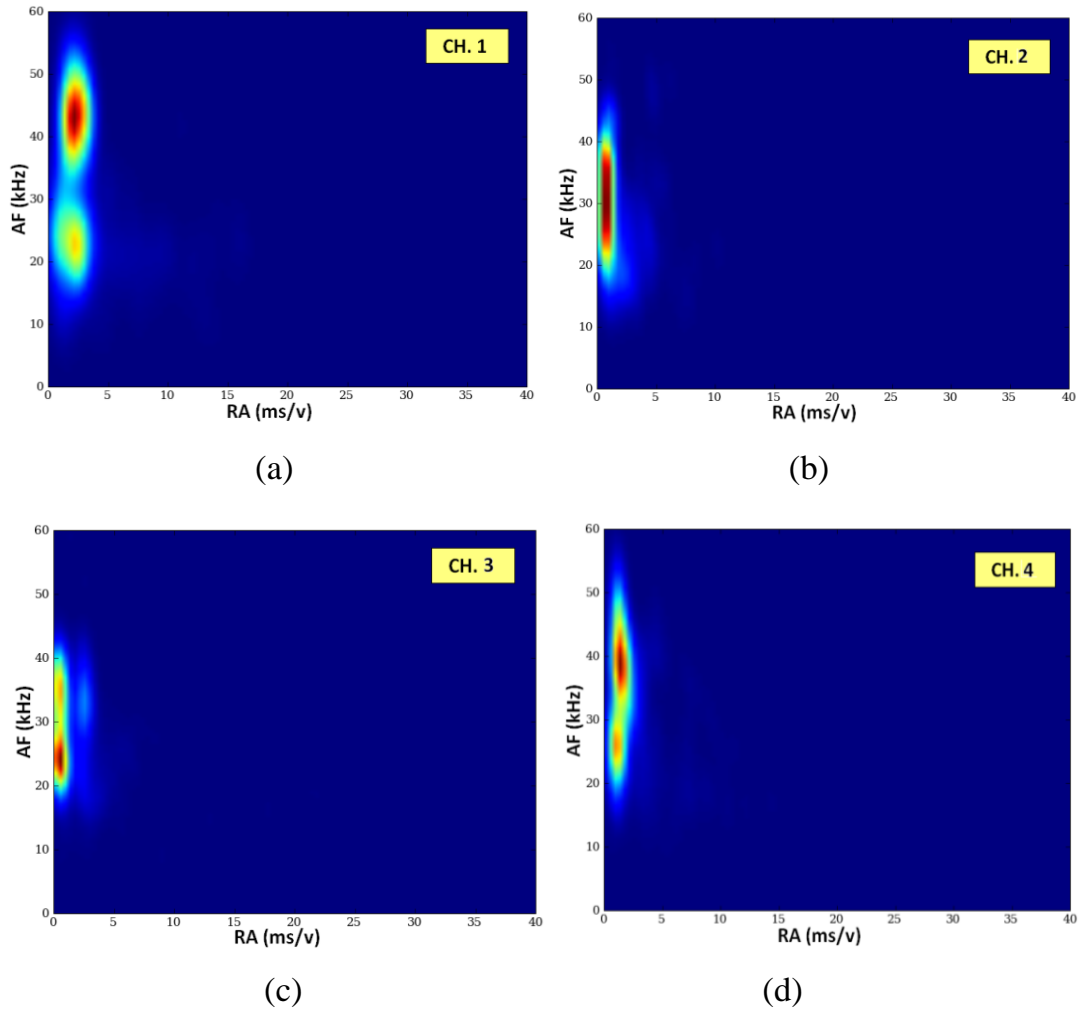
Figure 4. 39 Kernel Density Estimation of zone B (a) sensor 1, (b) sensor 2, (c) sensor 3 and (d) sensor 4.

4.4 Verification of AE due to corrosion alone

In order to investigate and distinguish only active corrosion, this test was performed for a short period, approximately 28 hours before any indication of micro and macro cracks occurred. This is representation of stage1 in Figure 4.22.

4.4.1 Experimental Procedure

The specimen was prepared and AE sensors were mounted and systems hardware was set-up as explained in the previous section (Section 4.3.1).

4.4.2 Results and Discussion

Figure 4.40 is a photograph of the top mortar surface after the end of the test (with sensor positions indicated) showing that no crack had occurred. The corrosion wires and corrosion product once the mortar had been removed is shown in Figure 4.41. It is evident that significant corrosion occurred in the upper wire.
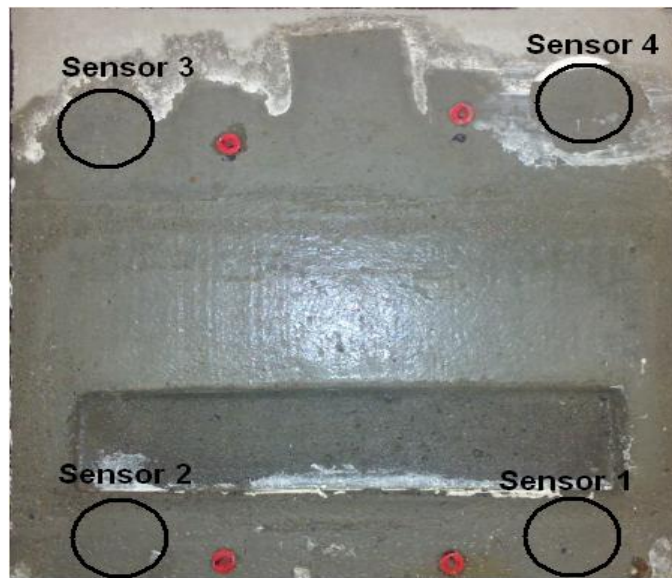
Figure 4. 40 Photo of top mortar surface

Figure 4. 41 Photograph of upper concrete surface and wires

All the detected and located signals with a minimum amplitude 45 dB detected by all sensors for almost 28 hr of continuous monitoring are shown in Figure 4.42 as signal amplitude against time and Figure 4.43 displays the cumulative hits against time. Figure 4.44 displays the same data set but this time as energy against time. The detected hits and their energy are attributed to active corrosion, noise and separation of the mortar from the concrete.
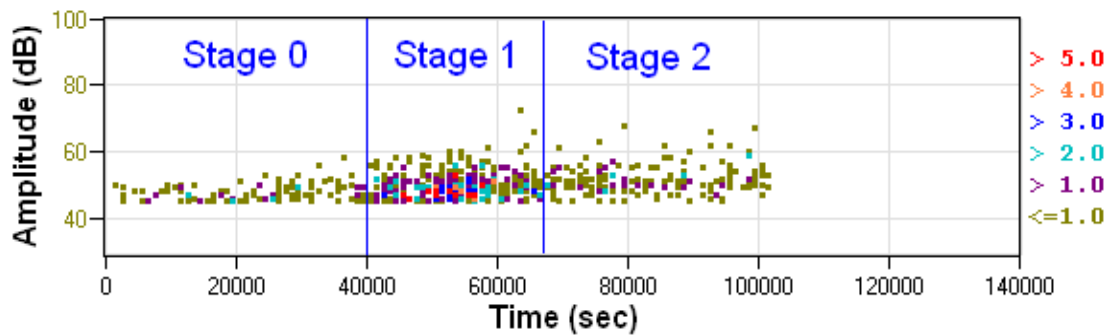
Figure 4. 42 Amplitude of detected signals for duration of investigation
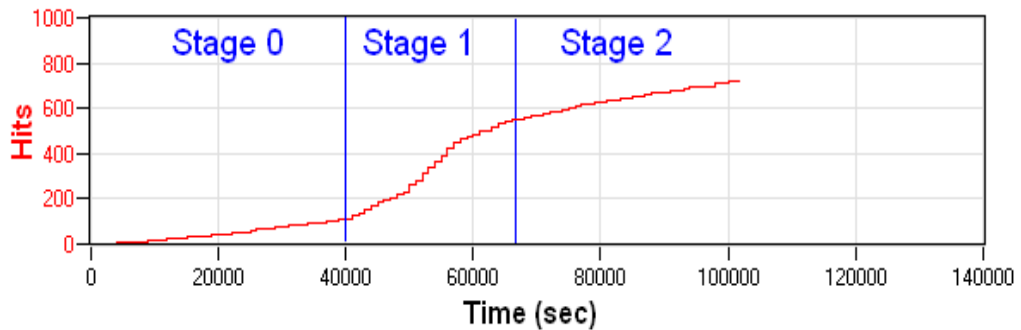
Figure 4. 43 Cumulative hits Vs time
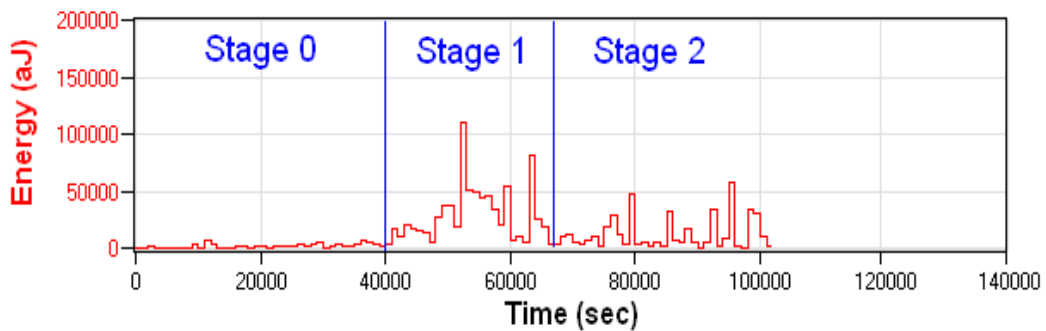
Figure 4. 44 Absolute energy of detected signals for duration of investigation

It can be noted that the whole time of the test can be divided into three significant stages, the first stage is stage 0 (0-40,000 sec) there are a small number of hits, low amplitude and with very low energy. The second stage (stage 1), which has an increase in the number of hits and higher energy emitted (peak of 12000 aJ) and is attributed to onset of corrosion and the build up of corrosion products on the corroding surface. The following decrease in the number of hits with smaller energy is attributed to a decrease in the rate of corrosion due to the corrosion products build up at stage 2. This behaviour is in remarkable agreement with the phases 1 and 2 of typical corrosion loss in the phenomenological model as illustrated in Figure 4.45 (Melchers 2006 and Ohtsu 2008). Figure 4.45 illustrates a typical corrosion loss during the corrosion process. The corrosion is initiated at phase 1. The corrosion rate process is controlled by the rate of transport of oxygen. At phase 2, the corrosion rate loss decreases due to the corrosion product build up on the corroding surface of the steel material which inhibits oxygen transfer. Further corrosion loss increases due to anaerobic corrosion in phases 3 and 4 (Robert 2006 and Ohtsu 2008).
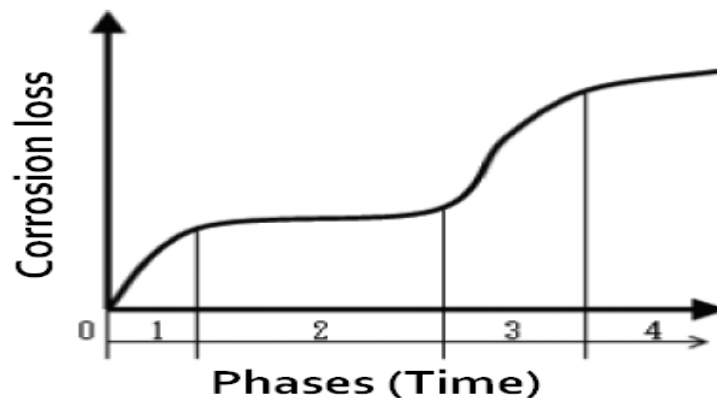
Figure 4. 45 Typical corrosion loss for steel in sea water immersion [Ohtsu 2008]

By comparing between stages in Figure 4.43 and phases in Figure 4.45 It can be seen that the stage 1 in Figures 4.43 could correspond to phase 1 in Figure

4.45 and the stage 2 corresponds to phase 2. It can be concluded that the onset of corrosion can be detected by determining the significant increase in AE activity and energy. Hence, the first increase of AE activity could be related to the onset of corrosion.

4.5 Reinforced concrete specimens test

4.5.1 Introduction

This section demonstrates the use of AE to monitor and assess stages of damage of reinforced mortar/concrete specimens induced by steel wire corrosion. A detailed description of the experimental work performed and the procedures followed are given. The materials, the initial casting and preparation of the specimens and test setup are described.

The data analysis involved the use of AE parameters such as hits, energy and location, corroborated by visual inspection as well as a study of the relationship between AF and RA values. KDEF was used to visualise these results.

4.5.2 Experimental procedure

- **Concrete and mortar preparation**

A concrete specimen (200×200×50mm) was manufactured .The water to cement ratio used was 0.4 and the material proportions were 1:2:2.5:0.4 by weight of cement, sand, aggregate and water respectively and the concrete design strength was about 58 MPa strength at 28 days.

Three days later, after the concrete specimen had completely cured, two wires (80 mm length and 4.88 mm diameter) combined were placed on the upper surface of this specimen. The mortar 200×200mm and 20 mm thickness was coated on the upper surface of the concrete. The water to cement ratio used

was 0.4 and the material proportions were 1:2:0.4 by weight of cement, sand and water respectively and the concrete design strength was about 56MPa strength at 28 days. The mortar should consist of one part cement to not more than three parts fine aggregate by weight. The construction is shown in Figure 4.46.

Figure 4. 46 Concrete and mortar specimen

- **Accelerated corrosion technique**

The corrosion acceleration set up was identical to previous tests, as described in section 4.3.1.

- **Acoustic Emission set-up**

Four AE sensors (R3I – 30 kHz resonant frequency) were mounted on the surface of the mortar using silicon sealant as an acoustic couplant and fixed on the upper surface of mortar with a U shaped plate attached with screws to hold the sensors and to ensure a good coupling. The threshold level for AE data acquisition was 40 dB. The sensitivity of the sensors was checked by using the

Hsu-Neilson source (Hsu 1979). A photograph of the set up is shown in Figure 4.47.
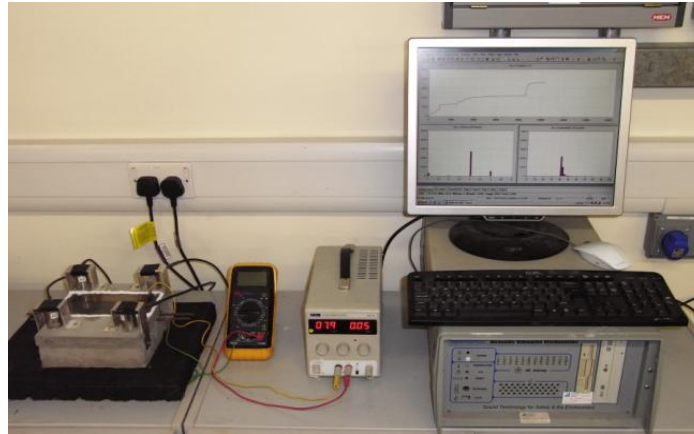
Figure 4. 47 Photograph of experimental set up

4.5.3 Results and discussion

AE monitoring was conducted for approximately seven days. As previously, to eliminate background noise a threshold of 48dB was used, this was found to provide a better distinction of location regions, the location of signals with minimum amplitude 48dB for the whole period of the test is shown in Figure 4.48. It can be noted that the highest hits concentration and highest energy region coincides with the position of maximum wire corrosion and the crack which was visibly observed post test as shown in Figures 4.49 and 4.50.
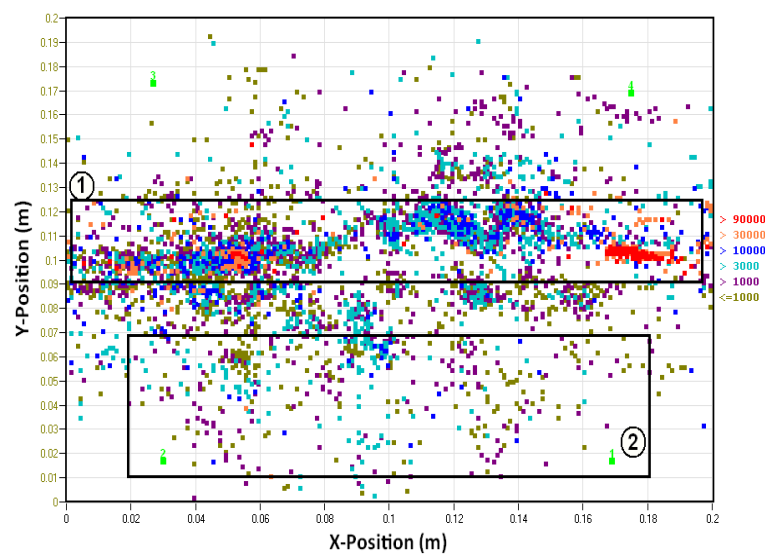
Figure 4. 48 Source locations for whole test with amplitudes greater than 48dB

Figure 4.49 is a photograph of the top mortar surface after the end of the test, showing the crack shape and sensors location on the mortar surface. Comparing this figure with the previous location plot reinforces the conclusion that the AE was detecting the concrete cracking as a result of wire corrosion within the specimen.
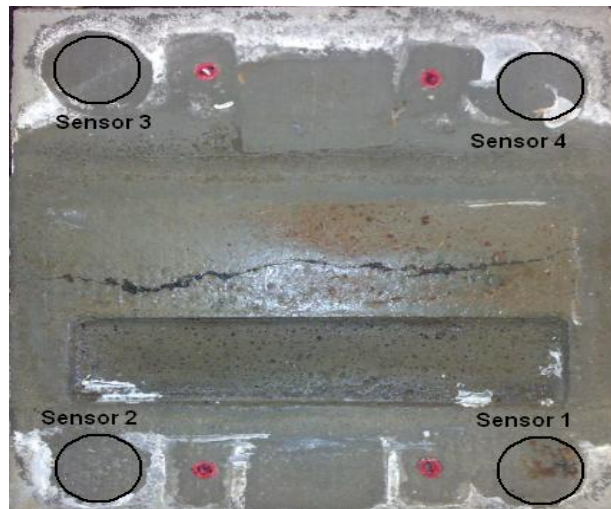
Figure 4. 49 Photo of top mortar surface

The corroded wires and corrosion product once the mortar had been removed is shown in Figure 4.50. It is evident that significant corrosion occurred in the upper wire and it was in this location that a large majority of AE signals were detected and located.

Figure 4. 50 Photo of upper concrete surface and wires

Two zones have been chosen as examples to distinguish between the crack area and noise and also to classify mode types. Areas were chosen based on visual observation (Figure 4.48 and Figure 4.49). Zone 1 in Figure 4.48 has a high concentration of hits and energy and is referred to the cracking area and zone 2 is no cracking area. Figure 4.51 (a and b) show the AF vs. RA values for different regions of concentration of events on the surface of mortar.

Figure 4.51 (a) shows the AF vs. RA for zone associated with the crack region containing a longitudinal crack due to the products of corrosion from wire 1 and wire 2. It can be seen that the most of data points have various AF values and low RA values (less than 10 ms/v) which is termed a "vertical trend". Therefore, based on Figure 2.5 (in section 2.4.1) and Figure 3.12 (in section 3.5.2), this indicates that the type of the crack is pure tensile. Figure 4.51 (b) shows the AF vs RA values for zone 2, an area where there is a low concentration of AE locations and no crack observed. It can be noted that in this area the RA value has a wide distribution (RA values 0-30 ms/v and AF values 10-40) (horizontal trend). This indicates that the trend indicates no tensile crack present.

(a)   (b)
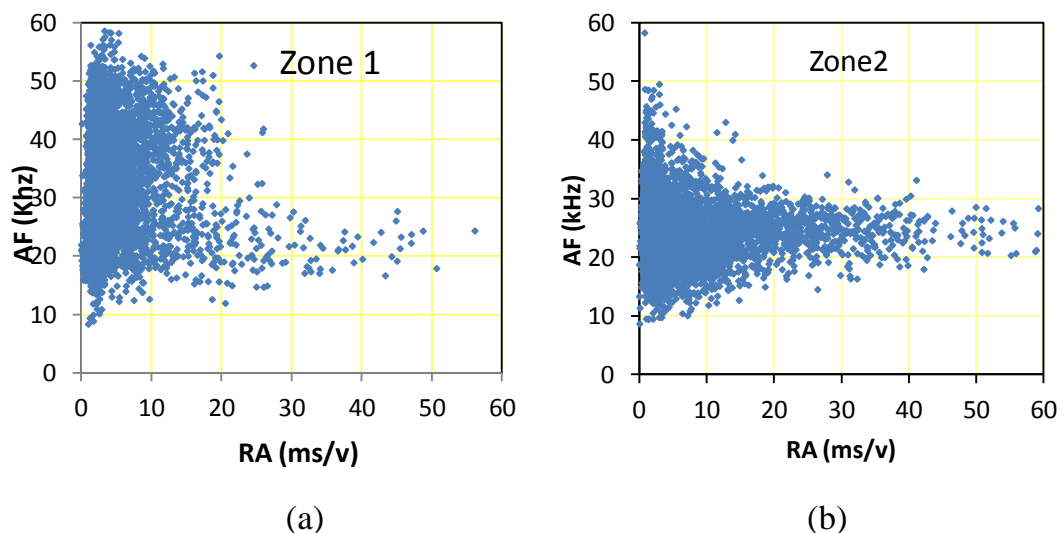
Figure 4. 51 Relation between the RA value and average frequency of (a) zone1 and (b) zone2

Furthermore, these areas can be visualised using KDEF as shown in Figure 4.52 (a and b). Regions of high concentration are more easily identified. The concentration value of the data is represented by different colours, brown for the highest number of data points and blue for lowest.

(a)   (b)
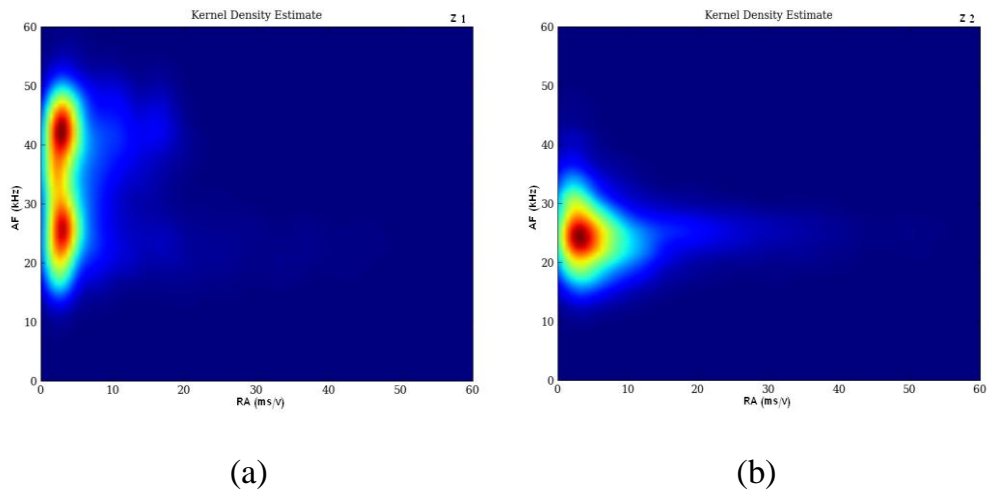
Figure 4. 52 Kernel Density Estimation of (a) zone 1 and (b) zone 2

All the detected and located signals with a minimum amplitude of 45 dB (better distinction of location regions) detected by all sensors for almost seven days of continuous monitoring are shown in Figure 4.53 as signal amplitude against time and Figure 4.54 displays the cumulative hits against time. Figure 4.55 displays the same data set but this time as energy against time. The detected energy is attributed to a number of sources; active corrosion, micro cracking, macro cracking, propagation of mortar cracking, separation of the mortar from the concrete and noise, as observed by visual inspection.
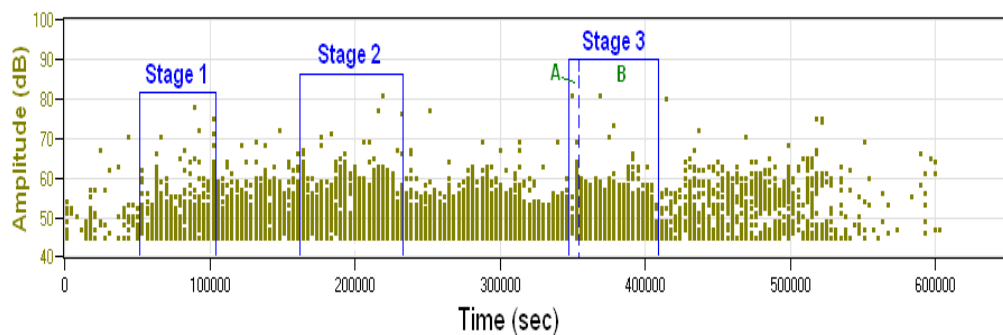
Figure 4. 53 Amplitude of detected signals for duration of investigation
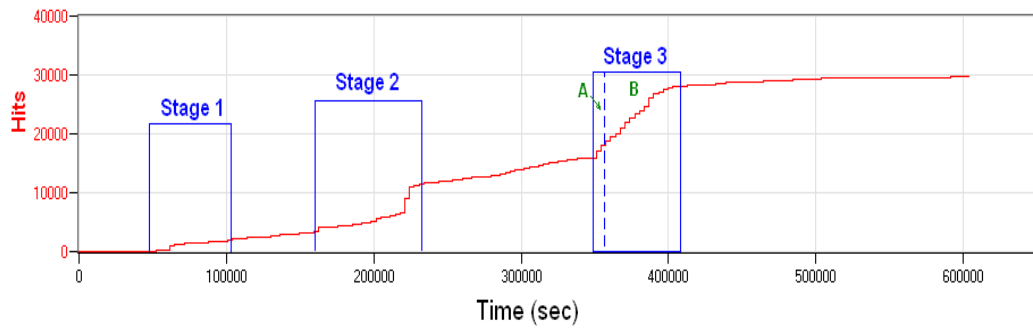
Figure 4. 54 Cumulative Hits Vs Time
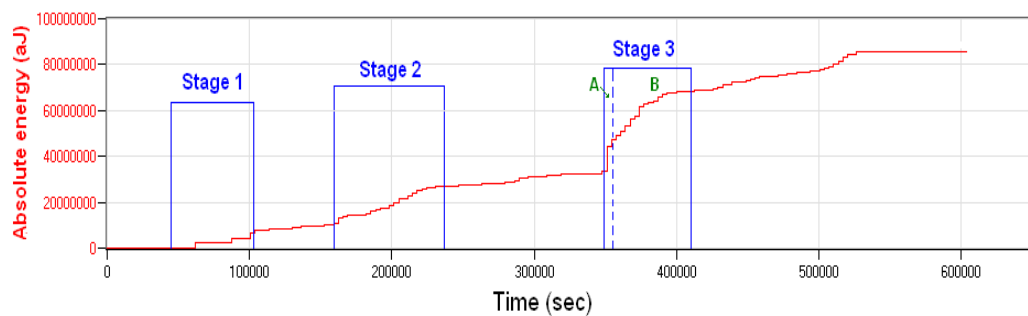
Figure 4. 55 Absolute energy of detected signals for duration of investigation

It can be seen that in Figure 4.53, 4.54 and 4.55 there are three significant stages which contain signals with a combination of large energy and an increased rate of hits. The increased hit rate, low amplitude and low energy in Stage 1 is attributed to the energy release from the corrosion activity (corrosion products accumulation at the interface of prestressed wire / mortar and concrete and the friction of corrosion products at the inner sides of the pores).

Stage 2 exhibits an increase in the number of hits with a slightly higher energy and amplitude and is attributed to micro crack formation.

Stage 3 is divided into two stages; A and B. In the first stage (3A) the sources emitted high energy and high amplitude over a short interval of time which is attributed to the energy release from the formation of the macro crack due to the products of corrosion from wire 1 and 2 as observed in visual inspection.

107

The following increase in the number of hits with smaller energy, smaller amplitude and longer interval of time than stage 3A is attributed to macro crack propagation.

It can thus be noted that different damage modes, including corrosion activity, micro/macro cracking formation and crack propagation) generate different types of AE signals with varying amplitudes and absolute energy emitted. The increase in the number of hits, low amplitude and low energy is attributed to the energy release from the corrosion activity (corrosion products accumulation at the interface reinforced wire / mortar and concrete and the friction of corrosion products at the inner sides of the pores).

The micro cracks emit a large number of signals with smaller amplitudes whereas macro cracks emit less signals but with larger amplitude. In addition, the absolute energy released from macro crack formation is higher than micro crack formation. The results have shown that the gradual increase of the number of hits emitted with higher energy than those due to micro crack formation and lower than those due to macro crack formation correspond to macro crack propagation.

The results show that the AE parameters behaviour (trend) gained from AE monitoring of stages of damage of reinforced mortar/concretes specimen due to wire corrosion is similar to prestressed mortar/concretes specimen with the same properties and under the same conditions. However, the energy emitted from signals of corrosion activity and crack of prestressed concrete is more than that from reinforced concrete. Furthermore, the corrosion rate process and crack formation in prestressed concrete is quicker than reinforced concrete. This result shows good agreement with the result demonstrated by Li et al. (2011). It has been reported that the corrosion rate of prestressing steel strands in concrete increases with the increase of the level of stresses applied (Li. et al. 2011).

4.6   Conclusions

The overall conclusions are summarized as follows:

- Laboratory-based tests were conducted to determine the applicability of the method to provide qualitative information concerning the condition of field prestressed concrete structures.

- This work on specimens representative of prestressed and reinforced concrete/mortar structures has provided invaluable information and experience in setting up and AE monitoring to assess and identify the corrosion process and damage stages of prestressed and reinforced concrete/mortar structures due to corrosion steel.

- The results confirm that AE could be used be effectively to detect and locate damage areas at a very early stage in representative specimens due to corrosion.

From these laboratory investigations and data analyses it has been demonstrated that:

- Different damage modes, including corrosion activity, micro/macro cracking formation, crack propagation and wire failure generate different of types of AE signals with varying amplitudes and absolute energy emitted.

- An increase in the number of hits, of low amplitude and low energy is attributed to the energy release from the corrosion activity (corrosion products accumulation at the interface prestressed wire / mortar and concrete and the friction of corrosion products at the inner sides of the pores).

- Micro cracks emit a large number of signals with smaller amplitudes whereas macro cracks emit less signals but with larger amplitude. In addition, the absolute energy released from macro crack formation is higher than micro crack formation. The results have shown that the gradual

increase of the number of hits emitted with higher energy than those due to micro crack formation and lower than those due to macro crack formation correspond to macro crack propagation.

- From analysis of the data it was demonstrated that the detected crack types can be distinguished and classified by identifying the relations between RA/AF values.

- The relationship between RA value and AF value can be used to determine the crack area and classify it as either tensile crack type, other type (shear movement) or no crack. If the relationship of RA/AF value has vertical trend this indicates tensile cracks However, if the relationship of RA/AF value has a horizontal trend this indicates signals arising from a region containing no tensile cracks.

- Use of KDEF provides better visualisation of the data to represent clearly the RA/AF values trend so it is recommended.

- The data analysis has shown that the RA/AF value trends are not affected by distance from damage source or sensor position and the number of sensor, making this an ideal approach.

- The AE parameters behaviour (trend) gained from AE monitoring of stages of damage of reinforced mortar/concrete specimen due to wire corrosion is similar to those observed in prestressed mortar/concrete specimen of the same properties and under the same conditions. However, the energy emitted from signals of corrosion activity and cracking of prestressed concrete is higher than that from reinforced concrete and the corrosion rate process and crack formation in prestressed concrete is faster than that in reinforced concrete.

CHAPTER 5: VALIDATION STUDY

5.1 Introduction

This chapter aims to validate the Acoustic Emission technique for use in the monitoring and assessment of the stages of damage in reinforced mortar/concrete specimens induced by steel wire corrosion, by using larger scale specimens.

A detailed description of the experimental work performed is presented including the procedures followed during the laboratory phase of the project and details of the materials, the initial casting and preparation of the specimens and test setup. Furthermore, the data acquired by the AE system is analysed by using the relationship between RA values and average frequencies for classification of crack type in reinforced concrete/mortar structures.

Two laboratory tests were performed on larger reinforced concrete specimens and this chapter give details for one such test which is indicative of both tests.

5.2 Aims and objectives

The aims and objective of this experiment using parameter analysis were:

- To assess the ability of AE to detect, locate and characterise damage areas at a very early stage in large-scale representative specimens due to corrosion.
- To investigate and distinguish active corrosion and stages of the corrosion process.
- To detect, locate, distinguish and classify the detected crack types.
- To investigate and distinguish micro cracks, macro cracks and crack propagation.
- To validate the AE technique for monitoring larger structures and real prestressed concrete pipes.

5.3 Experimental procedure

5.3.1 Concrete and mortar preparation

The concrete specimen (600×600×50mm) was prepared according to the technical specification for prestressed concrete cylinder pipe manufacturing used in GMRP, which is in accordance with AWWA C301-92 (Standard for Pre-stressed Concrete Pressure Pipe, Steel Cylinder Type, for water and other Liquids.)

The water to cement ratio used was 0.4 and the material proportions were 1:2:2.5:0.4 by weight of cement, sand, aggregate and water respectively and the concrete design strength was about 58.5MPa strength at 28 days.

Three days later, after the concrete specimen was completely cured, the wires combined with their holding frame were placed on the upper surface of this specimen. Mortar of 600×600mm and 20 mm thickness was coated on the upper surface of the concrete. The water to cement ratio used was 0.4 and the material proportions were 1:2:0.4 by weight of cement, sand and water respectively and the concrete design strength was 56.5MPa strength at 28 days. The mortar should consist of one part cement to not more than three parts fine aggregate by weight. The construction is shown in Figure 5.1
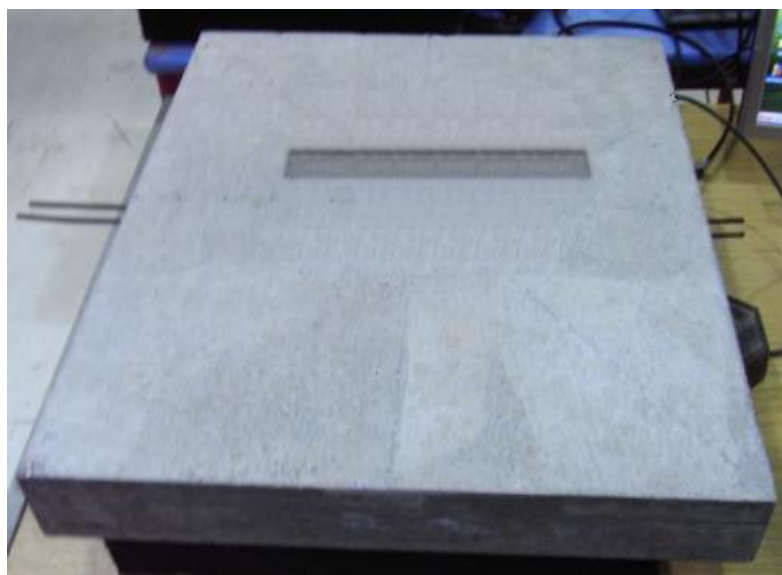
Figure 5. 1 Concrete / mortar specimen

5.3.2 Accelerated corrosion Technique

Wire corrosion was induced by impressed current (500µA/cm²). The prestressed wires were connected in an electrical circuit with positive pole of power supplier and the negative pole connected with a stainless steel plate (30×300 mm) resting on the upper mortar. A 4% NaCl solution was poured on the surface of the mortar. Silicon sealant was used to pool the solution on the upper surface (Elfergani et. al. 2011).

5.3.3 Acoustic Emission Set-up

Four AE sensors (R3I − 30 kHz resonant frequency) were mounted on the surface of the mortar using silicon sealant as an acoustic couplant and fixed on the upper surface of mortar with a U shaped plate attached with screws to hold the sensors and to ensure a good coupling. The threshold level for AE data acquisition was 40 dB. The sensitivity of the sensors was checked by using the Hsu-Neilson source (Hsu 1981). A photograph of the set up is shown in Figure 5.2.
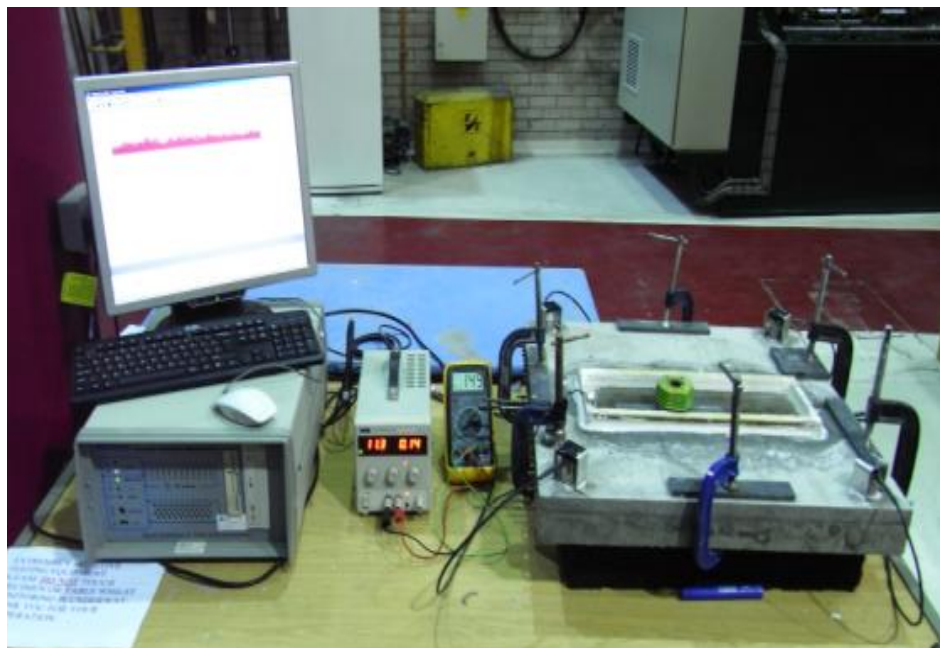
Figure 5. 2 Photograph of experimental set up

5.4 Results and discussion

AE monitoring was conducted for approximately seven days. In order to eliminate background noise and provide a better distinction of location regions a threshold of 45dB was used for data analysis. The location of signals with minimum amplitude 45dB for the whole period of the test is shown in Figure 5.3. It can be noted that the highest hits concentration and highest energy region coincides with the position of maximum wire corrosion and the crack position, which was monitored visually at regular intervals throughout the test and photographed post test as shown in Figure 5.4.

Figure 5.4 is a photograph of the top mortar surface after the end of the test (with sensor positions indicated) showing the crack shape. Comparing this figure with the previous location plot reinforces the conclusion that the AE was detecting the concrete cracking as a result of wire corrosion within the specimen.
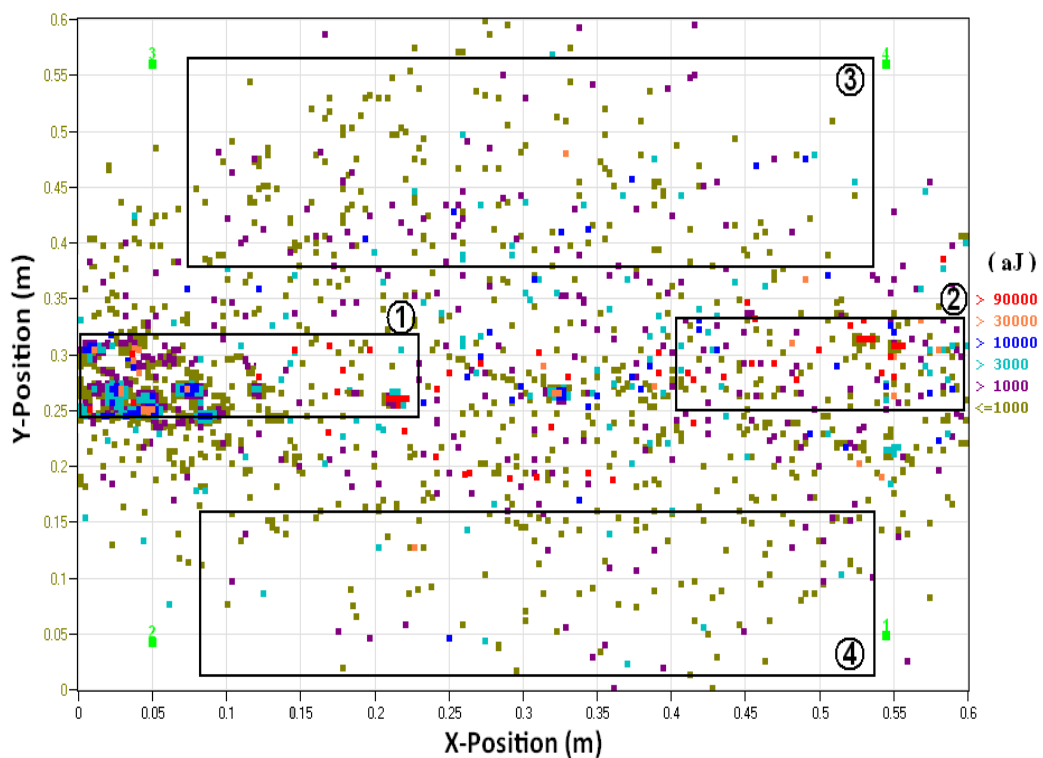
Figure 5. 3 Source locations for whole test with amplitudes greater than 45dB
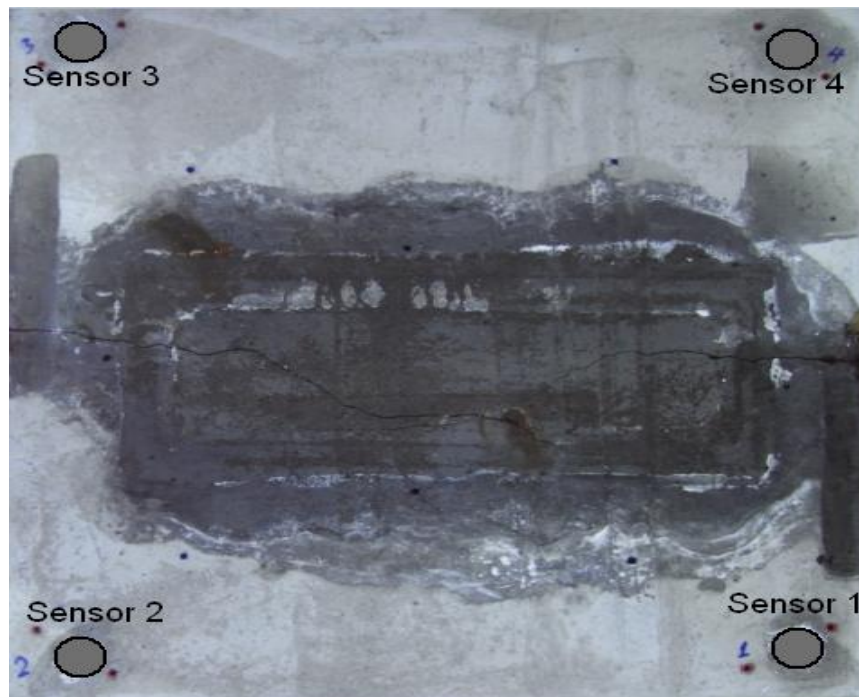
Figure 5. 4 Photo of top mortar surface

Four zones have been chosen as examples to distinguish between the crack area and noise and also to classify mode types. Areas were chosen based on visual observation (Figure 5.3 and Figure 5.4). Zones 1 and 2 in Figure 5.3 have a high concentration of hits and energy and are referred to the cracking areas and zone 3 and 4 are no cracking areas.

Figure 5.5 (a, b, c and d) shows the AF vs. RA values for different regions of concentration of events on the surface of the mortar. Figure 5.5 (a and b) shows the AF vs. RA for zones 1 and 2 associated with the crack region containing a longitudinal crack due to the products of corrosion from wires . It can be seen that the most of data points have various AF values and low RA values (less than 10 ms/v) which is termed a "vertical trend". Therefore, based on Figure 2.5 (in section 2.4.1) and Figure 3.12 (in section 3.5.2), this indicates that the type of the crack is pure tensile. Figure 5.5 (c and d) shows the AF vs RA values for zones 3 and 4, areas where there is a low concentration of AE locations and no crack observed. It can be noted that in

115

this area the RA value has a wide distribution (RA values 0-30 ms/v and AF values 10-40) (horizontal trend). This trend indicates no tensile crack present.

(a)

(b)

(c)

(d)
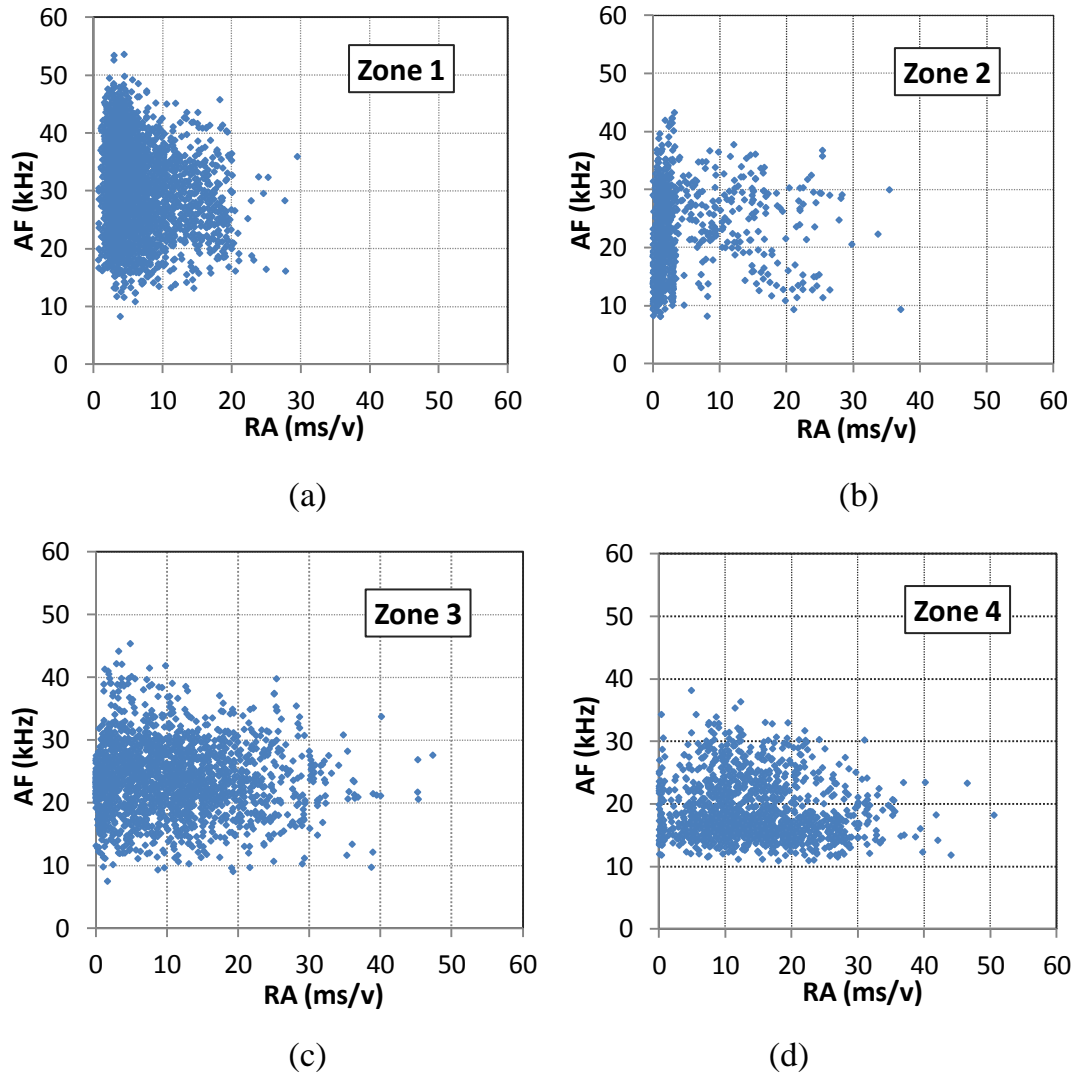
Figure 5. 5 Relation between the RA value and average frequency of (a)zone1, (b) zone2, (c) zone3 and (d) zone 4

Furthermore, these figures can be represented by using a KDEF for improved visualisation as shown in Figure 5.6 (a, b, c and d). Regions of high concentration are more easily identified. The concentration value of the data is represented by different colours, brown for the highest concentration of data points and blue for lowest.
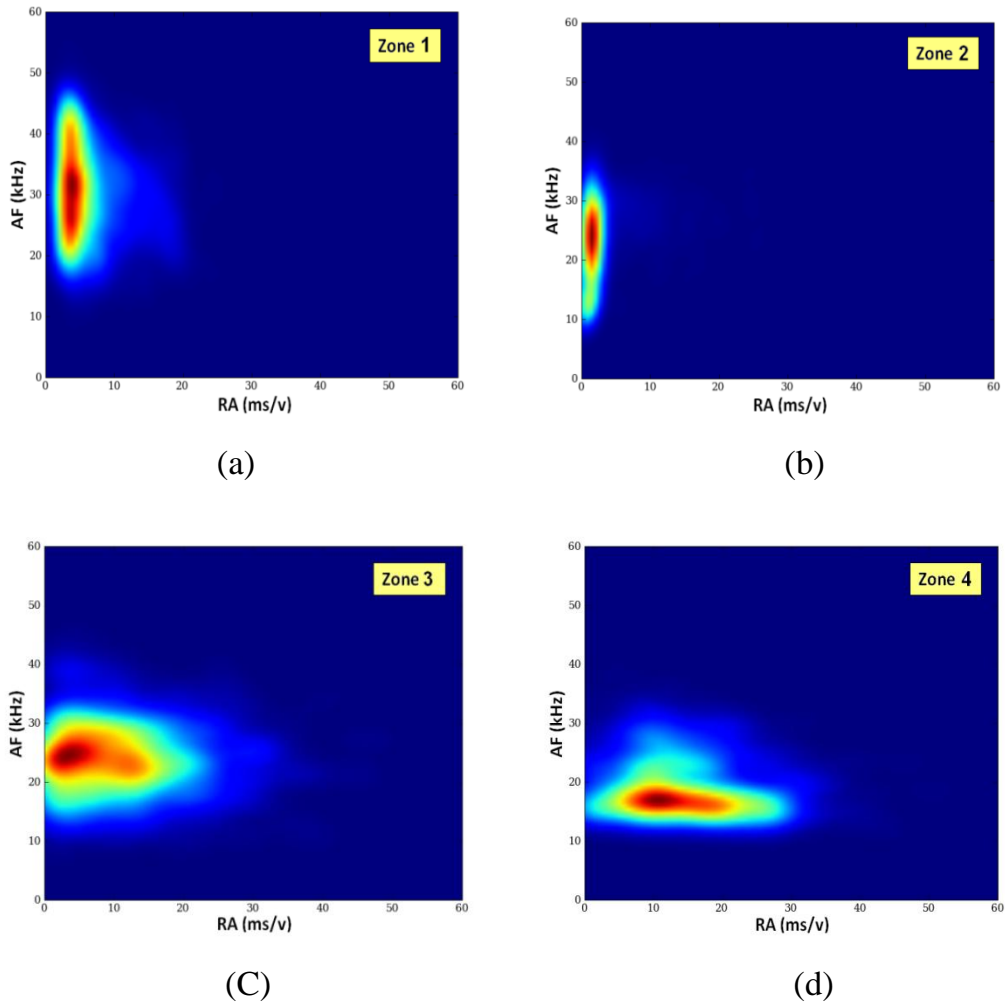
Figure 5. 6 Kernel Density Estimation of (a) zone 1 (b) zone 2 (c) zone 3 and (d) zone 4

All the detected and located signals with a minimum amplitude of 45 dB detected by all sensors for almost seven days of continuous monitoring are shown in Figure 5.7 as signal amplitude against time and Figure 5.8 displays the cumulative hits against time. Figure 5.9 displays the same data set but this time as energy against time.

The detected energy is attributed to a number of sources; active corrosion, micro cracking, macro cracking, propagation of mortar cracking, separation of the mortar from the concrete and noise, as observed by visual inspection.
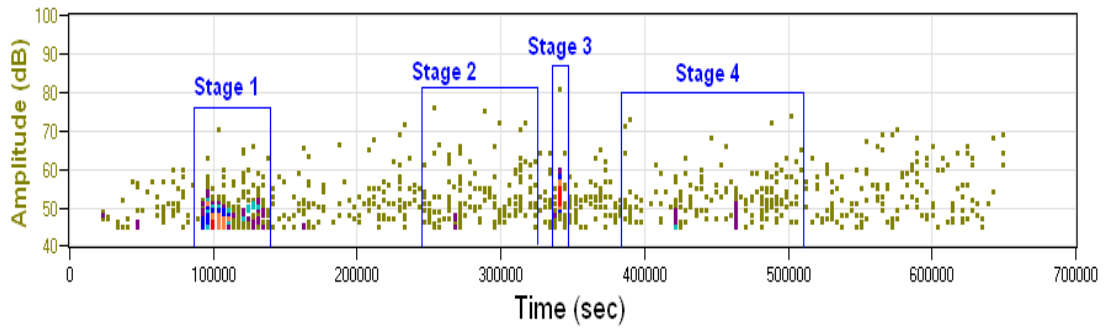
Figure 5. 7 Amplitude of detected signals for duration of investigation
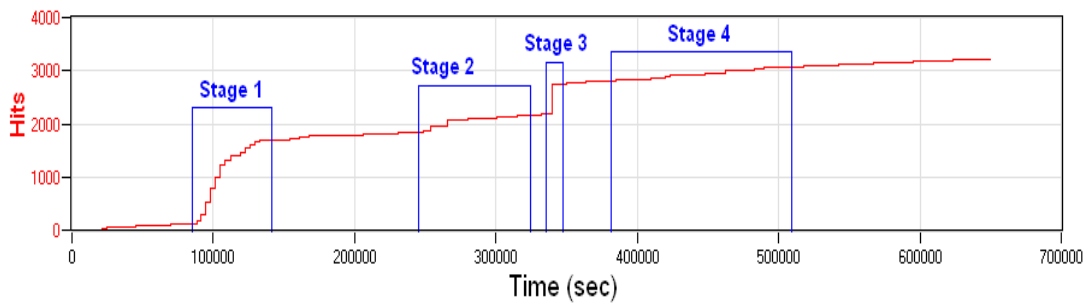
Figure 5. 8 Cumulative Hits Vs Time
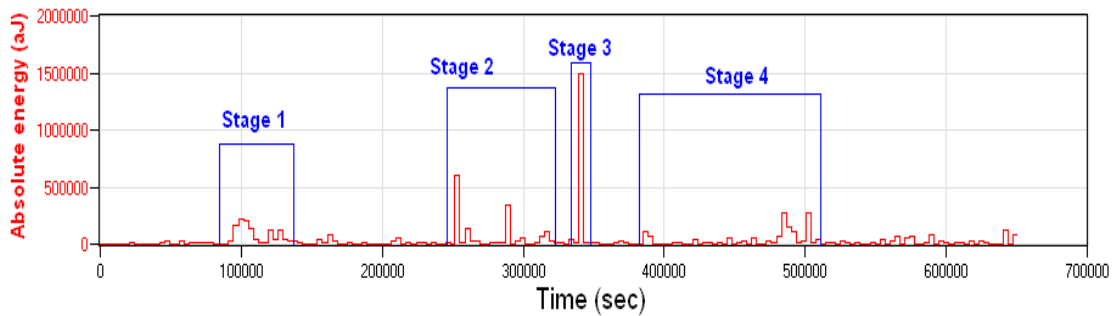
Figure 5. 9 Absolute energy of detected signals for duration of investigation

It can be seen that in Figure 5.7, 5.8 and 5.9 there are four significant stages which contain signals with a combination of high amplitude, large energy and an increased rate of hits. The increased hit rate, low amplitude and low energy in stage 1 is associated with the energy release from the corrosion activity (corrosion products accumulation at the interface of reinforced wire / mortar and concrete and the friction of corrosion products at the inner sides of the pores).

118

Stage 2 exhibits an increase in the number of hits with a slightly higher energy and amplitude and is attributed to micro crack formation. In Stage 3, the sources emitted high energy and high amplitude over a short interval of time which is attributed to the energy release from the formation of the macro crack due to the products of corrosion from wire 1 and 2 as observed in visual inspection. The following increase in the number of hits with smaller energy and smaller amplitude than Stage 3 and longer interval of time than Stage 2 is attributed to macro crack propagation as shown in Stage 4. These results are corroborated by visual observations throughout the test.

By comparing these results with visual observations during the test, the increase in the hits rate low amplitude and small energy is attributed to the energy release from the corrosion activity (corrosion products accumulation at the interface reinforced wire / mortar and concrete and the friction of corrosion products at the inner sides of the pores). This result shows a good agreement with results demonstrated by Assouli et al (2005) and Ohno and Ohtsu (2010). A large number of signals with smaller amplitudes is associated with micro cracks events. Macro crack events emit fewer signals in a small period but with larger amplitude and high energy. This result shows a good agreement with results demonstrated by Colombo et al (2003). By comparing between macro crack and micro crack events, the results and visual observation shown that the amplitude and absolute energy released from macro crack formation are higher than micro crack formation. This result shows good agreement with results demonstrated by Aggelis (2011). Furthermore, the gradual increase of the number of hits emitted with higher energy than those due to micro crack formation and lower than those due to macro crack formation correspond to macro crack propagation. This result shows good agreement with the result demonstrated by Aggelis (2011) and Muralidhara (2010).

In addition, the results show that the AE parameters behaviour (trend) gained from AE monitoring of different damage stages of large scale reinforced mortar/concretes specimen due to wire corrosion is similar to small scale

mortar/concrete specimen with the same properties and under the same conditions. This suggests that the AE technique is valid for any size of structure and real concrete pipes, although large scale monitoring tests would be required to fully validate the technique for use in the field.

5.5 Conclusion

This chapter investigated the use of AE to monitor, detect and locate damage in larger-scale reinforced mortar/concrete specimen (larger than the small scale specimen reported previously Chapter 4 by 9 times OF 200×200 mm specimen). The aim of the research was to demonstrate the validity of AE monitoring at a larger scale and hence the potential for monitoring real structures such as prestressed concrete pipes.

- The results show that the AE techniques can be successfully used to detect, locate and characterise the different stages of damage from larger-scale reinforced concrete/mortar specimen thus the use in real structures such as large concrete pipes is promising, although some limitations were demonstrated.

- The results confirm that AE could be used effectively to detect and locate damage areas at a very early stage in representative specimens due to corrosion.

- The AE parameters analysis of correlation amplitude, hits and energy versus time plots were shown to be useful indicators of corrosion onset, micro crack, macro crack and crack propagation.

- More advanced AE parameters data analysis (by identifying the relations between RA/AF values) was successfully used to determine the crack area and classify it as either a tensile crack type, other type (shear movement) or

no crack. If the relationship of RA/AF value has vertical trend this indicates tensile cracks. However, if the relationship of RA/AF value has a horizontal trend this indicates signals arising from a region containing no tensile cracks.

- The AE parameters behaviour (trend) observed during AE monitoring of different damage stages of larger scale reinforced mortar/concrete specimens due to wire corrosion shows a similar behaviour to those observed in small scale reinforced mortar/concrete specimen of the same properties and under the same conditions. However, the number of signals detected for large scale is less than small scale specimens due to attenuation of the signals over the larger distance between the sources and sensors.

- This test on larger scale specimen suggested it to be practical approach for real reinforced concrete structures and prestressed concrete pipes.

- In the practical application of pipes line, there are some factors that should be considered
    - Sensor numbers and their location in real pipes.
    - Environmental noise.
    - Moisture and temperature changes effects.

CHAPTER 6: CONCLUSIONS AND RECOMMENDATION FOR FUTURE WORK

6.1 Conclusions

This thesis has investigated the role of acoustic emission for the Structural Health Monitoring (SHM) of different sizes of laboratory based prestressed and reinforced composite concrete/mortar specimens. The aim of this research was to further the understanding of the AE technique for use in global and local structural monitoring of concrete/mortar damage for the evaluation of prestressed concrete pipes and reinforced concrete structures. This research has lead to the development of an innovative non-destructive corrosion detection technique where crack types can be distinguished by advanced AE analysis techniques. The developed procedures can be trialled in the field for commercial exploited in major prestressed and reinforced concrete pipe structures such as those used in the Great Man-Made River Project in Libya. The early detection of damage, including corrosion, in such structures is of paramount importance to avoid catastrophic failures which can lead to loss of water to homes and businesses.

Key findings of the research are:-

- The Time of Arrival (TOA) technique was successfully used to locate signals on reinforced and prestressed composite concrete/mortar specimens and has an acceptable accuracy, the average error is approximately 6 mm for this sample.

- A thorough investigation of wave propagation and attenuation in composite concrete/mortar specimens was completed and the following conclusions were drawn:

  - Propagation of the elastic waves through the surface of the mortar parallel to the interface of concrete/mortar is affected by the wire direction in the sample. This needs to be taken into consideration when mounting the sensors and locating the crack in the pipe. The

wave propagation through the mortar specimen is faster along the wire length when compared with other directions, suggesting that the wave travels along the steel wire, which acts as a wave guide.

- The attenuation through the mortar is less than that through concrete.

- Attenuation of the elastic waves in crossing the concrete-mortar wall of the pipe is very high and is affected by the complex nature of the concrete, steel plate, and concrete-mortar interaction. The reason for high attenuation is complex, due to several factors such as waves passing through different medias, scattering due to the presence of aggregate and reflections from the steel plate and/or concrete-mortar interface.

- Since the attenuation of waves through the thick composite wall is high, the noise effect inside the pipe due to water flow is considered to be very small.

- Primary tests were performed to investigate pure tensile crack type signals and to fully understand the trend of RA and AF values.

- The results show that use of the AE technique as a non-destructive technique can detect the onset of corrosion activity in wire in the interface between prestressed concrete and mortar as found in prestressed concrete pipes.

- The results show that by correlation between three parameters of classical AE analysis techniques (traditional parameters), damage can be detected and located whilst the corrosion area, macro crack and crack propagation can be identified. However, it cannot classify the crack type.

  - Different damage modes, including corrosion activity, micro/macro cracking formation, crack propagation and wire failure generate different of types of AE signals with varying amplitudes and absolute energy emitted.

  - An increase in the number of hits of low amplitude and low energy is attributed to the energy release from the corrosion activity (corrosion

products accumulation at the interface of prestressed wire / mortar and concrete and the friction of corrosion products at the inner sides of the pores).

- Micro cracks emit a large number of signals with smaller amplitudes whereas macro cracks emit less signals but with larger amplitude. In addition, the absolute energy released from macro crack formation is higher than that from micro crack formation. The results have shown that the gradual increase of the number of hits emitted with higher energy than those due to micro crack formation and lower than those due to macro crack formation correspond to macro crack propagation.

- A novel analysis approach has been used on composite materials (concrete, mortar and steel) to evaluate differing crack types by combination between the classical acoustic emission analysis technique and advanced analysis (RA and AF values); results proved the effectiveness of the developed techniques for damage detection and classification of crack types.

- From analysis of the data it was demonstrated that the detected crack types can be distinguished and classified by identifying the relations between RA/AF values.

- The relationship between RA value and AF value can be used to determine the crack area and classify it as either tensile crack type, other type (shear movement) or no crack. If the relationship of RA/AF value has vertical trend this indicates tensile cracks However, if the relationship of RA/AF value has a horizontal trend this indicates signals arising from a region containing no tensile cracks.

  - The data analysis has shown that the RA/AF value trends are not affected by distance from damage source or sensor position, making this an ideal approach.

- The AE parameters behaviour (trend) observed during AE monitoring of stages of damage of reinforced mortar/concrete specimen due to wire corrosion is similar to those observed in prestressed mortar/concrete

specimen of the same properties and under the same conditions. However, more energy is emitted from signals of corrosion activity and cracking of prestressed concrete than from reinforced concrete corrosion cracking and the corrosion rate process and crack formation in prestressed concrete is quicker than that in reinforced concrete.

- The AE parameters behaviour (trend) observed during AE monitoring of different damage stages of larger scale reinforced mortar/concrete specimens due to wire corrosion shows a similar behaviour to that observed in small scale reinforced mortar/concrete specimen of the same properties and under the same conditions. However, the number of signals detected for large scale specimens is less that in than small scale specimens due to attenuation of the signals over the larger distance between the sources and sensors.

- The study has demonstrated that the AE technique is valid in larger scale monitoring and hence the potential for monitoring real structures such as prestressed concrete pipes.

- It has been shown that by using AE and the relationship between RA and AF value, the crack area can be located and identified. Hence, it could be possible to provide a corrosion alarm and location prior to any wire breaks. Furthermore, by knowing the crack type it is possible to identify the damaged area before the mortar completely fails.

- The use of Kernel Density Estimation Function (KDEF) provides improved visualisation of the data to represent clearly the RA/AF values.

- The results offer encouragement to the use of the AE technique to detect early corrosion and macro cracks in large concrete pipe structures.
    - The primary aim is to obtain a reliable relationship that can be applied during the AE monitoring for condition assessment of a structural component. The methodology developed here could

contribute to an early warning system that is able to detect precursors of a failure.

- By identifying a period before failure assets can be protected.

- Tests on larger scale specimens proved the techniques are a practical approach for real reinforced concrete structures and prestressed concrete pipes.

- In the practical application of pipes line, there are some factors that should be considered
    - Sensor numbers and their location in real pipes.
    - Environmental noise.
    - Moisture and temperature changes effects.

- Although the AE technique may have some limitations for underground pipes, it could be very successful in other reinforced structures such as buildings, bridges and dams.

6.2 **Recommendations for further work**

In light of the conclusions of this work, the following topics are recommended for further study:

- Further investigation into the applicability of AE techniques for the monitoring real buried pipes, including access, long term stability and background noise.

- More experimental work should be conducted to investigate the influence of temperature variations on the AE detection of the corrosion.

- Experiments are required to examine the effect of cathodic protection on AE waves.

- More investigation should be conducted to detect hydrogen embrittlement stress cracking due to apply cathodic protection.

CHAPTER 7: REFERENCES

- Acciani G., Fornarelli G., Giaquinto A., Maiullari D. and Brunetti G., 2008, Non-Destructive Technique for Defect Localization in Concrete Structures Based on Ultrasonic Wave Propagation, ICCSA, Part II, LNCS 5073, pp 541-554.

- Aggelis D., Soulioti D., Sapouridis N., Barkoula N., Paipetis A. and Matikas T., 2011, Acoustic emission characterization of the fracture process in fibre reinforced concrete. Construction and Building Materials, 25, pp 4126–4131.

- Ahmad, S., 2003, Reinforcement corrosion in concrete structures, it's monitoring and service life prediction - A review, Cement & Concrete Composites, Vol. 25, pp. 459-471.

- AL NAHR CO., LTD., July 1999, Great Man-Made River Project phase III AL gardabiya/assdada link, Technical Specification for PCC Pipe Manufacturing.

- Aggelis D., 2011, Classification of cracking mode in concrete by acoustic emission parameters, Mechanics Research Communications, 38, pp 153-157.

- Ann K.Y., Ahn J. H. and Ryou J. S., 2009, The importance of chloride content at the concrete surface in assessing the time to corrosion of steel in concrete structures, Construction and Building Materials, 23, pp 239–245.

- Assoulia B., Simescua F., Debickib G., and Idrissia,H., 2005, Detection and identification of concrete cracking during corrosion of reinforced

concrete by acoustic emission coupled to the electrochemical techniques, NDT&E International, 38, pp. 682–689.

- ASTM A663/A663M-89. 2000. Specification for Steel Bars, Carbon, Merchant Quality, Mechanical Properties, American Society for Testing and Materials

- ASTM C876-91. 1999. Standard Test Method for Half-Cell Potentials of Uncoated Reinforcing Steel in Concrete, American Society for Testing and Materials.

- ASTM E 976 .1994. Standard guide for determining the reproducibility of acoustic emission sensor response, American Society for Testing and Materials.

- AWWA C301-92. 1999. Standard for Prestressed Concrete Pressure Pipe, Steel Cylinder Type, for Water and Other Liquids. American Water Works Association.

- Baron J. A. and Ying S.P., 1987, Acoustic Emission Source Location, Nondestructive Testing Handbook, American Society for Non-destructive Testing, Columbus, OH,5,6, pp 136-154.

- Baxter M., 2007, Ph.D. Thesis, Damage assessment by Acoustic Emission (AE) during landing gear fatigue testing, Cardiff School of Engineering, Cardiff University.

- Beck P., 2004, PhD Thesis, Quantitative damage assessment of concrete structures using acoustic emission, Cardiff School of Engineering, University of Wales, Cardiff.

- Benin A. V., 2006, Analysis of the Acoustic Emission Technique Used in Laboratory Tests of Reinforced-Concrete Structures, ISSN 1061-8309, Russian Journal of Non destructive Testing, Vol. 42, No. 12, pp. 790–793.

- Benson S.D.P., 2003, PhD Thesis, CARDIFRC®: development and constitutive behaviour, Cardiff School of Engineering, University of Wales, Cardiff.

- Berkeley K.G.C. and Pathmanaban S., 1990, Cathodic Protection Reinforced Steel in Concrete, Butterworth.

- Bertolini L., Elsener B., Pedeferri P. and Polder R. P., 2004, Corrosion of Steel in Concrete. Morlenbach: WILEY-VCH.

- Bond L., Kepler W. and Frangopol D., 2000, Improved, Assessment of mass concrete dams using acoustic travel time tomography Part I theory, Construction and Building Materials, 14, pp 133-146.

 Boving K.G., 1989, NDE Handbook: Non-destructive examination methods for condition monitoring, Butterworths, London.

- Bradford, S. A., 1993. Corrosion Control. New York: Van Nostrand Reinhold.

- Broomfield J. P., Davies K., Hladky K., 2002, The use of permanent corrosion monitoring in new and existing reinforced concrete structures, Cement & Concrete Composites, 24, pp 27–34.

- BS 1881 Testing Concrete. Part 201:1986, Guide to the use of non-destructive methods of test for hardened concrete.

- Bunnori N. M., 2008, Ph.D. Thesis, Acoustic Emission Techniques for the Damage Assessment of Reinforced Concrete Structures, Cardiff School Engineering, Cardiff University.

- Bunnori N., Pullin R., Holford K. M. and Lark R. J., 2006a, A practical investigation into Acoustic Wave propagation in concrete structures, Advanced Material Research, Vols. 13-14, pp 205-211.

- Bunnori N., Holford K. M. and Lark R. J., 2006b, The Application of Acoustic Emission Monitoring to the Assessment of concrete structures suffering from reinforcement corrosion. Concrete Communication Conference, University College London, 5-6 September 2006.

- Carpinteri A., Lacidogna G. and Pugno N., 2007, Structural damage diagnosis and life-time assessment by acoustic emission monitoring. Engineering Fracture Mechanics 74, pp 273–289.

- Carpinteri, A., G. Lacidogna, and Puzzi S., 2009, From criticality to final collapse: Evolution of the "b-value" from 1.5 to 1.0." Chaos, Solitons & Fractals 41(2): 843-853.

- Colombo I. S., Main I., Forde M., 2003, Assessing damage of reinforced concrete beam using ''b-value" analysis of acoustic emission signals, Journal of Materials in Civil Engineering, ASCE, pp. 280–286.

- Eaton M. 2007, Ph.D. Thesis, Acoustic Emission (AE) monitoring of buckling and failure in carbon fibre composite structures, Cardiff School of Engineering, Cardiff University.

- Enawaa K.M, 2002, M.Sc. Thesis, Technical Evaluation of Field Data from Commissioning of Retrofit Cathodic Protection System for 500Km of 4- meter Diameter Prestressed Concrete Pipeline (PCCP) Utilizing Sacrificial Anodes, Imperial College, University of London.

- Elfergani H., Pullin R. and Holford K., 2011, Acoustic emission analysis of prestressed Concrete structures, Journal of Physics: Conference Series, 305 (1), 012076.

- Elfergani H., Pullin R. and Holford K., 2012, Crack classification and location using Acoustic Emission Analysis in Prestressed Concrete Structures, the 9th fib international PhD symposium in civil engineering, 22-25 July, Karlsruhe, Germany.

- Elfergani H., Pullin R. and Holford K., 2013, Damage assessment of corrosion in prestressed concrete by acoustic emission, Construction and Building Materials, 40, pp 925–933.

- Elliott J., Stieb J. and Holley M., 2006, an integrated dynamic approach to PCCP integrity management. Pipeline Division Specialty Conference. Chicago, Illinois, United States. July 30 - August 2, Publisher: American Society of Civil Engineers, pp. 1-9.

- Essamin O. and Holley M., 2004, Great Man Made River Authority (GMRA): The Role of Acoustic Monitoring in the Management of the Worlds Largest Prestressed Concrete Cylinder Pipe Project , Proceedings

of the ASCE Annual International Conference on Pipeline Engineering and Construction, August 1-4, San Diego, California.

- Fuahashi M. and Bushman J.B., 1991, Technical Review of 100 mV Polarization Shift Criterion for Reinforcing Steel in Concrete, Corrosion-may Vol.47,no.5,pp 376-386.

- Fontana M. G. 1978. Corrosion Engineering. Tokyo: McGraw-HILL.

- Giannoulakis D., 2008, MS.c Thesis, Acoustic Emission Technology for Detection of Minor Damage in RC Structures, Cardiff School of Engineering, Cardiff University.

- Ha T. H., Muralidran S., Bae J. H., Ha Y. C., Lee H. G., Park K. W. and Kim D. K., 2007, Accelerated short-term techniques to evaluate the corrosion performance of steel in fly ash blended concrete, Building and Environment, Vol. 42, pp 78-85.

- Hellier C. J., 2001, Handbook of Non-destructive Evaluation, McGraw-Hill, USA.

- Holford K.M., 2000, Acoustic Emission-Basic Principles and Future Directions, Strain, Vol.36 No.2.

- Hsu N.N. and Breckenbridge F.R, 1979, Characterization and Calibration of Acoustic Emission Sensors, Materials Evaluation 39, pp 60-68.

- Idrissi H. and Liman A., 2003, Study and characterization by acoustic emission and electrochemical measurements of concrete deterioration

caused by reinforcement steel corrosion, NDT & E International, Vol. 36, pp 563-569.

- Ing M., Austin S. and Lyons R., 2005, Cover zone properties influencing acoustic emission due to corrosion, Cement and Concrete Research, 35, pp.284– 295.

- Ing M. J., 2003, Ph.D. Thesis, Detection of Reinforcement Corrosion by an Acoustic Technique, Loughborough University.

- Kawasaki Y., Tomoda Y. and Ohtsu M., 2010, AE monitoring of corrosion process in cyclic wet–dry test, Construction and Building Materials, 24, pp.2353–2357.

- JCMS-III B5706, 2003, Monitoring method for active cracks in concrete by AE, Construction Material Standards. Tokyo: Japan.

- Kuwairi A., 2006, Water mining: the Great Man-made River, Libya, Proceedings of ICE Civil Engineering, 159, May 2006, pp.39-43.

- Landis E., 1999, Micro-macro fracture relationships and acoustic emission in concrete, Construction and Building Materials, 13, pp.65-72.

- Leelalerkiet V., Shimizu T., Tomoda Y. and Ohtsu M., 2005, Estimation of corrosion in reinforced concrete by electrochemical techniques and acoustic emission, Journal of Advanced Concrete Technology, Vol. 3, No.1, pp.137-147.

- Li X., and Zhang, Y., 2008, Analytical Study of piezoelectric Paint for Acoustic Emission-Based Fracture Monitoring, Fatigue and Fracture of Engineering Materials and Structures, 31, pp.684-694.

- Melchers R. E., 2006, Modelling immersion corrosion of structural steels in natural fresh and brackish waters, Corrosion Science, Vol. 48, Issue 12, pp. 4174–4201

- Melchers R.E. and Li C.Q., 2009, Reinforcement corrosion initiation and activation times in concrete structures exposed to severe marine environments, Cement and Concrete Research, 39, pp.1068-1076.

- Miller R. K. and Hill E. V. K., 2005, Non-destructive Testing Handbook, Acoustic Emission Testing, Volume 6, USA.

- Miller, R.K. and Mclntire, P., 1987, Acoustic Emission Testing. NDT Handbook Vol 5, second edition, American Society for Nondestructive Testing, pp. 151.

- Minemura O., Sakata N., Yuyama S., Okamotod T. and Maruyama K., 1998, Acoustic emission evaluation of an arch dam during construction cooling and grouting, Construction and Building Materials, 12, pp. 385-392.

- Muralidhara S., Prasad B., Eskandri H. and Karihaloo B., 2010, Fracture process zone size and true fracture energy of concrete using acoustic emission, Construction and Building Materials, 24, pp 479-486.

- Nair A. and Cai C., 2010, Acoustic emission monitoring of bridges: Review and case studies, Engineering Structures, 32, pp. 1704-1714.

- Ohtsu M., 1989, Source Kinematics of acoustic emission based on moment tensor, NDT International, 22, pp. 14-20.

- Ohno K. and Ohtsu M., 2010, Crack classification in concrete based on acoustic emission, Construction and Building Materials, 24, pp. 2339-2346.

- Ohtsu M. and Tomoda Y., 2007a, Damage evaluation and corrosion detection in concrete by acoustic emission. Proc of the 6th international conference on fracture mechanics of concrete and concrete structures, Vol 2, pp. 981-989.

- Ohtsu M. and Tomoda Y., 2007b, Corrosion process in reinforced concrete identified by acoustic emission, Materials Transactions, Vol 48, pp.1184 - 1189.

- Ohtsu M., Uchida M., Okamoto T. and Yuyama S., 2002, Damage assessment of reinforced concrete beams qualified by Acoustic Emission. ACI Structural Journal (Technical paper) July-August, pp. 411-417.

- Perez N., 2004, Electrochemistry and corrosion science, Kluwer Academic publisher.

- Pollock A. A., 1986, Classical Wave Theory in Practical AE Testing, Progress in Acoustic Emission III, the Japanese of NDI.

- Poursaee A., 2010, Potentiostatic transient technique, a simple approach to estimate the corrosion current density and Stern–Geary constant of reinforcing steel in concrete, Cement and Concrete Research, 40, pp 1451–1458.

- Proust A. and Lenain J., 2000, Use of Acoustic Emission to Detect Location Corrosion Philosophy of Industrial use, Illustrated with Real Examples, Journal of Acoustic Emission, USA, Volume 18, pp.161-165.

- Pullin R. 2001, Ph.D. Thesis, Structural Integrity Monitoring of Steel Bridges Using Acoustic Emission Techniques, Cardiff School of Engineering, Cardiff University.

- Pullin R, Baxter M.G., Holford k. M. and Evans S. L. 2007, Novel Acoustic emission source location. 6th International Conference on Acoustic Emission. Lake Tahoe-Nevada, USA, pp.235-240.

- Ramadan S., Gaillet L., Tessier C. and Idrissi H., 2008, Detection of stress corrosion cracking of high-strength steel used in prestressed concrete structures by acoustic emission technique, Applied Surface Science, 254, pp. 2255–2261.

- Rindorf, H. J., 1981, Acoustic emission source location in theory and in practice, Bruel and Kjaer Technical Review, 2, pp. 3-44.

- Rippengill S., Worden K., Pullin R., and Holford K., 2003, Automatic classification of acoustic emission patterns, Strain, 39, pp. 31-41.

- Schiessl P., 1988, Corrosion of steel in concrete, London New York: CHAPMAN AND HALL.

- Scully J. C. 1990. The Fundamentals of Corrosion. Exeter: PERGAMON PRESS.

- Singh S. K., 2000, Ph.D. Thesis, Corrosion Studies on Prestressing Steel Wire, Imperial College, University of London.

- Shiotani T., 2006, Evaluation of Repair Effect for Deteriorated Concrete Piers of Intake Dam Using AE Activity, Advanced Materials Research, 13-14, pp 175-180.

- Song H and Saraswathy V, 2007, Corrosion Monitoring of Reinforced Concrete Structures − A Review, International Journal of Electrochemical. Science 2, pp.1- 28.

- Soulioti D., Barkoula N. M., Paipetis A., Matikas T.E, Shiotani T. and Aggelis D.G., 2009, Acoustic emission behaviour of steel fibre reinforced concrete under bending, Construction and Building Materials, 23, pp. 3532-3536.

- Travers F., 1997, Acoustic Monitoring of Prestressed Concrete pipe, Construction and Building Materials, Vol. 11, No. 3, pp. 175-187.

- Uddin A., Numata K., Shimasakia J., Shigeishi M. and Ohtsu M., 2004, Mechanisms of crack propagation due to corrosion of reinforcement in concrete by AE-SiGMA and BEM, Construction and Building Materials, 18, pp. 181–188.

- Watanabe T., Nishibata S., Hashimoto C. and Ohtsu M., 2007, Compressive failure in concrete of recycled aggregate by acoustic emission, Construction and Building Materials, 21, pp. 470-476.

- Wheat H. G., 2007, Monitoring Corrosion Behavior Using Acoustic Emission Techniques, NACE International, Corrosion, Conference &Expo, paper No 07291.

- Xiong H., Li P. and Li Q., 2010, FE model for simulating wire-wrapping during prestressing of an embedded prestressed concrete cylinder pipe, Simulation Modelling Practice and Theory, 18, pp. 624–636.

- Youping Liu, 1996, Ph.D. Thesis, Modelling the Time-to-Corrosion Cracking of the Cover Concrete in Chloride Contaminated Reinforced Concrete Structures, Faculty of the Virginia Polytechnic Institute and State University.

- Yun H., Choi W. and Seo S., 2010, Acoustic emission activities and damage evaluation of reinforced concrete beams strengthened with CFRP sheets, NDT & E International, 43, pp. 615–628.

- Yu J., Ziehl P., Zárate B. and Caicedo J., 2011, Prediction of fatigue crack growth in steel bridge components using acoustic emission, Journal of Constructional Steel Research, 67, pp. 1254–1260.

- Yuyama, S., Yokoyama K., Niitani, K., Ohtsu M. and Uomoto T., 2007, Detection and evaluation of failures in high-strength tendon of prestressed concrete bridges by acoustic emission, Construction and Building Materials, 21, No.3, pp. 491-500.

- Zongjin Li., Faming Li., Zdunek A., Landis E., and Shah S.,1998, Application of Acoustic Emission Technique to Detection of Rebar Corrosion in Concrete, ACI Materials Journal , 95, pp. 68-76.

APPENDIX A

SUMMARY OF TEST DETAILS

APPENDIX A: Summary of Test details

Test No.	Specimen size mm^3	Current Density (μA/cm²)	Pre-stress	First Crack start (hr)	Period whole test (Day)	Note
Test 01	200×200×50	495	NO	48	14	Trial
Test 02	200×200×50	350	YES	36	22	Trial
Test 03	200×200×50	350	YES	40	09	Trial
Test 04	200×200×50	250	No	72	11	
Test 05	200×200×50	450	YES	34	09	Section 4.3 (test 1)
Test 06	200×200×50	100	NO	120	12	
Test 07	200×200×50	700	NO	36	06	
Test 08	200×200×50	125	NO	96	09	
Test 09	200×200×50	500	NO	36	04	
Test 10	200×200×50	500	NO	48	07	Section 4.5 (Reinforced concrete test)
Test 11	200×200×50	500	NO	36	08	
Test 12	200×200×50	250	NO	78	09	
Test 13	200×200×50	250	NO	48	10	
Test 14	200×200×50	250	NO	60	08	
Test 15	200×200×50	150	NO	72	14	
Test 16	200×200×50	150	NO	48	14	
Test 17	200×200×50	250	YES	72	14	Section 4.3 (test 2)
Test 18	600×600×50	250	NO	48	10	
Test 19	600×600×50	250	NO	70	07	Chapter 5 (Large scale test)
Test 20	400×400×50	250	NO	78	10	
Test 21	200×200×50	500	NO	N/A	28	Section 4.4 (Corrosion alone-No cracking)
Test A	Dog-bone shape	NO	Tensile load	N/A	550 sec.	Section 3.5.2 (test 1)
Test B	Dog-bone shape	No	Tensile load	N/A	700 sec.	Section 3.5.2 (test 2)
Test C	600×600×50	NO	NO	N/A	N/A	Section 3.3 (Wave propagation)
Test D	400×400×230	NO	NO	N/A	N/A	Section 3.4 (attenuation)

APPENDIX B

SENSOR CALIBRATION CERTIFICATES

PHYSICAL ACOUSTICS CORPORATION

A MISTRAS Holdings Company

AE SENSOR CALIBRATION CERTIFICATE

Sensor Name:	R3I	Test Date:	11/27/00
Sensor S/N:	AM50	Tested By:	C.P.
Comment:			
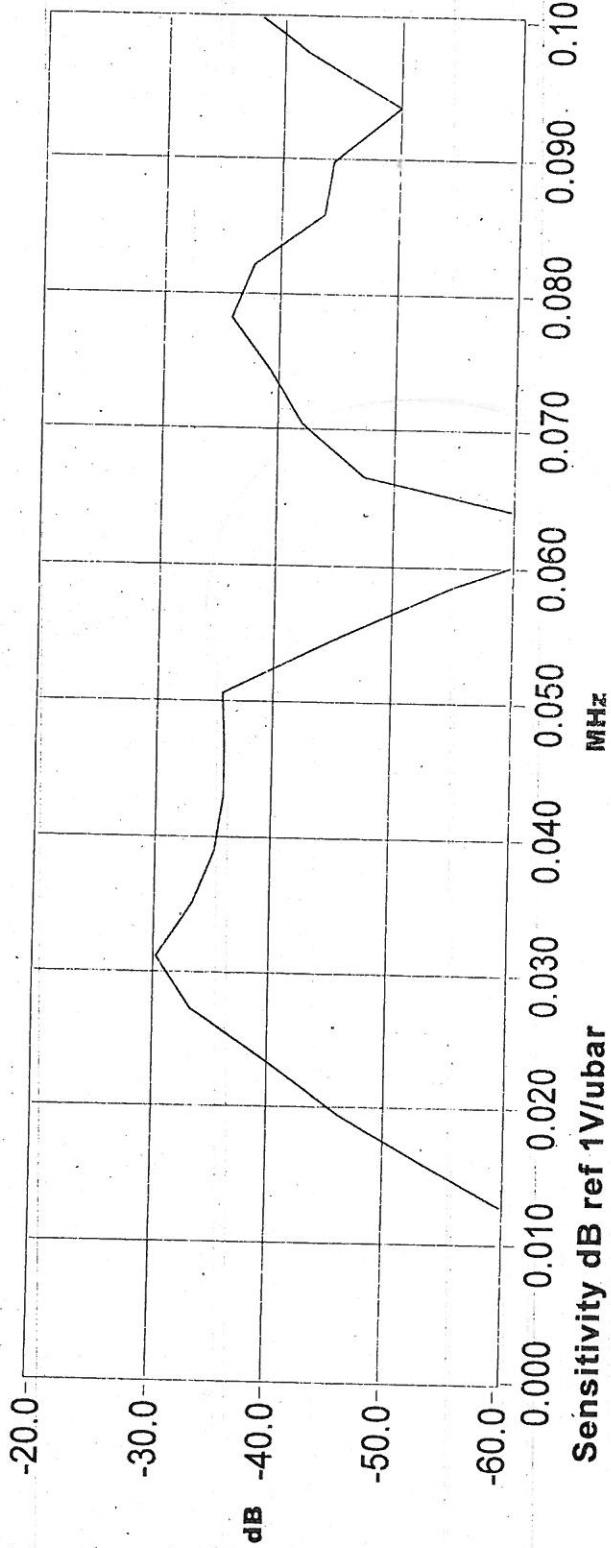
Max. Value (dB):	-30.25
Peak Freq.(kHz):	31.25

Sensitivity dB ref 1V/ubar

PAC Certifies that this sensor meets all performance, environmental and physical standards established in applicable PAC specifications. Calibration methodology based on ASTM standard E976- ""Guide for Determining the Reproducibility of Acoustic Emission Sensor Response."

LITHO IN U.S.A.

GOES 746

PHYSICAL ACOUSTICS CORPORATION
A MISTRAS Holdings Company

AE SENSOR CALIBRATION CERTIFICATE

Sensor Name:	R3I-AST	**Test Date:**	4/15/02
Sensor S/N:	AO13	**Tested By:**	KBG
Comment:			

Max. Value (dB): 121.18

Peak Freq.(kHz): 21.48

Sensitivity dB ref 1V/(m/s)

MHz

dB

PAC Certifies that this sensor meets all performance, environmental and physical standards established in applicable PAC specifications. Calibration methodology based on ASTM standard E1106- "Standard Method for Primary Calibration of Acoustic Emission Sensors."

PHYSICAL ACOUSTICS CORPORATION
A MISTRAS Holdings Company

AE SENSOR CALIBRATION CERTIFICATE

Sensor Name: R3I-AST **Test Date:** 4/15/02 **Max. Value (dB):** 119.96

Sensor S/N: AO14 **Tested By:** KBG **Peak Freq.(kHz):** 21.48

Comment:
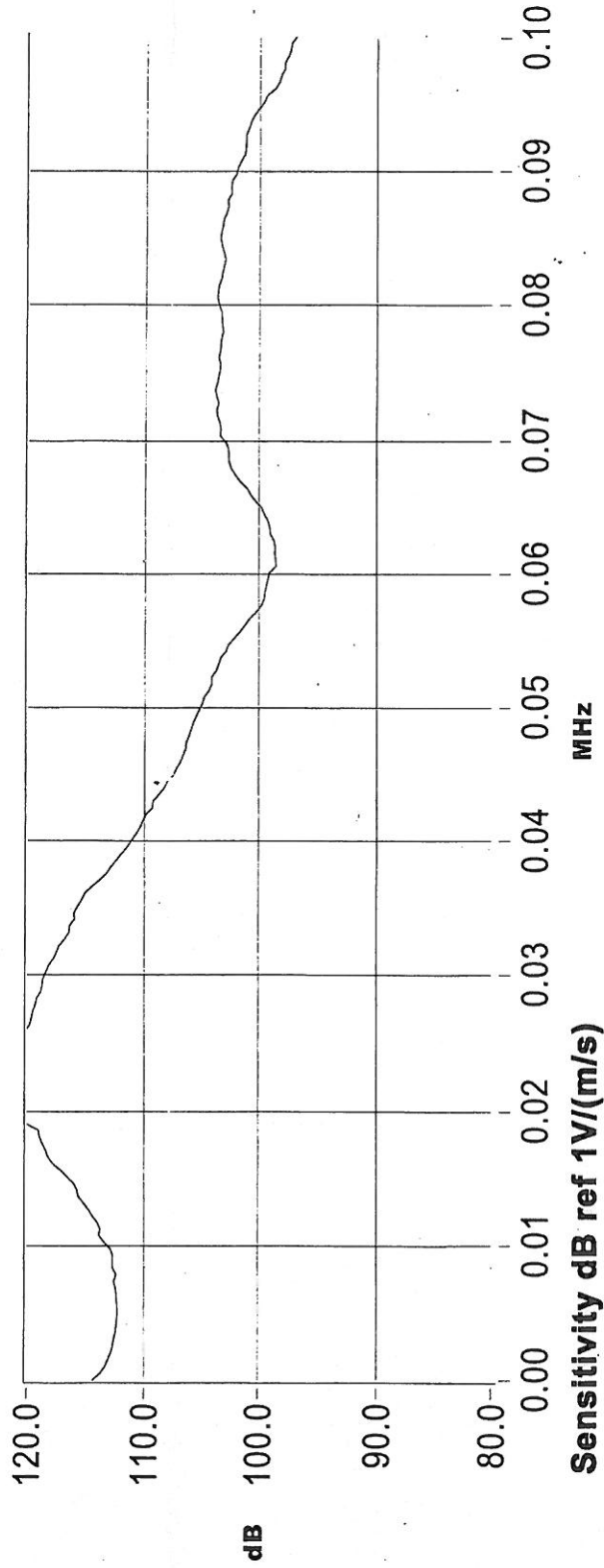

Sensitivity dB ref 1V/(m/s)

MHz

PAC Certifies that this sensor meets all performance, environmental and physical standards established in applicable PAC specifications. Calibration methodology based on ASTM standard E1106- "Standard Method for Primary Calibration of Acoustic Emission Sensors."

PHYSICAL ACOUSTICS CORPORATION

A MISTRAS Holdings Company

AE SENSOR CALIBRATION CERTIFICATE

Sensor Name: R3I-AST   **Test Date:** 4/15/02   **Max. Value (dB):** 119.97

Sensor S/N: AO17   **Tested By:** KBG   **Peak Freq.(kHz):** 19.53

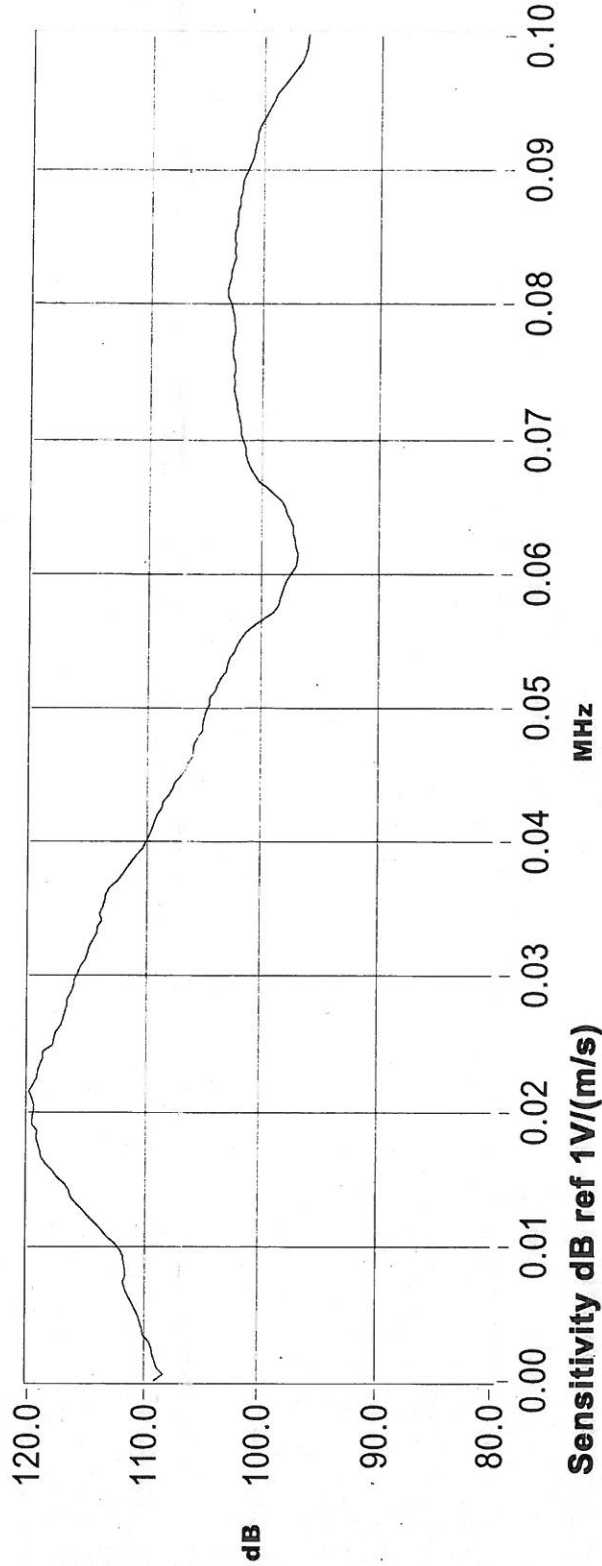**Comment:**

Sensitivity dB ref 1V/(m/s)

PAC Certifies that this sensor meets all performance, environmental and physical standards established in applicable PAC specifications. Calibration methodology based on ASTM standard E1106- "Standard Method for Primary Calibration of Acoustic Emission Sensors."

PHYSICAL ACOUSTICS CORPORATION

A MISTRAS Holdings Company

AE SENSOR CALIBRATION CERTIFICATE

Sensor Name:	R3I-AST	**Test Date:** 4/15/02
Sensor S/N:	AO18	**Tested By:** KBG
Comment:		

Max. Value (dB): 119.93

Peak Freq.(kHz): 21.48
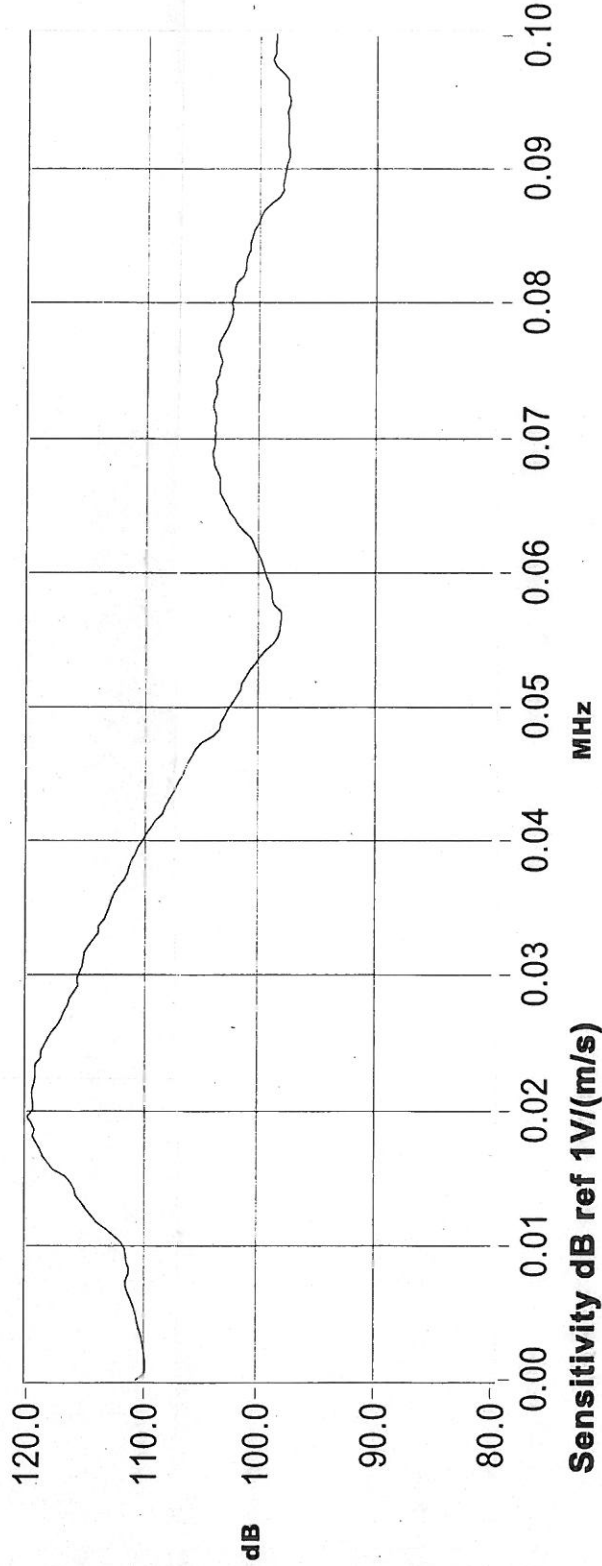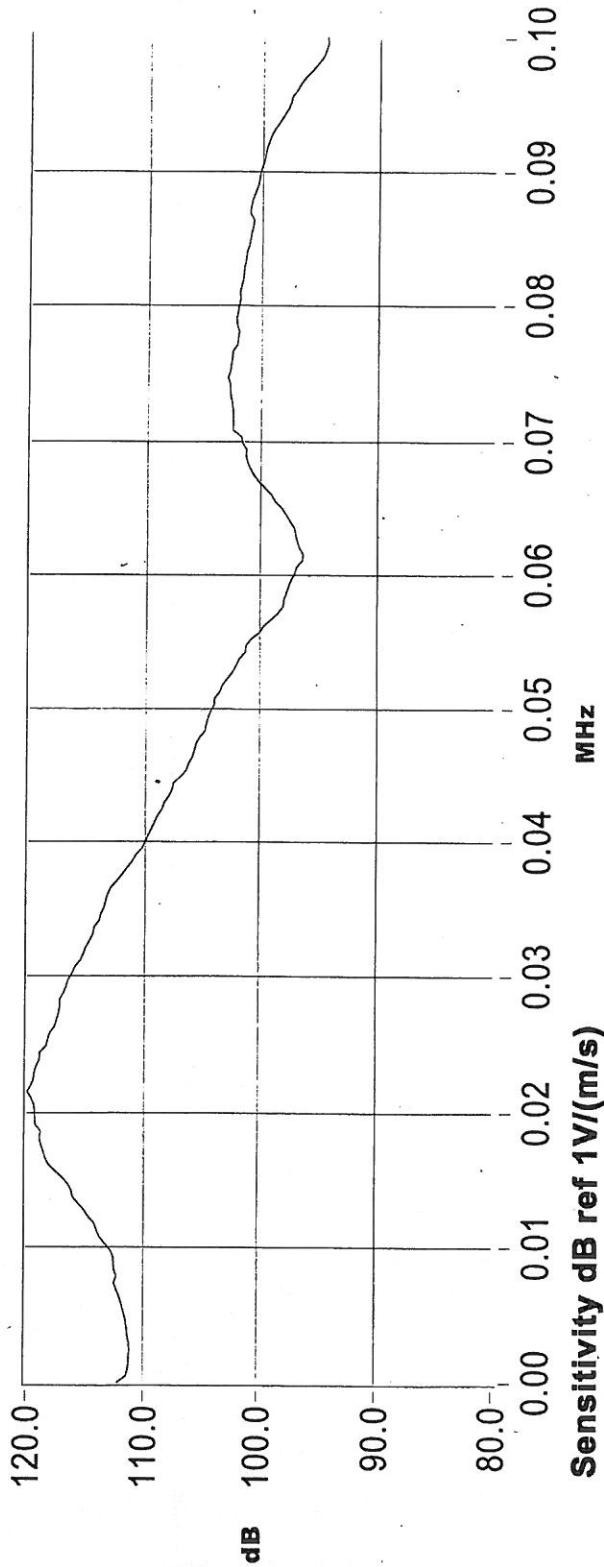

Sensitivity dB ref 1V/(m/s)

PAC Certifies that this sensor meets all performance, environmental and physical standards established in applicable PAC specifications. Calibration methodology based on ASTM standard E1106- "Standard Method for Primary Calibration of Acoustic Emission Sensors."

PHYSICAL ACOUSTICS CORPORATION
A MISTRAS Holdings Company

AE SENSOR CALIBRATION CERTIFICATE

Sensor Name:	R3I-AST	**Test Date:**	4/15/02
Sensor S/N:	AO21	**Tested By:**	KBG
Comment:			

Max. Value (dB): 120.58

Peak Freq.(kHz): 19.53

Sensitivity dB ref 1V/(m/s)

MHz

dB

APPENDIX C

PUBLISHED PAPERS

Damage assessment of corrosion in prestressed concrete by acoustic emission

Hisham A. Elfergani *, Rhys Pullin, Karen M. Holford

Cardiff School of Engineering, Cardiff University, Queen's Building, The Parade, Cardiff CF24 3AA, Wales, UK

HIGHLIGHTS

► Development of Acoustic Emission (AE) techniques for damage detection.
► Applications of AE to concrete reinforced structures including pipes.
► Successfully detected and located corrosion and wire cracking in laboratory.
► Characterised microcracks, macrocracks and crack movement with AE.
► Engineering solution developed for early stage corrosion detection.

ARTICLE INFO

ABSTRACT

Damage due to corrosion is most common in reinforced and prestressed concrete structures. Structural Health Monitoring (SHM) and detection of corrosion and cracks in initial stages is very important to avoid catastrophic failure. This paper reports on using the Acoustic Emission (AE) technique to detect and locate the early stages of corrosion and macrocracks and furthermore classify different crack types to aid maintenance priorities. The results presented indicate that AE is capable of detecting corrosion, macrocracks and crack propagation in representative structures. In addition, it can distinguish between tensile cracks and shear movement.

1. Introduction

Many structures like bridges, buildings, concrete pipes, storage tanks, dams, nuclear reactor protective shells, railway sleepers, piles and pressure vessels are made of prestressed concrete in which prestressing steel wires are put into a permanent state of tension to compensate for the inadequate tensile strength of the concrete. Tensile cracking in the concrete is minimised by ensuring that the concrete is in compression under normal working loads by prestressing the steel reinforcement. Generally prestressed steel is between four to five times stronger than mild steel. The main advantages of prestressed concrete structural materials are that they are stronger, lighter and "crack free" [1] and hence offer cost benefits.

Corrosion is a significant problem in numerous structures and the associated cost is estimated at billions of dollars every year [1]. The risk of corrosion in reinforced and prestressed structures must be given special consideration because failure may result in

the worst scenario of a loss of life and at best a loss of asset use and hence a financial loss. Most studies indicate that the main reason of failure of bridges and concrete pipes is corrosion during the short period after they were constructed [1,2]. The concrete provides the ideal environment to protect the steel wires which are embedded in it, possibly for over 50 years [2]. However, the life of a concrete structure becomes shorter due to steel corrosion, which may occur by aggressive ion attack from products of chloride or carbonation [3]. The concrete pipes which transport water are one such structure that has suffered from corrosion, for example, the pipes of Great man-made river project of Libya.

The Great Man-Made River Project (GMRP) is concerned with water transportation from the aquifers deep in the Sahara desert to the coastal region where over 90% of the population lives and the main regions of agriculture and industry are located. The high quality ground water is conveyed through almost 4000 km of pre-stressed concrete cylinder pipe (PCCP) networks as shown in Fig. 1 [1,4,5].

The majority of transportation line pre-stressed concrete cylinder pipes are 4.0 m in, inner diameter; with a length of 7.5 m, and over 70 tonnes in weight. The concrete pipe consists of a 225 mm

---

* Corresponding author.
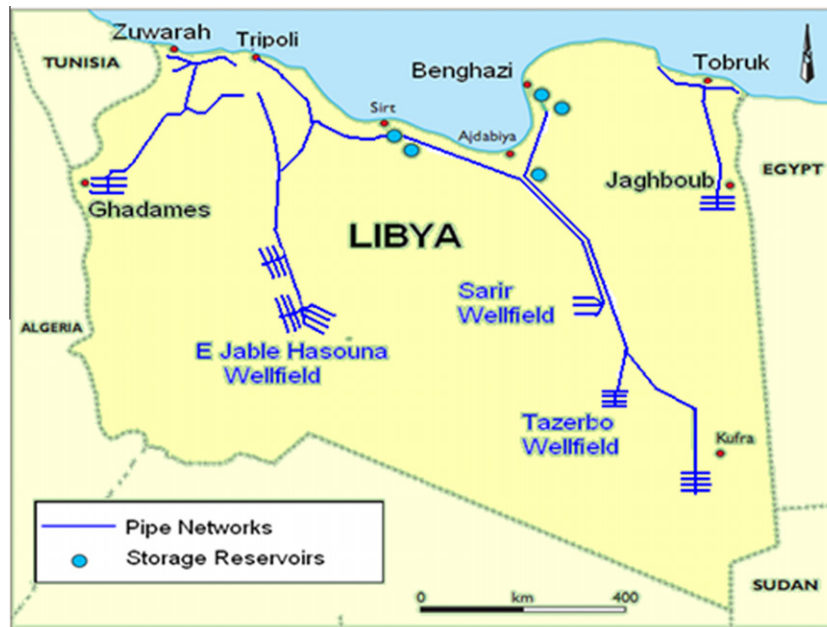   *E-mail address:* ElferganiH@Cardiff.ac.uk (H.A. Elfergani).

Fig. 1. Layout of the various phases of Great Man-Made River Project [4].
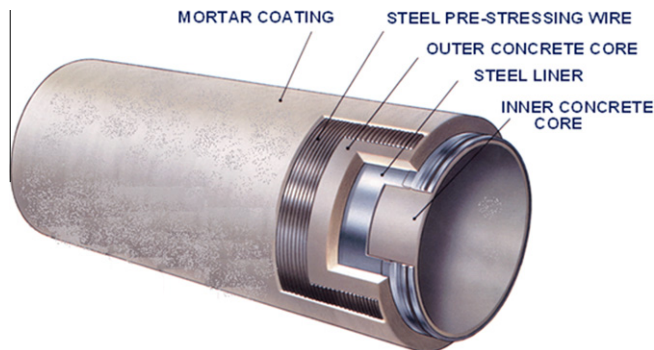

Fig. 2. Typical cross-section of the PCCP.

thick concrete core within an embedded thin steel cylinder and externally wrapping prestressed wires. The prestressed wires are covered by a 19 mm thick layer of cement mortar. A typical cross-section of the PCCP is shown in Fig. 2. In order to protect the pipelines from risks including temperature variations and other environmental conditions, they are laid in 7 m deep trenches.

Five catastrophic failures in 4 m diameter pipes occurred between 1999 and 2001 after 10 years of operation. The main reason for the damage is corrosion of prestressed wires in the pipes due to attack by the chloride ions from soil [4,5]. The project used non-destructive methods but they were unable to detect wire breaks and they could not detect the presence of corrosion and macro-cracks. Hence, in areas where no excavation has been completed, areas of serious damage can go undetected. In this respect, AE has significant advantages compared with other NDT methods because the AE technique is possibly the only one able to reliably detect the very early stages of the corrosion process, before significant damage to the concrete has occurred. Furthermore, it can indicate the level of damage occurring to the concrete [6–8].

The substantial challenges which faces the pipe engineers, apart from future corrosion protection, is to find the best way to detect the corrosion and macrocracking at an early stage and prevent the pipes from deteriorating further. This project aims to use the AE technique to detect the early stages of corrosion and macro-cracking prior to wire breaks and eventual failure of the concrete structures.

1.1. Acoustic emission technique

Acoustic Emission (AE) is defined as the elastic energy released from materials which are undergoing deformation. The rapid release of elastic energy, the AE event, propagates through the structure to arrive at the structure surface where a piezoelectric transducer is mounted. These transducers detect the displacement of the surface at different locations and convert it into a usable electric signal. By analysis of the resultant waveform in terms of feature data such as amplitude, energy and time of arrival, the severity and location of the AE source can be assessed [7,9]. In concrete research two primary areas of activity exist, application to structures and damage characterisation.

Numerous researchers have shown that the AE monitoring technique can be applied to reinforced concrete applications such as, bridges, viaducts, dams and buildings. Successful applications of AE in dam structures have been demonstrated by Minemura et al. [10] Bond et al. [11] and Shiotani [12]. Furthermore the use of AE on bridges has been reported by Nair, Yuyama et al. and Yu et al. [13–15]. In addition, using AE to characterise the damage process of steel fibre reinforced concrete under bending was studied by Aggelis et al. [16], whilst classification of cracking modes in concrete were studied by Aggelis [17] and Ohno and Ohtsu [18]. Directly related to this work, the AE process was utilised to identify micro–macro fracture relationships in concrete by Landis [19]. Further investigations which identified the corrosion process in reinforced concrete have been demonstrated by Uddin et al. [20] Ohtsu [21] and Kawasaki et al. [22].

Finally an estimation of the fracture process zone in concrete has been studied by Muralidhara et al. [23]. Despite this research activity in concrete structures, only a few works for using AE techniques in prestressed concrete structures and composite concrete (mortar and concrete) currently exist [24]. One study of the applicability of acoustic emission technique for detecting corrosion of rebar in concrete was performed by Zongjin et al. [25].Their results

demonstrated that there is a clear relationship between the AE events and rebar corrosion in concrete.

1.2. AE parameter analysis

AE parameter analysis is the fundamental method for identifying types of damage in a structure. It utilises features that describe the detected waveform. Typical parameters investigated include amplitude, energy, counts (number of threshold crossings), frequency, duration and rise time. The shape of AE waveforms is reported to be characteristic of the fracture mode (Fig. 3a and b). Shear events are characterised by longer rise time and usually higher amplitude than tensile events [12].

According to many researchers [17,18,21,26], the relationship between RA values (rise time/ amplitude) and average frequencies (counts/duration) can be used for classification of crack type in concrete structures. They reported that when an AE signal has low average frequency and high RA value it is classified as shear type crack/movement. However when it has a high average frequency and low RA value is classified as tensile type crack as in Fig. 4. It should be noted that some researchers describe the shear movement as a shear "crack" but that this is not strictly correct; concrete will crack under tensile forces and then move due to shear forces.

Furthermore, a size distribution of AE sources can be estimated by using b-value. The b-value is defined as relationship between the number of AE events, N, and amplitudes A, as:

$$\log_{10}N = a - b \log_{10}A \tag{1}$$

where a and b are empirical constants.

In the case that large scales of fracture is dominant then the b-value becomes small. Conversely, b-value is large when small scales of fracture are dominant [17,22,27]. Moreover, using moment tensor analysis to determine crack kinematics on locations, types and orientations are quantitatively [20,28]. This paper focuses on the use of RA/AF values for source characterisation.

2. Experimental program

The experimental program contains five key stages; development of a tension holding frame, wire preparation, concrete and mortar preparation, accelerated corrosion and AE monitoring.

2.1. Tension holding frame

This work aimed to simulate as close as possible the real physical conditions surrounding the high strength steel wires in concrete pipes. Therefore it was prudent to place and maintain all relevant wire samples under tension equal to 60% of their ultimate tensile strength as is found in the pipes in Libya. To achieve this objective a tension frame was designed and fabricated.
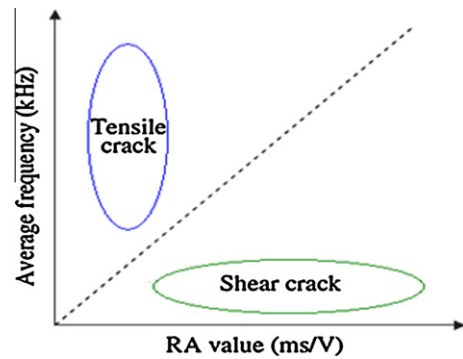

Fig. 4. Crack classification [12].

The frame consists of two blocks (190 mm × 45 mm × 45 mm) and two threaded steel bars (studding) having a diameter of 20 mm and a length of 500 mm. Two holes (20 mm diameter) and two (6 mm) are drilled in each block. Fig. 5 shows a schematic drawing for the tension holding frame. The two blocks are assembled via two threaded bars tightened by means of eight nuts.

2.2. Wire preparation

Two high strength steel wires samples were supplied from GMRA PCCP manufacturing plant in Libya. The metallurgical composition and mechanical properties as certified by the wire manufactures is summarised as follows: Carbon steel (carbon 0.8–0.84%, 0.85–1.00%Mn, 0.030% Max S, 0.035% Max P, 0.20–0.35% Si). The tensile strength of the wires is approximately 1738 MPa.

The two working wire samples were passed through 6 mm diameter holes in the steel blocks and then through two modified bolts and nuts (designed to control the tension load of each wire). Finally a steel cylinder was then threaded over the wire. The cylinder was then compressed in a load machine. In this way the modified nut and bolt could be expanded between the clamped cylinder and the steel block and as a result tension could be introduced into the wire. Each wire was subjected to a tensile force of 20 kN by adjusting the bolts and nuts and monitored via strain gauges mounted on the wires [29].

2.3. Concrete and mortar preparation

The concrete specimen (200 × 200 × 50 mm), representative of the inner pipe was prepared according to the technical specification for PCCP manufacturing used in Great Man-Made River Project, which is in accordance with AWWA C301-92 [30]. A day after casting the concrete specimen, the wires combined with their holding frame was placed on the upper surface of this specimen. Finally the mortar 200 × 200 mm and 20 mm thickness was coated on the upper surface of the concrete. The mortar consists of one part cement to not more than three parts fine aggregate by weight. The final construction is shown in Fig. 6 [29].

2.4. Accelerated corrosion technique

To accelerate the corrosion process, a corrosion cell was used with an impressed current (100 μA/cm²). This is reported as corresponding to the maximum corrosion rate for concrete in laboratory conditions and has been used by several researchers in the laboratory as discussed by Li and Zhang [31].
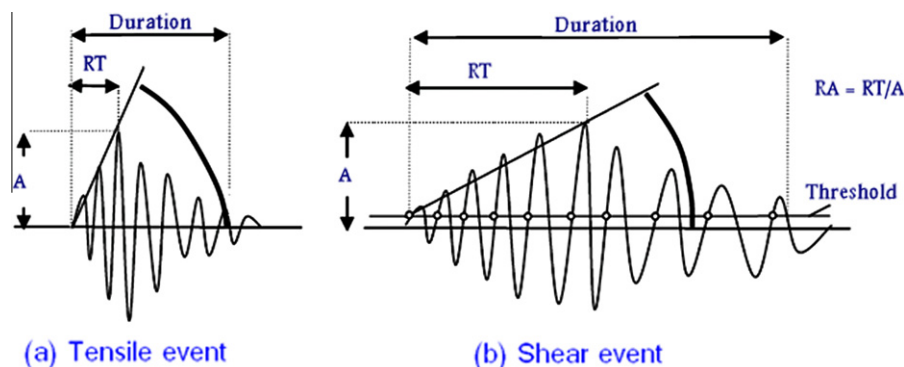
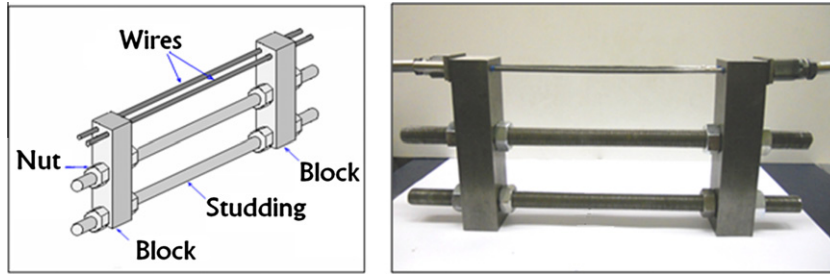

Fig. 3. Typical waveforms [12].

Fig. 5. Tension holding frame.
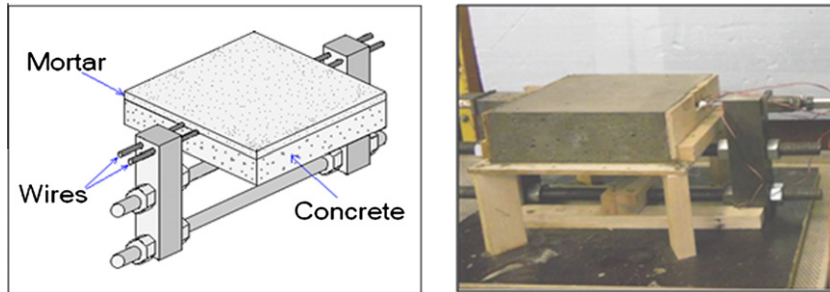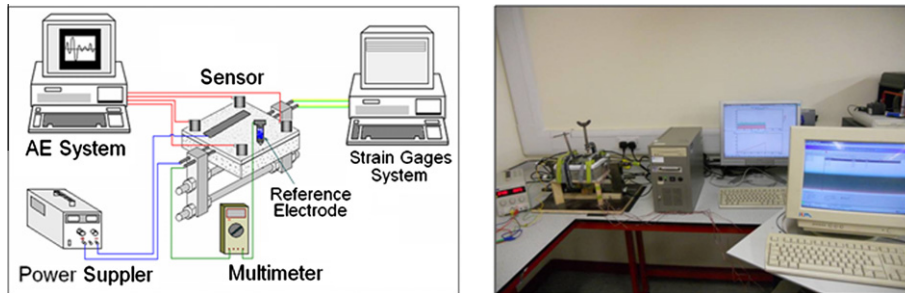

Fig. 6. Concrete and mortar specimen.

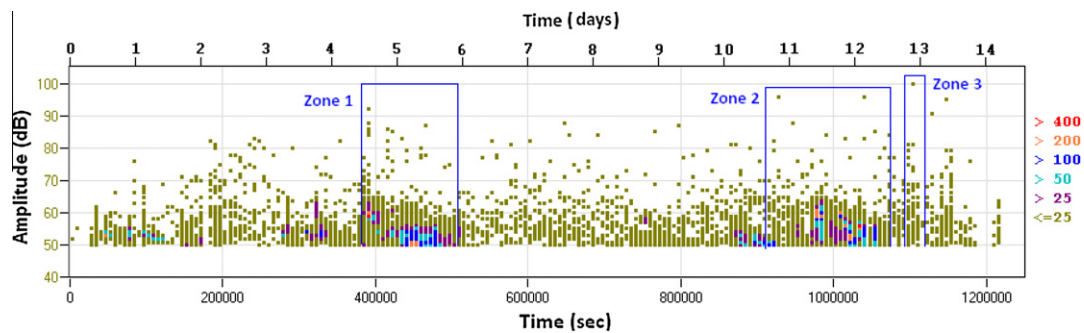**Fig. 7.** Schematic diagram and photo of experimental set up.

Fig. 8. Amplitude of detected signals for duration of investigation.

In this experimental work, the wire corrosion was induced by impressed current (500 μA/cm^2). The prestressed wires were contacted in an electrical circuit with positive pole of power supplier and the negative pole connected with a stainless steel plate (30 × 150 mm) resting on the upper mortar. A 4% NaCl solution was poured on the surface of the mortar. Silicon sealant was used to pool the solution on the upper surface [29].

2.5. Acoustic emission set-up

AE instrumentation typically consists of transducers, filters, amplifiers and analysis software. Four AE sensors (R3I – 30 kHz resonant frequency) were mounted on the surface of the mortar as shown in Fig. 7. The four AE sensors were

mounted using silicon sealant and were fixed on the upper surface of mortar with a U shaped plate attached with screws hold the sensors and to ensure a good coupling. The sensitivity of the sensors was checked by using the Hsu source [32].

3. Results and discussion

All the detected and located signals with a minimum amplitude 50 dB detected by all sensors for almost fourteen days of continuous monitoring are shown in Fig. 8 as signal amplitude against time. Fig. 9 displays the same data set but this time as energy
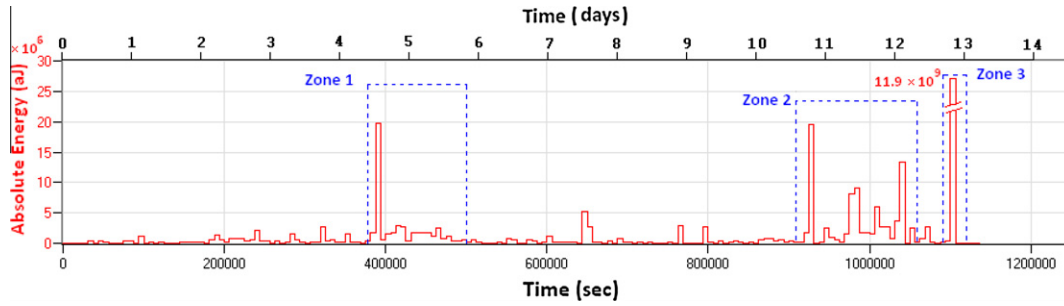
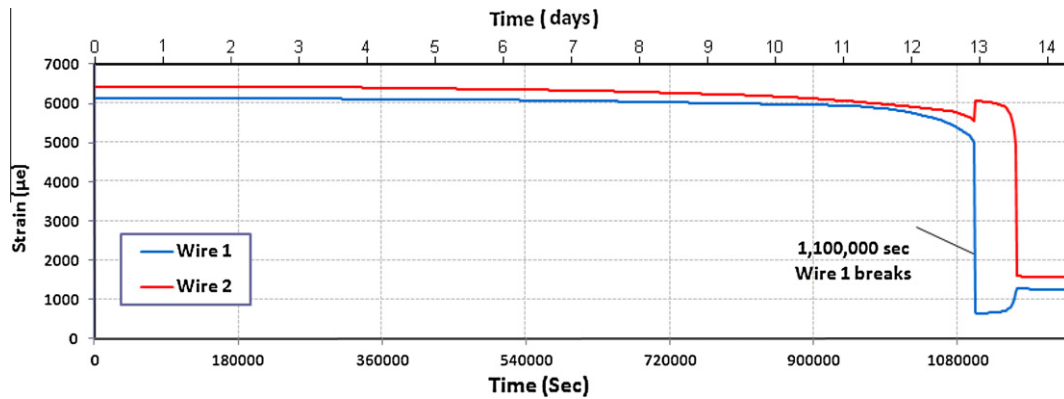**Fig. 9.** Absolute energy of detected signals for duration of investigation.

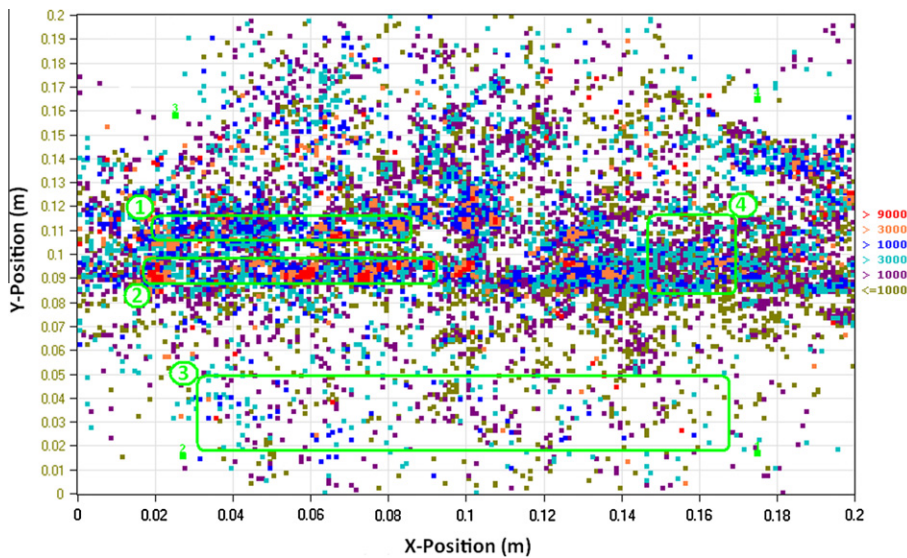**Fig. 10.** Recorded strain for duration of investigation.

Fig. 11. Source locations for whole test with amplitudes greater than 50 dB.

against time. The detected energy is attributed to a number of sources; active corrosion, microcracking, macrocracking, propagation of mortar cracking, separation of the mortar from the concrete, noise and wire breaks.

In Fig. 9, three zones are highlighted based on visual inspection, strain measurements, AE signal location and previous investigations.

It can be seen that in Fig. 9 there are three significant zones which contain signals of large energy. The high energy and high amplitude (at 390,000 s) in zone 1 is attributed to the energy re-

lease from the formation of macrolongitudinal crack due to the products of corrosion from wire 1 as observed in visual inspection. In addition, the energy release from macrocracks formation is higher than microcracks formation. This result shows good agreement with result demonstrated by Aggelis [17]. The following increase in the number of hits with smaller energy and smaller amplitude is attributed to macrocrack propagation.

The high energy and high amplitude in zone 2 corresponds to the formation of a macrolongitudinal crack due to the products of corrosion from wire 2 followed by an increase in the number
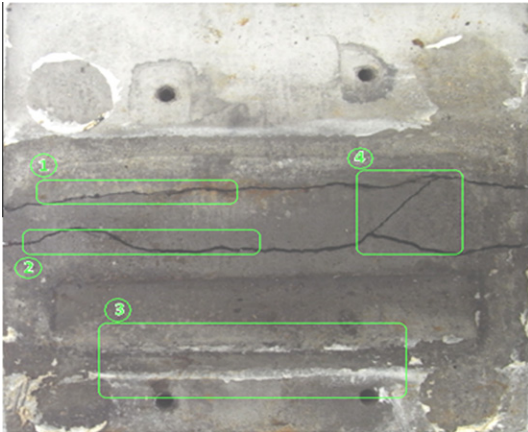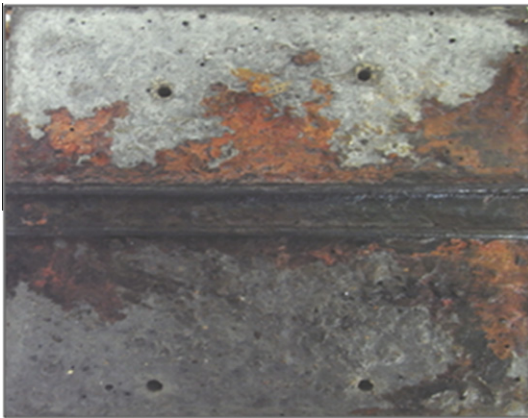
Fig. 12. Photo of top mortar surface.

Fig. 13. Photo of upper concrete surface and wires.

of hits with variable energy corresponds to mix of macrocrack propagation and the formation of a macroinclined crack between two longitudinal cracks. The highest energy and highest amplitude (100 dB) located in zone 3 is due to the wire 1 breaking. At this time the strain gauge reading suddenly decreased to almost zero.

The variation of measured strain of the embedded wires against time is shown in Fig. 10. It can be seen the load on the wires is constant for whole period until wire 1 failure at about 1,100,000 s and the load is then transferred to wire 2 which subsequently failed.

The location of signals with minimum amplitude 50 dB for the whole period of the test is shown in Fig. 11. Zones were allocated based on the damage observed as shown in Fig. 12. It can be noted that the highest hits concentration and highest energy in region coincides with maximum wire corrosion and the crack which was visibly observed post test as shown in Fig. 12.

Fig. 12 is a photograph of the top mortar surface after the end of the test, showing the crack shape. Comparing this figure with the previous location plot reinforces the conclusion that the AE was detecting the concrete cracking as a result of wire corrosion within the specimen.

The corrosion wires and corrosion product once the mortar had been removed is shown in Fig. 13. It is evident that significant corrosion occurred in the upper wire and it was in this location that a large majority of AE signals were detected and located.

Four zones have been chosen as examples to distinguish between the crack area and noise and also to classify mode types. Areas were chosen based on visual observation (Figs. 11 and 12) zone 1 and 2 represents crack areas where cracks shapes are parallel to the corroded wires (longitudinal crack), zone 4 represent a crack shape that is inclined crack between two longitudinal cracks whereas zone 3 no cracks were present. Fig. 14a–d shows the AF vs. RA values for different regions of concentration of events on surface of mortar.

Fig. 14a and b shows the AF vs. RA for zones associated with the crack regions which is longitudinal crack due to the products of corrosion from wire 1 and wire 2 respectively. It can be seen that
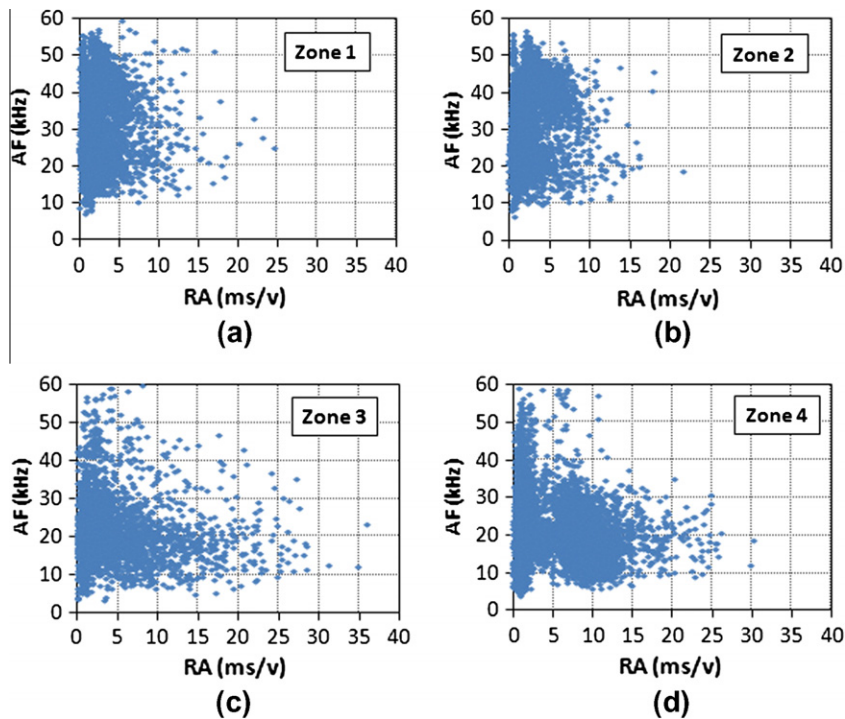

Fig. 14. Relation between the RA value and average frequency of (a) zone 1, (b) zone 2, (c) zone 3 and (d) zone 4.
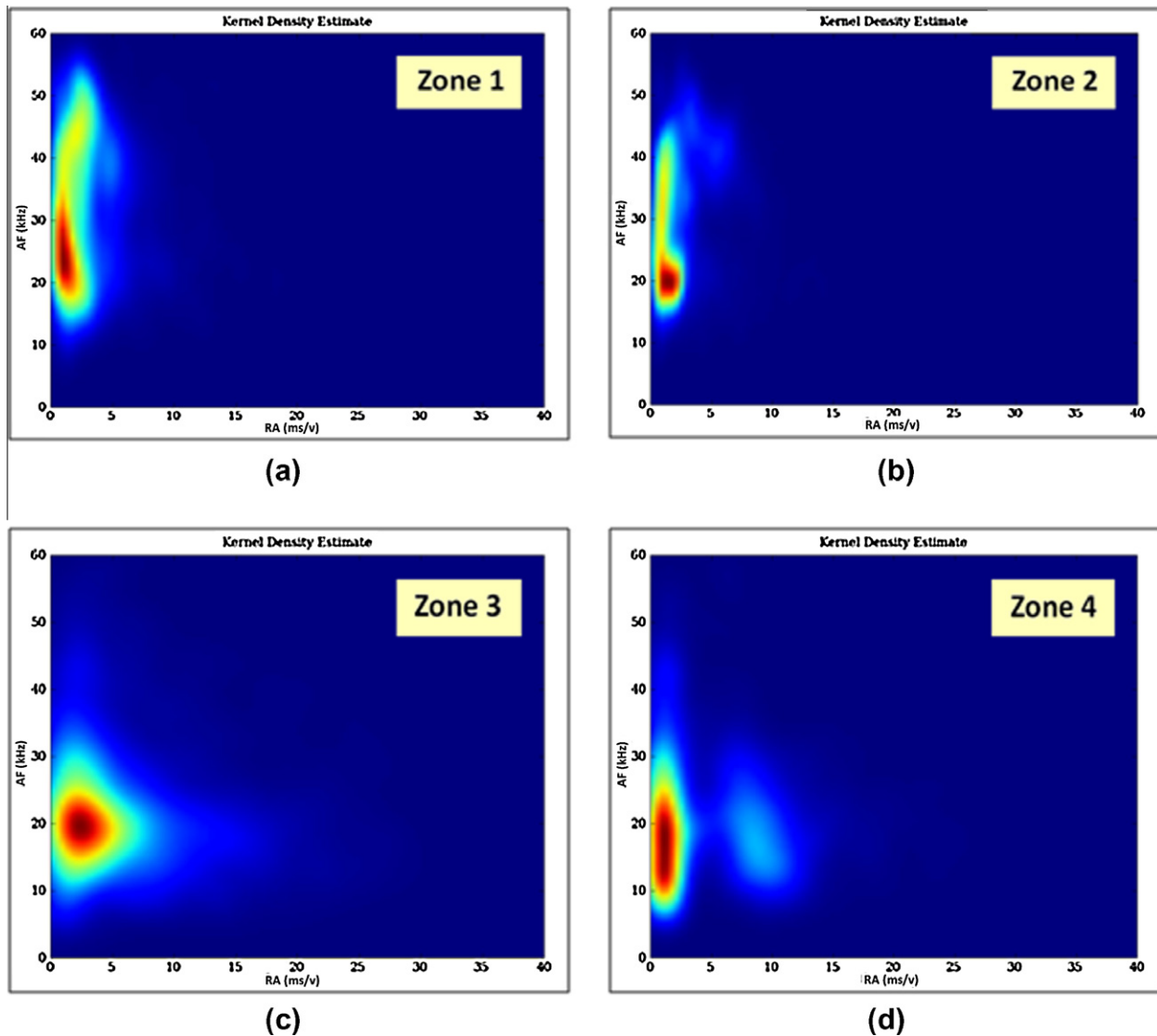
Fig. 15. Kernel Density Estimation of (a) zone 1, (b) zone 2, (c) zone 3 and (d) zone 4.

the most of data points have various AF and low RA value (less than 10 ms/v). Therefore, based on Fig. 4, this indicates that the type of the crack is pure tensile [17,18,21,26]. However Fig. 14c shows an area where there is a low concentration of locations. It can be noted that in this area the RA value has a wide distribution (RA values 0–30 ms/v and AF values 10–40). The Fig. 14d shows the relationship between RA value and AF associated with the crack region which is the inclined crack between two longitudinal cracks. Therefore, based on Fig. 4, this indicates that the crack type is mixed between two modes; tensile crack and shear mode movement [17,18,21,26].

Furthermore, these figures can be represented by using a Kernel Density Estimation Function (KDEF) as shown in Fig. 15a–d. KDEF can be used to better visualise the data as described by Rippengill et al. [33]. Regions of high concentration are more easily identified. The concentration value of the data is represented by different colours, brown for the highest number of data points whereas blue for lowest.

It clearly can be seen that zones 1 and 2 have various AF and low RA value (AF less than 5 kHz and RA values have range between 10 and 50 ms/v) and zone 3 has small various RA and AF has range between 0 and 10 ms/v. However, zone 3 has two parts:

one has various AF and low RA value (RA less than 5 kHz) and another has small ringed various AF (10–20 kHz) and RA has value ranged between 5 and 15 ms/v.

During the corrosion process a number of key stages occur. Initially there is delamination and cracking of the steel wire, this leads to product expansion and a material volume increase. This increase then leads to the mortar cover moving upwards in this example or radially outwards on the real pipe causing a surface crack to form. It can be seen that in this area, before the macro-crack occurred, an increasing number of signals with low amplitudes as shown in Figs. 8 and 9, occurred. This increase in signals is associated with the initial stages of corrosion prior to the larger amplitude signals associated with the mortar cover cracking. This demonstrates that the AE method can not only detect the cover cracking but evidence of the corrosion process can be observed.

In this example the longitudinal cracks grew along the lengths of both wires prior to a third crack forming at an incline/angle to the two already present (Fig. 12 – zone 4). This inclined crack would have initially been created by tensile forces, however as product expansion increases and the two faces of the mortar move upwards relative to each other a shear movement occurs. This is consistent with the findings in Figs. 14 and 15 that show zone 4
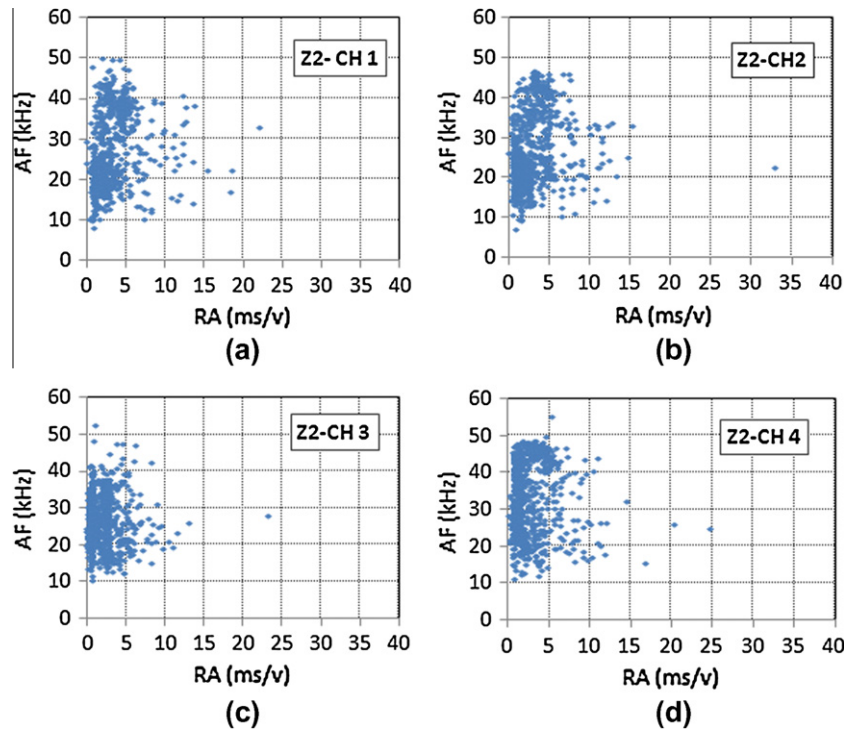
Fig. 16. Relation between the RA value and average frequency of data of (a) sensor 1, (b) sensor 2, (c) sensor 3 and (d) sensor 4.

is a mixed mode area of both tensile and shear movement whilst zones 1 and 2 are purely tensile. It has been shown that by using AE and the relationship between RA and AF value, the crack area can be located and identified (Figs. 11, 14 and 15). Hence, it could be possible to provide a corrosion alarm and location to pipe engineers prior to any wire breaks. Furthermore, by knowing the crack type it is possible to identify the damaged area before the mortar completely fails. Additional analysis has shown that the measured values are not affected by distance from damage source or sensor position making this an ideal approach.

This is revealed by comparing the analysis of data of AF vs. RA values for all the signals detected by the four sensors separately. It can be seen from Fig. 11 that every sensor has different distance from zone 2. Fig. 16a–d shows the AF vs. RA for every sensor for zone 2. It can be seen that the data is similar for every channel, suggesting that the results will not be affected by distance to source. A similar result was found for all zones.

Further work is being conducted to investigate the exact mechanisms within this structure that causes differing RA and AF values. Results suggest that AE techniques can be successfully used as an SHM system on concrete pipes and other concrete structures such as bridges. However, when applying AE techniques on site (in real pipe lines), some limitations need to be considered which include source attenuation, number and location of sensors, noise from the surrounding environment and noise from water flow. Further research studies are needed to overcome these limitations if AE is to be used to successfully monitor pipes.

4. Conclusions

In this paper, the AE technique was used to assess the damage of small scale pipe samples due to prestressing wire corrosion. It was shown that corrosion, macrocracks and crack propagation could be detected. A novel analysis approach to this application has been used to evaluate differing crack types.

The results show that using AE analysis damage can be detected and located whilst the corrosion area, macrocrack and crack propagation can be identified.

In addition, for better visualisation of the data the use of Kernel Density Estimation Function (KDEF) is recommended.

The results offer encouragement to the use of the AE technique to detect early corrosion and macrocracks in pipe structures.

Acknowledgements

References

[1] Singh SK. Corrosion studies on prestressing steel wire. Ph.D. thesis. Imperial College, University of London; 2000.
[2] Bertolini L, Elsener B, Pedeferri P, Polder RP. Corrosion of steel in concrete. 1st ed. Morlenbach: WILEY-VCH; 2004.
[3] Ann KY, Ahn JH, Ryou JS. The importance of chloride content at the concrete surface in assessing the time to corrosion of steel in concrete structures. Constr Build Mater 2009;23:239–45.
[4] Kuwairi A. Water mining: the Great Man-made River Libya. Proc ICE Civ Eng 2006;159(14382):39–43.
[5] Essamin O, Holley M. Great Man Made River Authority (GMRA): The role of acoustic monitoring in the management of the world's largest prestressed concrete cylinder pipe project. In: Proceedings of the ASCE pipeline division specialty congress – Pipeline engineering and, construction 2004; 283–90.
[6] Ing M, Austin S, Lyons R. Cover zone properties influencing acoustic emission due to corrosion. Cem Concr Res 2005;35:284–95.
[7] Hellier CJ. Handbook of non-destructive evaluation. USA: McGraw-Hill; 2001.
[8] Carpinteri A, Lacidogna G, Pugno N. Structural damage diagnosis and life-time assessment by acoustic emission monitoring. Eng Fract Mech 2007;74:273–89.
[9] Miller RK, Hill EVK, Moore PO. Non-destructive Testing Handbook Acoustic Emission Testing, vol. 6. USA: Amer Society for Nondestructive; 2005.

[10] Minemura O, Sakata N, Yuyama S, Okamotod T, Maruyama K. Acoustic emission evaluation of an arch dam During construction cooling and grouting. Constr Build Mater 1998;12:385–92.

[11] Bond L, Kepler W, Frangopol D. Improved assessment of mass concrete dams using acoustic travel time tomography Part I theory. Constr Build Mater 2000;14:133–46.

[12] Shiotani T. Evaluation of repair effect for deteriorated concrete piers of intake dam using AE activity. Adv Mater Res 2006;13–14:175–80.

[13] Nair A, Cai C. Acoustic emission monitoring of bridges: review and case studies. Eng Struct 2010;32:1704–14.

[14] Yuyama S, Yokoyama K, Niitani K, Ohtsu M, Uomoto T. Detection and evaluation of failures in high-strength tendon of prestressed concrete bridges by acoustic emission. Constr Build Mater 2007;21:491–500.

[15] Yu J, Ziehl P, Zárate B, Caicedo J. Prediction of fatigue crack growth in steel bridge components using acoustic emission. J Constr Steel Res 2011;67:1254–60.

[16] Aggelis D, Soulioti D, Sapouridis N, Barkoula N, Paipetis A, Matikas T. Acoustic emission characterization of the fracture process in fibre reinforced concrete. Constr Build Mater 2011;25:4126–31.

[17] Aggelis D. Classification of cracking mode in concrete by acoustic emission parameters. Mech Res Commun 2011;38:153–7.

[18] Ohno K, Ohtsu M. Crack classification in concrete based on acoustic emission. Constr Build Mater 2010;24:2339–46.

[19] Landis E. Micro–macro fracture relationships and acoustic emission in concrete. Constr Build Mater 1999;13:65–72.

[20] Uddin A, Numata K, Shimasakia J, Shigeishi M, Ohtsua M. Mechanisms of crack propagation due to corrosion of reinforcement in concrete by AE-SiGMA and BEM. Constr Build Mater 2004;18:181–8.

[21] Ohtsu M, Tomoda Y. Corrosion process in reinforced concrete identified by acoustic emission. Mater Trans 2007;48(6):1184–9.

[22] Kawasaki Y, Tomoda Y, Ohtsu M. AE monitoring of corrosion process in cyclic wet–dry test. Constr Build Mater 2010;24:2353–7.

[23] Muralidhara S, Prasad B, Eskandri H, Karihaloo B. Fracture process zone size and true fracture energy of concrete usin acoustic emission. Constr Build Mater 2010;24:479–86.

[24] Ing MJ. Detection of reinforcement corrosion by an acoustic technique. Ph.D. thesis, Loughborough University; 2003.

[25] Zongjin Li, Faming Li, Zdunek A, Landis E, Shah S. Application of acoustic emission technique to detection of rebar corrosion in concrete. ACI Mater J 1998;95:68–76.

[26] JCMS-III B5706. Monitoring method for active cracks in concrete by AE. Construction Material Standards. Tokyo: Japan; 2003.

[27] Watanabe T, Nishibata S, Hashimoto C, Ohtsu M. Compressive failure in concrete of recycled aggregate by acoustic emission. Constr Build Mater 2007;21:470–6.

[28] Ohtsu M. Source kinematics of acoustic emission based on moment tensor. NDT Int 1989;22:14–20.

[29] Elfergani H, Pullin R, Holford K. Acoustic emission analysis of prestressed concrete structures. J Phys: Conf Ser 2011;305(1):012076.

[30] Al NAHR CO. LTD. Technical report. Libya, July; 1999.

[31] Li X, Zhang Y. Analytical study of piezoelectric paint for acoustic emission-based fracture monitoring. Fatigue Fract Eng Mater Struct 2008;31:684–94.

[32] Hsu NN, Breckenridge FR. Characterization and calibration of acoustic emission sensor. Mater Eval 1981;39(1):60–8.

[33] Rippendgill S, Worden K, Pullin R, Holford K. Automatic classification of acoustic emission patterns. Strain 2003;39:31–41.

Acoustic Emission Analysis of Prestressed Concrete Structures

H.A. Elfergani, R. Pullin and K.M. Holford

Cardiff School of Engineering, Cardiff University, Queen's Building, The Parade,

Cardiff, CF24 3AA, Wales, UK

ElferganiH@Cardiff.ac.uk, PullinR@cardiff.ac.uk, holford@Cardiff.ac.uk

Abstract. Corrosion is a substantial problem in numerous structures and in particular corrosion is very serious in reinforced and prestressed concrete and must, in certain applications, be given special consideration because failure may result in loss of life and high financial cost. Furthermore corrosion cannot only be considered a long term problem with many studies reporting failure of bridges and concrete pipes due to corrosion within a short period after they were constructed. The concrete pipes which transport water are examples of structures that have suffered from corrosion; for example, the pipes of The Great Man-Made River Project of Libya. Five pipe failures due to corrosion have occurred since their installation. The main reason for the damage is corrosion of prestressed wires in the pipes due to the attack of chloride ions from the surrounding soil. Detection of the corrosion in initial stages has been very important to avoid other failures and the interruption of water flow. Even though most non-destructive methods which are used in the project are able to detect wire breaks, they cannot detect the presence of corrosion. Hence in areas where no excavation has been completed, areas of serious damage can go undetected. Therefore, the major problem which faces engineers is to find the best way to detect the corrosion and prevent the pipes from deteriorating. This paper reports on the use of the Acoustic Emission (AE) technique to detect the early stages of corrosion prior to deterioration of concrete structures.

1. Introduction

Several structures e.g. bridges, buildings, concrete pipes, strong tanks, dams, nuclear reactor protective shells, railway sleepers, piles and pressure vessels are made of prestressed concrete in which prestressing steel wires are put into a permanent state of tension to compensate for the inadequate tensile strength of the concrete. Tensile cracking in the concrete is minimised by ensuring that the concrete is in compression under normal working loads by prestressing the steel reinforcement. Generally prestressed steel is between four to five times stronger than mild steel. The main advantages of prestressed concrete structural materials are that they are stronger, lighter and "crack free" [1] and hence these materials offer cost benefits over other materials.

Corrosion is a big problem in numerous structures. The cost due to corrosion is estimated in billions of dollars every year. Department of Transport in the UK evaluated that, the cost of recondition of concrete structures damaged by corrosion problems is £755 million a year [2]. The problem of corrosion in this type of structure must be given special consideration because failure may result in the worst scenario a loss of life but at a minimum a loss in finance. Most studies indicate the main reason of failure of bridges and concrete pipes is due to corrosion during the short period after they were constructed. The concrete provides the ideal environment to protect the steel wires which are

embedded in it possibly for over 50 years [3]. However, the life of a concrete structure becomes shorter due to steel corrosion which may occur by aggressive ion attack from products of chloride or carbonation [2].

The concrete pipes which transport water are one such structure that has suffered from corrosion. For example, the pipes of Great man-made river project of Libya have suffered catastrophically from this affect. Five pipe failures due to corrosion have occurred since their installation. However, the big problem which faces the engineers, apart from future corrosion protection, is to find the best way to detect the corrosion and prevent the pipes from deteriorating [1]. This project aims to use the AE technique to detect the early stages of corrosion prior to deterioration and eventual failure of the concrete structures.

Acoustic emission (AE) is defined as the elastic energy released from materials which are undergoing deformation. Also it can be defined as "the transient elastic waves which are generated by the rapid release of energy from localized sources within a material" [4].The rapid release of elastic energy, the AE event, propagates through the structure to arrive at the structure surface where a piezoelectric transducer is mounted. These transducers detect the displacement of the surface at different locations and convert it into a usable electric signal. By analysis the resultant waveform in terms of feature data such as amplitude, energy and time of arrival, the severity and location of the AE source can be assessed.

The Great Man-Made River Project (GMRP) is the one of the major civil engineering projects of the 20th century located in Libya. The project is concerned with water transportation from the aquifers deep in the Sahara desert to the coastal region where over 90% of the population lives and the main regions of agriculture and industry are located. The high quality ground water is conveyed throughout almost 4000 km of prestressed concrete cylinder pipe (PCCP) networks as shown in Figure 1. The PCCP networks consist mainly of four metre diameter pipes and 6.6 million cubic metres water is transported every day. The purpose of the project is to transform thousands of hectares of semi-desert into rich fertile agricultural land. [1, 5, 6]

Pre-stressed concrete cylinder pipes are designed to take best advantage of the compressive strength and corrosion-inhibiting property of Portland cement concrete and mortar and the tensile strength of prestressing wire. Each transportation line pre-stressed concrete cylinder pipe is mainly 4.0 m in inner diameter; with a length of 7.5 m, and over 70 tonnes in weight. The concrete pipe consists of a 225 mm thick concrete core within an embedded thin steel cylinder and externally wrapping prestressed wires. The cured concrete core is prestressed by applying over-wrapping with high tensile steel wire at a close pitch under uniform tension. The prestressed wires are coved by a 19 mm thick layer of cement mortar to protect the wires against corrosion and mechanical harm. A typical cross-section of the PCCP is shown in Figure 2.
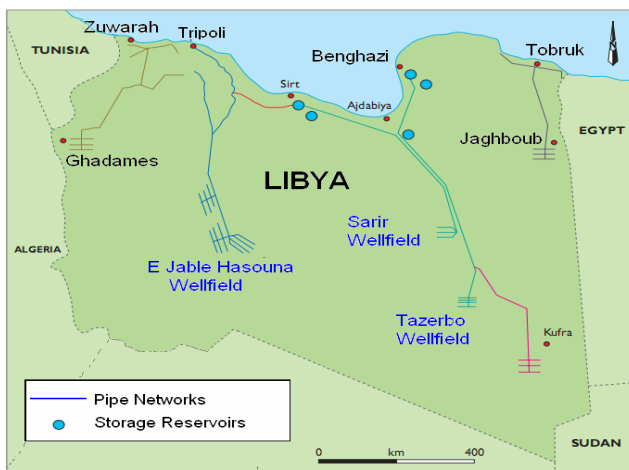

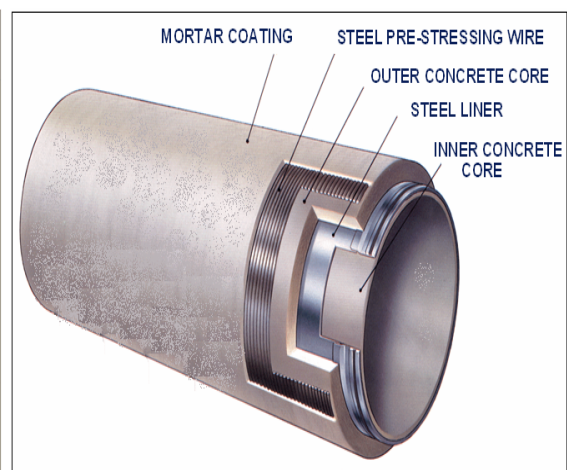Figure 1 Layout of the Pipe Networks of GMRP [5]   Figure 2 Typical Cross-Section of the PCCP

The pipe is designed in accordance to AWWA standard C301 [7]. The pressure evaluation is based on the maximum steady state operating pressure plus a safety factor of about 5m head of water, and accommodates transients up to 140% of rated pressure. Classifications of the primary transportation system range from 6 bar to 28 bar in 2 bar increases, the different classifications are controlled by changes in prestressing wire diameter, pitch and number of layers during pipe manufacture. In order to protect the pipelines from risks including temperature variations and other environmental conditions they are laid in seven metre deep trenches.

Due to prestressed wire corrosion in the concrete pipes induced by chloride ions absorbed from the aggressive soil, five catastrophic failures in four metre diameter white pipes occurred between 1999 and 2001 after ten years of operation. The main reason for the damage is corrosion of prestressed wires in the pipes due to attack the chloride ions from soil. Detection of the corrosion in initial stages has been very important to avoid other failures which will interrupt water flows. Initially traditional techniques such as potential mapping, tapping and close-interval potential surveys were used to make a vast survey of the current pipelines. Then, experts used electromagnetic inspection and acoustic monitoring was used to inspect and monitor the rate of deterioration of pipes [6]. The time and location of wire break events can be determined by this method, however the detection of corrosion was not considered. Even though most of non-destructive methods, which are used in the project, are able to detect wire break, they cannot detect the presence of corrosion. Hence in areas where no excavation has been completed, areas of serious damage can go undetected. In this respect AE has significant advantages compared with other NDT methods because the AE technique is the only one able to reliably detect the very early stages of the corrosion process, before significant damage to the concrete has occurred and furthermore it can indicate the level of damage occurring to the concrete. [8, 9, 10]

2 Experimental Procedure

2.1 Tension holding frame
Since it was intended in this work to simulate as close as possible the real physical conditions surrounding the high strength steel wires in concrete pipes, it was prudent to place and maintain all relevant wire samples under tension equal to 60% of their U.T.S in PCCP. To achieve this objective a tension frame was especially designed and fabricated.

The frame consists mainly of two blocks (190mm x 45mm x 45mm) and two threaded steel bars (studding) having a diameter of 20 mm and a length of 500 mm. Two holes (20 mm diameter) and two (6mm) are drilled in each block. Figure 3 shows a schematic drawing for the tension holding frame. The two blocks are assembled via two threaded bars tightened by means of eight nuts.
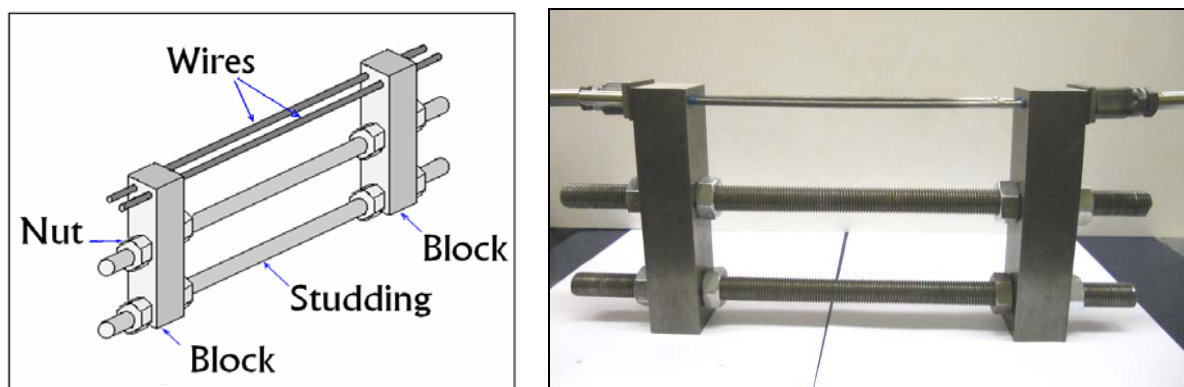

Figure 3 Tension holding frame

2.2 Wire preparation

The two working high strength steel wires samples were supplied from GMRA PCCP manufacturing plant in Libya. The metallurgical composition and mechanical properties as certified by the wire manufactures is summarized as follows: Carbon steel (carbon 0.8-0.84%, 0.85-1.00%Mn, 0.030 %Max S, 0.035% Max P, 0.20-0.35% Si). The tensile strength of the wires is almost 1738 MPa.

The two working wire samples were passed through 6 mm diameter holes in the steel blocks and then two modified bolts and nuts (designed to control the tension load of each wire). Finally a steel cylinder was then threaded over the wire. The cylinder was then compressed in a load machine. In this way the modified nut and bolt could be expanded between the clamped cylinder and the steel block and as a result tension could be introduced into the wire. Each wire was subjected to a tensile force of 20 kN by adjusting the bolts and nuts and monitored via strain gauges mounted on the wires.

2.3 Concrete and mortar preparation

The concrete specimen (200*200*50mm), representative of the inner pipe was prepared according to the technical specification for PCC Pipe Manufacturing used in Great Man-Made River Project, which is in accordance with AWWA C301-92 (Standard for Pre-stressed Concrete Pressure Pipe, Steel Cylinder Type, for Water and Other Liquids.) [11] Three days after casting the concrete specimen, the wires combined with their holding frame were placed on the upper surface of this specimen. Finally the mortar 200*200mm and 20 mm thickness was coated on the upper surface of the concrete. The mortar should consist of one part cement to not more than three parts fine aggregate by weight. The construction is shown in Figure 4.
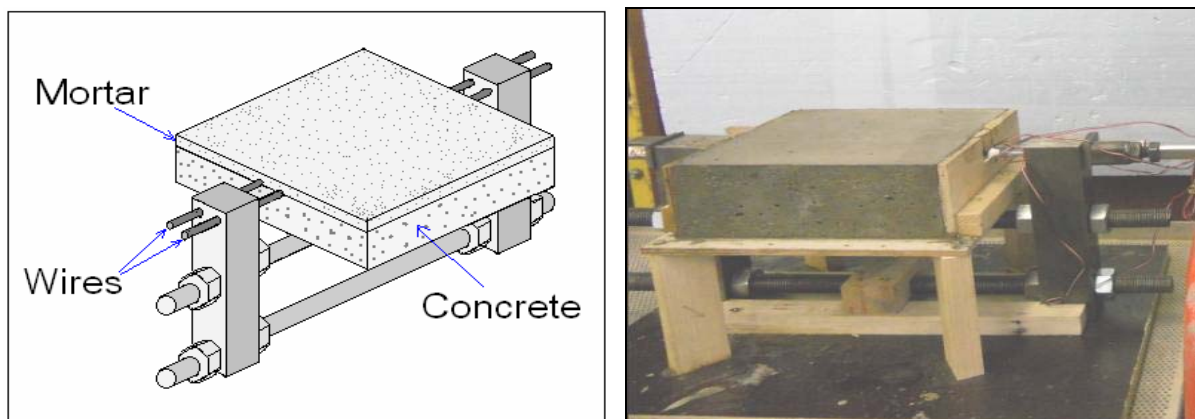

Figure 4 Concrete and mortar specimen

2.4 Accelerated corrosion technique

To study the effects of corrosion within a realistic time-scale, it is sometimes necessary to accelerate the initiation period and occasionally control the rate of corrosion during the propagation stage. To simulate the corrosion of prestressing steel wires, the corrosion cell was induced by impressed current ($100\mu A/cm^2$). This is reported as corresponding to the maximum corrosion rate for concrete in laboratory conditions and has been used by several researchers in the laboratory as discussed by Li and Zhang [12].

In this experimental work, the wire corrosion was induced by impressed current ($100\mu A/cm^2$). The prestressed wires were contacted in an electrical circuit with positive pole of power supplier and the negative pole connected with stainless steel plate attached the upper mortar. Then a 5% NaCl solution was poured on the surface of the mortar.

2.5 Acoustic emission set-up

Four Physical Acoustic Limited (PAL) AE sensors (R3I – resonance   30 kHz, R6D – resonance 60 kHz) were mounted to the surface of mortar as shown in Figure 5. A PAL DiSP system was used to acquire and capture all AE data. The sensitivity of the AE system was checked using the Hsu-Neilson source [13].
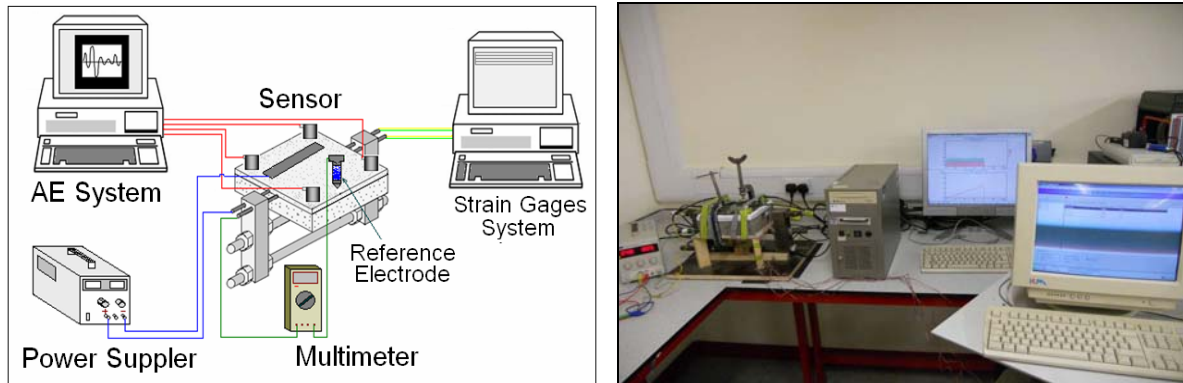

Figure 5 Schematic Diagram and Photo of Experimental set up

3. Results and Discussion

Figure 6 shows the cumulative acoustic energy as detected by all sensors for almost nine days of continuous monitoring. The detected energy is attributed to active corrosion and mortar cracking. The graph demonstrates the behaviour of the energy emission in three regions of time. Each period of time marked represent three days of monitoring.
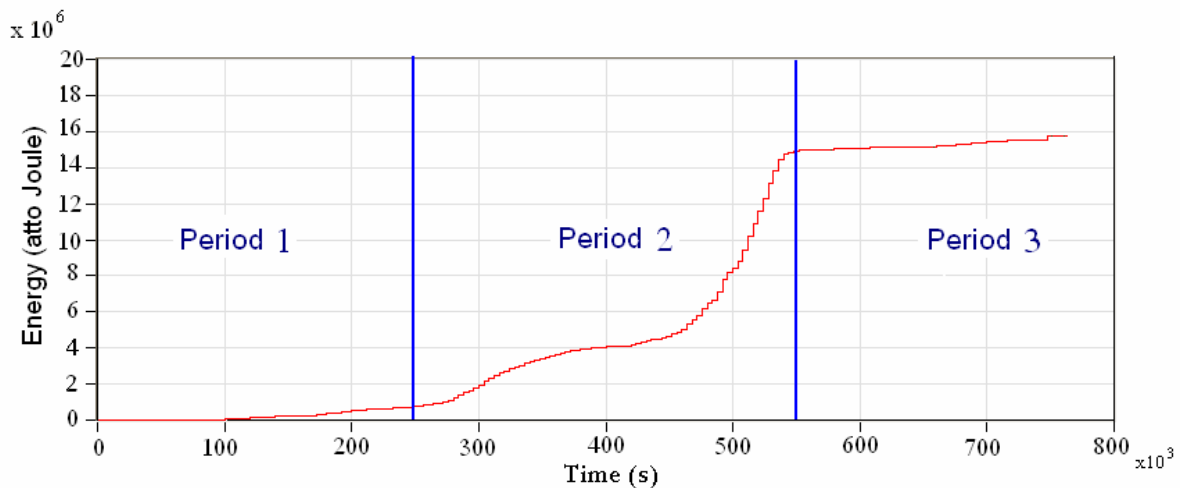

Figure 6 Energy vs. time

Figure 7 shows the variation strains of two wires (strains 1, 2 for wire 1 and strains 3, 4 for wire 2) with time. In addition, the current supply (corrosion rate) is added as a function of time.
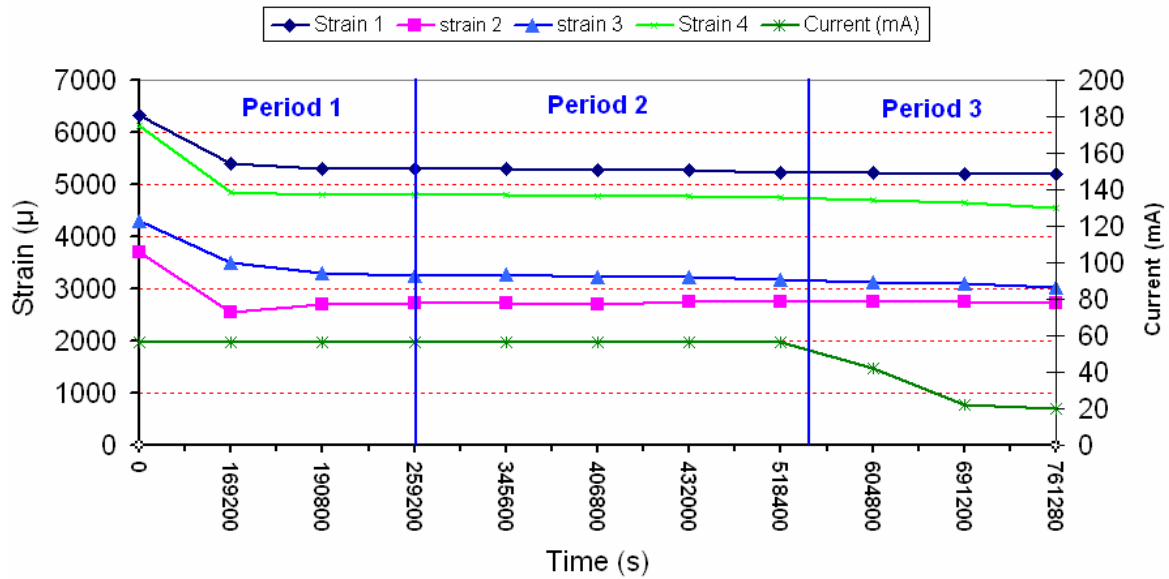
Figure 7 Strain and current vs. Time

Figure 8 shows source location of sample before supplying current (no corrosion) for about 20 hours. It can be seen that there is a low level of events prior to the onset of corrosion. A colour key that indicates the number of signals detected at a position is also provided.
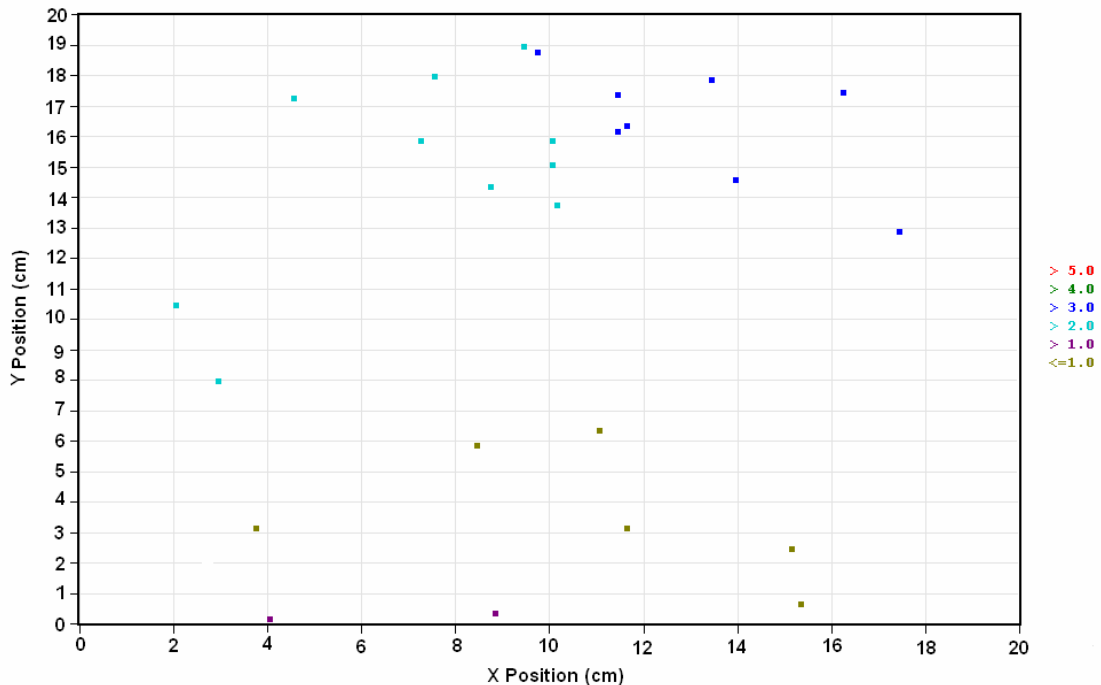

Figure 8 Source locations before supplying current (no corrosion)

The period of test is divided to three different stages as shown in Figures 6 and 7. The first stage, which is first three days, is named period 1. The energy emitted is attributed to constant corrosion

activity, a small visible crack and the separation of mortar from the concrete. It can be noted that in this stage, considerable decrease in strains is evident (Figure 7) due to initial crack in this location. Furthermore, Figure 9 shows the source location of signals within this period 1. It can be seen that the highest hits concentration appears in the region of corrosion reaction, where the stainless steel plate (cathodic reaction) and wire (anodic reaction) are placed.
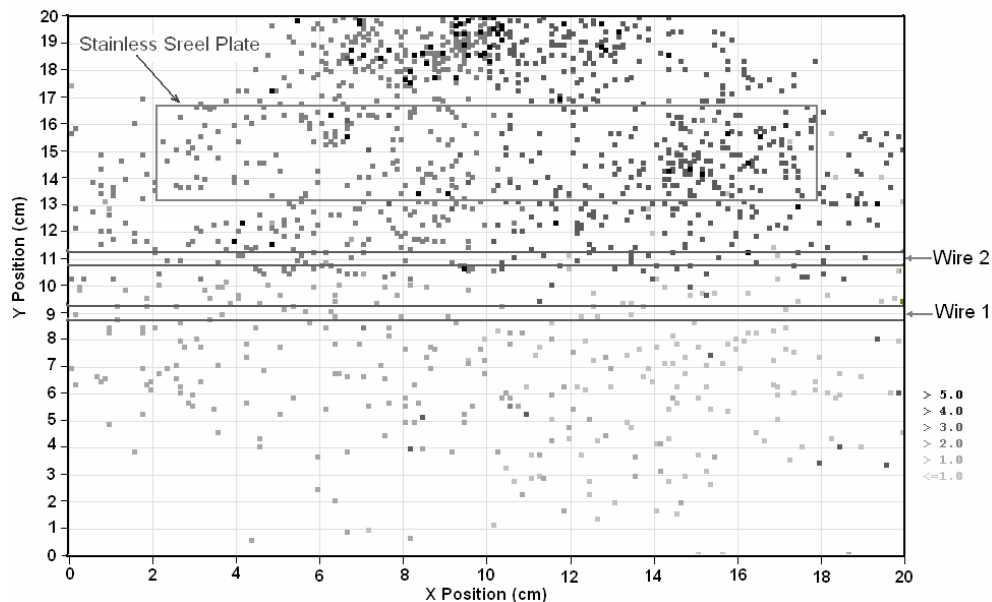

Figure 9 Source location for first three days (Period 1)

The second stage is between the fourth day and sixth day which is named period 2. In this stage, it can be seen that the current and strains are constant while the emission energy increases significantly as shown in Figure 6 and 7. Furthermore, it can be seen that in Figure 10 the locations considerably increase due to the growth of the crack and split of mortar from concrete. Also, a high concentration of hits in the area of corrosion reactions can be observed.
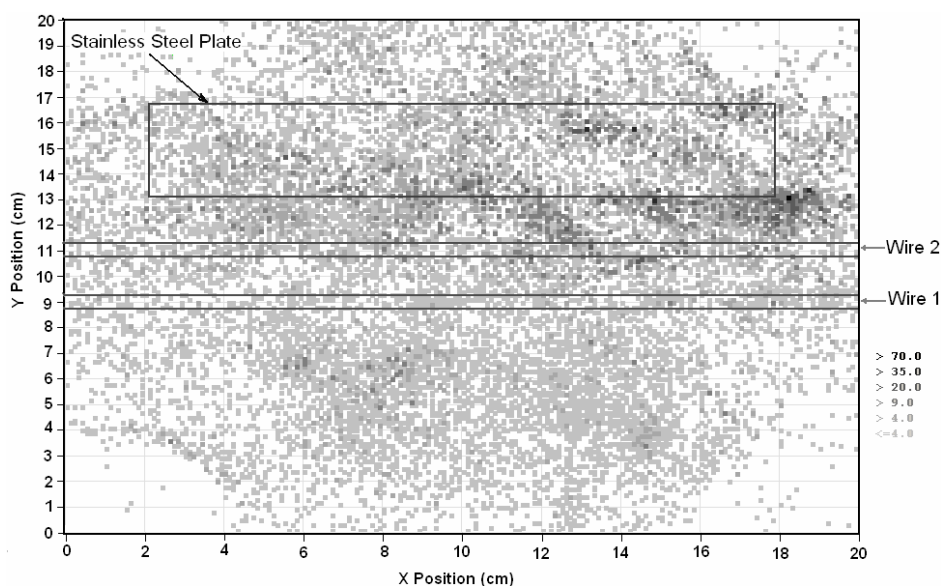

Figure 10 Source location for middle three days (Period 2)

During the final three days (period 3 in Figure 6 and Figure 7) it can be noted that the energy decreases due to decrease of current (corrosion rate). In addition, Figure 11 shows source location on the mortar surface. It can be seen that the number of hits is decreased from period two.
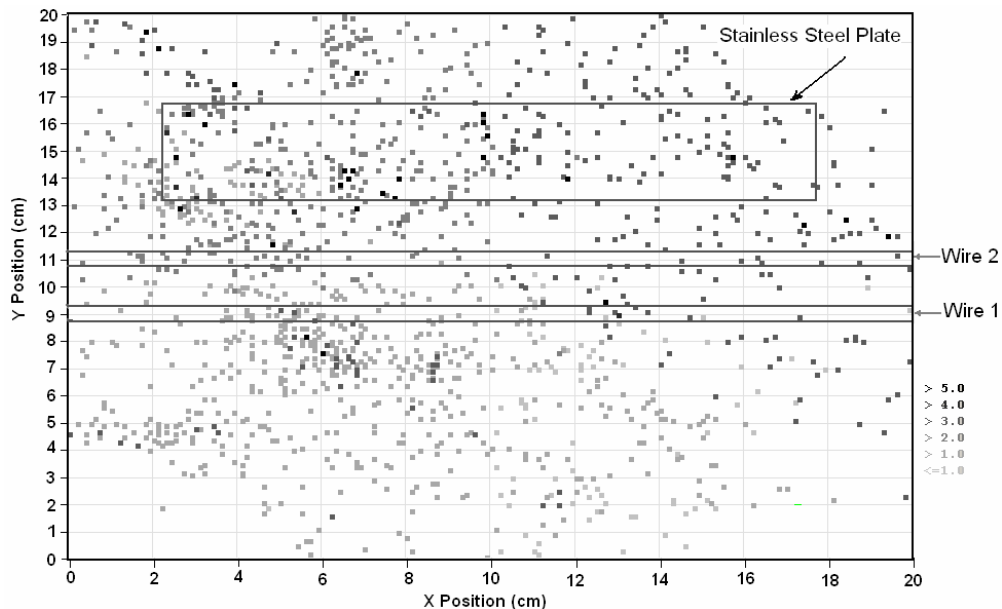

Figure 11 Source location for last three days (Period 3)

Figure 12 shows the distribution of hits with minimum amplitude 40dB for whole test (three periods) while Figure 13 shows hits distribution with amplitude greater than 47dB for whole period of the test. It can be noted that the highest hits concentration and highest energy in region coincide with maximum wire corrosion which was visibly observed post test.
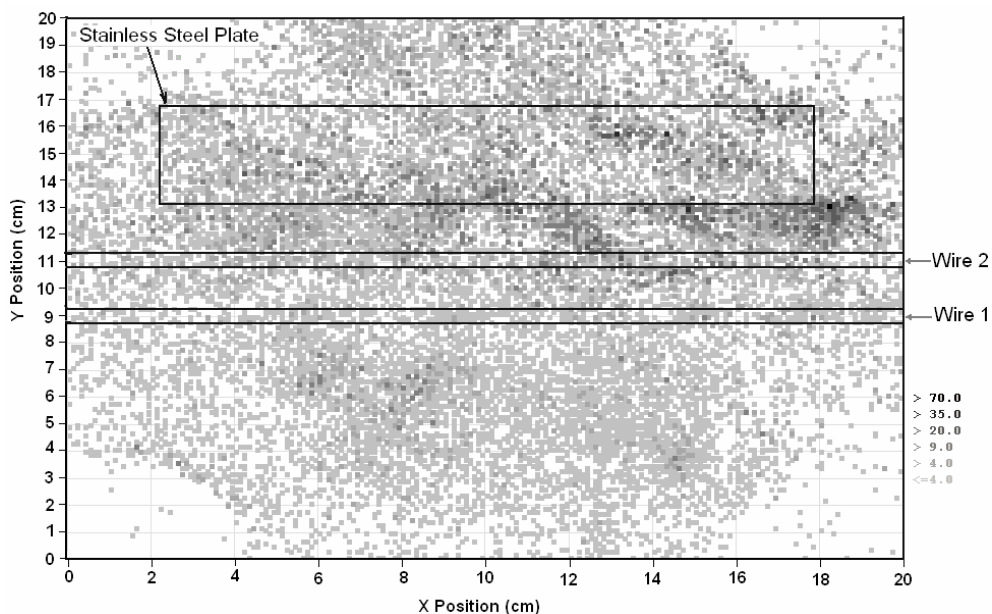

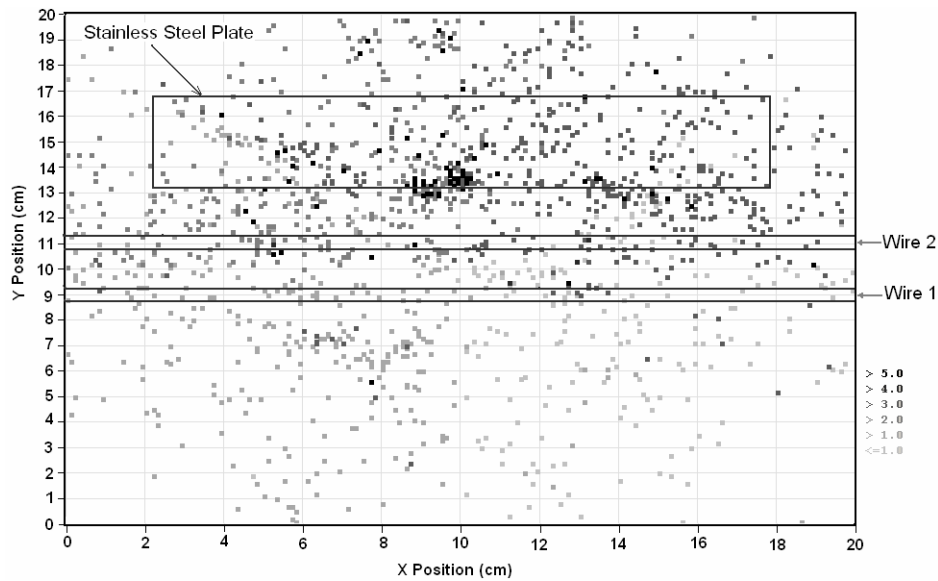Figure 12 Source locations for 9 days

Figure 13 Source locations for whole test with amplitudes greater than 47dB

Figure 14(a) is a schematic diagram of the specimen after testing. The figure shows the sensors mounted on mortar surface, wires, stain steel plate and crack shape. Figure 14b is a photograph of the top mortar surface after finish the test, again showing the crack shape. Comparing the two figures with previous locations reinforces that the AE was detecting the concrete cracking as a result of wire corrosion within the specimen.
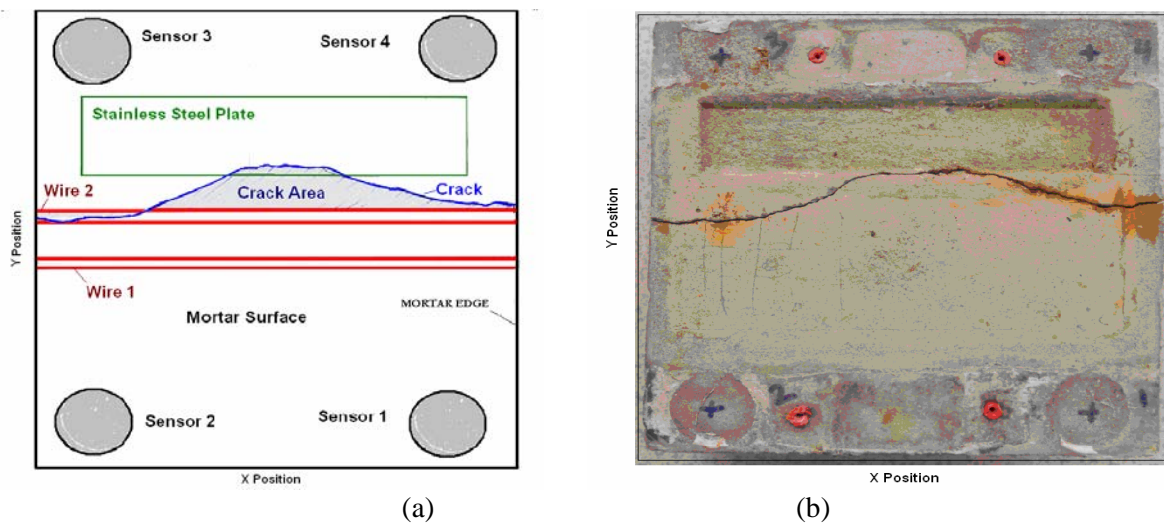

(a)   (b)

Figure 14 Schematic Diagram and photo of top mortar surface

The corrosion wires and corrosion product once the mortar had been removed is shown in Figure 15. It is evident that significant corrosion occurred in the upper wire and it was in this location that a large majority of AE signals were detected and located. The results offer encouragement to the use of the AE technique to detect early corrosion in pipe structures, however for full validation considerable larger specimens will have to be considered. A further series of investigations are planned that will utilise environmental chambers to assess temperature effects and geometric effects with the ultimate aim of producing a guide to detecting early corrosion in pipe structures using AE.

Figure 15 Photo of upper concrete surface and wires

4. Conclusion

This paper reveals that use of the AE technique as a non-destructive technique can detect the onset of corrosion activity in wire in the interface between prestressed concrete and mortar as found in prestressed concrete pipes. Furthermore, this technique is able to locate approximately the corrosion activity on small prestressed concrete samples.

5. Acknowledgements

References

[1]   Singh S. K., 2000 Corrosion Studies on Prestressing Steel Wire, Ph.D. Thesis, Imperial College, University of London.

[2]   Ann K.Y., Ahn J. H., Ryou J. S., 2009, The importance of chloride content at the concrete surface in assessing the time to corrosion of steel in concrete structures, Construction and Building Materials, 23, pp239–245.

[3]   Bertolini L., Elsener B., Pedeferri P., Polder R. P., 2004, Corrosion of Steel in Concrete. Morlenbach: WILEY-VCH.

[4]   Miller R. K., Hill E. V. K., Moore P. O., 2005, Non-destructive Testing Handbook, Acoustic Emission Testing, Volume 6, USA.

[5]   Kuwairi A., 2006, Water mining: the Great Man-made River, Libya, Proceedings of ICE Civil Engineering 159 May 2006 Pages 39-43 paper 14382.

[6]   Essamin O. and Holley M., 2004, Great Man Made River Authority (GMRA): The Role of Acoustic Monitoring in the Management of the Worlds Largest Prestressed Concrete Cylinder Pipe Project , Proceedings of the ASCE Annual International Conference on Pipeline Engineering and Construction, August 1-4, San Diego, California.

[7]   Al NAHR CO. LTD. In Libya, July 1999, Technical Report.

[8]   Ing M., Austin S., Lyons R., 2005, Cover zone properties influencing acoustic emission due to corrosion, Cement and Concrete Research 35 pp 284– 295.

[9]   Hellier C. J. , 2001, Handbook of Non-destructive Evaluation, McGraw-Hill, USA.

[10]   Carpinteri A., Lacidogna G., Pugno N. 2007, Structural damage diagnosis and life-time assessment by acoustic emission monitoring. Engineering Fracture Mechanics 74, pp273– 289.

[11]   Singh S. K., 2000 Corrosion Studies on Prestressing Steel Wire, Ph.D. Thesis, Imperial College, University of London

[12]   Li X. and Zhang Y., 2008, Analytical Study of piezoelectric Paint for Acoustic Emission-Based Fracture Monitoring, Fatigue and Fracture of Engineering Materials and Structures 31, pages 684-694.

[13]   Hsu N N, and Breckenridge, F. R. 1981, Characterization and Calibration of Acoustic Emission Sensor. Materials Evaluation 39 (1) pages 60-68.

Crack Classification and Location Using Acoustic Emission Analysis in Prestressed Concrete Structures

Hisham A. Elfergani

Cardiff School of Engineering, Cardiff University,
Queen's Building, The Parade ,
Cardiff, CF24 3AA, Wales, UK
Supervisor: Rhys Pullin and Karen M. Holford

Abstract

Deterioration, by corrosion of steel wire in reinforced and prestressed concrete is very serious and must be given special consideration; failure may result in the loss of life and a high financial cost. One application is prestressed concrete cylinder pipes which are widely used for conveying water and wastewater. The biggest problem in these pipes is corrosion of the prestressed wires which can lead to catastrophic failure. In the Great Man-mad River in Libya detection of the corrosion in its initial stages is very important to avoid water interruption to homes and industry. This paper reports on the use of the Acoustic Emission (AE) technique to detect and locate the early stages of corrosion and classify different crack types. Preliminary results presented indicate that AE is capable of detecting corrosion in representative structures. In addition, it can identify and classify the crack location and type.

1   Introduction

Corrosion is a significant problem in numerous structures. The cost due to corrosion is estimated at billions of dollars every year. The Department of Transport in the UK evaluated that the cost of repairing concrete structures damaged by corrosion problems as £755 million a year [1]. The risk of corrosion in this type of structure must be given special consideration because failure may result in the worst case a, loss of life, but at a minimum a financial loss. Most studies indicate that the main reason of the failure of bridges and concrete pipes is corrosion during the short period after they were constructed. However, the life of a concrete structure becomes even shorter due to steel corrosion, which may occur by aggressive ion attack from products of chloride or carbonation [1].

The concrete pipes which transport water are one such structure that has suffered from corrosion. For example, the pipes of Great Man-Made River project of Libya have suffered catastrophically from this affect. Five pipe failures due to corrosion have occurred since their installation. However, the substantial challenges which face the engineers, apart from future corrosion protection, is to find the best way to detect the corrosion and prevent the pipes from deteriorating [2]. This project aims to use the Acoustic Emission (AE) technique to detect the early stages of corrosion prior to deterioration and eventual failure of the concrete structures.

AE is defined as the elastic energy released from materials which are undergoing deformation. Also, it can be defined as "the transient elastic waves which are generated by the rapid release of energy from localised sources within a material" [3].The rapid release of elastic energy, the AE event, propagates through the structure to arrive at the structure surface where a piezoelectric transducer is mounted. These transducers detect the displacement of the surface at different locations and convert it into a usable electric signal. By analysis of the resultant waveform in terms of feature data such as amplitude, energy and time of arrival, the severity and location of the AE source can be assessed.

According to many of researches [4, 5, 6, 7] the relationship between RA values (rise time/ Amplitude) and average frequencies (counts/duration) can be used for classification of crack types. They reported that when an AE signal has low average frequency and high RA value it is classified as shear type crack. However when it has a high average frequency and low RA value classified as tensile type crack as shown Fig.1and 2.
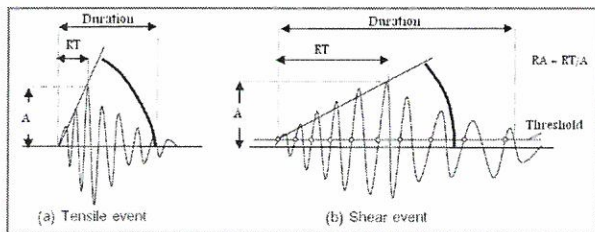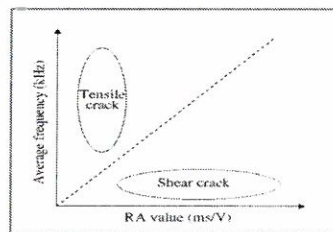
Fig. 1 Typical waveforms [4]

Fig. 2 Crack classification [4]

The Great Man-Made River Project (GMRP) is the one of the major civil engineering projects of the 20th century located in Libya. The project is concerned with water transportation from the aquifers deep in the Sahara desert to the coastal region where over 90% of the population lives. The water is conveyed throughout almost 4000 km of prestressed concrete cylinder pipe (PCCP) networks as shown in Fig. 3. [2, 8, 9]

Pre-stressed concrete cylinder pipes are designed to take the best advantage of the compressive strength and corrosion-inhibiting property of Portland cement concrete and mortar and the tensile strength of prestressing wire. The majority of pre-stressed concrete cylinder pipes are 4.0 m in inner diameter; with a length of 7.5 m, and over 70 tonnes in weight. The concrete pipe consists of a 225 mm thick concrete core within an embedded thin steel cylinder and externally wrapping prestressed wires. The cured concrete core is prestressed by applying over-wrapping with high tensile steel wire at a close pitch under uniform tension. The prestressed wires are coved by a 19mm thick layer of cement mortar to protect the wires against corrosion and mechanical harm. A typical cross-section of the PCCP is shown in Fig. 4.
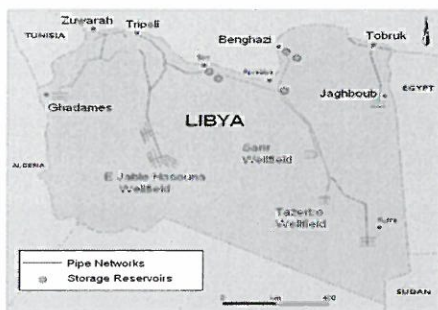

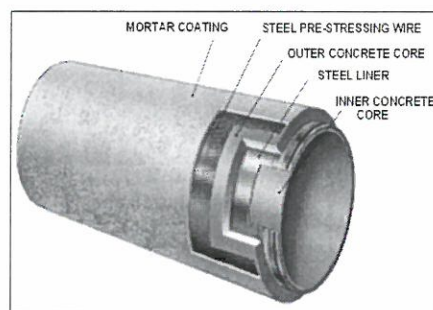Fig. 3 Pipe Networks of GMRP [8]

Fig. 4 Typical cross-section

Five catastrophic failures in four metre diameter pipes occurred between 1999 and 2001 after ten years of operation. The main reason for the damage is corrosion of prestressed wires in the pipes due to attack by the chloride ions from the surrounding soil. Detection of the corrosion in the initial stages has been very important to avoid other failures which will interrupt water flows. Even though most of the non-destructive methods which are used in the project are able to detect wire breaks, they cannot detect the presence of corrosion. Hence, in areas where no excavation has been completed, areas of serious damage can go undetected. In this respect, AE has significant advantages compared with other NDT methods because the AE technique is able to reliably detect the very early stages of the corrosion process, before significant damage to the concrete has occurred. Furthermore, it can indicate the level of damage occurring to the concrete. [10, 11, 12]

2 Experimental Procedure

2.1 Tension holding frame

Since it was intended in this work to simulate as close as possible the real physical conditions surrounding the high strength steel wires in concrete pipes, it was important to place and maintain all relevant wire samples under tension equal to 60% of their ultimate tensile strength in PCCP. To achieve this objective a tension frame was designed and fabricated.

The frame consists of two blocks (190mm x 45mm x 45mm) and two threaded steel bars (studding) having a diameter of 20 mm and a length of 500 mm. Two holes (20 mm diameter) and two (6mm) are drilled in each block. Fig. 5 shows a schematic drawing for the tension holding frame. The two blocks are assembled via two threaded bars tightened by means of eight nuts.
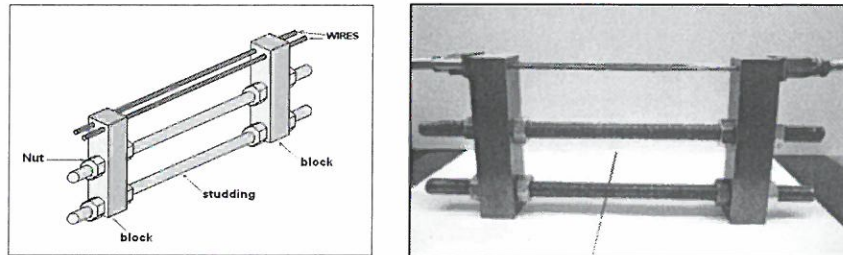

Fig. 5 Tension holding frame

2.2 Wire preparation

The two working high strength steel wires samples were supplied from GMRP manufacturing plant in Libya. The metallurgical composition and mechanical properties as certified by the wire manufactures is summarised as follows: Carbon steel (carbon 0.8-0.84%, 0.85-1.00%Mn, 0.030 %Max S, 0.035% Max P, 0.20-0.35% Si). The tensile strength of the wires is approximately 1738 MPa.

The two working wire samples were passed through 6 mm diameter holes in the steel blocks and then through the two modified bolts and nuts, designed to control the tension load of each wire. Finally a steel cylinder was then threaded over the wire. The cylinder was then compressed in a load machine. In this way the modified nut and bolt could be expanded between the clamped cylinder and the steel block and as a result tension could be introduced into the wire. Each wire was subjected to a tensile force of 20 kN by adjusting the bolts and nuts and the resulting strain was monitored via strain gauges mounted on the wires.

2.3 Concrete and mortar preparation

The concrete specimen (200×200×50mm), representative of the inner pipe was prepared according to the technical specification for PCCP manufacturing used in GMRP, which is in accordance with AWWA C301-92 (Standard for Pre-stressed Concrete Pressure Pipe, Steel Cylinder Type, for Water and Other Liquids)[2]. Three days after casting the concrete specimen, the wires combined with their holding frame were placed on the upper surface of this specimen. Finally the mortar 200×200mm and 20 mm thickness was coated on the upper surface of the concrete. The mortar consists of one part cement to not more than three parts fine aggregate by weight. The final construction is shown in Fig.6.
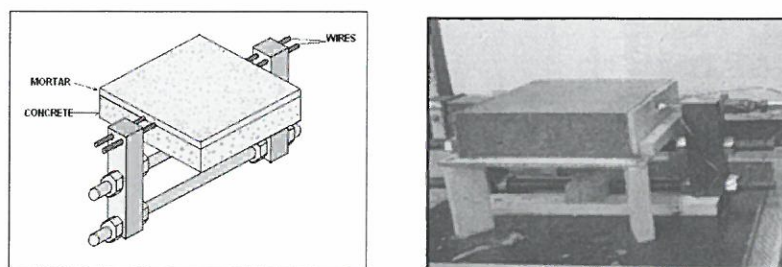

Fig. 6 Concrete and mortar specimen

2.4 Accelerated corrosion technique

To study the effects of corrosion within a realistic time-scale, it is sometimes necessary to accelerate the initiation period and occasionally control the rate of corrosion during the propagation stage. To simulate the corrosion of prestressing steel wires, the corrosion cell was induced by an impressed current ($100\mu A/cm^2$). This is reported as corresponding to the maximum corrosion rate for concrete in

laboratory conditions and has been used by several researchers in the laboratory as discussed by Li and Zhang [13]. In this experimental work, the wire corrosion was induced by impressed current ($100\mu A/cm^2$). The prestressed wires were contacted in an electrical circuit with positive pole of power supplier and the negative pole connected with a stainless steel plate (30*150 mm) resting on the upper mortar. A 4% NaCl solution was poured on the surface of the mortar. Silicon sealant was used to pool the solution on the upper surface.

2.5   Acoustic emission set-up

AE instrumentation typically consists of transducers, filters, amplifiers and analysis software. Four AE sensors (R3I – resonant frequency 30 kHz) were mounted to surface of mortar.The four AE sensors were mounted using silicon sealant and were fixed on the upper surface of mortar with a U shaped plate. The plate was screwed to hold the sensors down and to ensure a good coupling. Then the sensitivity of the sensors was checked by using the Hsu-Neilson source [14].

3   Results and Discussion

Figure 7a is a schematic diagram of the specimen after testing. The figure shows the sensors mounted on the mortar surface, wires position, the stainless steel plate and the crack shape. Fig. 7 b is a photograph of the top mortar surface the after of the test finished, again showing the crack shape

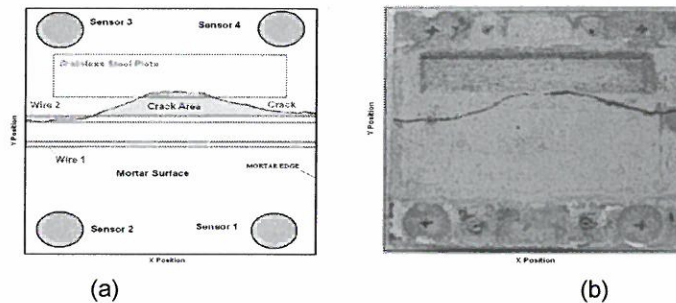(a)   (b)

Fig. 7 Schematic Diagram and photo of top mortar surface

Fig. 8 shows the location of hits with minimum amplitude 45dB for the whole period of the test. It can be noted that the highest hits concentration and highest energy coincides with maximum wire corrosion and the crack which was visibly observed post test. Four zones have been chosen as examples to differentiate between cracks and non cracked areas. Areas were chosen based on visual observation (Fig. 7b) zone 1 and 2 represent crack areas whereas zone 3 and 4 no cracks were present.

Fig. 9 (a, b, c, and d) Show the AF vs. RA value for different regions of concentration of events on surface of mortar. Fig. 9 (a and b) show the AF vs. RA for zones associated with the crack regions. It can be seen that the most of data points have various AF and low RA value (less than 10 ms/v). Therefore, based on Fig. 7, this indicates that the type of the crack is tensile cracks. However, the Fig. 9 (C and d) show the relationship between RA value and AF, where areas on the location with low concentration of hits. It can be noted that the RA value has a wide distribution (0-50 ms/v).
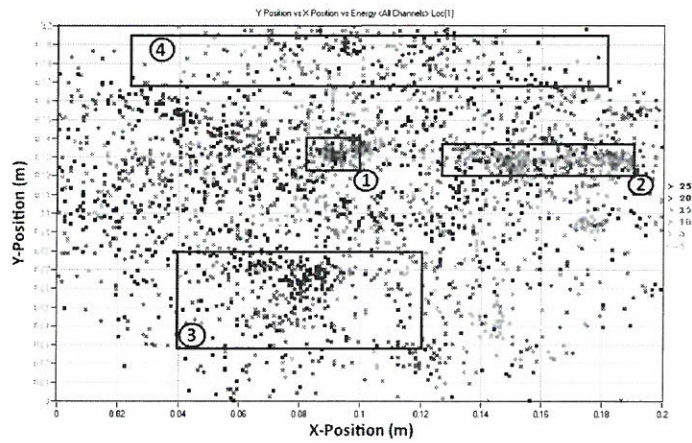
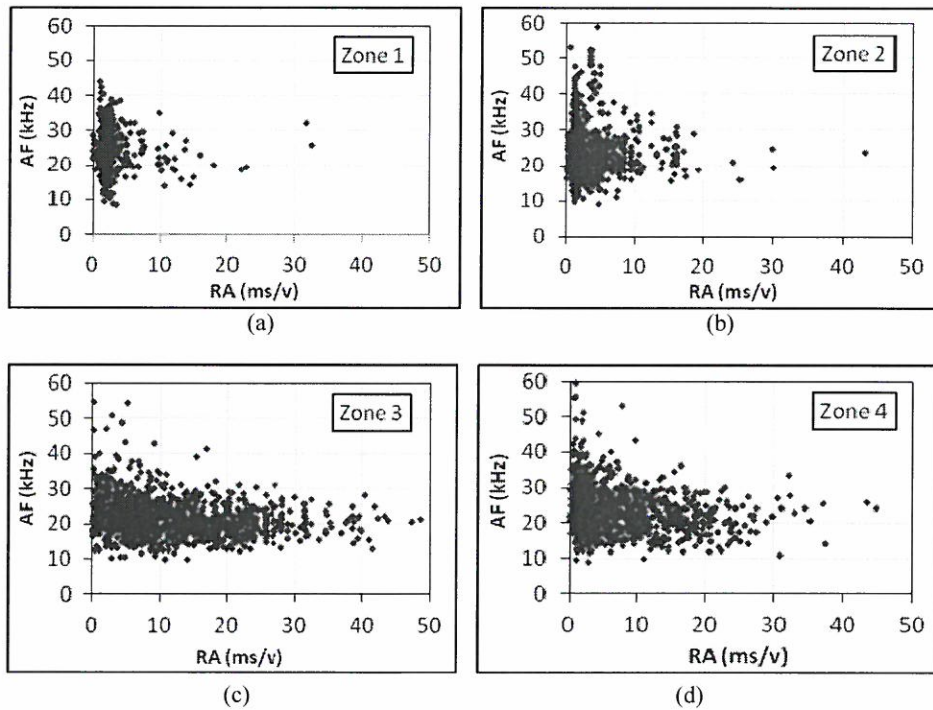Fig. 8 Source locations for whole test with amplitudes greater than 45dB

Fig. 9   Relation between the RA value and average frequency of (a) zone1, (b) zone2, (c) zone3 and (d) zone 4

Fig. 10 shows Relation between the RA value and average frequency of zone1 compared with zone 3. The black data points represent the crack region, while the grey represents the no crack region. It can be seen clearly the difference between two zones.
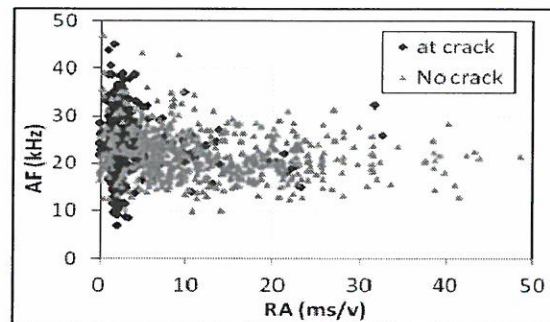
657

Fig. 10   Relation between the RA value and average frequency of Zone1 and zone 3

It has been demonstrated that by using relationship between RA and AF value, the crack area can be identified (Fig. 10). Hence, it could be possible to provide a corrosion alarm and location to pipe engineers prior to any wire breaks. Furthermore, by knowing the crack types it could be possible to identify the damaged area before the mortar completely fails. Additional analysis has shown that the measured values are not affected by distance making them an ideal approach. Further work is being conducted to investigate the exact mechanisms within this structure that causes differing RA and RF values. Results suggest that using AE techniques as structural health monitoring of the concrete pipes and other concrete structures such as bridges could be achieved. However, applying acoustic emission techniques on site (real pipes line), some limitations need to be considered which include source attenuation, number and location of sensors, noise from the surrounding environment and noise from water flow. Further research studies are needed to overcome these limitations if AE is to be used to monitor pipes.

4   Conclusion

The AE method has been applied to detect the corrosion in small scale pipe samples and a novel analysis approach to this application has been used to evaluate differing crack types. Using the relationship between RA value and AF value, the crack area and crack type can be identified and distinguish.

Acknowledgements

References

[1]   Ann, K.Y. et al.: The importance of chloride content at the concrete surface in assessing the time to corrosion of steel in concrete structures. In: Construction and Building Materials (2009) No. 23, pp239–245.

[2]   Singh, S. K.: Corrosion Studies on Prestressing Steel Wire. In: Ph.D. Thesis (2000) Imperial College, University of London.

[3]   Miller, R. K. et al.: Non-destructive Testing Handbook, Acoustic Emission Testing (2005) Volume 6, USA.

[4]   JCMS-III B5706: Monitoring method for active cracks in concrete by AE. In: Construction Material Standards (2003) Tokyo: Japan.

[5]   Ohtsu, M. and Tomoda, Y.: Corrosion process in reinforced concrete identified by acoustic emission. In: Materials Transactions (2007b) Vol. 48, No. 6, pp1184 to 1189.

[6]   Ohno, K. and Ohtsu, M.: Crack classification in concrete based on acoustic emission. In: Construction and Building Materials (2010) No. 4, pp. 2339-2346.

[7]   Aggelis, D.: Classification of cracking mode in concrete by acoustic emission parameters. In: Mechanics Research Communications (2011) No. 38, pp.153-157.

[8]   Kuwairi, A.: Water mining: the Great Man-made River, Libya. In: Proceedings of ICE Civil Engineering 159 May (2006) No.14382 pp.39-43.

[9]   Essamin, O. and Holley, M.: Great Man Made River Authority (GMRA): The Role of Acoustic Monitoring in the Management of the Worlds Largest Prestressed Concrete Cylinder Pipe Project. In: Proceedings of the ASCE Annual International Conference on Pipeline Engineering and Construction (2004) August 1-4, San Diego, California.

[10]   Ing, M. et al.: Cover zone properties influencing acoustic emission due to corrosion. In: Cement and Concrete Research (2005) No. 35 pp 284– 295.

[11]   Hellier, C. J.: Handbook of Non-destructive Evaluation (2001) McGraw-Hill, USA.

[12]   Carpinteri, A. et al.: Structural damage diagnosis and life-time assessment by acoustic emission monitoring. In: Engineering Fracture Mechanics (2007) No.74, pp273–289.

[13]   Li, X. and Zhang, Y.: Analytical Study of piezoelectric Paint for Acoustic Emission-Based Fracture Monitoring. In: Fatigue and Fracture of Engineering Materials and Structures (2008) No.31, pp 684-694.

[14]   Hsu, N. N. and Breckenridge, F. R.: Characterization and Calibration of Acoustic Emission Sensor. In: Materials Evaluation (1981) No. 39 (1) pp. 60-68.